

RANDOM WALK MODELS OF TURBULENT DISPERSION

A Thesis submitted for the degree of Doctor of Philosophy

by

David John Thomson

Meteorological Office, Bracknell

Department of Mathematics and Statistics, Brunel University

November 1988

Brunel University, Uxbridge

Department of Mathematics and Statistics

Author: David John Thomson

Title: Random Walk Models of Turbulent Dispersion

Year: 1988

Abstract: An understanding of the dispersion of contaminants in turbulent flows is important in many fields ranging from air pollution to chemical engineering, and random walk models provide one approach to understanding and calculating aspects of dispersion. Two types of random walk model are investigated in this thesis. The first type, so-called "one-particle models", are capable of predicting only mean concentrations while the second type, "two-particle models", are able to give some information on the fluctuations in concentration as well. Many different one-particle random walk models have been proposed previously and several criteria have emerged to distinguish good models from bad. In this thesis, the relationships between the various criteria are examined and it is shown that most of the criteria are equivalent. It is also shown how a model can be designed to (i) satisfy the criteria exactly and (ii) be consistent with inertial subrange theory. Some examples of models which obey the criteria are described. The theory developed for one-particle models is then extended to the two-particle case and used to design a two-particle model suitable for modelling dispersion in high Reynolds number isotropic turbulence. The properties of this model are investigated in detail and compared with previous models. In contrast to most previous models, the new model is three-dimensional and leads to a prediction for the particle separation probability density function which is in agreement with inertial subrange theory. The values of concentration variance from the new model are compared with experimental data and show encouraging agreement.

Contents.

Chapter 1 - Introduction	1
1.1 The Problem of Turbulent Dispersion	1
1.2 The Random Walk Approach	5
1.3 Alternative Modelling Approaches	7
1.4 Guide to Succeeding Chapters	12
Chapter 2 - Probability and Stochastic Differential Equations	14
2.1 Notation for Probabilistic Concepts	14
2.2 The Wiener Process	16
2.3 Stochastic Differential Equations	18
Chapter 3 - Mathematical Framework for Random Walk Models	21
3.1 Basic Equations	21
3.2 The Ensemble of Realisations	22
3.3 Transition Densities	24
Chapter 4 - Theoretical Aspects of One-Particle Random Walk Models ..	30
4.1 Introduction to One-particle Models	30
4.2 Some Criteria for the Selection of Random Walk Models	40
4.3 Choosing \underline{a} and \underline{B} - Additional Considerations	58
4.4 Some Examples of Random Walk Models	64
4.5 Summary	68
Chapter 5 - Two-Particle Random Walk Models	70
5.1 Introduction to Two-Particle Models	70
5.2 Theoretical Aspects of Two-Particle Models	74
5.3 The Role of Molecular diffusion	79
5.4 A New Two-Particle Model Applicable to Dispersion in High Reynolds Number Constant Density Isotropic Turbulence	85
5.5 Some Previously Proposed Two-Particle Models	92

5.6 Properties of the Two-Particle Transition P.D.F. in the Models ..	96
5.7 Summary	110
Chapter 6 - Predictions of Concentration Variance from the New Model	112
6.1 Isotropic Concentration Fields	112
6.2 Instantaneous Deterministic Sources	116
Chapter 7 - The Random Walk Modelling Technique - An Appraisal.....	128
Appendix A - Derivation of the Statistical Relations given in §3.3	133
Appendix B - Some Properties of Various Random Walk Models	137
Appendix C - Details of the Numerical Simulations	140
C.1 Details of Simulations Presented in Chapter 4	140
C.2 Details of Simulations Presented in Chapters 5 and 6	140
C.3 Justification of the "Particle Splitting" Technique	143
Appendix D - The relation between $\langle \delta\tilde{X}_1 ^2 \rangle$ and $\langle \delta\Delta\tilde{X} ^2 \rangle$	145
References	148

Acknowledgements.

It is a pleasure to thank the following individuals for their help and encouragement. First and foremost I would like to thank Professor Philip Chatwin, my supervisor at Brunel, for many stimulating discussions and constant encouragement throughout my studies. I would also like to thank my external supervisor at the Meteorological office, Dr Barry Smith, for originally suggesting that I should apply to study for a doctorate, and Dr David Carson who strongly supported and assisted in my application for sponsorship from the Meteorological office. Last, but by no means least, I would like to thank Dr Paul Mason (head of the Boundary-layer Branch of the Meteorological Office) for his encouragement and for his understanding of the amount of time it took to complete this study.

In addition, I would like to thank the Meteorological Office for their support throughout my period of study at Brunel University.

1. INTRODUCTION.

1.1 The Problem of Turbulent Dispersion.

One of the most characteristic properties of turbulence is its ability to disperse and mix contaminants. Indeed, in many problems involving turbulent flows, it is the dispersive properties of the turbulence which are of primary interest. Examples of such problems include the dispersion of pollutants in the atmosphere, rivers, seas and oceans; heat transfer in geophysical and engineering flows (in many respects heat behaves in the same way as a material contaminant); and mixing processes in chemical engineering. The range of dispersion problems is large. For example, in the case of atmospheric dispersion, one might be interested in dispersion over a few hundred metres in the case of odours from a factory or over several thousand kilometres in the case of acid rain. To understand these different problems requires an understanding of the atmospheric eddies over a wide range of scales, from micrometeorological turbulence to synoptic-scale depressions and anticyclones (see e.g. Pasquill and Smith (1983)). Further complications are the chemical properties of the dispersing substance (which affect, for example, the rate at which the substance is absorbed by the ground or transformed into other substances) and the density of the release (as typified by the difference between accidental releases of dense gases and hot buoyant plumes from chimneys).

In any particular turbulent flow, the flow field and the distribution of contaminants within the flow evolve in a very complicated fashion which shows great sensitivity to initial conditions and is unpredictable in detail. As a result it is usual in the study of turbulent flows to adopt a statistical approach (see e.g. Batchelor (1953) or Monin and Yaglom (1971)). In such an approach, the attempt to calculate the evolution of any particular flow is abandoned and instead an ensemble of realisations of the flow (in which the external

conditions are identical but in which the details of the turbulence differ) is considered. Attempts are then made to understand and predict the evolution of ensemble average quantities. Examples of such quantities include the ensemble mean, standard deviation and probability density function (p.d.f.) of the concentration at a particular point, and quantities reflecting the spatial and temporal structure of the concentration field such as correlation functions and spectra.

In many situations the ensemble mean concentration is the main quantity of interest. However there are also many flows in which some understanding of the fluctuations is desirable. At the simplest level it is useful to have an estimate of the extent to which the true concentration at a point might differ from the ensemble average. The fluctuations often have a standard deviation which is many times greater than the mean concentration (see e.g. Sawford (1987) or Mylne (1988)) and so the difference between the true and ensemble average concentrations is not necessarily small. Also, for many quantities in many situations, ensemble averages are equal to time averages (Monin and Yaglom (1971, §4.7) give sufficient conditions for this to be so), and, in such cases, knowledge of the concentration p.d.f., or of some gross statistic such as the standard deviation of the concentration, gives an indication of the variability in time of the concentration at a point. Such knowledge is often needed in atmospheric dispersion problems, especially those involving toxic, inflammable or odorous materials, or in flows involving chemical reactions. For example, in the case of a toxic or inflammable release, the peak concentrations can constitute a significant risk, even if the time average concentration is well within safety limits. Similarly, in the case of reacting substances, the instantaneous reaction rate is a function of the instantaneous concentrations of the various reacting species. In non-linear reactions, estimates of the average reaction rate calculated

from the average concentrations can be badly in error.

In many dispersion problems it is possible to assume that the contaminant is passive, i.e. the contaminant is non-reacting, moves only as a result of molecular diffusion and advection by the velocity field, and is present in sufficiently small concentrations so as not to affect the motion of the fluid (e.g. through buoyancy effects). This assumption, when it can be made, results in a considerable simplification of the problem since the contaminant concentration then satisfies a linear equation (the advection-diffusion equation) and it is possible to separate the problem of dispersion from the problem of turbulence, i.e. we can ask the question, "Given the statistics of the velocity field, what are the statistics of the concentration field?". Even with this simplification, experience shows that the problem is still very difficult and that there is little prospect of a solution being found in the near future, even for the simplest of flows. We simply do not have the mathematical tools necessary to tackle problems with so many degrees of freedom.

One of the few exact results that have been obtained, and certainly one of the most important is that obtained by Taylor (1921). Taylor considered the motion of fluid elements, i.e. infinitesimal points which travel at the local fluid velocity, and related their mean square displacement to the Lagrangian velocity correlation function. Suppose, for simplicity, that there is no mean flow (or that the mean flow is constant and that we are using a reference frame moving with the flow) and consider the motion in one direction only - say the x-direction. Let $X(t)$ be the trajectory of the fluid element which was at $x=0$ at the time zero and let $U(t)$ denote the fluid element velocity dX/dt . Then Taylor's result states that, provided the velocity $U(t)$ is a stationary random function, the mean square displacement of fluid elements is given by

$$\langle X(t)^2 \rangle = \int_0^t \int_0^t \sigma^2 R(t_1 - t_2) dt_1 dt_2, \quad (1.1)$$

where $\langle \rangle$ denotes an ensemble average, σ^2 is the variance of the fluid element velocities and R is the correlation function of the fluid element velocities, i.e. $R(t) = \langle U(t')U(t'+t) \rangle / \sigma^2$. For small and large times (1.1) has a particularly simple physical interpretation. For small t , $\langle X(t)^2 \rangle \approx \sigma^2 t^2$. This is simply a consequence of the fact that particle trajectories can be approximated by straight lines over short periods of time. For large times, provided the Lagrangian integral time-scale $\tau_I = \int_0^\infty R(t) dt$ is finite and non-zero, $\langle X(t)^2 \rangle \approx 2\sigma^2 \tau_I t$. This type of behaviour, with $\langle X(t)^2 \rangle$ proportional to t , is similar to that observed in molecular diffusion problems and can be understood by regarding the displacement $X(t)$ over a time t , $t \gg \tau_I$, as the sum of many approximately independent displacements over intervals which are long compared to τ_I but much shorter than t .

The importance of Taylor's result is that, provided molecular diffusion can be neglected, it gives an estimate of the spatial spread of the ensemble mean concentration field resulting from an instantaneous point source. Often it is possible to make an assumption about the shape of the ensemble mean concentration distribution. When this can be done, knowledge of the mean square spread can be used to calculate the ensemble average concentration field. For example, provided the fluid element velocities are stationary random functions with τ_I finite and non-zero, it seems likely on the basis of central limit theorem type arguments that the spatial distribution will be Gaussian at large times. Also the fixed point velocity distribution is often close to Gaussian and so the ensemble average concentration field will be close to Gaussian at small times as well. In such situations it is not too great a leap of faith to believe that the distribution is always close to Gaussian (see e.g. Monin and Yaglom (1971, pp540-541)).

Important as Taylor's result is (and it would be hard to overstate its importance), it leaves many questions unanswered. For example, in the majority of flows $U(t)$ is not a stationary random function. Even in cases where it is, the Lagrangian correlation function $R(t)$ is usually unknown. The Eulerian (i.e. fixed point) velocity statistics are usually better known (either from measurements or turbulence models) but it is not clear how $R(t)$ can be calculated from such statistics. Also Taylor's theory takes no account of molecular diffusion. However this is not so serious a problem because molecular diffusion is generally thought to have a negligible effect on ensemble mean concentrations in most high Reynolds number flows (Saffman 1960; Monin and Yaglom 1971, §10.2). (In fact Taylor's result can be modified to include molecular diffusion (Saffman 1960); however the result of this modification is to express the mean square displacement of molecules in terms of the correlation function of the flow velocity evaluated along molecular trajectories. Such correlations are generally no better known than Lagrangian correlations.) Finally Taylor's result gives no indication at all of the size of fluctuations in concentration which, as noted above, are often of considerable importance.

1.2 The Random Walk Approach.

In view of the difficulties noted above in calculating turbulent dispersion directly from the governing equations, it is often necessary to resort to approximate mathematical models of the dispersion process. One such modelling technique, which has been much exploited in recent years and which constitutes the main subject of this thesis, is the so-called "random walk" technique, also known as the random flight or random force method (see e.g. Obukhov (1959), Novikov (1963), Lin and Reid (1963), Jonas and Bartlett (1972), Hall (1975) and Reid (1979) for a selection of the early applications of this technique). The range of

dispersion problems to which this approach is applicable is rather modest compared with the full range of dispersion problems discussed in §1.1. In particular, random walk models assume that the dispersing material is passive and that the eddies have at least some of the randomness properties characteristic of three-dimensional turbulence. Thus the technique, at least in its basic form, is not directly applicable to buoyant or heavy plumes, reacting flows, or to long range atmospheric dispersion problems where the eddies responsible for the dispersion are predominantly two-dimensional.

The basic idea behind random walk models is to simulate the motion of many particles of the dispersing substance. The idea is a very natural one, since it is, of course, the motion of the individual elements of the dispersing substance which determines the dispersion. Figure 1.1 shows some simulated trajectories for the case of an elevated source in a neutral boundary layer. The particles are assumed to be drawn at random from among all the particles of the dispersing material in the ensemble of flows. To calculate the ensemble mean concentration at a particular place and time, a small box is constructed (metaphorically speaking) around the place in question and the number of trajectories in the box at the time in question is counted. In order to obtain statistically reliable values for the concentration, it is necessary to ensure that many particles pass through the box, and so a large number of trajectories, typically ten thousand, need to be computed. Of course in order to implement the above scheme, it is necessary to have a model of the way the particles move. The investigation of how such models should be formulated is one of the main aims of this thesis. In some cases the statistics of the particle trajectories, and hence the ensemble mean concentration field, can be calculated from the model analytically, without the need for the explicit simulation of many trajectories. However such situations are the exception rather than the rule.

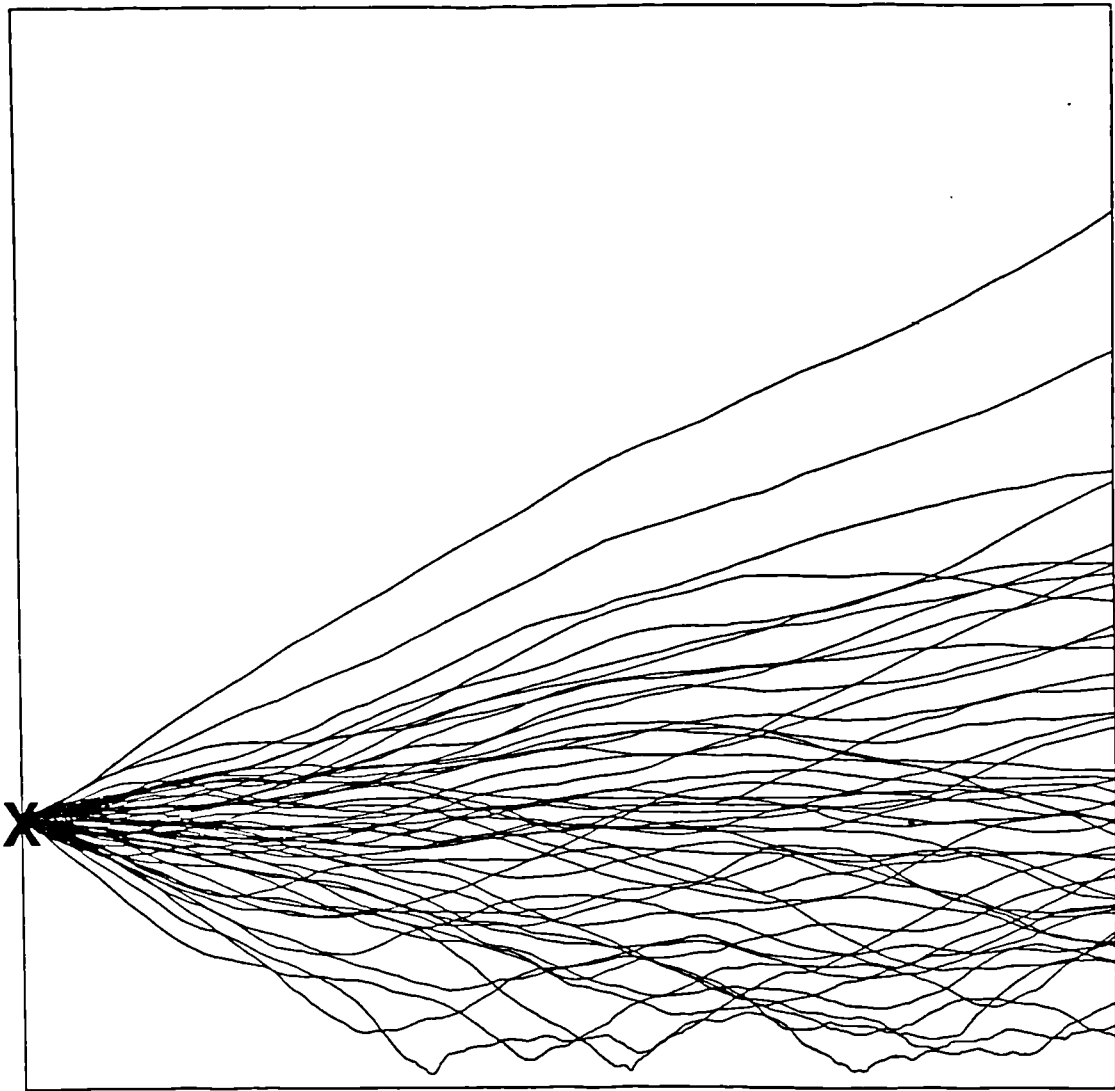


Figure 1.1: 50 trajectories from a random walk simulation of vertical dispersion downwind of an elevated source, marked x, in a neutral boundary layer.

If the trajectories of pairs of particles (instead of single particles) are simulated, random walk models can be used to predict the concentration variance as well as the ensemble mean concentration. The idea that the concentration variance can be expressed in terms of the motion of particle-pairs is due in essence to Batchelor (1952), but it is only comparatively recently (Durbin 1980) that this has been exploited by simulating the motion of particle-pairs numerically.

1.3 Alternative Modelling Approaches.

Of course the random walk approach is not the only possible approach to dispersion modelling, and it is appropriate to discuss briefly some of the alternative approaches. A discussion of the advantages and disadvantages of the random walk approach in relation to these alternative approaches will be given in chapter 7 after the random walk approach has been investigated in some detail.

Perhaps the most widely used practical method for modelling the ensemble mean concentrations resulting from steady sources in the atmosphere is the Gaussian plume model (see e.g. Pasquill and Smith (1983, p320)), in which the shape of the concentration distribution across the plume is assumed to be Gaussian. The reason for choosing a Gaussian shape is that, for dispersion in homogeneous stationary turbulence, the fluid element velocities are stationary random functions, and so a Gaussian shape is expected on the basis of central limit theorem type arguments (see §1.1). Of course atmospheric turbulence cannot be assumed to be homogeneous and stationary (especially in the vertical direction) and so the Gaussian assumption is unlikely to be exact. However it might be expected to be a reasonable approximation, an expectation which, in many (but not all) situations, is confirmed by experimental data (Pasquill and Smith 1973, §4.2, §4.5 and p320). In Gaussian plume models the width of the plume in the lateral and vertical directions is determined from tables or

nomograms based on experimental observations of plume behaviour. Although it will be a while before this method is superseded from a practical point of view, such models are essentially empirical and do not explain the dispersion in terms of the flow properties.

A second approach which has been extensively applied is the use of the diffusion equation (see e.g. Monin and Yaglom (1971, §§10.3-10.5) and Pasquill and Smith (1983, §§3.1 and 3.2)). In this approach it is assumed that the turbulent eddies disperse material in a way which is qualitatively similar to the action of molecular diffusion, i.e. it is assumed that the turbulent flux of material is proportional to the concentration gradient, the constant of proportionality being the diffusivity K . There are various ways in which the "eddy-diffusivity" K and its spatial and temporal variation can be estimated in terms of the flow properties. However, the fundamental assumption underlying the diffusion equation, namely that the length- and time-scales of the motions responsible for the dispersion are small compared with the scales on which the concentration and flow properties vary, is not true in general. This leads to a number of qualitative errors in the results. For example, the ensemble average plume from an elevated source grows linearly for small times after release (because fluid elements travel in straight lines over short distances) whereas the diffusion equation predicts parabolic growth as in figure 1.2. Also, in many flows, a substantial part of the turbulence energy is contained in large eddies whose sizes are comparable to the domain size; in such cases the diffusion equation can fail to represent the most important features of the dispersion. A good example of such a flow is the convective boundary layer (see e.g. Willis and Deardorff (1976, 1978 and 1981), Lamb (1982), de Baas, van Dop and Nieuwstadt (1986), Sawford and Guest (1987) and Weil (1988)). In such boundary layers the dispersion is dominated by large scale convective eddies of size comparable to the boundary layer depth. These large eddies cause many

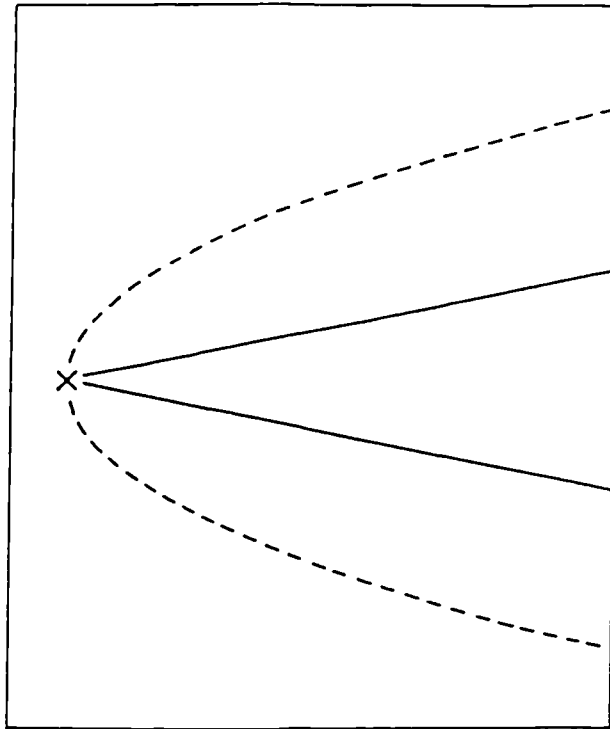


Figure 1.2: Plume growth downwind of an elevated source in the atmospheric boundary layer. The solid line indicates the true behaviour at short distances from the source and the dashed line gives the result of using the diffusion equation. x marks the source position.

non-diffusive effects such as the "lift-off" of plumes from ground level sources. There are however some situations in which the eddy-diffusivity approach does give good results. For example we saw above in discussing Taylor's (1921) result that, provided the conditions required for Taylor's result are fulfilled, an eddy-diffusion assumption is likely to be good at large times. Another example is the case of vertical diffusion from a surface source in a neutral surface layer. In this flow the eddies become small as we approach the surface. If the eddies responsible for dispersing the contaminant were much smaller than the cloud of contaminant at all stages of the dispersion then we could be confident that an eddy-diffusivity assumption would be valid. Although this is not the case (and so an eddy-diffusivity assumption cannot be formally justified), it is true that the eddies are never much larger than the cloud and so an eddy-diffusivity assumption might be expected to be an acceptable (although inexact) approximation. Experimental evidence (Pasquill and Smith 1983, §4.6) supports this view.

High-order closure models constitute a promising technique which overcomes some of the problems associated with eddy-diffusivity models. However, these models cannot represent the initial stages of the evolution of the ensemble mean concentration in a natural way and cannot easily represent the dispersion from complex source distributions (Deardorff 1978). The difficulty is that an eddy-diffusivity assumption needs to be made for the flux of some higher order moment, and this assumption is no more justified than the use of an eddy-diffusivity for the flux of contaminant. The most common form of high-order closure is second-order closure, and such models can be (but are not always - see Deardorff (1978)) formulated in a way which enables them to predict concentration variance as well as the mean concentration (see e.g. Newman, Launder and Lumley (1981) or Sykes, Lewellen and Parker (1984)). However, these models sometimes

have difficulty in providing good predictions of the concentration variance, especially if the length-scale of the concentration fluctuations is not closely related to that of the velocity field. The reason for this is that second-order closure models describe the flow solely in terms of one-point statistics, and so do not carry information on the spatial structure of the concentration field. These difficulties occur even in what is perhaps the simplest possible flow involving fluctuations in concentration, namely the decay of an isotropic concentration field in decaying isotropic turbulence. The grid turbulence experiments of Warhaft and Lumley (1978) and Sreenivasan, Tavoularis, Henry and Corrsin (1980) provide a good approximation to this flow and show that the power law exponent of the decay of concentration variance depends strongly on the ratio of the length-scales of the scalar and velocity fields. The early second-order closure models assumed, following Spalding (1971), that the ratio of the time-scales for the decay of the scalar and velocity fields was a universal constant and were consequently unable to explain the variation in decay rate. Newman et al (1981) succeeded in designing a model which reproduces the observed decay, although at the cost of violating the principle of superposition of scalar fields (Pope 1983; Lumley and Van Cruyningen 1985), a principle which follows from the linearity of the advection-diffusion equation. This suggests that a completely consistent second-order closure model may not be possible.

So-called p.d.f. models (Pope 1985) provide an approach to modelling which has much in common with both high-order closure models and the random walk approach. These models enable predictions of the p.d.f. of the concentration at each point to be obtained. However such models are usually formulated in terms of one-point statistics and so are likely to suffer from the same problems as high-order closure models in predicting properties of the fluctuations in concentration.

More soundly based models for calculating concentration variance are provided by two-point closures, of which the "eddy-damped quasi-normal Markovian approximation" is perhaps the most widely applied (see e.g. Lesieur (1987)), and two-point two-time closures such as the direct interaction approximation or its Lagrangian modification (see e.g. Leslie (1973)). In these models, the description of the flow includes a specification of the (second-order) spatial structure of the concentration field. As a result such models avoid the problems encountered by the one-point closures discussed above and can describe the decay of an isotropic concentration field in isotropic turbulence easily and naturally (Larчевêque, Chollet, Herring, Lesieur, Newman and Schertzer 1980). However such models are usually formulated in terms of spectra and are hard to extend to flows where the velocity or concentration field is inhomogeneous (of course in such cases a description in terms of power spectra is impossible).

A rather different type of approach is possible in cases where the dispersion of material depends on only a small number of physical quantities. In such situations it is possible to obtain some information on the dispersion by dimensional analysis. The results of such analyses usually imply similarity between some aspects of the concentration distribution at different times or places, and so the use of this technique is often referred to as the application of similarity theory. Although there are only a few situations to which such an approach can be applied, the technique, when applicable, generally gives important insights into the dispersion. The two most successful examples of applications of similarity theory to dispersion have been in the investigation of vertical dispersion from an instantaneous ground level source in the neutral atmospheric surface layer (Batchelor 1964) and in inquiries into those aspects of dispersion which are governed by the inertial subrange part of the turbulence spectrum (Monin and Yaglom 1975, §§21.6 and 24.1-24.3). A disadvantage of

similarity theory is that it gives only limited information about the dispersion. For example, in the case of an instantaneous ground level source in the neutral atmospheric surface layer, it gives no information on the shape of the concentration distribution in the vertical, other than that it is the same at all times. In addition the similarity is usually not exact. For example, it is thought that the integral length-scale of the turbulent velocity field has a weak influence on the inertial subrange structure as a result of its effect on fluctuations in dissipation rate (Monin and Yaglom 1975, §25), an effect which is neglected in the dimensional analysis.

1.4 Guide to Succeeding Chapters.

The main objective of the work presented in this thesis is to clarify theoretical aspects of the problem of how to formulate one- and two-particle random walk models, and to apply two-particle models to the problem of predicting concentration variance in some simple flows. No applications of one-particle models are presented here; however many examples of applications can be found in the references cited.

Chapters 2 and 3 are concerned with various preliminaries which are necessary for the discussion of random walk models. With the exception of some ideas in §3.3, most of this material is not original, having previously been discussed quite extensively by other authors. The random walk models themselves are most easily expressed in terms of the language of stochastic differential equations, and chapter 2 gives a brief description and summarizes the main properties of such equations. Chapter 3 is concerned with developing the mathematical framework for describing turbulent dispersion. The equations satisfied by the fluid dynamic variables are presented (§3.1), the statistical approach outlined in §1.1 is described in more detail (§3.2) and the statistical relations between the concentration field and the trajectories of particles and particle-pairs are described (§3.3). The

main new results obtained in this thesis are presented in chapters 4, 5 and 6. In chapter 4 the theory of how one-particle random walk models should be formulated is developed. Chapter 5 extends this theory to two-particle models and investigates some of the properties of such models in what is perhaps the simplest possible flow, namely isotropic turbulence. In chapter 6 predictions of the concentration variance are compared with experimental data. Finally, in chapter 7, a discussion is given of the strengths and weaknesses of random walk models, both in absolute terms and in relation to other modelling techniques.

2. PROBABILITY AND STOCHASTIC DIFFERENTIAL EQUATIONS.

This chapter outlines some aspects of the theory of probability and stochastic differential equations, primarily in order to establish notation and provide a summary of those results which will be used frequently in chapters 3, 4 and 5. The random processes which are described in §2.2 and §2.3 were introduced originally to model Brownian motion and molecular diffusion. These applications are discussed briefly in order to give a physical picture of the processes. Applications to turbulent dispersion are deferred to chapter 4.

2.1 Notation for Probabilistic Concepts.

The notations which will be used for probabilistic concepts are similar to those used in so-called p.d.f. models of turbulence by Pope (1985) and others. The probability density function (p.d.f.) of a real-valued random variable X , which always exists if "function" is interpreted in the generalised sense (Pope 1985; Lumley 1970, p9), will be denoted by $p_X(x)$. If the expectation of X exists, it will be denoted by $\langle X \rangle$. The joint p.d.f. of several random variables X_1, \dots, X_n will be denoted by $p_{X_1, \dots, X_n}(x_1, \dots, x_n)$ or, if the random variables X_1, \dots, X_n are the components of a (finite-dimensional) random vector \underline{X} , by $p_{\underline{X}}(\underline{x})$. The expectation of such a random vector \underline{X} (defined component-wise) will be written $\langle \underline{X} \rangle$. Superscripts will be used to denote components of vectors and the summation convention will be used.

Just as expectations can be expressed in terms of probabilities, so the probabilities associated with a random variable X can be expressed in terms of expectations. For example, the probability that the random variable X is less than or equal to x is given by the expectation of the random variable χ_x defined by

$$\chi_x = \begin{cases} 1 & \text{if } X \leq x \\ 0 & \text{otherwise.} \end{cases}$$

Hence the p.d.f. of X is given by

$$p_X(x) = d\langle\chi_x\rangle/dx = \langle\delta(x-X)\rangle \quad (2.1a)$$

where δ denotes the Dirac delta function. Similarly

$$p_{X_1, \dots, X_n}(x_1, \dots, x_n) = \langle\delta(x_1-X_1)\dots\delta(x_n-X_n)\rangle \quad (2.1b)$$

and

$$p_{\underline{X}}(\underline{x}) = \langle\delta(\underline{x}-\underline{X})\rangle. \quad (2.1c)$$

In chapter 3 we will need the concept of the X -weighted p.d.f. of Y , where X and Y are random variables. This is defined, by analogy with (2.1), to be $\langle X \delta(y-Y)\rangle$. Just as knowledge of the p.d.f. of Y enables expectations of functions of Y to be calculated using the relation $\langle f(Y)\rangle = \int f(y) p_Y(y) dy$, so knowledge of the X -weighted p.d.f. of Y enables X -weighted expectations to be calculated from $\langle X f(Y)\rangle = \int f(y) \langle X \delta(y-Y)\rangle dy$.

If X and Y are random variables, the conditional p.d.f. of X given $Y = y$, which is defined by $p_{X,Y}(x,y)/p_Y(y)$, will be denoted by $p_{X|Y}(x|y)$. The conditional expectation of X given $Y = y$ will be denoted by $\langle X|Y=y\rangle$ and is defined by

$$\langle X|Y=y\rangle = \int x p_{X|Y}(x|y) dx.$$

It has the property that

$$\begin{aligned} p_Y(y) \langle X|Y=y\rangle &= \int x p_{X,Y}(x,y) dx \\ &= \int x \delta(y-y') p_{X,Y}(x,y') dx dy' \\ &= \langle X \delta(y-Y)\rangle. \end{aligned}$$

The definitions and notations for weighted p.d.f.s, conditional p.d.f.s and conditional expectations will also be used with the obvious modifications when X and Y are (finite-dimensional) random vectors or (finite) collections of random variables.

2.2 The Wiener Process.

A random process which plays an important role in random walk models is the Wiener process (Feller 1971, pp99 and 181; Schuss 1980, §2.1; Gihman and Skorohod 1980, p158), originally introduced to model Brownian motion. A random process $\zeta(t)$ which is defined for $t \geq 0$ is a Wiener process if it has the following properties: (i) all its sample paths are continuous, (ii) for $t_2 \geq t_1$, the increment $\zeta(t_2) - \zeta(t_1)$ has a probability distribution depending only on $t_2 - t_1$, (iii) the increments in non-overlapping intervals are independent (i.e. $\zeta(t_4) - \zeta(t_3)$ is independent of $\zeta(t_2) - \zeta(t_1)$ for $t_4 \geq t_3 \geq t_2 \geq t_1$), (iv) for $t_2 \geq t_1$, the increment $\zeta(t_2) - \zeta(t_1)$ is a Gaussian random variable with zero mean and variance $t_2 - t_1$, and (v) $\zeta(0) = 0$. We will also be interested in multi-dimensional Wiener processes $\underline{\zeta}(t)$ which are simply vector-valued processes with independent components, each component of which is a one-dimensional Wiener process. The symbol ζ will be reserved throughout this thesis for Wiener processes.

Somewhat surprisingly, any vector-valued process $\underline{X}(t)$ which is defined for $t \geq 0$ and which has continuous sample paths and stationary independent increments (i.e. which satisfies multi-dimensional analogues of conditions (i), (ii) and (iii)) can be expressed in terms of a Wiener process by suitable scaling and the addition of a mean drift and initial (possibly random) displacement, i.e. it can be expressed in the form

$$X^i(t) = a^i t + b^{ij} \zeta^j + X^i(0) \quad (2.2)$$

for some Wiener process $\underline{\zeta}(t)$. This is because the increment of such a process over the interval $[t_2, t_1]$ can be expressed as the sum of the n increments which occur over the n non-overlapping time intervals $[t_1 + (t_2 - t_1)(i-1)/n, t_1 + (t_2 - t_1)i/n]$, $i=1, \dots, n$. Each of these increments has the same distribution and also, since the sample paths are continuous, the expected number of these increments which exceed ε (for

any given $\epsilon > 0$) tends to zero as $n \rightarrow \infty$. Hence, by the central limit theorem, the increment $\underline{X}(t_2) - \underline{X}(t_1)$ must be Gaussian. It follows that, with an appropriate choice of \underline{a} and \underline{b} , $\underline{X}(t)$ takes the form (2.2). A more rigorous proof of this can be found in Gihman and Skorohod (1980, pp189-190).

As is well known, small particles suspended in a fluid (such as smoke particles in air) undergo a random motion (called Brownian motion) as a result of the impacts of the fluid molecules. As mentioned above, the Wiener process (suitably scaled and with the addition of an initial displacement) is often used as a model for this motion (Einstein 1956; Schuss 1980, §2.1; Gihman and Skorohod 1980, p158; Wax 1954). The displacement of a particle results from the combined effect of an enormous number of impacts by molecules. Provided the properties of the medium in which the particle is moving are uniform in space and time, the effects of these impacts in non-overlapping time intervals are likely to be independent due to the random nature of molecular motions; also the p.d.f. of an increment over an interval is likely to depend only on the length of the interval. Hence the Wiener process should be a good model for such motions, at least on time-scales much longer than the time-scale on which the Brownian particle exchanges momentum with the fluid. The Wiener process is not such a good model over shorter time intervals. To see this note that the mean square derivative of a Wiener process is infinite (since the mean square of the increment over an interval Δt is equal to Δt and is not of order $(\Delta t)^2$) whereas the velocity of a particle must of course be finite. In the Wiener process model of Brownian motion, the velocity of a particle, which has a very large mean square value (relative to the average velocity of the particle over a "macroscopic" time interval) and a very short correlation time-scale (relative to the length of a macroscopic time interval), is modelled by an idealised process with infinite mean square value and

zero correlation time-scale.

For similar reasons, the Wiener process is a good model for the random displacement of molecules in a fluid over time intervals which are much longer than the time-scale on which a molecule exchanges momentum with other molecules.

2.3 Stochastic Differential Equations.

The Wiener process, although a good model for Brownian or molecular motions in a uniform medium, is not sufficiently general for our purposes. A natural generalisation is to consider processes in which the properties of the increments vary with position and time. Such processes can be described by Itô stochastic differential equations (Gihman and Skorohod 1979; Schuss 1980):

$$dX^i = a^i(\underline{X}(t), t) dt + b^{ij}(\underline{X}(t), t) d\zeta^j. \quad (2.3)$$

Informally this equation can be regarded as a generalisation of (2.2) with \underline{a} and \underline{b} depending on $\underline{X}(t)$ and t . For our purposes it is sufficient to regard (2.3) as being the limit as $\Delta t \rightarrow 0$ of the difference equation

$$X^i(t+\Delta t) - X^i(t) = a^i(\underline{X}(t), t)\Delta t + b^{ij}(\underline{X}(t), t)(\zeta^j(t+\Delta t) - \zeta^j(t)). \quad (2.4)$$

For given \underline{a} and \underline{b} , equation (2.3) does not of course determine the process $\underline{X}(t)$; to do this it is also necessary to specify the p.d.f. $p_{\underline{X}(0)}$ of $\underline{X}(0)$ (assuming the process $\underline{X}(t)$ is to be defined for $t \geq 0$). For suitable choice of \underline{a} and \underline{b} , such a process is a good model of the motion of Brownian particles or molecules in a fluid which is in motion. Indeed, it will be seen below that (for suitable \underline{a} and \underline{b}) the p.d.f. $p_{\underline{X}(t)}$ obeys the usual advection-diffusion equation for the evolution of the concentration of a passive contaminant.

For processes described by Itô stochastic differential equations it is straightforward to derive equations for the evolution of $P_{\underline{X}(t)|\underline{X}(s)}$ and $p_{\underline{X}(t)}$. First note that $\underline{X}(t)$ is Markovian, i.e. given the value of \underline{X} at time t , the values at times greater than t are independent of the values at times less than t . A consequence of this is that $P_{\underline{X}(t)|\underline{X}(s)}$ obeys the Chapman-Kolmogorov equation

$$P_{\underline{X}(t)|\underline{X}(s)}(\underline{x}|\underline{y}) = \int P_{\underline{X}(t)|\underline{X}(r)}(\underline{x}|\underline{z}) P_{\underline{X}(r)|\underline{X}(s)}(\underline{z}|\underline{y}) d\underline{z}$$

for any r with $t \geq r \geq s$ (Schuss 1980, p101; Gihman and Skorohod 1980, p160). Hence, for $t \geq s$,

$$\begin{aligned} P_{\underline{X}(t+\Delta t)|\underline{X}(s)}(\underline{x}|\underline{y}) &= \int P_{\underline{X}(t+\Delta t)|\underline{X}(t)}(\underline{x}|\underline{z}) P_{\underline{X}(t)|\underline{X}(s)}(\underline{z}|\underline{y}) d\underline{z} \\ &= \int P_{\Delta\underline{X}|\underline{X}(t)}(\underline{x}-\underline{z}|\underline{z}) P_{\underline{X}(t)|\underline{X}(s)}(\underline{z}|\underline{y}) d\underline{z} \\ &= \int P_{\Delta\underline{X}|\underline{X}(t)}(\Delta\underline{x}|\underline{x}-\Delta\underline{x}) P_{\underline{X}(t)|\underline{X}(s)}(\underline{x}-\Delta\underline{x}|\underline{y}) d\Delta\underline{x} \end{aligned}$$

where $\Delta\underline{X} = \underline{X}(t+\Delta t) - \underline{X}(t)$. Now, because the trajectories $\underline{X}(t)$ are continuous, the main contribution to the integral will come from values of $\Delta\underline{x}$ close to zero. Expanding in a Taylor series in $\Delta\underline{x}$ yields

$$\begin{aligned} P_{\underline{X}(t+\Delta t)|\underline{X}(s)}(\underline{x}|\underline{y}) &= \sum_{l=0}^{\infty} \sum_{m=0}^{\infty} \sum_{n=0}^{\infty} \frac{(-1)^{l+m+n}}{l!m!n!} \times \\ &\times \frac{\partial^{l+m+n}}{(\partial x^1)^l (\partial x^2)^m (\partial x^3)^n} \left(\langle (\Delta X^1)^l (\Delta X^2)^m (\Delta X^3)^n | \underline{X}(t) = \underline{x} \rangle P_{\underline{X}(t)|\underline{X}(s)}(\underline{x}|\underline{y}) \right). \end{aligned} \quad (2.5)$$

From (2.4), the conditional p.d.f. $P_{\Delta\underline{X}|\underline{X}(t)}(\Delta\underline{x}|\underline{x})$ of $\Delta\underline{X}$ given $\underline{X}(t) = \underline{x}$ is Gaussian with mean $\underline{a}(\underline{x}, t)\Delta t$ and covariance matrix $2B^{ij}(\underline{x}, t)\Delta t$ where $B^{ij}(\underline{x}, t) = \frac{1}{2}b^{ik}(\underline{x}, t)b^{jk}(\underline{x}, t)$. Hence $\langle \Delta X^i | \underline{X}(t) = \underline{x} \rangle = a^i(\underline{x}, t)\Delta t$, $\langle \Delta X^i \Delta X^j | \underline{X}(t) = \underline{x} \rangle = 2B^{ij}(\underline{x}, t)\Delta t$ and all higher moments are $o(\Delta t)$. By letting $\Delta t \rightarrow 0$ in (2.5), it follows that $P_{\underline{X}(t)|\underline{X}(s)}(\underline{x}|\underline{y})$ satisfies

$$\frac{\partial p}{\partial t} = - \frac{\partial}{\partial x^i} (a^i(\underline{x}, t)p) + \frac{\partial^2}{\partial x^i \partial x^j} (B^{ij}(\underline{x}, t)p) \quad (2.6)$$

for $t \geq s$ (Schuss 1980, p109). This is called the forward Kolmogorov or Fokker-Planck equation for the process $\underline{X}(t)$. For suitable \underline{a} and \underline{b} this

is, as noted above, the usual advection-diffusion equation.

$P_{\underline{X}(t)|\underline{X}(s)}(\underline{x}|\underline{y})$ also satisfies the backward Kolmogorov equation

$$\frac{\partial p}{\partial s} = - a^i(\underline{y}, s) \frac{\partial p}{\partial y^i} - B^{ij}(\underline{y}, s) \frac{\partial^2 p}{\partial y^i \partial y^j} \quad (2.7)$$

for $t \geq s$. This can be derived in the same way as the forward equation starting from the Chapman-Kolmogorov equation in the form

$$P_{\underline{X}(t)|\underline{X}(s)}(\underline{x}|\underline{y}) = \int P_{\underline{X}(t)|\underline{X}(s+\Delta t)}(\underline{x}|\underline{z}) P_{\underline{X}(s+\Delta t)|\underline{X}(s)}(\underline{z}|\underline{y}) d\underline{z}.$$

In addition the unconditional p.d.f. $P_{\underline{X}(t)}(\underline{x})$, which can be expressed as

$$P_{\underline{X}(t)}(\underline{x}) = \int P_{\underline{X}(t)|\underline{X}(0)}(\underline{x}|\underline{y}) P_{\underline{X}(0)}(\underline{y}) d\underline{y},$$

also satisfies (2.6).

Although (2.3) is formally similar to an ordinary differential equation, it cannot be manipulated in all respects in the same way as an ordinary differential equation because the size of the random increment $d\underline{\zeta}$ is of order $(dt)^{1/2}$ and not of order dt . As a result, if $f(\underline{x}, t)$ is a function of \underline{x} and t , the differential of $f(\underline{X}(t), t)$ is given not by the chain rule, but by Itô's formula (Schuss 1980, pp79-80 and 112):

$$df(\underline{X}(t), t) = \left(\frac{\partial f}{\partial t} + a^i(\underline{X}(t), t) \frac{\partial f}{\partial x^i} + B^{ij}(\underline{X}(t), t) \frac{\partial^2 f}{\partial x^i \partial x^j} \right) dt + b^{ij}(\underline{X}(t), t) \frac{\partial f}{\partial x^i} d\underline{\zeta}^j. \quad (2.8)$$

3. MATHEMATICAL FRAMEWORK FOR RANDOM WALK MODELS.

In this chapter the basic fluid dynamic equations and the statistical approach to turbulence are outlined and the mathematical framework which forms the starting point for random walk models is presented.

3.1 Basic Equations

The basic fluid dynamic equations which describe the evolution of the velocity and density fields in a Newtonian fluid are well known. Many derivations can be found in the literature (e.g. Batchelor (1967), Monin and Yaglom (1971) or Libby and Williams (1980)) and so we simply state these equations here. The velocity and density fields, $\underline{u}_e(\underline{x}, t)$ and $\rho(\underline{x}, t)$, satisfy the mass and momentum conservation equations

$$\partial\rho/\partial t = -\nabla\cdot(\rho\underline{u}_e) \quad (3.1)$$

$$D\underline{u}_e/Dt = \underline{F} \quad (3.2)$$

where D/Dt is the material derivative $\partial/\partial t + \underline{u}_e\cdot\nabla$ and $\underline{F}(\underline{x}, t)$ is the net force per unit mass applied to the fluid, either by the fluid itself (e.g. pressure or viscous forces) or by external forces (e.g. gravity). The subscript e in \underline{u}_e is used to indicate the Eulerian velocity field and to distinguish it from the last three coordinates of a point $(\underline{x}, \underline{u})$ in the phase space which will be introduced in §3.3. If the density and viscosity μ of the fluid are constant and the external forces are negligible (or conservative), equation (3.2) takes the form $D\underline{u}_e/Dt = - (1/\rho)\nabla\Pi + \nu\nabla^2\underline{u}_e$ where Π is the (modified) pressure and $\nu = \mu/\rho$ is the kinematic viscosity. Although most of our interest will centre on this case, the consideration of more general situations (in particular variable density flows) is useful, in that it provides some insight into a number of aspects of random walk models.

In this thesis, only the dispersion of passive contaminants (see §1.1) will be considered. The concentration $c(\underline{x}, t)$ of a passive contaminant obeys the equation

$$\partial c / \partial t = - \nabla \cdot (c \underline{u}_e) + \nabla \cdot (\kappa \rho \nabla (c / \rho)) + S \quad (3.3)$$

where $S(\underline{x}, t)$ is the source strength, i.e. the amount of tracer released per unit space-time volume, and κ is the molecular diffusivity which will be assumed constant (Libby and Williams 1980). It will be assumed that the concentration c is zero at the initial time (which will be taken to be $t=0$) and hence that all the contaminant enters the flow via the source strength S and not via the initial conditions. This assumption of course implies no real restriction on the physics, referring to the nature of the mathematical description of the flow and not to the flow itself.

3.2 The Ensemble of Realisations

One does not have to watch a turbulent flow for long to realise that there is little hope of being able to predict the evolution of the flow in detail over a time much in excess of the time-scale of a single eddy. This is because, although the equations governing the flow are deterministic, the solution of these equations is very sensitive to initial and boundary conditions, giving the appearance of randomness. As indicated in §1.1, the usual response to this problem (which will also be followed here) is to abandon any attempt to calculate the evolution of a particular flow and to adopt a statistical approach (see e.g. Batchelor (1953, §§1.1-2.2) or Monin and Yaglom (1971, §§3.2-3.3)).

Suppose one decides on a particular set of external conditions for a turbulence experiment. For example, one might set up a wind tunnel in a particular way, with a turbulence generating grid and a nozzle for releasing contaminant into the flow. Because of the great sensitivity of turbulent flows to the initial conditions, the details of the flow

will not be predictable, no matter how carefully the experiment is prepared. There will however be probabilities associated with various events; for example there will be a certain probability that the concentration c measured at a given space-time point lies in a given range. As a result it is natural to use the language of probability theory to describe a turbulent flow. The velocity \underline{u}_e , density ρ , contaminant concentration c and source strength S are then random fields. Although in many cases the source strength will be deterministic, it is useful to allow it to be random. Such randomness might be caused, for example, by a mechanism for releasing the contaminant in which the release rate depends on the flow properties, or by some other source of randomness in the release mechanism, unrelated to the turbulence. The set or "ensemble" of all possible outcomes or "realisations" of the flow will be denoted by Ω .

In the statistical approach, no attempt is made to predict anything other than the expectations of random variables (or the probabilities associated with random variables, which, as noted in §2.1, contain the same information as the expectations). Such an expectation will often be referred to as an "ensemble average value" or an "average over the ensemble". In principle, if we had sufficient knowledge of the probability distribution of the initial and boundary conditions (and of any probabilistic process within the contaminant release mechanism), then we could calculate such quantities from the equations governing the flow. In practice however such a calculation is, except for some simple low Reynolds number flows for which "direct simulations" (Schumann and Friedrich 1986) can be carried out, beyond the reach of the combined forces of today's mathematical knowledge and computational technology. As a result it is (as noted in §1.2) necessary to use mathematical models which involve assumptions and approximations that cannot be justified rigorously. Ultimately such models can only be justified by comparison with experimental data,

although of course mathematical and physical arguments can play an important role in designing such models. Random walk models of the type to be considered in this thesis are models of this sort. In these models, the values of certain low order statistics of ρ , u_x and S are assumed known and, with these values as input, the random walk model gives predictions for the values of various low order statistics involving the contaminant concentration. In practice the turbulence statistics which are required as input could be obtained from measurements or estimated from turbulence models.

In stationary or homogeneous flows it is often possible to interpret ensemble average values as time or space averages (for time averages this was discussed briefly in §1.1). The required conditions for this to be valid are quite mild and can usually be assumed to be satisfied (Monin and Yaglom 1971, §4.7). This is particularly useful in comparing experimental data, which often take the form of time-averaged quantities, with ensemble average predictions from models.

3.3 Transition Densities

In this section various relations will be given which express statistical quantities involving the contaminant concentration in terms of probabilities associated with the motion of "fluid particles". These relations form the necessary mathematical framework for discussing random walk models. The relations in question (equations (3.4) to (3.7) below) are very natural and indeed, at least in the case of the ensemble mean concentration, almost obvious. As a result we simply present these relations here and give the derivation in Appendix A. Of these relations, (3.4) and (3.6) were originally derived by Batchelor (1949, 1952) for the case of zero molecular diffusivity and the extensions to non-zero diffusivity have been discussed by Egbert and Baker (1984) and Sawford and Hunt (1986).

Before presenting these relations, some discussion of what is meant by "fluid particle" is desirable. Two cases arise corresponding to the presence or absence of molecular diffusion. If $\kappa = 0$, fluid particles are simply points which are advected by the flow velocity \underline{u}_e . If $\kappa > 0$ however, fluid particles will be taken to be molecules of fluid which are advected by \underline{u}_e and also undergo a random molecular motion. It is convenient to use the term fluid particle to cover both cases, although in most of the literature the term fluid particle is used only in the first case. The term "fluid element" will be used when we wish to emphasise that we are considering the case $\kappa = 0$.

Let $\underline{X}(t)$ denote the trajectory of a fluid particle chosen at random from all fluid particles in the ensemble of flows. A discussion of the precise meaning of "a fluid particle chosen at random" is given in Appendix A. Then provided S/ρ is independent of the velocity and density fields,

$$\langle c(\underline{x}, t) \rangle = \int_{s \leq t} P_{\underline{X}(t) | \underline{X}(s)}(\underline{x} | \underline{y}) \langle S(\underline{y}, s) \rangle d\underline{y} ds. \quad (3.4)$$

This expresses $\langle c(\underline{x}, t) \rangle$ in terms of the p.d.f. of the position of fluid particles which were at \underline{y} at time s . The physical interpretation of the assumption that S/ρ is independent of the velocity and density fields is that the source simply "marks" a certain fraction of the fluid particles which pass by, this fraction being independent of the flow.

Because most random walk models take the form of stochastic differential equations for the evolution of the position and velocity of fluid particles, it is useful to obtain a result similar to (3.4) for the distribution of fluid particles in position-velocity (or "phase") space. $g_p(\underline{x}, \underline{u}, t)$ and $g_c(\underline{x}, \underline{u}, t)$ will be used to denote $\langle \rho(\underline{x}, t) \delta(\underline{u} - \underline{u}_e(\underline{x}, t)) \rangle$ and $\langle c(\underline{x}, t) \delta(\underline{u} - \underline{u}_e(\underline{x}, t)) \rangle$ respectively. These are the density- and concentration-weighted velocity p.d.f.s (see §2.1) and

can also be regarded as the phase space mass densities of fluid and contaminant. If $\underline{U}(t)$ denotes the value of the flow velocity \underline{u}_o at the location $\underline{X}(t)$ of the randomly chosen fluid particle, then g_c is given by

$$g_c = \int_{s \leq t} P_{\underline{X}(t), \underline{U}(t) | \underline{X}(s), \underline{U}(s)}(\underline{x}, \underline{u} | \underline{y}, \underline{v}) \times \\ \times g_p(\underline{y}, \underline{v}, s) \langle S(\underline{y}, s) / \rho(\underline{y}, s) \rangle d\underline{v} d\underline{y} ds. \quad (3.5)$$

This equation indicates how the phase space density of tracer particles is related to the source $g_p \langle S/\rho \rangle$ of particles in phase space by the transition density $P_{\underline{X}(t), \underline{U}(t) | \underline{X}(s), \underline{U}(s)}$.

In a similar way, let $\underline{X}_1(t)$ and $\underline{X}_2(t)$ denote the trajectories of a pair of fluid particles chosen at random from all pairs of fluid particles in the ensemble of flows (here a pair of fluid particles means two fluid particles, both belonging to the same realisation). Then, again assuming that S/ρ is independent of the velocity and density fields, $\langle c(\underline{x}_1, t_1) c(\underline{x}_2, t_2) \rangle$ is given by

$$\langle c(\underline{x}_1, t_1) c(\underline{x}_2, t_2) \rangle = \int_{s_1 \leq t_1, s_2 \leq t_2} P_{\underline{X}_1(t_1), \underline{X}_2(t_2) | \underline{X}_1(s_1), \underline{X}_2(s_2)}(\underline{x}_1, \underline{x}_2 | \underline{y}_1, \underline{y}_2) \times \\ \times \langle S(\underline{y}_1, s_1) S(\underline{y}_2, s_2) \rangle d\underline{y}_1 d\underline{y}_2 ds_1 ds_2. \quad (3.6)$$

This expresses the covariance function of c in terms of the joint p.d.f. of the position of the first particle at time t_1 and the position of the second particle at time t_2 , given that the first particle was at \underline{y}_1 at time s_1 and the second was at \underline{y}_2 at time s_2 . If we define \hat{g}_p and \hat{g}_c to be

$$\hat{g}_p(\underline{x}_1, \underline{u}_1, t_1, \underline{x}_2, \underline{u}_2, t_2) = \\ \langle \rho(\underline{x}_1, t_1) \rho(\underline{x}_2, t_2) \delta(\underline{u}_1 - \underline{u}_o(\underline{x}_1, t_1)) \delta(\underline{u}_2 - \underline{u}_o(\underline{x}_2, t_2)) \rangle$$

and

$$\hat{g}_c(\underline{x}_1, \underline{u}_1, t_1, \underline{x}_2, \underline{u}_2, t_2) = \\ \langle c(\underline{x}_1, t_1) c(\underline{x}_2, t_2) \delta(\underline{u}_1 - \underline{u}_o(\underline{x}_1, t_1)) \delta(\underline{u}_2 - \underline{u}_o(\underline{x}_2, t_2)) \rangle,$$

then the phase space analogue of (3.6) is

$$\begin{aligned} \hat{g}_c = & \int_{s \leq t} P_{\underline{X}_1}(t_1), U_1(t_1), \underline{X}_2(t_2), U_2(t_2) | \underline{X}_1(s_1), \dots, U_2(s_2) (\underline{x}_1, \dots, \underline{u}_2 | \underline{y}_1, \dots, \underline{v}_2) \times \\ & \times \hat{g}_\rho(\underline{y}_1, \underline{v}_1, s_1, \underline{y}_2, \underline{v}_2, s_2) \langle S(\underline{y}_1, s_1) S(\underline{y}_2, s_2) / \rho(\underline{y}_1, s_1) \rho(\underline{y}_2, s_2) \rangle \times \\ & \times d\underline{v}_1 d\underline{v}_1 ds_1 d\underline{v}_2 d\underline{v}_2 ds_2, \end{aligned} \quad (3.7)$$

where $U_i(t) = u_{\theta}(\underline{X}_i(t), t)$ for $i=1,2$.

Equations (3.4) to (3.7) enable us to calculate the values of $\langle c(\underline{x}, t) \rangle$, $\langle c(\underline{x}_1, t_1) c(\underline{x}_2, t_2) \rangle$, g_c and \hat{g}_c from models of the motion of particles and particle-pairs. For example, a stochastic model for the evolution of $\underline{X}(t)$ enables $P_{\underline{X}(t) | \underline{X}(s)}$ to be evaluated and hence $\langle c \rangle$ can be found from (3.4). In many cases such models are not amenable to analytic treatment; then $P_{\underline{X}(t) | \underline{X}(s)}$ can be estimated by calculating many sample trajectories numerically. In practice it is often easier to evaluate $\langle c \rangle$ directly by calculating trajectories which have random initial conditions with density proportional to $\langle S(\underline{x}, t) \rangle$.

If the value of $\langle c(\underline{x}, t) \rangle$, $\langle c(\underline{x}_1, t_1) c(\underline{x}_2, t_2) \rangle$, g_c or \hat{g}_c at a specific point (or pair of points) is required, it is often convenient to calculate the trajectories backwards in time from the specified point to the source. The idea of considering reverse trajectories was put forward originally by Corrsin (1952) and first utilised in random walk models by Durbin (1980). It avoids the waste of calculating many forward trajectories which do not pass near the specified point and so do not contribute to the result. $\langle c(\underline{x}, t) \rangle$, $\langle c(\underline{x}_1, t_1) c(\underline{x}_2, t_2) \rangle$, g_c and \hat{g}_c can be expressed in terms of the statistics of backward trajectories by using certain symmetry relations obeyed by the transition densities (see Lundgren (1981) or Egbert and Baker (1984) for the special case of constant density flows). Consider the probability of a fluid particle lying, at time t , in the elemental region $d\underline{x}$ surrounding the point \underline{x} and, at time s , in the region $d\underline{y}$ surrounding the point \underline{y} . This

probability is equal to the probability of it occupying the region $d\mathbf{x}$ at time t given that it occupies $d\mathbf{y}$ at time s - i.e. $P_{\mathbf{X}(t)|\mathbf{X}(s)}(\mathbf{x}|\mathbf{y})d\mathbf{x}$ - multiplied by the probability of it occupying $d\mathbf{y}$ at time s - i.e. $\langle \rho(\mathbf{y},s) \rangle d\mathbf{y}/M$, where M is the total mass of the fluid. Hence the probability equals

$$P_{\mathbf{X}(t)|\mathbf{X}(s)}(\mathbf{x}|\mathbf{y})\langle \rho(\mathbf{y},s) \rangle d\mathbf{x}d\mathbf{y}/M.$$

By symmetry, the probability is also given by

$$P_{\mathbf{X}(s)|\mathbf{X}(t)}(\mathbf{y}|\mathbf{x})\langle \rho(\mathbf{x},t) \rangle d\mathbf{x}d\mathbf{y}/M$$

and so

$$P_{\mathbf{X}(t)|\mathbf{X}(s)}(\mathbf{x}|\mathbf{y})\langle \rho(\mathbf{y},s) \rangle = P_{\mathbf{X}(s)|\mathbf{X}(t)}(\mathbf{y}|\mathbf{x})\langle \rho(\mathbf{x},t) \rangle. \quad (3.8)$$

As a result (3.4) can also be expressed as

$$\frac{\langle c(\mathbf{x},t) \rangle}{\langle \rho(\mathbf{x},t) \rangle} = \int_{s \leq t} P_{\mathbf{X}(s)|\mathbf{X}(t)}(\mathbf{y}|\mathbf{x}) \frac{\langle S(\mathbf{y},s) \rangle}{\langle \rho(\mathbf{y},s) \rangle} d\mathbf{y} ds. \quad (3.9)$$

Similarly, by considering a pair of particles,

$$P_{\mathbf{X}_1(t_1), \mathbf{X}_2(t_2)|\mathbf{X}_1(s_1), \mathbf{X}_2(s_2)}(\mathbf{x}_1, \mathbf{x}_2 | \mathbf{y}_1, \mathbf{y}_2) \langle \rho(\mathbf{y}_1, s_1) \rho(\mathbf{y}_2, s_2) \rangle = \quad (3.10)$$

$$P_{\mathbf{X}_1(s_1), \mathbf{X}_2(s_2)|\mathbf{X}_1(t_1), \mathbf{X}_2(t_2)}(\mathbf{y}_1, \mathbf{y}_2 | \mathbf{x}_1, \mathbf{x}_2) \langle \rho(\mathbf{x}_1, t_1) \rho(\mathbf{x}_2, t_2) \rangle$$

and so, from (3.6), $\langle c(\mathbf{x}_1, t_1) c(\mathbf{x}_2, t_2) \rangle$ can be expressed as

$$\frac{\langle c(\mathbf{x}_1, t_1) c(\mathbf{x}_2, t_2) \rangle}{\langle \rho(\mathbf{x}_1, t_1) \rho(\mathbf{x}_2, t_2) \rangle} = \int_{s_1 \leq t_1, s_2 \leq t_2} P_{\mathbf{X}_1(s_1), \mathbf{X}_2(s_2)|\mathbf{X}_1(t_1), \mathbf{X}_2(t_2)}(\mathbf{y}_1, \mathbf{y}_2 | \mathbf{x}_1, \mathbf{x}_2) \times$$

$$\times \frac{\langle S(\mathbf{y}_1, s_1) S(\mathbf{y}_2, s_2) \rangle}{\langle \rho(\mathbf{y}_1, s_1) \rho(\mathbf{y}_2, s_2) \rangle} d\mathbf{y}_1 d\mathbf{y}_2 ds_1 ds_2. \quad (3.11)$$

Analogous relations also hold in phase space. For example

$$P_{\mathbf{X}(t), \mathbf{U}(t)|\mathbf{X}(s), \mathbf{U}(s)}(\mathbf{x}, \mathbf{u} | \mathbf{y}, \mathbf{v}) g_p(\mathbf{y}, \mathbf{v}, s) = \quad (3.12)$$

$$P_{\mathbf{X}(s), \mathbf{U}(s)|\mathbf{X}(t), \mathbf{U}(t)}(\mathbf{y}, \mathbf{v} | \mathbf{x}, \mathbf{u}) g_p(\mathbf{x}, \mathbf{u}, t)$$

and so g_c can be expressed in terms of the backwards probabilities. A similar result holds for pairs of particles.

Some insight into the way particle-pairs move can be obtained by considering a pair of particles with trajectories $\underline{X}_1(t)$ and $\underline{X}_2(t)$ as a single entity with a trajectory $\hat{\underline{X}}(t) = (\underline{X}_1(t), \underline{X}_2(t))$ in a six-dimensional space. In a single realisation the mass density of contaminant particle-pairs in the six-dimensional space is given by $\hat{c}(\hat{\underline{x}}, t) = c(\underline{x}_1, t)c(\underline{x}_2, t)$ where $\hat{\underline{x}} = (\underline{x}_1, \underline{x}_2)$ while the mass density of fluid particle-pairs is $\hat{\rho}(\hat{\underline{x}}, t) = \rho(\underline{x}_1, t)\rho(\underline{x}_2, t)$. It follows from (3.3) that, away from any sources, \hat{c} evolves according to

$$\partial \hat{c} / \partial t = - \nabla \cdot (\hat{c} \hat{\underline{u}}_e) + \nabla \cdot (\kappa \hat{\rho} \nabla (\hat{c} / \hat{\rho}))$$

where $\hat{\underline{u}}_e(\hat{\underline{x}}, t) = (\underline{u}_e(\underline{x}_1, t), \underline{u}_e(\underline{x}_2, t))$ is the velocity field in the six-dimensional space. Comparison with (3.3) shows that particle-pairs are advected and diffused in the six-dimensional space in the same way that single particles are advected and diffused in three dimensions. Note that the six-dimensional density and velocity fields $\hat{\rho}$ and $\hat{\underline{u}}_e$ are consistent with each other in the sense that they satisfy a "mass conservation" equation which is of the same form as (3.1):

$$\partial \hat{\rho} / \partial t = - \nabla \cdot (\hat{\rho} \hat{\underline{u}}_e).$$

4. THEORETICAL ASPECTS OF ONE-PARTICLE RANDOM WALK MODELS.

In order to make use of the relations derived in §3.3, it is necessary to have a model for the way particles (or pairs of particles) move. In this chapter, models for the motion of single particles are discussed and the way in which such models should be formulated is investigated.

4.1 Introduction to One-particle Models.

For simplicity it will be assumed throughout this chapter that $\kappa = 0$, so that fluid particles are simply advected by the local flow velocity. In justification we note that it is generally thought that molecular diffusion has little effect on ensemble mean concentrations in high Reynolds number flows (Monin and Yaglom 1971, §10.2), although no proof of this has yet been found. This assumption will be discussed in more detail when we consider two-particle models in chapter 5. In this introductory section 4.1 we will assume in addition that the flow is of constant density.

One of the simplest ways of modelling the motion of single particles in a turbulent flow is to assume that the turbulent motions of the particles are similar to the random motions of Brownian particles or molecules. With this assumption, the particle trajectories evolve according to a stochastic differential equation of the form (2.3) and, from (2.6) and (3.4), it can be shown that $\langle c \rangle$ satisfies the equation (2.6) with the addition of a source term $\langle S \rangle$ on the right hand side. Because $\langle c \rangle$ satisfies an advection-diffusion equation, models based on (2.3) are equivalent to the eddy-diffusivity models discussed in §1.3 (this is of course to be expected since both types of model are based on analogies with molecular diffusion) and so suffer from all the problems associated with such models. Some of these problems are associated with the fact (discussed in §2.2) that,

for stochastic differential equations of the form (2.3), the mean square velocity is infinite and uncorrelated in time. While this is not a bad approximation for molecular diffusion or Brownian motion (provided one is not interested in properties of particle motions over very short time intervals), it is not so good for turbulent diffusion which takes place by "continuous movements" (Taylor 1921), i.e. the trajectories of the fluid elements have continuous derivatives.

These problems can be overcome by considering models in which the position and velocity of a particle satisfy a coupled set of stochastic differential equations:

$$dX^i = U^i dt \quad (4.1a)$$

$$dU^i = a^i(\underline{X}(t), \underline{U}(t), t) dt + b^{ij}(\underline{X}(t), \underline{U}(t), t) d\zeta^j. \quad (4.1b)$$

In such a model the velocity of a particle changes continuously in time, while the acceleration has infinite mean square value and is uncorrelated in time. While this is still unphysical, it is not as serious a problem as the uncorrelated velocity in models of the form (2.3). This is because, in high Reynolds number flows, the particle accelerations are very large (relative to integral length- and time-scales) and are only significantly correlated over very short times of the order of the Kolmogorov time-scale τ_η (Monin and Yaglom 1975, pp369-370). In the atmospheric surface layer, τ_η is typically between a tenth and a hundredth of a second. As a result it seems reasonable to hope that a model of the form (4.1) could give a good description of the motion of particles, at least over time intervals in excess of the Kolmogorov time-scale. (Note that, although the changes in velocity over successive intervals Δt , $\Delta t \gg \tau_\eta$, are only weakly correlated, they cannot be completely independent or the variance of the particle velocities would grow indefinitely. Such weak dependencies are represented in the model through the presence of the term $\underline{a}dt$ in (4.1b). This term results in a non-zero covariance between the acceleration at different times, even though, as a result of the

infinite mean square acceleration, the correlation is zero.)

Alternative models for particle motions have been proposed which overcome the worst failings of eddy-diffusivity models, but these tend to be less successful and less physically plausible than those based on (4.1). Examples include models in which the particle velocities can take only a finite number of discrete values with the velocities changing by discrete jumps at random times (Taylor 1921; Monin and Yaglom 1971, §10.6) and models in which the velocities change by random jumps but in which the range of possible velocities is continuous (Smith 1984; Smith and Thomson 1984). The first of these types of models has much in common with high-order closure models (van Stijn and Nieuwstadt 1986).

The first model of the form (4.1) was proposed by Langevin (1908), not in order to model turbulent diffusion, but in order to give a more accurate description of Brownian motion than that given by the Wiener process model described in §2.2 (as noted in §2.2, the Wiener process model is not a good model for Brownian motion over very short time intervals). For simplicity, consider the motion of a particle in one direction only, say the x -direction (here, and also on occasion below, x , y and z will be used instead of x^1 , x^2 and x^3 in order to simplify notation). In Langevin's model, it is assumed that the velocity U of the particle in this direction obeys the stochastic differential equation

$$dU = -\alpha U dt + b d\zeta. \quad (4.2)$$

Equation (4.2) is known as the Langevin equation, and the resulting velocity process is an Uhlenbeck-Ornstein process, or, more precisely, becomes one when scaled so that $\alpha = b = 1$ (Feller 1971, p99). An intuitive interpretation of (4.2) is that over a time interval dt the particle loses a small fraction $\alpha U dt$ of its momentum to the surrounding fluid and in return receives a random impulse $b d\zeta$. It can

easily be seen (see Appendix B) that $U(t)$ is (or, more precisely, can be if the distribution of the initial velocity $U(0)$ is chosen appropriately) a stationary Gaussian process with mean square value $\frac{1}{2}b^2/\alpha$ and correlation function $R(t) = \langle U(s)U(s+t) \rangle / \langle U(s)^2 \rangle = \exp(-\alpha t)$. If (4.2) is to be a reasonable model for the motion of a particle in homogeneous stationary turbulence, α and b should be chosen so that the model velocity process has the correct variance and integral time-scale. This will ensure that the mean square displacement of particles is correct for small and large times (see discussion of Taylor's (1921) result in §1.1). Hence we must set $b^2 = 2\sigma^2/\tau_I$ and $\alpha = 1/\tau_I$ where σ^2 is the Lagrangian velocity variance and τ_I is the Lagrangian integral time-scale $\int_0^\infty R(t)dt$. (Throughout this thesis, τ_I will be used to denote the Lagrangian integral time-scale, while τ will be used to indicate some more general measure of the time-scale on which particle velocities become decorrelated.) For this model, the mean square displacement of particles can be obtained from Taylor's result (1.1) and is equal to

$$\int_0^t \int_0^t \sigma^2 R(t_1 - t_2) dt_1 dt_2 = 2\sigma^2 \tau_I^2 (\exp(-t/\tau_I) - 1 + t/\tau_I).$$

In addition, because of the Gaussianity of the velocity process, the distribution of the displacements is Gaussian (see Appendix B). It follows that at large times the $\langle c \rangle$ distribution is the same as that obtained from an eddy-diffusivity model with $K = \sigma^2 \tau_I$. The model (4.2) for particle motions in homogeneous stationary turbulence has also been discussed by Novikov (1963), Lin and Reid (1963), Jonas and Bartlett (1972) and Durbin (1983), and is closely related to the ideas of Obukhov (1959) and Smith (1968).

For several reasons the Langevin equation model is a plausible model for the motion of a particle in homogeneous stationary turbulence although, as with all turbulence models, a rigorous justification is impossible, at least with the current state of our mathematical

knowledge. Firstly the experimental evidence indicates that the distribution of Eulerian velocities at any single given point is Gaussian to quite high accuracy in homogeneous turbulence (Batchelor 1953, pp169-170; Monin and Yaglom 1971, p540). Because of Lumley's result that Lagrangian and Eulerian velocity distributions are equal in an incompressible homogeneous turbulent flow (see Monin and Yaglom (1971, pp573-574)), it follows that the single time Lagrangian velocity distributions are also Gaussian. Secondly, as noted above, the particle accelerations in high Reynolds number turbulence are only significantly correlated over very short time intervals. Thirdly, the exponential correlation function, although almost certainly not exact, has many features which are qualitatively correct (Tennekes 1979) such as the correct inertial subrange form $1-t/\tau_1+o(t)$ at small times (Monin and Yaglom 1975, pp358-359).

For homogeneous stationary turbulence, Taylor's result (1.1) provides a solid basis for understanding the evolution of $\langle c \rangle$, and random walk models can add only a little to our knowledge. Hence, if random walk models are to make a useful contribution to our understanding, it is important that they can be applied to more complex flows in which the flow properties are non-uniform in space or time (there is of course no equivalent of Taylor's result for general flows). Many of the early attempts to do this were based on an equation of the same form as the Langevin equation (4.2), but with α and b being made functions of position and time in order to reflect the fact that the turbulence properties are not uniform. More precisely, $\frac{1}{2}b^2/\alpha$ was set equal to the local Eulerian (i.e. fixed point) velocity variance $\sigma^2(x)$, while $1/\alpha$ was set equal to an estimate $\tau(x)$ of the "local Lagrangian time-scale", i.e. the time-scale on which the velocities of the particles near x become decorrelated. In addition some of these models dealt with the problem of dispersion in more than one dimension and took account of the presence of a mean velocity in

the flow, possibly varying with position. Among such models are those considered by Hall (1975), Reid (1979), Wilson, Thurtell and Kidd (1981a), Ley (1982) and Legg (1983).

In many of the situations to which these models were applied, results were obtained which showed quite good agreement, both qualitatively and quantitatively, with experimental data. This is in spite of the fact that there is no justification for simply setting α and b equal to local values. For example, the Eulerian velocity variance σ^2 at a given point is not, in general, equal to the velocity variance of particles of contaminant passing the point in question. This is because the concentration of contaminant particles at the point will vary from realisation to realisation and so the set of contaminant particles passing the given point is not a representative sample of all fluid particles passing the point. It follows that the velocities of these particles will not necessarily be a representative sample of the velocities of all particles passing the point and so will not be a representative sample of Eulerian velocities at the point. (This line of reasoning is due in essence to Batchelor (1964), who pointed out that the Eulerian mean velocity is not in general equal to the mean velocity of contaminant particles.) Also, the velocity of a particle moving according to (4.2) depends on the values of α and b at all points along its path. Hence there is no reason to expect the velocity variance of model particles passing a fixed point to equal $\frac{1}{2}b^2/\alpha$.

However in situations where the Eulerian velocity variance varies significantly with position, the results obtained were far from satisfactory, with the particles accumulating unphysically in regions where σ^2 was small (e.g. Janicke (1983)). The reason for this can be seen by considering a situation where the profile of $\langle c \rangle$ is initially uniform. Consider a particle moving according to (4.2) with α and b chosen as indicated above. The velocity of such a particle depends on

the values of σ^2 at all points along its path, the magnitude of the velocity being in general larger the larger σ^2 is. It follows that the velocity of particles arriving at a given point from a region where σ^2 is large will be moving faster than those arriving from a region where σ^2 is small. Hence there will be a net flux of particles into the region where σ^2 is small, leading to a non-uniform $\langle c \rangle$ profile.

A large number of models have been tried in attempting to overcome this problem (Wilson, Thurtell and Kidd 1981b; Legg and Raupach 1982; Janicke 1983; Runca, Bonino and Posch 1983; Ley and Thomson 1983; Wilson, Legg and Thomson 1983; Thomson 1984; van Dop, Nieuwstadt and Hunt 1985). It does not seem appropriate to review all of these approaches in detail here - instead we will outline the main ideas involved. Legg and Raupach (1982), Runca et al (1983) and Ley and Thomson (1983) noticed that, when the velocity variance varies with position, the particles passing through a particular point have a non-zero mean acceleration even if the mean Eulerian velocity is zero everywhere. For example, suppose the mean velocity is zero and the turbulence is stationary and homogeneous in the y- and z-directions. Now consider the motion of particles in the x-direction and suppose the fixed point variance of the x-component of velocity (to be denoted by σ^2) varies with x. Then the mean acceleration in the x-direction of particles passing a given point is equal to

$$\langle Du_e^1/Dt \rangle = \langle \partial u_e^1/\partial t \rangle + \langle \nabla \cdot (\underline{u}_e u_e^1) \rangle = \partial \sigma^2/\partial x$$

(here u_e^1 indicates the first component of the Eulerian velocity \underline{u}_e and we have used the fact that the flow is of constant density, i.e. $\nabla \cdot \underline{u}_e = 0$). Legg and Raupach (1982), Runca et al (1983) and Ley and Thomson (1983) added this mean acceleration to the right hand side of the Langevin equation to obtain

$$dU = (-U/\tau + \partial \sigma^2/\partial x) dt + (2\sigma^2/\tau)^{1/2} d\zeta.$$

Although this model reduces the extent of particle accumulation, it does not always remove it entirely, especially if the variation of σ^2

is rapid (Wilson et al 1983).

Concurrently with these ideas, a number of papers appeared in which attempts were made to force the random walk model to yield a uniform steady state $\langle c \rangle$ profile by modifying the Langevin equation appropriately (Wilson et al 1981b; Janicke 1983; Thomson 1984). Janicke (1983) and Thomson (1984) in fact required somewhat stronger conditions to be satisfied, with the strongest condition (that proposed by Thomson (1984)) being that, if $g_c = g_p$ at some time, then g_c should remain equal to g_p at all subsequent times (g_p being assumed known), i.e. if the particles are well-mixed in phase space they should remain so. We will call this the well-mixed condition. Somewhat surprisingly this approach led to the use of a non-zero mean acceleration equal to that used by Legg and Raupach. The approach also indicated the need for a number of more subtle modifications of the Langevin equation, although it was not clear what form these modifications should take. The suggestions of Thomson (1984) included changing the moments of $d\zeta$ and, following Wilson et al (1981b), using a Langevin equation for U/σ instead of for U . The need for such modifications was also demonstrated by van Dop et al (1985) by considering $\langle D(u_0^1)^2/Dt \rangle$ and higher order quantities in the same way that Legg and Raupach had considered $\langle Du_0^1/Dt \rangle$. Again it is somewhat surprising that the two different approaches (i.e. insisting on a well-mixed steady state and considering the small time behaviour of the moments of velocity) lead to similar results.

Although in many situations the approaches of Thomson (1984) and van Dop et al (1985) (see also Sawford (1986)) yield models which show little sign of an unnatural accumulation of particles, there are still some unsatisfactory features in these approaches. In particular, although these approaches yield a number of constraints on the form of the model, there are situations in which no model (of the type

considered by Thomson or van Dop et al) satisfies the constraints. For example, the models of Thomson (1984) and van Dop et al (1985) sometimes require the random term in the equation for U to have negative variance (de Baas et al 1986)! The reason for these problems is that the models considered were the wrong sort of generalisations of the Langevin equation. For example, in Thomson (1984), an attempt was made to construct a process which is more general than that given by (4.2) but which still looks locally like a process with independent increments, by generalising the random forcing $d\zeta$ in (4.2) and allowing it to have a non-Gaussian distribution. This is inadmissible because of the result quoted in §2.2 - if a process has continuous sample paths and looks locally like a process with independent increments, then the infinitesimal increments must be Gaussian. As a result the model considered by Thomson (1984) is, in general, either non-existent (in the sense that no random process ζ exists which has increments $d\zeta$ with the required moments) or has discontinuous trajectories. Consider for example an inhomogeneous flow in which the fixed point velocity distribution is Gaussian. For this situation the model in question requires the first three moments of the random increment $d\zeta$ to be $O(dt)$ with higher moments $o(dt)$. Now any random variable X must satisfy $(\overline{X^3})^2 \leq \overline{X^2} \overline{X^4}$ (Feller 1971, p152). Hence there is no random forcing with the required moments. As mentioned above, the situation can be even worse in some cases, with the model requiring increments with negative variance. Of course in some cases such models can be implemented in an approximate form, and this has been done with successful results by a number of authors (Thomson 1984; de Baas et al 1986; Sawford and Guest 1987; Brière 1987). However this approach is rather unsatisfactory mathematically and it is difficult to estimate theoretically the effect of such approximations.

In order to overcome these problems we will consider general models of the form (4.1) and investigate in §4.2 the constraints on \underline{a} and \underline{b} which are needed to ensure that the model satisfies the well-mixed condition. It turns out that the model (4.1) is sufficiently general to ensure that satisfying the well-mixed condition is always possible. We will also consider various other constraints which are satisfied in reality and which we would like random walk models to obey. Firstly there is the condition (discussed above) that the velocity distribution of particles from a point source should evolve correctly at small times (van Dop et al 1985). Secondly the model should be consistent with the Eulerian equations (3.1), (3.2) and (3.3) in the sense discussed by van Dop et al (1985) (complete consistency with these equations would imply the model is exact, which is rather too much to ask for!). Thirdly, the model should satisfy the exact result (3.12) which relates the forward and backward transition probabilities. This type of constraint was originally put forward by Egbert and Baker (1984) in the context of two-particle models, although in a somewhat weaker form (Egbert and Baker only considered the two-particle equivalent of (3.8), i.e. (3.10), and not the two-particle equivalent of (3.12)). Finally we will consider the constraint proposed by Durbin (1983, 1984), who suggested that random walk models should be designed so that they reduce to an eddy-diffusivity model as the Lagrangian time-scale tends to zero. It will be shown that the first three of these conditions actually provide the same constraints on the form of the model as the well-mixed condition, explaining the somewhat surprising similarity, noted above, between models which were designed to satisfy the well-mixed condition and models designed to give the correct small time behaviour. It will also be shown that Durbin's (1983, 1984) condition is strictly weaker. Although these conditions provide strong constraints on the form of the model, they do not determine it completely. Various ways of reducing the remaining

indeterminacy are discussed in §4.3.

4.2 Some Criteria for the Selection of Random Walk Models.

(i) Some properties of the model (4.1).

Before discussing the various constraints on the formulation of random walk models described above, it is useful to summarize the results on stochastic differential equations obtained in §2.3, as they apply to the system (4.1). In discussing physical interpretations of (2.3) we concentrated, for obvious reasons, on the case where $\underline{X}(t)$ is a three-dimensional vector. However, the analysis in §2.3 applies quite generally to processes in any finite number of dimensions. Now the system (4.1) can be regarded as a six-dimensional version, and hence a special case, of (2.3), and so the results obtained in §2.3 can be applied to (4.1). It follows that $P_{\underline{X}(t), \underline{U}(t) | \underline{X}(s), \underline{U}(s)}$ satisfies the forward and backward Kolmogorov equations appropriate to the system (4.1), namely

$$\frac{\partial p}{\partial t} = - \frac{\partial}{\partial x^i} (u^i p) - \frac{\partial}{\partial u^i} (a^i(\underline{x}, \underline{u}, t) p) + \frac{\partial^2}{\partial u^i \partial u^j} (B^{ij}(\underline{x}, \underline{u}, t) p) \quad (4.3)$$

and

$$\frac{\partial p}{\partial s} = - v^i \frac{\partial p}{\partial y^i} - a^i(\underline{y}, \underline{v}, s) \frac{\partial p}{\partial v^i} - B^{ij}(\underline{y}, \underline{v}, s) \frac{\partial^2 p}{\partial v^i \partial v^j}, \quad (4.4)$$

for $t \geq s$. Here $B^{ij} = \frac{1}{2} b^{ik} b^{jk}$ as in §2.3. Note that although \underline{B} does not determine \underline{b} , knowledge of \underline{a} and \underline{B} is sufficient to determine all statistics of the motion of the model particles. Also, away from any sources of contaminant, $g_c(\underline{x}, \underline{u}, t)$ satisfies (4.3), expressing the fact that the flux of contaminant in the x^i -direction, $u^i g_c$, and that in the u^i -direction, $a^i g_c - \partial(B^{ij} g_c) / \partial u^j$, together balance the rate of change of the phase space density g_c . Equation (4.3) can be written in the form

$$\frac{\partial p}{\partial t} = - \frac{\partial}{\partial x^i} (u^i p) + \psi_{\underline{X}}(p) \quad (4.5)$$

where, for fixed \underline{x} , $\psi_{\underline{x}}$ is a linear operator which maps p (considered as a function of \underline{u}) to a new function $\psi_{\underline{x}}(p)$ of \underline{u} . For many of the arguments given below it is only assumed that the evolution equations for p and g_c have the form (4.5). A consequence of this is that many of the results obtained below on the relationships between the different constraints are applicable to more general models than (4.1), such as the models with non-Gaussian forcing discussed above (when they exist) and the models of the type presented by Smith (1984) (see also Smith and Thomson (1984)). In Smith's model the particle velocities do not change continuously but in discrete jumps which occur at random times.

As noted in §2.3, if $f(\underline{x}, \underline{u}, t)$ is a function of \underline{x} , \underline{u} and t , then the differential of $f(\underline{X}(t), \underline{U}(t), t)$ is given, not by the chain rule, but by Itô's formula. For the model (4.1), this takes the form

$$df(\underline{X}(t), \underline{U}(t), t) = \left(\frac{\partial f}{\partial t} + u^i \frac{\partial f}{\partial x^i} + a^i(\underline{X}(t), \underline{U}(t), t) \frac{\partial f}{\partial u^i} + B^{ij}(\underline{X}(t), \underline{U}(t), t) \frac{\partial^2 f}{\partial u^i \partial u^j} \right) dt + b^{ij}(\underline{X}(t), \underline{U}(t), t) \frac{\partial f}{\partial u^i} d\zeta^j. \quad (4.6)$$

Some of the arguments which follow are more easily expressed in terms of the characteristic functions (Feller 1971, chapter 15) of g_c and g_p than in terms of g_c and g_p themselves. These characteristic functions will be denoted by $\tilde{\cdot}$, i.e. $\tilde{g}_c(\underline{x}, \underline{\theta}, t) = \int g_c(\underline{x}, \underline{u}, t) \exp(i\underline{u} \cdot \underline{\theta}) d\underline{u}$ and $\tilde{g}_p(\underline{x}, \underline{\theta}, t) = \int g_p(\underline{x}, \underline{u}, t) \exp(i\underline{u} \cdot \underline{\theta}) d\underline{u}$. Note that, using the definitions of g_c and g_p given in §3.3, \tilde{g}_c and \tilde{g}_p can be expressed as $\tilde{g}_c = \langle c \exp(i\underline{u}_e \cdot \underline{\theta}) \rangle$ and $\tilde{g}_p = \langle p \exp(i\underline{u}_e \cdot \underline{\theta}) \rangle$. In terms of characteristic functions, the evolution equation for g_c can be expressed as

$$\frac{\partial \tilde{g}_c}{\partial t} = i \frac{\partial^2 \tilde{g}_c}{\partial x^i \partial \theta^i} + \tilde{\psi}_{\underline{x}}(\tilde{g}_c) \quad (4.7)$$

where $\tilde{\psi}_{\underline{x}}$ maps \tilde{g}_c to $\int \psi_{\underline{x}}(g_c) \exp(i\underline{u} \cdot \underline{\theta}) d\underline{u}$.

In the following \underline{U}_e will be used to denote the density-weighted mean Eulerian velocity while \underline{V}_e will denote the density-weighted covariance matrix of the velocity components at a fixed point, i.e. $\underline{U}_e = \langle \rho \underline{u}_e \rangle / \langle \rho \rangle$ and $V_e^{ij} = \langle \rho (u_e^i - U_e^i)(u_e^j - U_e^j) \rangle / \langle \rho \rangle$. In isotropic turbulence, σ^2 will be used to indicate the (density-weighted) variance of any one component of the velocity at a fixed point. We will often have cause to consider situations where the density-weighted velocity distribution at any point is Gaussian. In such situations, which we will call Gaussian turbulence, g_p takes the form

$$g_p = \frac{\langle \rho \rangle}{(2\pi)^{3/2} (\det \underline{V}_e)^{1/2}} \exp\{-\frac{1}{2} (u^i - U_e^i) (\underline{V}_e^{-1})^{ij} (u^j - U_e^j)\}.$$

There are a number of situations (e.g. in the atmospheric boundary layer) where the flow is homogeneous (or approximately homogeneous) in directions parallel to a certain plane. Often the main interest is then in dispersion in the direction perpendicular to the plane, which will be taken to be the x-direction. In such situations, it seems reasonable to assume that a one-dimensional model in which $X^1(t)$ and $U^1(t)$ evolve according to a coupled pair of stochastic differential equations will provide a reasonable model of the dispersion. This assumption is in the same spirit as the assumption that the three-dimensional displacement and velocity can be modelled by equations of the form (4.1). However, as an assumption about the evolution of $X^1(t)$ and $U^1(t)$ it is slightly stronger, since it implies that a^1 and B^{11} in (4.1) do not depend on U^2 or U^3 . (Of course it also implies that a^1 and B^{11} do not depend on X^2 or X^3 , but this follows from the assumed homogeneity in the x^2 - and x^3 -directions.) In such situations, as in the discussion of the Langevin equation in §4.1, quantities such as X^1 , U^1 , x^1 and u^1 will be written as scalar quantities X , U , x and u to reflect the fact that we are considering a

one-dimensional situation and the equivalents of \underline{a} , \underline{b} and \underline{B} for our pair of scalar stochastic differential equations will be written as a , b and B . Also σ^2 will be used to indicate the (density-weighted) variance of the x -component of velocity at a fixed point. \underline{u}_e will however always be written as a vector as a reminder of the fact that the turbulent velocity field is always three-dimensional even if the flow statistics depend on one coordinate only. In addition, $g_p(x, u, t)$ and $g_c(x, u, t)$ will be used to denote the density- and concentration-weighted p.d.f.s of u_e^1 , averaged or integrated as appropriate in the x^2 - and x^3 -directions. $g_p(x, u, t)$ and $g_c(x, u, t)$ can also be regarded as the densities of the distributions of $X(t)$ and $U(t)$ for fluid and contaminant particles respectively.

For some of the arguments which follow it is necessary to make a mild assumption about the behaviour of g_c and g_p as $|\underline{u}| \rightarrow \infty$. Consider an expression consisting of g_c , g_p or a derivative of g_c or g_p , multiplied by a number of terms, each term being a component of \underline{u} , \underline{a} , \underline{B} or a derivative of \underline{a} or \underline{B} . It is assumed that g_c and g_p tend to zero sufficiently rapidly as $|\underline{u}| \rightarrow \infty$ so that the integral of the expression over \underline{u} -space exists.

(ii) The well-mixed condition.

The well-mixed condition requires that, if the initial phase space distribution of contaminant is proportional to the distribution of fluid, then it should remain so (provided of course that there are no sources of contaminant subsequent to the initial time). In mathematical terms this means that g_p should satisfy (4.3) when substituted for p . This leads to the condition

$$a^i g_p = \frac{\partial}{\partial u^j} (B^{ij} g_p) + \phi^i \quad (4.8)$$

where ϕ^i is a function of \underline{x} , \underline{u} and t which satisfies

$$\frac{\partial \phi^i}{\partial u^i} = - \frac{\partial g_p}{\partial t} - \frac{\partial}{\partial x^i} (u^i g_p). \quad (4.9)$$

Note that, from (4.9) and the assumptions about g_p discussed at the end of §4.2(i), it follows that the integral over \underline{u} -space of a component of ϕ times various components of \underline{u} , \underline{a} , \underline{B} and their derivatives must exist. In particular $\phi \rightarrow 0$ as $|\underline{u}| \rightarrow \infty$. It is always possible to choose \underline{a} , \underline{B} and ϕ to satisfy these equations. For example, ϕ can be chosen to satisfy (4.9), \underline{B} chosen to be any covariance matrix, and then \underline{a}^i set equal to the right hand side of (4.8) divided by g_p . Hence a random walk model of the form (4.1) can always be made to satisfy the well-mixed condition, no matter what form g_p takes. In terms of $\tilde{\psi}$, the well-mixed condition can be expressed as

$$\frac{\partial \tilde{g}_p}{\partial t} = i \frac{\partial^2 \tilde{g}_p}{\partial x^i \partial \theta^i} + \tilde{\psi}_{\underline{x}}(\tilde{g}_p). \quad (4.10)$$

(iii) The small time behaviour of the velocity distribution of particles.

Consider now the behaviour of the velocity distribution of particles from an instantaneous point source located at (\underline{x}_s, t_s) . The p.d.f. of the velocity of these particles will be denoted by $h(\underline{u}, t)$. Now g_c is the mass density of contaminant particles in phase space. Hence $g_c(\underline{x}, \underline{u}, t) / \int \langle c(\underline{x}, t) \rangle d\underline{x}$ is the p.d.f. of the position and velocity of contaminant particles and so $h(\underline{u}, t) = \int g_c(\underline{x}, \underline{u}, t) d\underline{x} / \int \langle c(\underline{x}, t) \rangle d\underline{x}$. Integrating (4.7) with respect to \underline{x} and noting that $\int \langle c(\underline{x}, t) \rangle d\underline{x}$ is independent of t yields

$$\left(\int \langle c \rangle d\underline{x} \right) \frac{\partial \tilde{h}}{\partial t} = \int \tilde{\psi}_{\underline{x}}(\tilde{g}_c) d\underline{x}$$

where $\tilde{h}(\underline{\theta}, t)$ denotes $\int h(\underline{u}, t) \exp(i\underline{u} \cdot \underline{\theta}) d\underline{u}$. At $t = t_s$, \tilde{g}_c is zero except at $\underline{x} = \underline{x}_s$, and so $\tilde{\psi}_{\underline{x}}$ can be replaced by $\tilde{\psi}_{\underline{x}_s}$. Hence, using the linearity of $\tilde{\psi}_{\underline{x}_s}$,

$$\left(\frac{\partial \tilde{h}}{\partial t}\right)_{t_s} = \tilde{\psi}_{\underline{x}_s}(\tilde{h}(\underline{\theta}, t_s)),$$

the subscript t_s indicating that the derivative is evaluated at time t_s . Initially h is identical to the velocity distribution of fluid particles at the source and so $\tilde{h}(\underline{\theta}, t_s) = \tilde{g}_\rho(\underline{x}_s, \underline{\theta}, t_s) / \langle \rho(\underline{x}_s, t_s) \rangle$. Hence, using again the linearity of $\tilde{\psi}_{\underline{x}_s}$,

$$\left(\frac{\partial \tilde{h}}{\partial t}\right)_{t_s} = \frac{\tilde{\psi}_{\underline{x}_s}(\tilde{g}_\rho(\underline{x}_s, \underline{\theta}, t_s))}{\langle \rho(\underline{x}_s, t_s) \rangle}. \quad (4.11)$$

At small times however we can calculate the true behaviour of the velocity distribution of contaminant particles. From (3.1), (3.2) and (3.3) it follows that

$$\left(\frac{\partial}{\partial t} - i \frac{\partial^2}{\partial x^i \partial \theta^i}\right)(c \exp(i\underline{u}_e \cdot \underline{\theta})) = i c \exp(i\underline{u}_e \cdot \underline{\theta}) \underline{\theta} \cdot \frac{D\underline{u}_e}{Dt}$$

and

$$\left(\frac{\partial}{\partial t} - i \frac{\partial^2}{\partial x^i \partial \theta^i}\right)(\rho \exp(i\underline{u}_e \cdot \underline{\theta})) = i \rho \exp(i\underline{u}_e \cdot \underline{\theta}) \underline{\theta} \cdot \frac{D\underline{u}_e}{Dt}.$$

Taking the ensemble average yields

$$\left(\frac{\partial}{\partial t} - i \frac{\partial^2}{\partial x^i \partial \theta^i}\right) \tilde{g}_c = i \langle c \exp(i\underline{u}_e \cdot \underline{\theta}) \underline{\theta} \cdot \frac{D\underline{u}_e}{Dt} \rangle \quad (4.12)$$

and

$$\left(\frac{\partial}{\partial t} - i \frac{\partial^2}{\partial x^i \partial \theta^i}\right) \tilde{g}_\rho = i \langle \rho \exp(i\underline{u}_e \cdot \underline{\theta}) \underline{\theta} \cdot \frac{D\underline{u}_e}{Dt} \rangle. \quad (4.13)$$

By integrating (4.12) with respect to \underline{x} it can be seen that

$$\left(\int \langle c \rangle d\underline{x}\right) \left(\frac{\partial \tilde{h}}{\partial t}\right)_{t_s} = i \langle \int c d\underline{x} \exp(i\underline{u}_e \cdot \underline{\theta}) \underline{\theta} \cdot \frac{D\underline{u}_e}{Dt} \rangle (\underline{x}_s, t_s).$$

However the amount of material released in any realisation (i.e. $\int c d\underline{x}$) is proportional to the value of ρ at the source (see §3.3 and Appendix A) and so, using (4.13), we obtain

$$\left(\frac{\partial \tilde{h}}{\partial t}\right)_{t_s} = \frac{1}{\langle \rho(\underline{x}_s, t_s) \rangle} \left(\frac{\partial \tilde{g}_\rho}{\partial t} - i \frac{\partial^2 \tilde{g}_\rho}{\partial x^i \partial \theta^i}\right) (\underline{x}_s, t_s). \quad (4.14)$$

Comparing (4.11) and (4.14) shows that for the velocity distribution of particles from a point source to behave correctly at small times, it is necessary and sufficient that

$$\frac{\partial \tilde{g}_\rho}{\partial t} = i \frac{\partial^2 \tilde{g}_\rho}{\partial x^i \partial \theta^i} + \tilde{\psi}_{\underline{x}}(\tilde{g}_\rho)$$

at the source. Hence we see that requiring the correct small time behaviour of the velocity distribution of particles from a point source is equivalent to the well-mixed condition (4.10).

- (iv) The requirement of compatibility with the Eulerian equations, and the relation between random walk and high-order closure models.

As noted in (iii) above, it is possible to derive equations for \tilde{g}_c and \tilde{g}_ρ (namely (4.12) and (4.13)) from the fundamental equations (3.1), (3.2) and (3.3). Unfortunately, there is no random walk model of the form (4.1) for which the evolution equation (4.7) takes the form (4.12). This is because (4.12) contains terms involving $Du_{\underline{e}}/Dt$ which cannot in general be expressed exactly in terms of \tilde{g}_c and \tilde{g}_ρ . However a random walk model can produce an evolution equation of the same form as (4.12) with the right hand side of (4.12) being parametrized in terms of \tilde{g}_c and \tilde{g}_ρ . Comparing (4.7) and (4.12) shows that, for a random walk model of the form (4.1), the parametrization of the right hand side of (4.12) is given by

$$i \langle c \exp(iu_{\underline{e}} \cdot \underline{\theta}) \underline{\theta} \cdot \frac{Du_{\underline{e}}}{Dt} \rangle = \tilde{\psi}_{\underline{x}}(\tilde{g}_c). \quad (4.15)$$

Although the parametrizations corresponding to some models will clearly be better than those corresponding to others, there is only one obvious constraint which the exact equations (4.12) and (4.13) impose on the parametrization. If $c = \rho$ in each realisation, then $\tilde{g}_c = \tilde{g}_\rho$ and the right hand side of (4.12) equals the left hand side of (4.13). If the parametrization of the right hand side of (4.12) is also to have this

property, then

$$\left(\frac{\partial}{\partial t} - i \frac{\partial^2}{\partial x^i \partial \theta^i} \right) \tilde{g}_p = \tilde{\psi}_x(\tilde{g}_p) \quad (4.16)$$

must be satisfied. This is simply the well-mixed condition. If we regard the model as being "compatible" with the Eulerian equations whenever the parametrization satisfies (4.16), then the model is compatible with the Eulerian equations if and only if the well-mixed condition is satisfied. Of course the possibility that (4.12) and (4.13) imply other more subtle constraints cannot be ruled out - to be completely consistent with (4.12) and (4.13) there must exist an ensemble of velocity and density fields satisfying (3.1) for which the model (4.1) is exact - see §4.2(vii) below.

The equations (3.1), (3.2) and (3.3) give rise to an infinite sequence of equations for the evolution of the moments $\langle cu_e^i \dots u_e^m \rangle$ and $\langle \rho u_e^i \dots u_e^m \rangle$. These equations contain the same information that we have expressed more compactly in equations (4.12) and (4.13) by using characteristic functions. By differentiating (4.12) successively with respect to $\theta^i, \dots, \theta^m$, and setting θ equal to zero, we can obtain the equation for $\langle cu_e^i \dots u_e^m \rangle$. The left hand side of this equation takes the form

$$\frac{\partial}{\partial t} \langle cu_e^i \dots u_e^m \rangle + \frac{\partial}{\partial x^n} \langle cu_e^i \dots u_e^m u_e^n \rangle$$

while the right hand side contains the terms involving Du_e/Dt . In high order closure models of turbulent dispersion (e.g. Deardorff (1978)) the first few equations in this infinite sequence are used with suitable parametrizations for the unknown terms. As in random walk models, it is necessary in such models to parametrize the terms involving Du_e/Dt . In high-order closure models however, some terms of the form $\partial \langle cu_e^i \dots u_e^m u_e^n \rangle / \partial x^n$ have also to be parametrized, in order to obtain a closed set of equations. This is a consequence of the fact that high-order closure models describe only a finite number of the low

order concentration-weighted velocity moments $\langle cu_e^1 \dots u_e^m \rangle$ instead of the entire concentration-weighted velocity p.d.f. g_c , and so need to parametrize some effects which are represented explicitly in random walk models.

By expressing $\tilde{\psi}$ in terms of \underline{a} and \underline{B} and using (4.15), it can be seen that the parametrization (4.15) can be expressed as

$$i \langle c \exp(i\underline{u}_e \cdot \underline{\theta}) \underline{\theta} \cdot \frac{D\underline{u}_e}{Dt} \rangle = \int \left(- \frac{\partial}{\partial u^i} (a^i g_c) + \frac{\partial^2}{\partial u^i \partial u^j} (B^{ij} g_c) \right) \exp(i\underline{u}_e \cdot \underline{\theta}) d\underline{u}$$

$$= i \theta^i \langle ca^i(\underline{x}, \underline{u}_e, t) \exp(i\underline{u}_e \cdot \underline{\theta}) \rangle - \theta^i \theta^j \langle c B^{ij}(\underline{x}, \underline{u}_e, t) \exp(i\underline{u}_e \cdot \underline{\theta}) \rangle \quad (4.17)$$

By noting that $i \langle c \exp(i\underline{u}_e \cdot \underline{\theta}) \underline{\theta} \cdot D\underline{u}_e / Dt \rangle$ is equal to $\langle c \rangle$ times the average value of $d(\exp(i\underline{u}(t) \cdot \underline{\theta})) / dt$ for particles of tracer at \underline{x} , Itô's formula for (4.1) can be used to derive (4.17) directly. The first two moments of this parametrization are given by

$$\langle c (Du_e^i / Dt) \rangle = \langle ca^i \rangle$$

$$\langle c (u_e^i (Du_e^j / Dt) + u_e^j (Du_e^i / Dt)) \rangle = \langle c (u_e^i a^j + u_e^j a^i) \rangle + 2 \langle c B^{ij} \rangle.$$

Now, if the model does satisfy the condition (4.16), it follows that the two equations above are also satisfied with c replaced by ρ or, neglecting variations in ρ , by unity. Hence, if we neglect variations in ρ , the first two moments of the parametrization can be expressed as

$$\langle c' (Du_e^i / Dt)' \rangle = \langle c' a^i' \rangle \quad (4.18a)$$

$$\langle c' (u_e^i' (Du_e^j / Dt)' + u_e^j' (Du_e^i / Dt)') \rangle =$$

$$= \langle c' (u_e^i' a^j' + u_e^j' a^i') \rangle + 2 \langle c' B^{ij}' \rangle \quad (4.18b)$$

where a prime denotes the departure of a quantity from its ensemble average. Examples of the parametrizations which arise in specific cases will be discussed in §4.4 and related to the parametrizations occurring in high order closure models.

(v) Forward and Reverse Dispersion.

It was shown in §3.3 that, in reality, $P_{\underline{X}(t), \underline{U}(t) | \underline{X}(s), \underline{U}(s)}$ and g_p satisfy

$$P_{\underline{X}(t), \underline{U}(t) | \underline{X}(s), \underline{U}(s)}(\underline{x}, \underline{u} | \underline{y}, \underline{v}) g_p(\underline{y}, \underline{v}, s) = P_{\underline{X}(s), \underline{U}(s) | \underline{X}(t), \underline{U}(t)}(\underline{y}, \underline{v} | \underline{x}, \underline{u}) g_p(\underline{x}, \underline{u}, t). \quad (4.19)$$

For $t > s$, $P_{\underline{X}(t), \underline{U}(t) | \underline{X}(s), \underline{U}(s)}(\underline{x}, \underline{u} | \underline{y}, \underline{v})$ can be calculated from the model (4.1), it being simply the p.d.f. of the positions and velocities of fluid particles which commence at $(\underline{y}, \underline{v})$ at time s . In principle, the quantity $P_{\underline{X}(s), \underline{U}(s) | \underline{X}(t), \underline{U}(t)}(\underline{y}, \underline{v} | \underline{x}, \underline{u})$ could also be calculated from the model (again for $t > s$) by considering all trajectories resulting from a well-mixed distribution of particles (i.e. a distribution with phase space density function proportional to g_p) at time s , and then noting the position and velocity at time s of those trajectories which pass through $(\underline{x}, \underline{u})$ at time t . It seems reasonable to propose that the values of p obtained in this way should satisfy (4.19) if the model is to be acceptable. In fact it is easy to see that this requirement is equivalent to the well-mixed condition. Suppose the well-mixed condition is satisfied and consider all model trajectories resulting from a well-mixed distribution of particles at time s . Then the argument given in §3.3 which leads to (4.19) applies equally well to the model trajectories and so (4.19) is satisfied. Conversely, if (4.19) is satisfied, the integral of the left hand side of (4.19) with respect to \underline{y} and \underline{v} is proportional to the phase space density of tracer at time t resulting from a well-mixed distribution at time s , and the integral of the right hand side is equal to $g_p(\underline{x}, \underline{u}, t)$. Hence the well-mixed condition is satisfied.

As an aside from the main theme of this section (namely the investigation and comparison of various exact results which we would like random walk models to satisfy), it is of some interest to see if there is a way of calculating $P_{\underline{X}(s), \underline{U}(s) | \underline{X}(t), \underline{U}(t)}(\underline{y}, \underline{v} | \underline{x}, \underline{u})$ for $t > s$

from the model that is simpler than that given above. For example, consider a situation with an extended source distribution $S(\underline{x})$ and suppose that we are only interested in the value of $\langle c \rangle$ at a particular space-time point. In such a situation it is, as noted in §3.3, wasteful to calculate many forward trajectories, only a few of which will pass through the point. The obvious approach is to try to simulate the motion of particles backwards in time. In order to do this, we need a random walk model of the backwards trajectories of particles which will yield the same results as the forwards model. However it is not immediately obvious how such a model should be formulated. We will now investigate this.

Let us set $t' = -t$ and $\underline{u}' = -\underline{u}$ (for this section only) so that t' increases as we go back in time and denote the stochastic differential equation which we hope will describe the backward trajectories by

$$d\underline{X}' = \underline{U}' dt' \quad (4.20a)$$

$$dU'^i = a'^i(\underline{X}'(t'), \underline{U}'(t'), t') dt' + b'^{ij}(\underline{X}'(t'), \underline{U}'(t'), t') d\zeta^j. \quad (4.20b)$$

To simplify notation let $\hat{a}^i(\underline{x}, \underline{u}, t) = (1/g_p) \partial(B^{ij} g_p) / \partial u^j$. Then $\underline{a} = \hat{\underline{a}} + \underline{\phi}/g_p$. Using (4.4), (4.8), (4.9) and (4.19) it can be seen that

$P_{\underline{X}'(s), \underline{U}'(s) | \underline{X}'(t), \underline{U}'(t)}(\underline{y}, \underline{v} | \underline{x}, \underline{u})$ satisfies

$$\frac{\partial p}{\partial s} = - \frac{\partial}{\partial v^i} (v^i p) - \frac{\partial}{\partial v^i} \left[\left(\frac{\phi^i}{g_p} - \hat{a}^i \right) p \right] - \frac{\partial^2}{\partial v^i \partial v^j} (B^{ij} p)$$

for $t > s$, where $\underline{\phi}$, g_p , $\hat{\underline{a}}$ and \underline{B} are all evaluated at $(\underline{y}, \underline{v}, s)$. The forward transition density for our model (4.20), which is defined for $t' \geq s'$ only, will be denoted by

$$P_{\underline{X}'(t'), \underline{U}'(t') | \underline{X}'(s'), \underline{U}'(s')}(\underline{x}, \underline{u}' | \underline{y}, \underline{v}').$$

We want this to equal the reverse transition density function

$P_{\underline{X}'(-t'), \underline{U}'(-t') | \underline{X}'(-s'), \underline{U}'(-s')}(\underline{x}, -\underline{u}' | \underline{y}, -\underline{v}')$. For this to be so it is necessary that $P_{\underline{X}'(t'), \underline{U}'(t') | \underline{X}'(s'), \underline{U}'(s')}(\underline{x}, \underline{u}' | \underline{y}, \underline{v}')$ should satisfy

$$\frac{\partial p}{\partial t'} = - \frac{\partial}{\partial x^i} (u'^i p) - \frac{\partial}{\partial u'^i} \left[\left(\frac{\phi^i}{g_p} - \hat{a}^i \right) p \right] + \frac{\partial^2}{\partial u'^i \partial u'^j} (B^{ij} p)$$

for $t' > s'$, where $\underline{\phi}$, g_p , $\hat{\underline{a}}$ and \underline{B} are evaluated at $(\underline{x}, -\underline{u}', -t')$. If the

model (4.20) is to give rise to this forward equation, then we must have

$$\underline{a}'(\underline{x}, \underline{u}', t') = - \underline{\hat{a}} + \underline{\phi}/g_p$$

$$\underline{b}'(\underline{x}, \underline{u}', t') = \underline{b}$$

with $\underline{\phi}$, g_p , $\underline{\hat{a}}$ and \underline{b} evaluated at $(\underline{x}, -\underline{u}', -t')$. Note that $\underline{a}'(\underline{x}, \underline{u}', t')$ is not simply equal to $\underline{a}(\underline{x}, -\underline{u}', -t')$ as it would be if we were trying to formulate a backwards version of the ordinary differential equation $d\underline{U}/dt = \underline{a}$. Instead the two parts of \underline{a} (i.e. $\underline{\hat{a}}$ and $\underline{\phi}/g_p$) transform differently under time reversal, with $\underline{\hat{a}}$ changing its sign. The above results show how a model for the reverse trajectories should be formulated in order to ensure that the predictions for $\langle c \rangle$ and g_c are the same as would result from a given model for the forward trajectories.

(vi) The small time-scale limit.

Durbin (1983, 1984) posed the requirement that a random walk model should reduce to an eddy-diffusivity model as the Lagrangian time-scale, τ , tends to zero. In this section we investigate this requirement and its relation to the well-mixed condition.

Suppose the shortest time after the release of material at which we are interested in the dispersion is T and that the time-scale on which conditions change as viewed by a particle (due to inhomogeneity or unsteadiness in the turbulence) is τ_H . In investigating the behaviour of the model for small τ , it is convenient to non-dimensionalise quantities as follows. Let us non-dimensionalise all times with respect to $\min(T, \tau_H)$ and all lengths with respect to some measure of the spatial extent of the $\langle c \rangle$ field which results from an instantaneous point source at a time of $\min(T, \tau_H)$ after the release. To avoid unnecessary notational complexity, a non-dimensional quantity will be denoted by the same symbol as its dimensional equivalent. In justification, we note that the non-dimensional quantities are simply

the ordinary quantities measured in particular units.

Let us now assume that the non-dimensional τ is small. The non-dimensional turbulent energy must be large to make up for the small time-scale (otherwise the non-dimensional spatial extent of the $\langle c \rangle$ field at time $\min(T, \tau_H)$ will not be of order unity) and so we put $g_p = \varepsilon^3 f(\underline{x}, \underline{v}, t)$ where $\underline{v} = \varepsilon(\underline{u} - \underline{U}_e)$ and ε is a small parameter. It is not yet clear how \underline{a} and \underline{B} scale. However, because the particle velocities are large and rapidly changing, it is clear that \underline{B} must be large. In anticipation of the result we put $\underline{B} = \beta/\varepsilon^4$ and assume that ϕ is of order ε^0 or smaller; if \underline{B} is not of order ε^{-4} or ϕ is larger than ε^0 it can be shown, by repeating the analysis below with different assumptions about the size of \underline{B} and ϕ , that the non-dimensional spatial extent of the $\langle c \rangle$ field is not of order unity at non-dimensional times of order unity. Of course ϕ needs to be no larger than $O(\varepsilon)$ in order to satisfy (4.9) and in one-dimensional models it cannot be larger than this. The scaling for \underline{B} can be made plausible by considering diffusion in one dimension in homogeneous stationary Gaussian turbulence with no mean flow. (4.1) can then take the form of the Langevin equation (4.2) for which the non-dimensional diffusivity at times $t \gg \tau$ equals σ^4/B (σ and B here being non-dimensionalised quantities). ε has been defined so that $\sigma^2 = O(\varepsilon^{-2})$ and so B must be of order ε^{-4} if the non-dimensional diffusivity is to be of order unity (which it must be if the non-dimensional extent of the $\langle c \rangle$ field is to be of order unity at non-dimensional times of order unity).

Assuming the model satisfies the well-mixed condition, (4.3), (4.8) and (4.9) yield

$$\begin{aligned} \frac{\partial g_c}{\partial t} = & - \left(\frac{v^i}{\varepsilon} + U_e^i \right) \left(\frac{\partial g_c}{\partial x^i} - \varepsilon \frac{\partial g_c}{\partial v^j} \frac{\partial U_e^j}{\partial x^i} \right) + \frac{1}{\varepsilon^2} \frac{\partial}{\partial v^i} \left(\beta^{ij} f \frac{\partial}{\partial v^j} \left(\frac{g_c}{f} \right) \right) \\ & - \frac{1}{\varepsilon^2} \frac{\partial}{\partial v^i} \left(\frac{\phi^i g_c}{f} \right) \end{aligned} \quad (4.21)$$

with ϕ satisfying

$$\begin{aligned} \frac{\partial \phi^i}{\partial v^i} = & - \varepsilon v^i \frac{\partial f}{\partial x^i} - \varepsilon^2 \frac{\partial f}{\partial t} - \varepsilon^2 U_e^i \frac{\partial f}{\partial x^i} + \varepsilon^2 v^i \frac{\partial f}{\partial v^j} \frac{\partial U_e^j}{\partial x^i} + \\ & + \varepsilon^3 \frac{\partial f}{\partial v^i} \left(\frac{\partial U_e^i}{\partial t} + U_e^j \frac{\partial U_e^i}{\partial x^j} \right). \end{aligned}$$

From §4.2(ii), it is clear that $\phi \rightarrow 0$ faster than any power of $|\underline{v}|$ as $|\underline{v}| \rightarrow \infty$. Also, because there is no flux of particles through the phase space boundary at $|\underline{u}| = \infty$ (or alternatively from the assumptions about g_c stated at the end of §4.2(i)) it follows that the integral of $a^i g_c - \partial(B^{ij} g_c) / \partial u^j$ over the surface at $|\underline{u}| = \infty$ is zero. Using (4.8), this becomes

$$\int \left(\beta^{ij} f \frac{\partial}{\partial v^j} \left(\frac{g_c}{f} \right) - \frac{\phi^i g_c}{f} \right) dS^i = 0$$

where dS^i is an element of the surface at $|\underline{v}| = \infty$. Also, on physical grounds, we assume that g_c/f remains bounded as $|\underline{v}| \rightarrow \infty$.

The reasoning which follows is similar to that used by Schuss (1980, p134). Let us pose asymptotic expansions for g and ϕ , namely

$$g_c = g_0 + \varepsilon g_1 + \varepsilon^2 g_2 + \dots, \quad \phi = \phi_0 + \varepsilon \phi_1 + \varepsilon^2 \phi_2 + \dots$$

The leading order (ε^{-2}) terms in (4.21) yield

$$\frac{\partial}{\partial v^i} \left(\beta^{ij} f \frac{\partial}{\partial v^j} \left(\frac{g_0}{f} \right) \right) - \frac{\partial}{\partial v^i} \left(\frac{\phi_0^i g_0}{f} \right) = 0$$

with g_0/f bounded and

$$\int \left(\beta^{ij} f \frac{\partial}{\partial v^j} \left(\frac{g_0}{f} \right) - \frac{\phi_0^i g_0}{f} \right) dS^i = 0.$$

Because $\partial \phi_0^i / \partial v^i = 0$, this has a solution $g_0 = C(\underline{x}, t) f$; indeed all solutions are of this form. The order ε^{-1} terms in (4.21) yield

$$\frac{\partial}{\partial v^i} \left(\beta^{ij} f \frac{\partial}{\partial v^j} \left(\frac{g_1}{f} \right) \right) - \frac{\partial}{\partial v^i} \left(\frac{\phi_0^i g_1}{f} \right) = v^i f \frac{\partial C}{\partial x^i} \quad (4.22)$$

with g_1/f bounded and

$$\int \left(\beta^{ij} f \frac{\partial}{\partial v^j} \left(\frac{g_1}{f} \right) - \frac{\phi_0^i g_1}{f} \right) dS^i = 0. \quad (4.23)$$

In order for (4.22) and (4.23) to have a solution it is necessary that $\int v^i f(\partial C/\partial x^i) d\underline{v} = 0$ which is automatically satisfied. The order ϵ^0 equation becomes

$$\frac{\partial}{\partial v^i} \left(\beta^{ij} f \frac{\partial}{\partial v^j} \left(\frac{g_2}{f} \right) \right) - \frac{\partial}{\partial v^i} \left(\frac{\phi_0^i g_2}{f} \right) = f \left(\frac{\partial C}{\partial t} + U_e^i \frac{\partial C}{\partial x^i} \right) + v^i \frac{\partial g_1}{\partial x^i} + \frac{\partial}{\partial v^i} \left(\frac{\phi_1^i g_1}{f} \right)$$

with g_2/f bounded and

$$\int \left(\beta^{ij} f \frac{\partial}{\partial v^j} \left(\frac{g_2}{f} \right) - \frac{\phi_0^i g_2}{f} \right) dS^i = 0.$$

For these equation to have a solution it is necessary that

$$\left(\frac{\partial C}{\partial t} + U_e^i \frac{\partial C}{\partial x^i} \right) \int f d\underline{v} + \frac{\partial}{\partial x^i} \int v^i g_1 d\underline{v} = 0 \quad (4.24)$$

where g_1 is a solution of (4.22) and (4.23). By noting that $\int f d\underline{v} = \langle \rho \rangle$, $\partial \langle \rho \rangle / \partial t + \partial (\langle \rho \rangle U_e^i) / \partial x^i = 0$ and $C \propto \langle c \rangle / \langle \rho \rangle$ to leading order in ϵ , (4.24) yields

$$\frac{\partial \langle c \rangle}{\partial t} + \frac{\partial}{\partial x^i} (\langle c \rangle U_e^i) = \frac{\partial}{\partial x^i} \left(\langle \rho \rangle K^{ij} \frac{\partial}{\partial x^j} \left(\frac{\langle c \rangle}{\langle \rho \rangle} \right) \right)$$

where $K^{ij} = \int (u^i - U_e^i) G^j d\underline{u} / \int g_\rho d\underline{u}$ and G^k is a solution of

$$\frac{\partial}{\partial u^i} \left(B^{ij} g_\rho \frac{\partial}{\partial u^j} \left(\frac{G^k}{g_\rho} \right) \right) - \frac{\partial}{\partial u^i} \left(\frac{\phi_0^i G^k}{g_\rho} \right) = (u^k - U_e^k) g_\rho$$

with G^k/g_ρ bounded and

$$\int \left(B^{ij} g_\rho \frac{\partial}{\partial u^j} \left(\frac{G^k}{g_\rho} \right) - \frac{\phi_0^i G^k}{g_\rho} \right) dS^i = 0.$$

(Although G is not unique, all solutions differ by g_ρ times a vector function of \underline{x} and t which does not affect the value of K .) Hence we see that the model reduces to an eddy-diffusivity model. After some algebra it can be shown that K is positive definite and, if $\phi_0 = 0$, symmetric.

Unfortunately, it is not always possible to calculate \underline{K} analytically. However, for the class of models in which $(1/g_p)(\partial(B^{ij}g_p)/\partial u^j + \phi_0^i)$ is a linear function of $\underline{u} - \underline{U}_e$, $-L^{ij}(u^j - U_e^j)$ say, (i.e. those models for which \underline{a} is a linear function of $\underline{u} - \underline{U}_e$ to leading order in ε), \underline{K} can be calculated and is given by $K^{ij} = (\underline{L}^{-1})^{ik}V_e^{kj}$. This class of models includes most models proposed to date. K can also be found easily in one-dimensional models. In such models ϕ_0 is automatically zero and $K = \int (q^2/Bg_p)du/\int g_p du$ where $q = \int_{-\infty}^u (u' - U_e)g_p(x, u', t)du'$. In Gaussian turbulence, this reduces to $\int (\sigma^4 g_p/B)du/\int g_p du$. These expressions show how the model's diffusivity is related to \underline{a} and \underline{B} . If we know from other arguments what value the diffusivity should take, then these results can be used to help choose the values of \underline{a} and \underline{B} . This is discussed further in §4.3(iii) below.

We have seen that, if the model satisfies the well-mixed condition, it reduces to an eddy-diffusivity model as the Lagrangian time-scale tends to zero. Now the limit $\tau \rightarrow 0$ is, when rescaled, equivalent to $\min(t, \tau_H) \rightarrow \infty$. Hence, in homogeneous stationary turbulence (where $\tau_H = \infty$), the model becomes an eddy-diffusivity model as $t \rightarrow \infty$. Also, if the inhomogeneity or non-stationarity is weak (i.e. $\tau_H \gg \tau$), then the model is approximately an eddy-diffusivity model for $t \gg \tau$. However, if the inhomogeneity or non-stationarity is stronger (i.e. $\tau_H \leq \tau$), then it is not clear whether the model becomes an eddy-diffusivity model at large times or indeed whether it should.

If (4.1) reduces to an eddy-diffusivity model as the time-scale tends to zero, then the model need not satisfy the well-mixed condition. Hence we see that requiring the model to reduce to an eddy-diffusivity model as $\tau \rightarrow 0$ is a weaker condition than the well-mixed condition. Durbin (1984) suggested that, as well as reducing to an eddy-diffusivity model as $\tau \rightarrow 0$, a random walk model should give the correct variance for the particle velocities in

homogeneous stationary turbulence. However this is insufficient to ensure the well-mixed condition is satisfied and, strictly speaking, implies nothing about the behaviour of the model in inhomogeneous or non-stationary conditions.

(vii) Discussion.

Five constraints which it is desirable for random walk models to satisfy have been discussed. It has been shown that four out of the five constraints are equivalent and that the fifth constraint is satisfied if any of the others are. In retrospect the equivalence of so many of the constraints is not so surprising; all four of the equivalent constraints demand that some aspect of the model is consistent with the assumed form of g_p , and so the constraints are all of a similar nature.

A natural question to ask is, "If the well-mixed condition is satisfied, is the model completely consistent with the assumed form of g_p , in the sense that there exists an ensemble of mass conserving velocity and density fields (i.e. an ensemble of velocity and density fields satisfying (3.1), but not necessarily (3.2)) for which (i) the phase space density of all the fluid particles equals g_p , and (ii) the random walk model prediction of the dispersion is exactly correct?" If this is so then it sheds some light on why the well-mixed condition implies the other constraints - if the model is completely consistent with g_p , then any constraint involving g_p must automatically be satisfied. Of course this would not imply that the model predicts the dispersion correctly for any ensemble for which g_p takes the assumed form and, in particular, will not necessarily give the correct result for the true ensemble determined by the governing equations. It would however imply that the model is consistent with any deductions that could be made from (3.1), (3.3) (with $\kappa = 0$) and the assumed form of g_p . Conversely, if the answer to the question is no, then the model is

not consistent with every deduction that can be made from (3.1), (3.3) and the assumed form of g_p .

In fact the answer to the question is yes, at least if we allow the density fields in the ensemble to involve generalised functions. To see this, consider the ensemble of particle trajectories obtained from the model in the case where the initial phase space distribution of particles at time zero is well-mixed, i.e. has density function $g_p(\underline{x}, \underline{u}, 0)/M$, M being the total mass of fluid in the flow. Because the model is assumed to satisfy the well-mixed condition, the distribution of particles at time t has density function $g_p(\underline{x}, \underline{u}, t)/M$. We will now construct an ensemble of velocity and density fields by constructing a velocity and density field for each particle trajectory. More specifically, for each particle trajectory $(\underline{X}(t), \underline{U}(t))$, we consider a density field in which all the material is concentrated at $\underline{X}(t)$ (so that the realisation only contains a single particle!) and a velocity field which is uniform in space and equal to $\underline{U}(t)$. In mathematical terms this means $\rho(\underline{x}, t) = M\delta(\underline{x} - \underline{X}(t))$ and $\underline{u}_e(\underline{x}, t) = \underline{U}(t)$. The ensemble of such fields has the required properties. Although the ensemble is rather unphysical (as noted above, each realisation contains only a single particle), it is sufficient to explain the equivalence of the constraints.

One would like there to be a more physically realistic ensemble with the right properties. It seems likely that such an ensemble exists although it is not clear how to prove it rigorously. There must exist a physically realistic ensemble of velocity and density fields $\underline{u}_0(\underline{x})$, $\rho_0(\underline{x})$ for which the phase space density of fluid particles equals $g_p(\underline{x}, \underline{u}, 0)$. For each $(\underline{u}_0, \rho_0)$, it might be possible to define an ensemble of velocity and density fields by setting $\underline{u}_e(\underline{x}, 0) = \underline{u}_0(\underline{x})$, $\rho(\underline{x}, 0) = \rho_0(\underline{x})$ and letting the fluid particles move according to the model, perhaps with the same realisation of the Wiener process $\zeta(t)$

being used for all the fluid particles in any particular member of the ensemble. If this idea can be made precise, the ensemble formed by superimposing the ensembles formed from each $(\underline{u}_0, \rho_0)$ will have the right properties, although it is not clear if such an ensemble can be defined for all $t > 0$ (for example there is no guarantee that the velocity fields will not develop singularities). Also, if g_p is such that ρ could be constant (i.e. $\int g_p d\underline{u}$ independent of \underline{x} and $\partial(\int u^i g_p d\underline{u})/\partial x^i = 0$), then one might hope that there exists an ensemble of constant density flows for which the model is exact, but it is not clear if this is so.

4.3 Choosing \underline{a} and \underline{B} - Additional Considerations.

(i) Introduction.

It has been shown that all the criteria considered above will be satisfied if the well-mixed condition is satisfied, i.e. if \underline{a} and \underline{B} satisfy (4.8) and (4.9). In one dimension, (4.9) and the fact that $\phi \rightarrow 0$ as $|\underline{u}| \rightarrow \infty$ determine ϕ uniquely and only B is left to be determined since a can then be found from (4.8). In more than one dimension however, ϕ is unique only up to the addition of a component which is solenoidal in \underline{u} -space and tends to zero rapidly as $|\underline{u}| \rightarrow \infty$. To determine \underline{a} and \underline{B} completely some additional considerations are required. For the remainder of this chapter we assume that ρ is constant for simplicity.

(ii) The small time behaviour of the particles from a point source.

It was seen in §4.2(iii) that the well-mixed condition ensures that certain aspects of the small time behaviour of particles from an instantaneous point source are correct. However it does not ensure the correctness of all aspects of the small time behaviour. As in §4.2(iii), we take the point source to be at (\underline{x}_s, t_s) and consider the phase space trajectories $(\underline{X}(t), \underline{u}(t))$ of contaminant particles emerging

from the source. At times $(t-t_s) \ll \tau_h$, where τ_h is the Kolmogorov time-scale, the Lagrangian structure function $D^{ij} = \langle (U^i(t) - U^i(t_s))(U^j(t) - U^j(t_s)) \rangle$ has the form

$$\langle (Du_e^i/Dt)(Du_e^j/Dt) \rangle (t - t_s)^2 + o((t - t_s)^3) \quad (4.25)$$

(see Monin and Yaglom (1975, pp359 and 533)). At larger times with the time lag $(t-t_s)$ lying in the inertial subrange, D^{ij} has the form

$$D^{ij} = \delta^{ij} C_0 \varepsilon (t - t_s) \quad (4.26)$$

(Monin and Yaglom 1975, p359) where δ is the Kronecker delta, ε is the ensemble average rate of dissipation of energy and C_0 is a universal constant. The value of C_0 is rather uncertain. Experimental evidence indicates $C_0 = 4.0 \pm 2.0$ (Hanna (1981) - our C_0 is Hanna's $2\pi^2 B$) while recent direct simulations suggest that C_0 is at least as large as 4.0 (Yeung and Pope 1988). In the model (4.1), the assumption that $(\underline{x}, \underline{u})$ is a Markov process means that the model can only describe the particle motions correctly on time-scales larger than τ_h . Hence we should expect the model structure function to have the form (4.26) at small times. Now at small times (4.1) implies

$$D^{ij} = 2 \langle B^{ij} \rangle (t - t_s) + o((t - t_s)^2)$$

where $\langle B \rangle$ denotes $\langle B(\underline{x}_s, \underline{u}_s, t_s) \rangle$, i.e. $\int B g_p d\underline{u} / \int g_p d\underline{u}$. Hence for accurate results at small times we should choose

$$2 \langle B^{ij} \rangle = \delta^{ij} C_0 \varepsilon. \quad (4.27)$$

This idea can be traced back to Obukhov (1959) and Novikov (1963) (see also Monin and Yaglom (1975, pp547 and 571-573)) and was discussed further by van Dop et al (1985), Haworth and Pope (1986) and Pope (1987). Van Dop et al (1985) considered (4.27) in the context of a model in which \underline{a} was a linear function of \underline{u} . Van Dop et al found it was impossible in general to ensure that the model structure function had the form (4.26) at small times while also ensuring that the small time behaviour of the mean and variance of the particle velocities was

correct. If the mean and variance are correct, their model yields a structure function which depends on the inhomogeneity or unsteadiness in the turbulence as well as ε . By considering the more general model (4.1) we have avoided this problem.

So far we have only considered the small time behaviour of the velocity of particles. It is of some interest to consider also the distribution of particle positions. If the model satisfies the well-mixed condition we have, by applying Itô's formula (4.6),

$$\langle X^i - x_s^i \rangle = \langle u_e^i \rangle (t - t_s) + \frac{1}{2} \left(\frac{\partial}{\partial t} \langle u_e^i \rangle + \frac{\partial}{\partial x^j} \langle u_e^i u_e^j \rangle \right) (t - t_s)^2 + 0((t - t_s)^3)$$

and

$$\langle (X^i - x_s^i)(X^j - x_s^j) \rangle = \langle u_e^i u_e^j \rangle (t - t_s)^2 + \left(\frac{1}{2} \left(\frac{\partial}{\partial t} \langle u_e^i u_e^j \rangle + \frac{\partial}{\partial x^k} \langle u_e^i u_e^j u_e^k \rangle \right) - \frac{1}{3} \langle B^{ij} \rangle \right) (t - t_s)^3 + 0((t - t_s)^4).$$

We can also obtain an exact Taylor expansion for the behaviour of $\langle X^i - x_s^i \rangle$ and $\langle (X^i - x_s^i)(X^j - x_s^j) \rangle$ at small times (van Dop et al 1985), although, because small time in the model means that the time lag $(t-t_s)$ lies in the inertial subrange and not that $(t-t_s) \ll \tau_\eta$, we should not necessarily expect this to agree with the model. In fact the exact small time behaviour is the same as the model result given above, but without the $-(1/3)\langle B^{ij} \rangle (t-t_s)^3$ term. Hunt (1985) has shown how to calculate the small time behaviour of $\langle (X^i - x_s^i)(X^j - x_s^j) \rangle$ under the assumption that \underline{D} is given by (4.26) and not by (4.25). Provided the model satisfies (4.27), the result is in agreement with the model result given above, showing that the addition of the term $-(1/3)\langle B^{ij} \rangle (t-t_s)^3$ is the correct way to adjust the Taylor expansion to account for the fact that $(t-t_s)$ lies in the inertial subrange and is not much less than τ_η . It is of interest to note that models in which \underline{a} is a linear function of \underline{u} do not give the correct expression for the second moments of \underline{X} (van Dop et al 1985). This is connected with the

inability of such models to satisfy (4.26) and illustrates again the advantages of considering the more general model (4.1). In the same way we can consider higher order moments of $\underline{X} - \underline{x}_s$. The model prediction for such moments at small times is

$$\begin{aligned} \langle (X^i - x_s^i) \dots (X^m - x_s^m) \rangle &= \langle u_s^i \dots u_s^m \rangle (t - t_s)^r + \\ &+ \left(\frac{1}{2} \left(\frac{\partial}{\partial t} \langle u_s^i \dots u_s^m \rangle + \frac{\partial}{\partial x^n} \langle u_s^i \dots u_s^m u_s^n \rangle \right) - \frac{r(r-1)}{6} \langle B^{(ij)u^k} \dots u^m \rangle \right) (t - t_s)^{r+1} + \\ &+ O((t - t_s)^{r+2}). \end{aligned}$$

where r is the number of indices $i \dots m$ and $B^{(ij)u^k} \dots u^m$ denotes $B^{ij}u^k \dots u^m$ with the indices symmetrized. Apart from the term involving $\langle B^{(ij)u^k} \dots u^m \rangle$, this is in agreement with the exact small time expansion. However, in contrast to the situation which obtained when considering the second moments of $\underline{X} - \underline{x}_s$, we cannot say whether the term involving $\langle B^{(ij)u^k} \dots u^m \rangle$ is the correct adjustment to the Taylor expansion to take account of the fact that $(t - t_s)$ is not much less than τ_h . This is because the correct value of such an adjustment cannot be calculated exactly without making further assumptions about the turbulence.

One way to determine the dependence of \underline{a} and \underline{B} on \underline{u} would be to conduct a conditional release experiment, i.e. an experiment in which tracer is released only if the velocity at the source is equal to a particular value, \underline{u}_s say. (In practice such an experiment would probably be conditional on just one component of velocity or the velocity direction, not the vector velocity). For such a situation the model (4.1) yields

$$\begin{aligned} \langle U^i - u_s^i \rangle &= a^i(\underline{x}_s, \underline{u}_s, t_s)(t - t_s) + O((t - t_s)^2) \\ \langle (U^i - u_s^i)(U^j - u_s^j) \rangle &= 2B^{ij}(\underline{x}_s, \underline{u}_s, t_s)(t - t_s) + O((t - t_s)^2) \quad (4.28) \\ \langle X^i - x_s^i \rangle &= u_s^i(t - t_s) + \frac{1}{2}a^i(\underline{x}_s, \underline{u}_s, t_s)(t - t_s)^2 + O((t - t_s)^3) \\ \langle (X^i - \langle X^i \rangle)(X^j - \langle X^j \rangle) \rangle &= \frac{2}{3}B^{ij}(\underline{x}_s, \underline{u}_s, t_s)(t - t_s)^3 + O((t - t_s)^4). \end{aligned}$$

If the value of \underline{u}_g is varied, the dependence of \underline{a} and \underline{B} on \underline{u} could be estimated experimentally. Hanna (1979) presented some data in which tetraon trajectories were grouped into cases with the same initial velocity, thus providing data similar to that which could be obtained from a conditional release. This data is consistent with \underline{B} being independent of \underline{u} and \underline{a} depending linearly on $\underline{u} - \underline{u}_g$. However, these forms for \underline{a} and \underline{B} cannot both be exactly correct in all situations without violating the well-mixed condition.

Strictly speaking, inertial subrange theory requires the quantity $(U^i(t) - U^i(t_g))(U^j(t) - U^j(t_g))$ to be independent of $\underline{u}_g(\underline{x}_g, t_g)$ for small $(t - t_g)$ (Monin and Yaglom 1975, p359). If the model is to be consistent with this, it follows from (4.28) that $\underline{B}(\underline{x}, \underline{u}, t)$ should be independent of \underline{u} . However, inertial subrange theory is not exact (Monin and Yaglom 1975, p584-585) and this particular aspect of it is likely to be violated if the local instantaneous dissipation rate is correlated with the velocity. For example, in a convective boundary layer it seems likely that the dissipation is larger in the vigorous updraughts than in the gently subsiding air.

(iii) Weakly Inhomogeneous Flows.

In flows which are only weakly inhomogeneous or slightly non-stationary (i.e. $\tau_H \gg \tau$) the classical theory of Taylor (1921) and Batchelor (1949) applies for $t - t_s \ll \tau_H$. It follows that, when $t - t_s \ll \tau_H$, the second moments of the spread of the tracer depend only on \underline{V}_g (the covariance matrix of the velocity components at a fixed point) and on the Lagrangian correlation function $\underline{R}(t)$, which is defined by

$$R^{ij}(t) = \frac{\langle U'^i(s)U'^j(s+t) \rangle}{(V^{ii}V^{jj})^{1/2}},$$

where $\underline{U}' = \underline{U} - \underline{u}_g$ and the average is over all particles with given initial position (here, and in all other expressions involving \underline{R} or τ_I ,

defined below, the summation convention does not apply). In addition, Pasquill (1974, pp131-132) has shown that, if the Lagrangian integral time-scales are fixed, the dispersion is relatively insensitive to the shape of \underline{R} . There is therefore some merit in designing the model so that the Lagrangian integral time-scales

$$\tau_I^{ij} = \frac{1}{2} \int_0^{\infty} (R^{ij}(t) + R^{ji}(t)) dt$$

are correct. In order to be able to do this it is necessary to be able to calculate the integral time-scales of the model. From Batchelor's (1949) three-dimensional extension of Taylor's (1921) theory, the time-scales of the model are related to the model's diffusivity by $K^{ij} + K^{ji} = 2(V^{ii}V^{jj})^{1/2} \tau_I^{ij}$ and so the time-scales can be obtained from the value of \underline{K} which can in turn be calculated as indicated in §4.2(vi).

Although the shape of \underline{R} does not strongly influence the dispersion, it is of interest to consider what range of shapes can be obtained from a model of the form (4.1). If $a^i = -L^{ij}(u^j - U_0^j)$ with \underline{L} symmetric, then \underline{R} takes an exponential form (see Appendix B). In other cases it is not clear how to calculate \underline{R} analytically, and so some numerical calculations were carried out. The details of the calculation procedure are given in Appendix C and some examples are shown in Figure 4.1 for the case of Gaussian turbulence. The forms of \underline{B} and ϕ chosen have no special significance and were chosen simply to provide a range of different shapes for \underline{R} . The variations in the shape of \underline{R} caused by varying \underline{B} are small and, although greater variations can be produced by varying ϕ , it seems unlikely that the model can be tuned in this way to produce any desired shape for $\underline{R}(t)$. This is not a serious problem because, as noted above, Pasquill (1974, pp131-132) has shown that, if τ_I is fixed, the dispersion is relatively insensitive to the shape of $\underline{R}(t)$. Also experimental evidence (Draxler 1976) shows that \underline{R} can often be approximated by an exponential function.

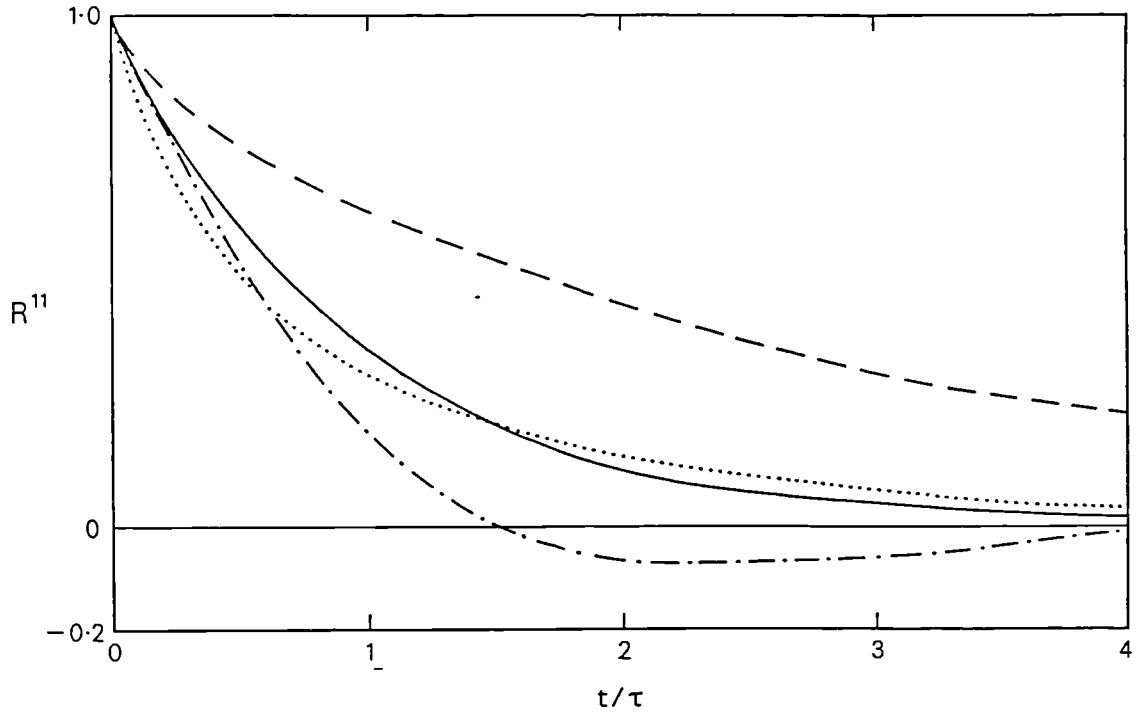


Figure 4.1: Results of numerical calculations of $R^{11}(t)$ in isotropic stationary Gaussian turbulence with no mean flow using various random walk formulations. The various curves correspond to the following values of \underline{B} and $\underline{\phi}$: —, $B^{ij} = \delta^{ij}\sigma^2/\tau$, $\underline{\phi} = 0$; - - - -, $B^{ij} = \delta^{ij}\sigma^2/\tau$, $\underline{\phi} = g_p(-u^2, u^1, 0)/\tau$; - - - - -, $B^{ij} = \delta^{ij}\sigma^2(0.2+(u^1/\sigma)^2)/1.2\tau$, $\underline{\phi} = 0$; ·····, $B^{ij} = 1.2\delta^{ij}\sigma^2/(0.2+(u^1/\sigma)^2)\tau$, $\underline{\phi} = 0$. With the exception of the first of these forms for \underline{B} and $\underline{\phi}$, τ is not the Lagrangian integral time-scale, but is simply a general measure of the time-scale on which the particle velocities become decorrelated. In the three examples with $\underline{\phi} = 0$, u^2 and u^3 do not affect u^1 ; hence these are essentially one-dimensional calculations.

(iv) Discussion.

For models which satisfy the well-mixed condition, the values of \underline{a} and \underline{B} have been seen to influence some of the more subtle aspects of the dispersion as predicted by the model, e.g. the dispersion from a conditional release and the shape of the Lagrangian correlation function. However, because the true evolution of $(\underline{X}, \underline{U})$ does not satisfy a pair of equations of the form (4.1), it may well be that some aspects of the dispersion can only be represented more accurately at the expense of the representation of other aspects. In the absence of sufficient data or a theory giving the values of \underline{a} and \underline{B} , it is sensible to keep the model as simple as possible, consistent with satisfying the well-mixed condition. The simplest choice for \underline{B} is to choose \underline{B} to be independent of \underline{u} . This also has the merit of being consistent with inertial subrange theory. If $\tau_H \gg \tau$, then, in view of Pasquill's result quoted above, \underline{B} should be chosen so that the integral time-scales of the model are correct. In more general conditions equation (4.27) offers what is perhaps the most rational choice for \underline{B} . In one-dimensional models, the value of B determines the model uniquely, as discussed in §4.3(i). In three-dimensional models however, there are many functions ϕ which satisfy (4.9) and tend to zero at infinity. In order to determine \underline{a} , and hence fix the model, it is necessary to select one of these functions. It is not clear in general what the simplest choice for ϕ is. Examples are given in the next section.

4.4 Some Examples of Random Walk Models.

In this section, some examples of random walk models based on the theoretical ideas discussed above are presented. Perhaps the simplest case is that which arises in modelling the motion of particles in one dimension (say the x -direction) in homogeneous stationary Gaussian turbulence with no mean flow. If we choose B to be independent of u

then the model takes the form of the Langevin equation (4.2):

$$dU = - \frac{BU}{\sigma^2} dt + (2B)^{1/2} d\zeta.$$

For this model the Lagrangian correlation function is $\exp(-tB/\sigma^2)$ and so, if we are to choose B on the basis of the ideas discussed in §4.3(iii), we should choose $B = \sigma^2/\tau_I$. This leads to the Langevin equation in its more traditional form:

$$dU = - \frac{U}{\tau_I} dt + \left(\frac{2\sigma^2}{\tau_I}\right)^{1/2} d\zeta.$$

The first two moments of the Eulerian parametrization corresponding to this model are, from (4.18a) and (4.18b),

$$\langle c' (Du_e^1/Dt)' \rangle = \langle c' u_e^1 \rangle / \tau_I \quad (4.29a)$$

$$\langle c' u_e^1 (Du_e^1/Dt)' \rangle = \langle c' (u_e^1)^2 \rangle / \tau_I. \quad (4.29b)$$

As in §4.2(iv), a prime denotes the departure of a quantity from its ensemble average. These parametrizations are qualitatively sensible and have been used in high-order closure models (Deardorff 1978).

Let us now consider the problem of modelling the motion of a particle in one dimension in inhomogeneous or non-stationary Gaussian turbulence. For simplicity we assume the mean flow \underline{U}_e is zero. For this case the solution of (4.9) for $\phi(x, u, t)$ is

$$\frac{\phi}{g_p} = \frac{1}{2} \frac{\partial \sigma^2}{\partial x} + \frac{1}{2\sigma^2} \frac{\partial \sigma^2}{\partial t} u + \frac{1}{2\sigma^2} \frac{\partial \sigma^2}{\partial x} (u)^2.$$

If we choose B to be independent of u as above, then, from (4.8), a is given by

$$a(x, u, t) = - \frac{B}{\sigma^2} u + \frac{\phi}{g_p}.$$

As in the Langevin equation it is useful to put $B = \sigma^2/\tau$. In weakly inhomogeneous or slightly non-stationary conditions (i.e. when $\tau_H \gg \tau$), the arguments in §4.3(iii) show that τ is equal to the Lagrangian

integral time-scale τ_1 . In conditions of stronger inhomogeneity or unsteadiness however, τ is not the integral time-scale, but is simply a (rather loosely defined) "local decorrelation time-scale". This model can be expressed more simply in the form

$$d(U/\sigma) = -\frac{(U/\sigma)}{\tau} dt + \frac{\partial \sigma}{\partial x} dt + \left(\frac{2}{\tau}\right)^{1/2} d\zeta$$

showing that the model is a simple modification of a Langevin equation for U/σ . This model is essentially that described by Wilson et al (1983, equation 3'') and Thomson (1984, §5). The first two moments of the Eulerian parametrization corresponding to this model are

$$\begin{aligned} \langle c' (Du_e^1/Dt)' \rangle &= k_1 \langle c' u_e^1 \rangle + k_2 \langle c' (u_e^1)^2 \rangle \\ \langle c' u_e^1 (Du_e^1/Dt)' \rangle &= k_1 \langle c' (u_e^1)^2 \rangle + k_2 \langle c' (u_e^1)^3 \rangle - \langle c' u_e^1 \rangle \sigma^2 \end{aligned}$$

where $k_1 = (1/2\sigma^2)\partial\sigma^2/\partial t - 1/\tau$ and $k_2 = (1/2\sigma^2)\partial\sigma^2/\partial x$. These equations contain terms depending on the inhomogeneity and unsteadiness which are absent in (4.29). It is hard to assess whether these extra terms yield a more accurate parametrization than (4.29). To the author's knowledge these terms have not been used to date in high-order closure parametrizations.

For Gaussian turbulence in more than one dimension there are many possible choices for $\phi(\underline{x}, \underline{u}, t)$ satisfying (4.9), of which the simplest is perhaps

$$\begin{aligned} \frac{\phi^i}{g_\rho} &= \frac{1}{2} \frac{\partial v_e^{i1}}{\partial x^1} + \frac{\partial U_e^i}{\partial t} + U_e^1 \frac{\partial U_e^i}{\partial x^1} + \\ &+ \left(\frac{(v_e^{-1})^{1j}}{2} \left(\frac{\partial v_e^{i1}}{\partial t} + U_e^m \frac{\partial v_e^{i1}}{\partial x^m} \right) + \frac{\partial U_e^i}{\partial x^j} \right) (u^j - U_e^j) + \\ &+ \frac{(v_e^{-1})^{1j}}{2} \frac{\partial v_e^{i1}}{\partial x^k} (u^j - U_e^j)(u^k - U_e^k). \end{aligned} \quad (4.30)$$

$\underline{a}(\underline{x}, \underline{u}, t)$ is then given by

$$a^i = -B^{ij} (v_e^{-1})^{jk} (u^k - U_e^k) + \phi^i/g_\rho.$$

Various choices for \underline{B} are possible as indicated in §4.3. The Eulerian parametrization corresponding to this model is similar to the one-dimensional case and is not presented here. The above model is similar to that utilised by Thomson (1986a). The form of ϕ proposed by Thomson was slightly more complex, although, in the application of the model described by Thomson (1986a), the principal axes of \underline{V}_e and \underline{B} were assumed parallel - in these circumstances the form of ϕ proposed by Thomson is identical to (4.30) above. Sawford and Guest (1988) have recently found an alternative form of ϕ satisfying (4.9) and of comparable "simplicity" to (4.30), and have tested it against (4.30) in a simple shear flow. The differences between the models were not insignificant, indicating the desirability of obtaining some theoretical arguments as to what form ϕ should take. However, it is far from clear how such arguments might be formulated.

Random walk models can also be designed to satisfy the well-mixed condition in non-Gaussian turbulence, provided of course that the form of g_p is known or can be estimated. As an illustration, suppose we wish to model the motion of particles in one dimension in a flow for which

$$g_p = \frac{\langle \rho \rangle}{(2\pi)^{1/2} \sigma} (\frac{1}{2} s^2 v^2 - sv + 1 - \frac{1}{2} s^2) \exp(-\frac{1}{2} v^2) \quad (4.31)$$

where $v = u/\sigma - s$ and s is a parameter. This form of g_p was chosen simply as a convenient form with adjustable skewness which can be manipulated easily and which depends smoothly on u - otherwise the form is quite arbitrary. The first three velocity moments of this distribution are $\langle u_e^1 \rangle = 0$, $\langle (u_e^1)^2 \rangle = \sigma^2$ and $\langle (u_e^1)^3 \rangle = \sigma^3 s^3$, and so s is a measure of the skewness of the velocity distribution. Provided $|s| < 1$, g_p is positive everywhere and, if $s = 0$, the turbulence is Gaussian. The graph of g_p for $s^3 = 0.331$ (the value used in the simulation below) is shown in figure 4.2. The solution of (4.9) for $\phi(x, u, t)$ is

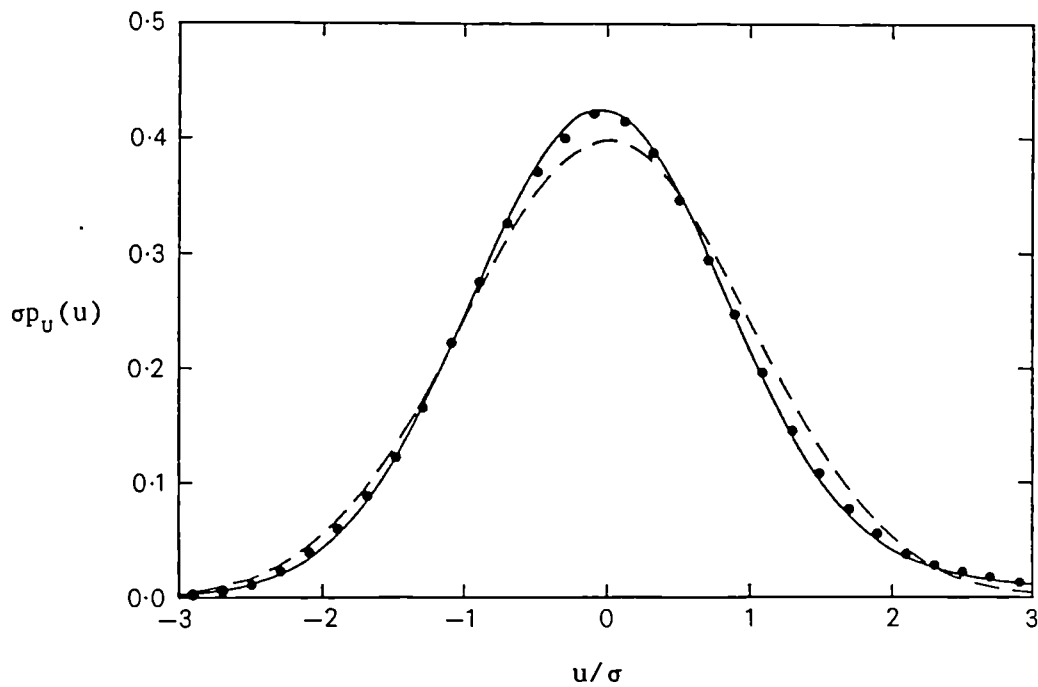


Figure 4.2: -----, Gaussian velocity distribution; —, velocity distribution implied by equation (4.31); •, velocity distribution of particles as given by a numerical computation of dispersion in homogeneous stationary turbulence with g_p given by (4.31), using the model based on equations (4.32) and (4.33). The results obtained from the numerical simulation are averaged over the time period between $8\sigma^2/B$ and $10\sigma^2/B$ after the release of the particles.

$$\begin{aligned}
\phi = & \frac{\langle \rho \rangle}{(2\pi)^{1/2}} \left(\frac{1}{2} v^4 s^2 \frac{\partial \sigma}{\partial x} + v^3 \left((s^3 - s) \frac{\partial \sigma}{\partial x} + \frac{1}{2} s^2 \sigma \frac{\partial s}{\partial x} \right) + \right. \\
& + v^2 \left((1 + \frac{1}{2} s^4 - 2s^2) \frac{\partial \sigma}{\partial x} + \frac{1}{2} s^3 \sigma \frac{\partial s}{\partial x} \right) + v(s - 3s^3/2) \frac{\partial \sigma}{\partial x} \\
& \left. + (1 + \frac{1}{2} s^2 - \frac{1}{2} s^4) \frac{\partial \sigma}{\partial x} - \frac{1}{2} s^3 \sigma \frac{\partial s}{\partial x} \right) \exp(-\frac{1}{2} v^2). \quad (4.32)
\end{aligned}$$

If B is chosen to be independent of u, it follows from (4.8) and (4.31) that a(x,u,t) is given by

$$a = - \frac{B(\frac{1}{2} s^2 v^3 - s v^2 + (1 - 3s^2/2)v + s)}{\sigma(\frac{1}{2} s^2 v^2 - s v + 1 - \frac{1}{2} s^2)} + \frac{\phi}{g_p}. \quad (4.33)$$

As an illustration, a simulation was conducted of particle trajectories in homogeneous turbulence with a skew velocity distribution ($s^3 = 0.331$). The details of the simulation procedure are given in Appendix C. The initial velocity distribution of the contaminant particles was Gaussian. The velocity distribution of the contaminant particles after a time $8\sigma^2/B$ is close to that given by (4.31) (see figure 4.2), confirming that the analysis leading to (4.32) and (4.33) is correct. An example of a simulation of dispersion in a convective surface layer using this model can be found in Thomson (1987). A similar model, based on the ideas presented here but using a different form for g_p , has been used by Weil (1988) to model vertical dispersion throughout the depth of a convective boundary layer. The results of Weil's simulations show encouraging agreement with experimental data.

4.5 Summary.

We have considered models of particle trajectories in which the trajectories in phase space are described by a coupled pair of stochastic differential equations of the form (4.1). This class of models includes many previously proposed models as special cases. One

of the advantages of considering the general model (4.1) is that it can be designed to satisfy the well-mixed condition exactly in any situation.

Various criteria for determining how such models should be formulated have been discussed. It has been shown that the well-mixed condition is equivalent to (i) requiring the small time behaviour of the velocity distribution of particles from a point source to be correct, (ii) requiring compatibility with the Eulerian equations, and (iii) demanding that the forward and reverse transition p.d.f.s are consistent. This simplifies the problem of designing a random walk model because there is no need to consider more than one these criteria. It has also been found that the well-mixed condition is more restrictive than Durbin's (1984) requirement that the model reduces to an eddy-diffusivity model as the Lagrangian time-scale tends zero. The fact that random walk models can be made consistent with so many of the physical constraints gives increased confidence in such models.

If the well-mixed condition is satisfied then the model is consistent with the known one-point density-weighted Eulerian statistics of the flow. To determine the model uniquely some further assumptions have to be made about the Lagrangian properties of the flow. It has been shown in §4.3 how the model can be designed to have the correct form of the structure function at small times or, if the flow is only weakly inhomogeneous or slightly non-stationary, the correct integral time-scales. In contrast to some previous models (van Dop et al 1985) it is always possible, at small times, to ensure that the model's structure function and the second moments of the cloud's spread are consistent with inertial subrange theory.

5. TWO-PARTICLE RANDOM WALK MODELS.

In this chapter the ideas developed in the previous chapter are extended to cover two-particle random walk models. Molecular diffusion plays a more important role in two-particle dispersion than in one-particle dispersion, and this is discussed in §5.3. Finally a two-particle model appropriate for isotropic turbulence in a constant density fluid is developed and its properties are compared and contrasted with previous models.

5.1 Introduction to Two-Particle Models.

Although the statistics of the motions of single particles of contaminant contain much useful information about the dispersion of the contaminant, these statistics give a far from complete description of the dispersion process. For example, it is impossible from such statistics to tell the difference between (i) a situation in which the cloud of contaminant is, in every realisation, spread evenly over a certain area and (ii) a situation in which the cloud remains very compact, but in which the centroid of the cloud moves to a different part of the area in each realisation. Such a distinction can be made from knowledge of the statistics of the motion of pairs of particles, although of course such statistics also give only incomplete information. Richardson (1926) was the first to consider pairs of particles and he showed that the mean square spread of a cloud relative to its centre of mass (the position of the centre of mass being evaluated separately in each realisation) is equal to half the mean square separation of all pairs of particles in the cloud. For our purposes it is more relevant to note that the second moments of concentration can be calculated from knowledge of the motion of particle pairs via (3.6).

In his 1926 paper, Richardson proposed a model for the separation of pairs of particles in which the p.d.f. of the separation satisfies a diffusion equation with an eddy-diffusivity proportional to separation to the power $4/3$. The decrease in the diffusivity with decreasing separation was intended to reflect the fact that, when the pair separation is small, all the turbulent eddies which are larger than the separation simply move the pair around without increasing the separation significantly. By taking the diffusivity proportional to separation to the four-thirds, Richardson produced a model which is consistent with inertial subrange scaling. However this must be regarded as somewhat fortuitous since Richardson wrote his paper long before inertial subrange theory was conceived and obtained his four-thirds law empirically from various experimental data, many of which were obtained in situations to which inertial subrange theory does not apply. Although this model does represent what is perhaps the most important aspect of the separation of pairs, namely the increase in dispersive power with separation, there are one or two aspects of the model which are unsatisfactory. Firstly, the use of an eddy diffusivity is conceptually unsatisfactory (for the same reasons that it is unsatisfactory in the one-particle case), although it is not clear how serious a problem this is. If the separation of particles were governed by eddies which were much smaller than the particle separation, then an eddy-diffusivity assumption would be reasonable. Of course in reality the eddy sizes which influence the separation most are of comparable size to the separation itself. However, because they are not much larger than the separation, it is possible that, for particles that are initially close, an eddy-diffusivity assumption might give acceptable results, as in the case of the vertical diffusion of single particles from a ground level source in a neutral surface layer (see the discussion in §1.3). Secondly, the model only describes the separation of pairs and does not give any information on the motion

of the centroid of a pair of particles. Such information is, in most situations, needed if one wishes to calculate the second moments of the concentration. Batchelor (1952) criticised Richardson's model on the grounds that the eddy-diffusivity is a statistical quantity and so should not depend on the particle separation which is a random quantity. Although this has generated much discussion (Sullivan 1971; Monin and Yaglom 1975, pp573-577), the criticism does not appear so serious if we regard a pair of particles as a single entity in a six-dimensional space, as suggested in §3.3. Indeed, when viewed in this way, the criticism is no more valid than criticising a single particle eddy-diffusivity model in which the eddy-diffusivity K is a function of position, on the grounds that K (a statistical quantity) should not be a function of the particle position (a random quantity).

A number of more recent models for the motion of pairs of particles in constant density flows have been proposed which overcome some of the problems associated with Richardson's model. Novikov (1963) and Lin and Reid (1963) proposed models which avoid the eddy diffusivity assumption, but they do not discuss the motion of the centroid of the pair of particles. In addition, Thiebaut (1975) proposed a model for the evolution of both the particle separation and centre of mass, but one which was still based on eddy-diffusivity concepts. Although it was seen above that an eddy-diffusivity assumption might be acceptable for the separation of particles, such an assumption is less satisfactory for the centroid motion, which is governed mainly by the energy-containing eddies. More recently still, a number of models have been proposed which avoid the eddy-diffusivity assumption and describe the motion of the centroid as well as the particle separation (Durbin 1980; Lamb 1981; Sawford 1982; Gifford 1982; Lee and Stone 1983; Sawford and Hunt 1986). Although such models have had some success in comparison with experimental data (Durbin 1982; Sawford 1985; Stapountzis, Sawford, Hunt and Britter 1986), the

correct way to formulate such models has not been investigated in detail. Recently a number of theoretical problems have been identified in connection with such models. For example, Durbin's (1980) model is inconsistent with the constant density constraint and, if the particle-pairs in the model are well-mixed initially, they do not remain so (Egbert and Baker 1984; Thomson 1986b). The models can be divided into two classes according to the predicted shape of the particle separation p.d.f. (Sawford 1983). The majority of the models (Lamb 1981; Sawford 1982; Gifford 1982; Lee and Stone 1983) predict that the p.d.f. is Gaussian (at least for initially coincident particles), while Durbin's (1980) model leads to a strongly peaked p.d.f. which tends to infinity at the origin. This difference in shape is important as it leads to very different predictions for the concentration fluctuations in some situations. Neither of these shapes seems very plausible, inertial subrange theory predicting that the p.d.f. should vary like $\alpha - \beta \Delta^{2/3}$ near $\Delta=0$ (where Δ is the magnitude of the particle separation). This sheds some doubt on whether any of the stochastic models are showing the correct qualitative behaviour. Richardson's (1926) model is of course consistent with the inertial subrange form $\alpha - \beta \Delta^{2/3}$.

In this chapter it will be shown that some understanding of these problems can be obtained by considering the one-particle theory described in chapter 4. It was noted in chapter 4 that, in inhomogeneous turbulence, one-particle stochastic models can be badly in error unless they are formulated carefully. In §4.1 we considered a situation in which the mean velocity is zero and the turbulence is stationary and homogeneous in the y- and z-directions. It was shown in §4.1 that if the fixed point variance of the x-component of velocity varies with x, then, unless the model is formulated carefully, a contaminant which is initially well-mixed becomes "un-mixed" and non-uniform in space at later times, with the particles accumulating

where the velocity variance is small. Such problems are also likely to occur in two-particle models, even in homogeneous turbulence. This is because of the variation of the two-point velocity covariance with the separation between the two points, something which is analogous to the variation of velocity variance with position in a one-particle model.

The aim of this chapter is (i) to extend the one-particle theory described in chapter 4 to two-particle models, (ii) to apply this theory in designing a two-particle model suitable for modelling dispersion in isotropic turbulence in a constant density fluid, and (iii) to investigate whether such a model overcomes the theoretical problems described above and results in a particle separation p.d.f. which is consistent with inertial subrange theory. Comparison of the model predictions with experimental data is deferred to chapter 6. Some initial steps towards these aims were taken by Thomson (1986b) using a one-dimensional model. In contrast the work presented here is three-dimensional. This is more satisfactory since the mixing processes which affect pair separation and concentration variance are essentially three-dimensional. Also, unless the three-dimensionality of the turbulence is taken account of, it is impossible to choose a form for the two-point velocity correlation function (a quantity which needs to be specified in most approaches to two-particle random walk models) which is consistent with the constant density constraint.

5.2 Theoretical Aspects of Two-Particle Models.

It is straightforward to extend the results of chapter 4 to the two-particle case. As was noted at the end of §3.3, a pair of particles with trajectories $\underline{X}_1(t)$ and $\underline{X}_2(t)$ can be regarded as a single entity with trajectory $\hat{\underline{X}}(t) = (\underline{X}_1(t), \underline{X}_2(t))$ in a six-dimensional space. The velocity of the particle-pair in this space is defined to be $\hat{\underline{U}}(t) = (\underline{U}_1(t), \underline{U}_2(t))$. As in the case of one-particle models, $d\hat{\underline{X}}/dt$ equals $\hat{\underline{U}}$ in the absence of molecular diffusion. The type of models which we

will be considering here are those in which $\hat{\underline{X}}$ and $\hat{\underline{U}}$ satisfy a coupled set of stochastic differential equations of the the same form as (4.1):

$$d\hat{X}^i = \hat{U}^i dt \quad (5.1a)$$

$$d\hat{U}^i = \hat{a}^i(\hat{\underline{X}}(t), \hat{\underline{U}}(t), t) dt + \hat{b}^{ij}(\hat{\underline{X}}(t), \hat{\underline{U}}(t), t) d\zeta^j \quad (5.1b)$$

(with the superscripts running from 1 to 6 instead of from 1 to 3).

The majority of the models mentioned in §5.1 above are of this type. As in the one-particle case described in chapter 4, this type of model implies infinite mean square particle accelerations and so cannot be an exact model of the motion of pairs. However it seems reasonable to hope that such a model may be able to provide a satisfactory description of particle-pair motions over time-scales in excess of the Kolmogorov time-scale τ_η . This is because, as in chapter 4, the particle accelerations in high Reynolds number flows are very large (relative to integral length- and time-scales) and are only significantly correlated over very short times of the order of the Kolmogorov time-scale. Hence the changes in $\hat{\underline{U}}(t)$ over successive time intervals Δt are, if $\Delta t \gg \tau_\eta$, only weakly correlated. Of course, as in the case of single particles, they cannot be completely independent or the variance of $\hat{\underline{U}}$ would grow indefinitely. In making the assumption that $\hat{\underline{X}}$ and $\hat{\underline{U}}$ obey equations of the form (5.1) it is assumed that this dependence can be accounted for by allowing the velocity increments to depend on the particle-pair's velocity $\hat{\underline{U}}$ and position $\hat{\underline{X}}$. Of course a model of the form (5.1) cannot describe the details of the particle motions over times of order τ_η . In the following \hat{B}^{ij} will be used to denote $\frac{1}{2}\hat{b}^{ik}\hat{b}^{jk}$ in the same way as in §2.3 and chapter 4.

It was noted in §3.3 that the mass densities of contaminant particle-pairs and fluid particle-pairs in the six-dimensional space (i.e. $\hat{c}(\hat{\underline{x}}, t)$ and $\hat{\rho}(\hat{\underline{x}}, t)$) and the velocity field in the six-dimensional space (i.e. $\hat{\underline{u}}(\hat{\underline{x}}, t)$) are related in the same way as c , ρ and \underline{u}_e are in ordinary space. Using these quantities we can define phase space densities of contaminant and fluid particle-pairs in the same way that

g_c and g_p were defined in ordinary space by setting

$$\hat{g}_c(\underline{\hat{x}}, \underline{\hat{u}}, t) = \langle \hat{c}(\underline{\hat{x}}, t) \delta(\underline{\hat{u}} - \underline{\hat{u}}_e(\underline{\hat{x}}, t)) \rangle$$

and

$$\hat{g}_p(\underline{\hat{x}}, \underline{\hat{u}}, t) = \langle \hat{p}(\underline{\hat{x}}, t) \delta(\underline{\hat{u}} - \underline{\hat{u}}_e(\underline{\hat{x}}, t)) \rangle.$$

Note that there is a slight change of notation here from that used in §3.3. In §3.3 the quantities which are represented here by $\hat{g}_c(\underline{\hat{x}}, \underline{\hat{u}}, t)$ and $\hat{g}_p(\underline{\hat{x}}, \underline{\hat{u}}, t)$ were written as $\hat{g}_c(\underline{x}_1, \underline{u}_1, t, \underline{x}_2, \underline{u}_2, t)$ and $\hat{g}_p(\underline{x}_1, \underline{u}_1, t, \underline{x}_2, \underline{u}_2, t)$ where $(\underline{x}_1, \underline{x}_2) = \underline{\hat{x}}$ and $(\underline{u}_1, \underline{u}_2) = \underline{\hat{u}}$. If the fluid has constant density, $\int g_p d\underline{u}$ is independent of $\underline{\hat{x}}$ and $g_p(\underline{\hat{x}}, \underline{\hat{u}}, t)$ is proportional to the p.d.f. of the velocity $\underline{u}_e(\underline{\hat{x}}, t)$, i.e. g_p contains the same information as the two-point Eulerian velocity statistics.

It follows immediately from the above that most of the analysis which was carried out for the one-particle case in chapter 4 holds for the two-particle case as well, with \underline{X} , \underline{U} , \underline{x} , \underline{u} , ρ , c , \underline{u}_e , g_c , g_p , \underline{a} , \underline{b} , and \underline{B} replaced by $\underline{\hat{X}}$, $\underline{\hat{U}}$, $\underline{\hat{x}}$, $\underline{\hat{u}}$, $\hat{\rho}$, \hat{c} , $\underline{\hat{u}}_e$, \hat{g}_c , \hat{g}_p , $\underline{\hat{a}}$, $\underline{\hat{b}}$, and $\underline{\hat{B}}$. In particular, it was noted in chapter 4 that, if g_c equals g_p at some time, then it will in reality remain equal to g_p (the "well-mixed condition"). In the same way, if \hat{g}_c equals \hat{g}_p at some time, they will remain equal. It is clearly desirable that the model should also have this property and this can be achieved by ensuring that $\underline{\hat{a}}$ and $\underline{\hat{B}}$ satisfy the equivalent of (4.8) and (4.9). As in chapter 4, this also ensures that the small time behaviour of \hat{g}_c for dispersion from an instantaneous source is correct, that the relation (3.10) and its phase space equivalent which relate the forward and reverse transition probabilities is satisfied, and that the model is compatible with the Eulerian equations in the sense described in §4.2(iv). Also, it follows from the discussion in §4.2(iv) that a two-particle model of the form (5.1) is equivalent to a two-point closure assumption on terms of the form

$$\langle c(\underline{x}_1) c(\underline{x}_2) u_e^i(\underline{x}_1) \dots u_e^m(\underline{x}_1) u_e^n(\underline{x}_2) \dots u_e^q(\underline{x}_2) \frac{D}{Dt} u_e(\underline{x}_1) \rangle.$$

Because the particle-pairs are advected and diffused in $\underline{\hat{x}}$ -space in the same way as single particles are in \underline{x} -space it might be thought that the construction of a stochastic model for the motion of particle pairs would not be significantly more difficult than for single particles. However there are some complications due to the special nature of the flow field $\underline{\hat{u}}_e$. Firstly, because the joint distribution of $\underline{u}_e(\underline{x}_1, t)$ and $\underline{u}_e(\underline{x}_2, t)$ depends on the separation $\underline{x}_1 - \underline{x}_2$, the field $\underline{\hat{u}}_e$ is always inhomogeneous, even in homogeneous turbulence. This is not a serious problem but it implies that there is no situation in which we can use a model as simple as the Langevin equation, which was seen in chapter 4 to be appropriate for modelling particle motions in homogeneous stationary velocity fields. Secondly, if A denotes the subspace of points $\underline{\hat{x}} = (\underline{x}_1, \underline{x}_2)$ with $\underline{x}_1 = \underline{x}_2$, then, at points in A, the direction of $\underline{\hat{u}}_e$ lies within A (i.e. $\underline{u}_e(\underline{x}_1, t) = \underline{u}_e(\underline{x}_2, t)$ if $\underline{x}_1 = \underline{x}_2$), thereby preventing particle-pairs escaping from the subspace A except by molecular diffusion. In other words, if the two particles in the pair are coincident, they can only be separated by molecular processes. This complication is discussed in the §5.3 below.

Before describing a third complication resulting from the special nature of the flow field $\underline{\hat{u}}_e$, it is appropriate to comment on the meaning of the word "coincident" in the above. If there is no molecular diffusion then fluid particles are simply fluid elements, and two particles which are coincident are simply the same fluid particle, and so can never separate. If $\kappa > 0$ however, we are committed to interpreting fluid particles as molecules (see §3.3). In this case the statement that two particles are "coincident" means that the molecule separation is small compared to all macroscopic scales and not of course that the two molecules are actually the same molecule! Such molecules can of course subsequently separate. Alternatively, if we adopt the stochastic differential equation model of molecular motions described in §2.3 and Appendix A, we can interpret "coincident"

literally; in this model of molecular motions there is no difficulty in two different molecules actually occupying the same position.

The third complication caused by the special nature of \hat{u}_e results from the fact that the first three components of \hat{u}_e are independent of x_2 and the second three are independent of x_1 . This is a property of \hat{u}_e which has no analogue in u_e . Unfortunately it is not clear what the full implications of this are, nor is it clear how to ensure the model is consistent with these implications. One obvious implication of this third complication (for the case of constant density flows) is the following. Consider for the moment a single realisation of the flow and consider the trajectory $\hat{X}(t) = (X_1(t), X_2(t))$ of the pair of fluid elements for which, at time s , the first element is at y_1 and the second at y_2 . From this trajectory, we can obtain a single particle trajectory $X_1(t)$ in x -space. This trajectory satisfies $dX_1/dt = u_{e1}(\hat{X}(t), t)$ and $X_1(s) = y_1$, where u_{e1} denotes the vector consisting of the first three components of \hat{u}_e . Because of the property of \hat{u}_e described above, u_{e1} depends only on X_1 and t and hence the single particle trajectory obtained would be the same, no matter what value y_2 takes (this result can of course also be seen directly by working in x -space, but it is useful to relate it to the special properties of the \hat{u}_e field described above). If we now consider the ensemble of such particle and particle-pair trajectories occurring in the ensemble of flows (one particle or particle-pair trajectory for each member of the ensemble) it is clear that:

$$\begin{aligned} &\text{For fixed } y_1, \text{ the ensemble of trajectories} \\ &X_1(t) \text{ is the same for all choices of } y_2. \end{aligned} \quad (5.2)$$

In particular, it follows that

$$\int P_{X_1(t_1), X_2(t_2) | X_1(s_1), X_2(s_2)}(x_1, x_2 | y_1, y_2) dx_2 \quad (5.3)$$

is independent of y_2 . This can of course also be seen directly by noting that (5.3) is simply the one-particle transition density

$P_{\underline{X}}(t_1) | \underline{X}(s_1) (\underline{x}_1 | \underline{y}_1)$. (5.2) also applies to the motion of particles in the presence of molecular diffusion. Indeed the above argument remains valid in this case, except that the equation for $\underline{X}_1(t)$, i.e. $d\underline{X}_1/dt = \underline{u}_{e_1}(\hat{\underline{X}}(t), t)$, is modified by the addition of a random term representing the molecular motions (see Appendix A). The condition (5.2) will be discussed further in §5.4, §5.5 and §5.6 below.

5.3 The Role of Molecular diffusion.

In this section the effect of molecular diffusion on the motion of particle-pairs will be discussed. However it is useful to consider first the simpler one-particle case. In flows with high Reynolds (Re) and Peclet (Pe) numbers, such as the atmosphere, it seems very likely that, except very close to a small source or close to boundaries, the effect of molecular diffusion on the statistics of the motions of single particles, and hence on $\langle c \rangle$, is small. Although this has not been proved rigorously, Saffman (1960) has provided a convincing intuitive argument in its support. Hence, as discussed in chapter 4, the one-particle models used to calculate $P_{\underline{X}}(t) | \underline{X}(s) (\underline{x} | \underline{y})$ and $\langle c \rangle$ can be formulated on the assumption that the particles of tracer move at the local velocity of the fluid.

Close to rigid boundaries however, molecular diffusion becomes important. In the absence of molecular diffusion, particles in the interior of the flow cannot reach the boundary, nor can particles which are on the boundary ever leave it. Hence, in the absence of molecular diffusion, there would be strong gradients of concentration across the "viscous sub-layer" (see e.g. Monin and Yaglom (1971, §5.3)) which adjoins the boundary. In practice however κ is always finite and molecular diffusion acts to smooth out the concentration gradients across the viscous sub-layer. This shows that taking $\kappa = 0$ will lead to incorrect estimates of surface concentrations. The time-scale on which this smoothing process occurs is of order the thickness of the

viscous sub-layer squared divided by κ , i.e. of order $(\nu/u_*^2)Sc$ where u_* is the friction velocity and Sc is the Schmidt number, which is defined to be ν/κ . Although this time-scale varies with Sc , it will, in flows with high Reynolds and Peclet numbers, be much smaller in general than the time-scale on which $\langle c \rangle$ varies in the interior of the flow. This means that molecular diffusion will act sufficiently quickly to produce an approximately uniform profile of $\langle c \rangle$ across the viscous sub-layer, and the values of $\langle c \rangle$ at the surface will be insensitive to the precise value of κ . It follows that it is not necessary to model the viscous sub-layer and the effect of κ in detail in a random walk model - provided the particles in the model are provided with the means to cross the viscous sub-layer in a time which is short compared to the time-scale on which $\langle c \rangle$ changes, satisfactory results should be obtained. (However it should be pointed out that in many laboratory experiments the Reynolds number is not sufficiently high for this to apply - see Chatwin (1971)).

The situation for two-particle models is rather more complex. Consider the motion of a particle-pair with trajectory $\hat{\underline{x}}(t) = (\underline{x}_1(t), \underline{x}_2(t))$ in $\hat{\underline{x}}$ -space. Re and Pe are assumed large. If the particle separation is large it seems likely, as in the one particle case, that the effect of molecular diffusion on the motion of the particle-pair is negligible in comparison to the effect of the turbulence. At large separations the fluid viscosity ν also has a negligible effect on the pair's motion because ν affects only the small scale components of the turbulence. When the particles are close together however, $\underline{u}_e(\underline{x}_1, t) \approx \underline{u}_e(\underline{x}_2, t)$ and so molecular diffusion can have a significant effect on the particle separation; indeed, as noted above, if the two particles are coincident they can only separate by molecular processes. Also ν influences the small scale components of the turbulence strongly and so will affect the motion of the particle-pair when the separation is sufficiently small. In some ways

this situation is analogous to the case of the motion of single particles in a flow with a boundary, although the analogy is not exact. In more detail, there is, adjacent to the "surface" $\underline{x}_1 = \underline{x}_2$ in $\underline{\hat{x}}$ -space, a "layer" in which viscosity affects the velocity field. The thickness of this layer depends on ν and is much less than the outer length-scale of the turbulence. Also particle-pairs cannot migrate across this layer without the aid of molecular diffusion.

In the previous paragraph we have centred our discussion on the motion of particle-pairs rather than on the quantity $\langle c(\underline{x}_1, t)c(\underline{x}_2, t) \rangle$. It has been shown that κ has an important effect on the motion of pairs when they are close together and it follows from (3.6) that κ is likely to have an important effect on $\langle c(\underline{x}_1, t)c(\underline{x}_2, t) \rangle$. It may help to clarify things to remark that it is easy to see directly that κ has a significant effect on $\langle c(\underline{x}_1, t)c(\underline{x}_2, t) \rangle$. For example, in a constant density fluid with no molecular diffusion, the concentration does not change following a fluid element (Chatwin and Sullivan 1979) and hence the integral $\int c^2 d\underline{x}$ is conserved (at least at times when there is no source of contaminant). This is clearly at odds with the observed fact that turbulence does lead to a rapid dilution of contaminant, implying that, in reality, κ has an important effect. The connection between this and the separation of pairs can be seen from (3.11) - if coincident particle-pairs cannot separate, (3.11) implies that $\int c^2 d\underline{x}$ is conserved in constant density flows (at least at times when there is no source of contaminant). In terms of the concentration field $c(\underline{x}, t)$, the effect of κ is to smooth out the strong gradients of concentration which form as a result of the distortion of the cloud of contaminant by advection (Monin and Yaglom 1971, pp592-593).

How small must the particle separation be for the effect of κ or ν on the motion of a pair of particles to be significant? Let d be the maximum particle separation for which κ or ν has a significant effect

on the motion of the pair of particles. Since we are assuming Re and Pe to be large, d will be much smaller than the outer length-scales of the turbulence. Hence, from Kolmogorov's theory of the universal equilibrium of the small scale components of high Reynolds number turbulence (Monin and Yaglom 1975, chapter 8), d can depend only on κ , ν , and the ensemble average dissipation rate ε . Dimensional analysis then yields $d = f_1(Sc) (\nu^3/\varepsilon)^{1/4}$ where f_1 is a function of the Schmidt number $Sc = \nu/\kappa$. If the particle separation is less than d , then the typical time taken for the particle separation to reach d will also depend only on κ , ν and ε , and will be of order $t_d = f_2(Sc) (\nu/\varepsilon)^{1/2}$ where f_2 is another function of Sc . Once the particles have separated to a distance d any further separation is caused only by the turbulence occurring in the inertial subrange and on larger scales; molecular diffusion no longer plays a significant role in the separation process.

For sufficiently large Re and fixed Sc , d and t_d can be made arbitrarily small compared with the outer length- and time-scales of the turbulence. As in the viscous sub-layer case considered above, it seems reasonable to expect that the precise manner in which the particle separation changes from zero to d (or vice versa) will not be important in calculating $\langle c(\underline{x}_1, t)c(\underline{x}_2, t) \rangle$; provided particles in the model are provided with the means to change their separation from zero to d in a time which is not greatly in excess of t_d , satisfactory results should be achieved. Following Durbin (1980), this can be achieved by ensuring that coincident particles can separate and by assuming that the inertial subrange of the turbulence in the model extends to arbitrarily small scales, so that if the separation of two particles is positive (no matter how small) they can be separated by the inertial subrange turbulence. The time required for inertial subrange turbulence to separate two particles to a distance d is, on dimensional grounds, of order $(d^2/\varepsilon)^{1/3}$ which is, for fixed Sc , of order t_d . In a sense this procedure can be regarded as modelling not

the real flow, but the flow which would occur in the limit $Re \rightarrow \infty$ with Sc and the outer length- and time-scales fixed. We will call this the high Reynolds number limit.

An alternative way to justify this procedure is as follows. First note that, for fixed values of Sc and the outer length- and time-scales, the form of $\langle c(\underline{x}_1, t)c(\underline{x}_2, t) \rangle$ for separations $|\underline{x}_1 - \underline{x}_2|$ much greater than the Kolmogorov length-scale $(\nu^3/\epsilon)^{1/4}$ is insensitive to the Reynolds number. Also the fractional change in $\langle c(\underline{x}_1, t)c(\underline{x}_2, t) \rangle$ as $|\underline{x}_1 - \underline{x}_2|$ changes from the Kolmogorov scale to zero (with \underline{x}_1 , say, fixed) is, for sufficiently large Re and fixed Sc , a negligible fraction of $\langle c(\underline{x}_1)^2 \rangle$. These two results follow from the theory of the small scale structure of scalar fields (Batchelor 1959; Batchelor, Howells and Townsend 1959; Monin and Yaglom 1975, §§21.6 and 22.4). It follows that the form of $\langle c(\underline{x}_1, t)c(\underline{x}_2, t) \rangle$ will converge to a limit in the limit $Re \rightarrow \infty$ and, if the true Reynolds number is sufficiently high, the form of $\langle c(\underline{x}_1, t)c(\underline{x}_2, t) \rangle$ in this limit will be a good approximation to reality.

It should be pointed out that these arguments break down when considering measurements of $\langle c(\underline{x}_1, t)c(\underline{x}_2, t) \rangle$ at points close to small sources (i.e. points where the travel time from a source whose size is of order d or less is of order t_d or less). The precise value of κ is clearly important in such cases, as it would be for short range dispersion from a source in a viscous sub-layer.

The above arguments suggest that for sufficiently high Re there is no need to consider explicitly the effects of viscosity and molecular diffusivity. The arguments can hardly be called rigorous, but are very suggestive. Some support for the conclusion has been obtained from the two-particle model of Sawford and Hunt (1986) which includes diffusive and viscous effects explicitly. This model also gives an indication of how large Re must be (for a given Sc) for the high Reynolds number

limit to be a good approximation. However Sawford and Hunt's model is based on that of Durbin (1980) which, as will be seen below, is not completely satisfactory. It would be of interest to repeat their work with a model based on that described in §5.4 below, although the following argument suggests that all random walk models of the type considered here (both one- and two-particle) may have difficulties in providing a good explicit representation of viscous and diffusive effects. Firstly note that the arguments which led us to expect models of the form (4.1) and (5.1) to be able to give a good description of dispersion depended on the fact that the particle accelerations are weakly correlated over times much in excess of τ_η . Over short times of the order of τ_η (the time-scale on which viscous and diffusive processes act) the particle acceleration correlations cannot be assumed small. Secondly, the usual way to include molecular diffusivity in a random walk model is, as in (A.1), to add a term representing the random molecular motion of a particle or pair of particles to (4.1a) or (5.1a) as appropriate (Durbin 1982; Sawford and Hunt 1986). For simplicity consider the one-particle case. Then (4.1) becomes

$$dX^i = U^i dt + (2\kappa)^{1/2} d\zeta'^i$$

$$dU^i = a^i(\underline{X}(t), \underline{U}(t), t) dt + b^{ij}(\underline{X}(t), \underline{U}(t), t) d\zeta^j.$$

where ζ' is a Wiener process independent of ζ . In homogeneous turbulence, \underline{a} and \underline{b} must be independent of $\underline{X}(t)$ and so the displacement of a model particle is simply the sum of the displacements which would result from the molecular and turbulent processes acting separately. Hence the model cannot represent the destructive interference between the two processes discussed by Saffman (1960). In addition such models cannot satisfy all the criteria discussed in §4.2. For example, for the above model the well-mixed condition (§4.2(ii)) takes the form

$$\frac{\partial \tilde{g}_\rho}{\partial t} = i \frac{\partial^2 \tilde{g}_\rho}{\partial x^i \partial \theta^i} + \tilde{\psi}_{\underline{X}}(\tilde{g}_\rho) + \frac{\partial^2}{\partial x^i \partial x^i} (\kappa \tilde{g}_\rho)$$

while demanding that the velocity distribution evolves correctly at

small times (§4.2(iii)) requires the condition

$$\frac{\partial \tilde{g}_\rho}{\partial t} = i \frac{\partial^2 \tilde{g}_\rho}{\partial x^i \partial \theta^i} + \tilde{\Psi}_{\underline{x}}(\tilde{g}_\rho) - \frac{\partial^2}{\partial x^i \partial x^i} (\kappa \tilde{g}_\rho)$$

to be satisfied (here we have assumed ρ is constant for simplicity). If g_ρ varies with position these conditions are incompatible. The above suggests that, although random walk models may be able to provide a satisfactory representation of dispersion by large scale and inertial subrange eddies, they are not well suited to modelling viscous and diffusive processes.

5.4 A New Two-Particle Model Applicable to Dispersion in High Reynolds Number Constant Density Isotropic Turbulence.

In this section the ideas discussed above are used to derive a model for the motion of particle-pairs. For simplicity we consider only isotropic constant density flows and always refer to a reference frame moving with the mean velocity. The Reynolds number is assumed to be large. This means, as indicated in the discussion in §5.3 above, that molecular diffusion can be neglected except when the two particles are coincident, and the inertial subrange of the turbulence can be assumed to extend to arbitrarily large wave numbers. Except when the particles are coincident, the particles can be assumed to move at the local fluid velocity, i.e. as if they are fluid elements.

It is convenient in the following to denote the first three components of $\hat{\underline{u}}_e$ by \underline{u}_{e1} and the last three by \underline{u}_{e2} so that $\hat{\underline{u}}_e = (\underline{u}_{e1}, \underline{u}_{e2})$. Also, it is often convenient, following Durbin (1980), to use a rotated coordinate system in the six-dimensional $\hat{\underline{x}}$ -space, in which the components of a point $\hat{\underline{x}} = (\underline{x}_1, \underline{x}_2)$ are related to the components of the separation vector $\underline{x}_1 - \underline{x}_2$ and the centroid $\underline{x}_1 + \underline{x}_2$. If we define $\Delta \underline{x} = (\underline{x}_1 - \underline{x}_2)/\sqrt{2}$ and $\Sigma \underline{x} = (\underline{x}_1 + \underline{x}_2)/\sqrt{2}$, then, in the new rotated coordinate system, $\hat{\underline{x}} = (\Delta \underline{x}, \Sigma \underline{x})$. Similarly it is useful in phase space to define $\Delta \underline{u} = (\underline{u}_1 - \underline{u}_2)/\sqrt{2}$ and $\Sigma \underline{u} = (\underline{u}_1 + \underline{u}_2)/\sqrt{2}$, so that, in the rotated

coordinate system, $\hat{\underline{u}} = (\Delta\underline{u}, \Sigma\underline{u})$. In the same way we can define $\Delta\underline{u}_e = (\underline{u}_{e1} - \underline{u}_{e2})/\sqrt{2}$, $\Sigma\underline{u}_e = (\underline{u}_{e1} + \underline{u}_{e2})/\sqrt{2}$, $\Delta\underline{x} = (\underline{x}_1 - \underline{x}_2)/\sqrt{2}$, $\Sigma\underline{x} = (\underline{x}_1 + \underline{x}_2)/\sqrt{2}$, $\Delta\underline{U} = (\underline{U}_1 - \underline{U}_2)/\sqrt{2}$ and $\Sigma\underline{U} = (\underline{U}_1 + \underline{U}_2)/\sqrt{2}$. It follows that, in the rotated coordinate system, the Eulerian velocity in the six-dimensional space is given by $\hat{\underline{u}}_e = (\Delta\underline{u}_e, \Sigma\underline{u}_e)$ and the position and velocity of a particle-pair are given by $\hat{\underline{x}} = (\Delta\underline{x}, \Sigma\underline{x})$ and $\hat{\underline{U}} = (\Delta\underline{U}, \Sigma\underline{U})$. In the sequel, $\Delta\underline{x}$ will often, for simplicity, be referred to as "the particle separation", ignoring the factor $1/\sqrt{2}$.

As indicated above, $\hat{\underline{a}}$ and $\hat{\underline{B}}$ will be selected by applying the theoretical ideas described in chapter 4 and §5.2. In order to apply these ideas we need to assume a form for the density function \hat{g}_p . For simplicity, the two-point velocity distributions, which determine \hat{g}_p up to a multiplicative constant in a constant density flow, are assumed to be Gaussian with

$$\begin{aligned} \langle u_{e1}^i u_{e1}^j \rangle &= \langle u_{e2}^i u_{e2}^j \rangle = \sigma^2 \delta^{ij} \\ \langle u_{e1}^i u_{e2}^j \rangle &= \langle u_{e2}^i u_{e1}^j \rangle = \sigma^2 R^{ij}(\Delta\underline{x}) \end{aligned} \quad (5.4)$$

or, equivalently,

$$\begin{aligned} \langle \Delta u_e^i \Delta u_e^j \rangle &= \sigma^2 (\delta^{ij} - R^{ij}(\Delta\underline{x})) \\ \langle \Sigma u_e^i \Sigma u_e^j \rangle &= \sigma^2 (\delta^{ij} + R^{ij}(\Delta\underline{x})) \\ \langle \Delta u_e^i \Sigma u_e^j \rangle &= 0 \end{aligned} \quad (5.5)$$

where \underline{R} is the two-point velocity correlation tensor. Because we are assuming the flow to be of constant density, $\partial R^{ij} / \partial \Delta x^j = 0$ (Batchelor 1953, p27) and, since \underline{R} is assumed isotropic, it can be written in the form

$$R^{ij} = F(\Delta) \Delta x^i \Delta x^j + G(\Delta) \delta^{ij}$$

where $\Delta = |\Delta\underline{x}|$ and F and G satisfy $4F + \Delta \partial F / \partial \Delta + (1/\Delta) \partial G / \partial \Delta = 0$. Following Durbin (1980) we take the longitudinal correlation function, $f = F\Delta^2 + G$, to be

$$f = 1 - (\Delta^2/(\Delta^2 + l^2))^{1/3}. \quad (5.6)$$

This form is qualitatively reasonable and gives the correct inertial subrange form at small Δ . The integral scale L of f , $\int f(\Delta) d(\Delta/2)$, is equal to 1.061. In the inertial subrange $f = 1 - C(\epsilon\Delta/2)^{2/3}/(2\sigma^2)$ (Monin and Yaglom 1975, p353) where C is the Kolmogorov constant which is taken here to be 2.0 (Monin and Yaglom 1975, p485). Hence, in terms of σ^2 and ϵ , $l = \sigma^3/(\epsilon/2)$. This is consistent with the longitudinal integral scale being of order $0.8\sigma^3/\epsilon$ (Townsend 1976, p61). F and G can be calculated from f . The six-dimensional covariance tensor $\langle \hat{u}_e^i \hat{u}_e^j \rangle$ will be denoted by \hat{V}_e^{ij} . The various components of \hat{V}_e are given, in the (x_1, x_2) coordinate system, by (5.4) and, in the rotated $(\Delta x, \Sigma x)$ coordinate system, by (5.5). In reality \hat{g}_p is not Gaussian, especially when Δ is small (Batchelor 1953, pp170-173), and it is hard to assess the error incurred by assuming that it is. This deserves further investigation. (Of course the model does not assume that the velocity and concentration fields are jointly Gaussian and allows the mixed velocity-concentration two-point third-order moments to be non-zero. This is essential in any model of $\langle c^2 \rangle$ since $\langle c(x_1)c(x_2)\hat{u}_e(\hat{x}) \rangle = \langle \hat{c}(\hat{x})\hat{u}_e(\hat{x}) \rangle$ represents the flux of pairs of contaminant particles in \hat{x} -space.)

From §4.2(ii) and the discussion in §5.2 above, it is clear that in order to satisfy the well-mixed condition it is necessary for \hat{a} to satisfy

$$\hat{a}^i \hat{g}_p = \partial(\hat{B}^{ij} \hat{g}_p) / \partial \hat{u}^j + \hat{\phi}^i \quad (5.7)$$

where $\hat{\phi}$ satisfies

$$\partial \hat{\phi}^i / \partial \hat{u}^i = - \partial \hat{g}_p / \partial t - \partial(\hat{u}^i \hat{g}_p) / \partial \hat{x}^i \quad (5.8)$$

and

$$\hat{\phi} \rightarrow 0 \text{ as } |\hat{u}| \rightarrow \infty. \quad (5.9)$$

For our value of \hat{g}_p ,

$$\frac{\hat{\phi}^i}{\hat{g}_p} = \frac{1}{2} \frac{\partial \hat{V}_e^{i1}}{\partial \hat{x}^1} + \frac{1}{2} (\hat{V}_e^{-1})^{1j} \frac{\partial \hat{V}_e^{i1}}{\partial t} \hat{u}^j + \frac{1}{2} (\hat{V}_e^{-1})^{1j} \frac{\partial \hat{V}_e^{i1}}{\partial \hat{x}^k} \hat{u}^j \hat{u}^k \quad (5.10)$$

is perhaps the simplest choice of $\hat{\phi}$ satisfying (5.8) and (5.9) (see equation (4.30)). In our situation the term $\frac{1}{2} \partial \hat{V}_e^{i1} / \partial \hat{x}^1$ is in fact zero because of the constant density constraint on \underline{R} .

\hat{B} remains to be chosen. In choosing \hat{B} for our two-particle model we will be guided by the one-particle case discussed in §4.3 and also by the ideas about the motion of particle-pairs discussed by Novikov (1963) and Monin and Yaglom (1975, p573). In high Re flows the acceleration correlation function is short-ranged in space as well as time (Monin and Yaglom 1975, §21.5) and so the acceleration of any particle is only weakly correlated with that of any other. However the accelerations cannot be completely independent or, at large times, all the particles would be moving independently. In (5.1), the acceleration of the first particle in a pair of particles consists of two parts, \hat{a}^i and $\hat{b}^{ij} d\zeta^j/dt$, $i = 1, 2, 3$. It seems reasonable to suppose that the part of the acceleration which is uncorrelated from one moment to the next, namely $\hat{b}^{ij} d\zeta^j/dt$, is also uncorrelated with the position, velocity or acceleration of the other particle. Also, for simplicity and consistency with inertial subrange theory, we would like \hat{B} to be independent of \underline{u} (see §4.3 for a discussion of the analogous one particle case). Together with the assumed isotropy of the turbulence, this leads to the choice $\hat{B}^{ij} = \hat{B} \delta^{ij}$. Because \hat{B} represents the high frequency part of the acceleration, \hat{B} should depend only on ε , i.e. $\hat{B} = \frac{1}{2} C_0 \varepsilon$ for some C_0 . (5.1) then implies that the one-particle Lagrangian structure function $D^{ij} = \langle (U_1^i(t) - U_1^i(s))(U_1^j(t) - U_1^j(s)) \rangle$ (the average here being over particles with a given position at time s or, equivalently, over all particle-pairs with a given $\underline{X}_1(s)$) takes the form $C_0 \varepsilon \delta^{ij} (t-s)$ for small time intervals $t-s$, as in the case of one-particle models (see §4.3(ii)). Hence, as in the one-particle

case, C_0 can be identified with the universal constant occurring in the inertial subrange part of \underline{D} . As noted in §4.3(ii), C_0 lies in the range 4.0 ± 2.0 (Hanna 1981). In the calculations presented below, C_0 will be taken to be 4.0. The above derivation of the form of $\hat{\underline{B}}$ can be understood more informally by noting that the high frequency part of the acceleration, being independent from particle to particle, should take the same form as in the one-particle case discussed in §4.3(ii). In the following \hat{B} will often be written as σ^2/τ . It will be shown below that τ can be interpreted as a Lagrangian time-scale. Because $\hat{\underline{B}}$ remains constant as $\Delta \rightarrow 0$ the model allows coincident particles to separate and no special measures are needed to ensure this. With the above value of $\hat{\underline{B}}$ and with $\hat{\underline{\phi}}$ given by (5.10), (5.7) becomes

$$\hat{a}^i = -\frac{\sigma^2}{\tau} (\hat{\underline{v}}_e^{-1})^{ij} \hat{u}^j + \frac{1}{2} (\hat{\underline{v}}_e^{-1})^{1j} \frac{\partial \hat{v}_e^{i1}}{\partial t} \hat{u}^j + \frac{1}{2} (\hat{\underline{v}}_e^{-1})^{1j} \frac{\partial \hat{v}_e^{i1}}{\partial x^k} \hat{u}^j \hat{u}^k.$$

To complete the specification of the model, we note that the initial value of $\hat{\underline{U}}$ for a particle-pair commencing at $(\underline{y}_1, \underline{y}_2)$ at time s is chosen at random from the two-point velocity distribution at $(\underline{y}_1, \underline{y}_2)$.

When the particles are far apart, the particles move independently and the motion of a single particle obeys the stochastic differential equations

$$d\underline{X}_1 = \underline{U}_1 dt \tag{5.11}$$

$$d\underline{U}_1 = \left(-\frac{1}{\tau} + \frac{1}{\sigma} \frac{\partial \sigma}{\partial t} \right) \underline{U}_1 dt + \sigma \left(\frac{2}{\tau} \right)^{1/2} d\underline{\zeta}.$$

This is an appropriate model for the motion of a single particle in isotropic Gaussian turbulence and, from the results given in §4.4, satisfies a one-particle version of the well-mixed condition. (5.11) can be expressed more simply as

$$d\underline{X}_1 = \sigma \tilde{\underline{U}}_1 dt \tag{5.12}$$

$$d\tilde{\underline{U}}_1 = -(\tilde{\underline{U}}_1/\tau) dt + (2/\tau)^{1/2} d\underline{\zeta}$$

where $\tilde{\underline{U}}_1 = \underline{U}_1/\sigma$. In stationary situations this is simply a

three-dimensional version of the Langevin equation and so $\langle U_1^i(t)U_1^j(s) \rangle = \sigma^2 \delta^{ij} \exp(-(t-s)/\tau)$. Hence τ is the Lagrangian integral time-scale of the model. $C_0 = 4.0$ implies $\tau\sigma/L = 0.67$ which is within the scatter of observed values (Pasquill and Smith 1983, §2.7). In non-stationary conditions τ is not the integral time-scale, but is simply a measure of the time-scale on which particle velocities become decorrelated.

The above model has been designed to be consistent with the assumed form of \hat{g}_p and can claim to be more faithful in this respect than previous models. However it is not completely satisfactory as it ignores one aspect of the field $\hat{u}_e(\hat{x}, t)$ which is not reflected in \hat{g}_p , namely the fact that u_{e1} does not depend on x_2 and u_{e2} does not depend on x_1 (as discussed in §5.2). In particular, the model trajectories do not satisfy (5.2). For example consider the evolution of $\langle U_1^i(t)U_1^i(t) \rangle$ and $\langle U_2^i(t)U_2^i(t) \rangle$ for particle-pairs with position (y_1, y_2) in \hat{x} -space at time s . If $|y_1 - y_2| \gg l$, the particles move according to (5.11) and it follows that

$$\langle U_1^i(t)U_1^i(t) \rangle = \langle U_2^i(t)U_2^i(t) \rangle = 3\sigma^2. \quad (5.13)$$

If the model is to satisfy (5.2), then (5.13) must be true for all initial separations and hence $\langle \hat{U}^i(t)\hat{U}^i(t) \rangle = 6\sigma^2$ for all initial separations. However, using either the Fokker-Planck equation or Itô's formula for the system (5.1), the above model yields

$$\begin{aligned} \langle \hat{U}^i(t)\hat{U}^i(t) \rangle = 6\sigma^2 - \sigma^4 \left(F\Delta^2(2\Delta dF/d\Delta + 5F) \right)_{\Delta=|y_1-y_2|/\sqrt{2}}(t-s)^2 + \\ + O((t-s)^3), \end{aligned} \quad (5.14)$$

showing that the model trajectories do indeed violate (5.2) (it is easy to see that $F\Delta^2(2\Delta dF/d\Delta + 5F)$ cannot be identically zero).

It is of interest to ask if the model can be modified to satisfy (5.2) and the well-mixed condition by choosing a different form for $\hat{\phi}$ (the physical reasoning leading to the choice of \hat{B} given above is strong and so we do not wish to alter the form of \hat{B}). Although it may

be possible to choose $\hat{\phi}$ so that $\langle \hat{U}^i(t)\hat{U}^i(t) \rangle$ is correct to order $(t-s)^2$, the author thinks it is unlikely that $\hat{\phi}$ can be chosen so that $\langle \hat{U}^i(t)\hat{U}^i(t) \rangle$ is correct to all orders, and hence even less likely that $\hat{\phi}$ can be chosen so that (5.2) is satisfied. The author has however been unable to prove the impossibility of satisfying both (5.2) and the well-mixed condition.

Although the fact that the model violates (5.2) is a little unsatisfactory in principle, the results of a number of numerical simulations, presented below, suggest that this is not too serious in practice.

In the calculations of mean and mean square concentration presented in chapter 6 below, it is convenient to follow the particles backwards and to use (3.11) (with ρ assumed constant) to calculate $\langle c^2 \rangle$ at a point (the point from which the trajectories start). When the trajectories are evaluated in the forward direction, only the mean square of c averaged over some finite sample volume can be obtained since a large number of pair trajectories need to pass through the receptor to reduce statistical error. For the isotropic Gaussian turbulence considered in this paper the calculation of the reverse trajectories is straightforward. Let $(\hat{\underline{X}}'(t), \hat{\underline{U}}'(t))$ denote the ensemble of forward trajectories starting at $(\hat{\underline{y}}, -\hat{\underline{v}})$ at time $-s$ calculated from the model with $\sigma(t)$, $l(t)$, $\varepsilon(t)$ and $\tau(t)$ replaced by $\sigma(-t)$, $l(-t)$, $\varepsilon(-t)$ and $\tau(-t)$ respectively. The theory presented in §4.2(v) implies that the ensemble of trajectories $(\hat{\underline{X}}(t), \hat{\underline{U}}(t)) = (\hat{\underline{X}}'(-t), -\hat{\underline{U}}'(-t))$ is the required ensemble of backwards trajectories starting at $(\hat{\underline{y}}, \hat{\underline{v}})$ at time s .

5.5 Some Previously Proposed Two-Particle Models.

It is appropriate to compare the above model with some of the models that have been proposed previously, and which were described briefly in §5.1. In this section several such models will be described and some of their basic properties discussed. A more detailed comparison of these models with the new model described in §5.4 will be given in the next section where the values of the two-particle transition p.d.f.s for the various models will be compared.

The first model which we will consider is Richardson's (1926) model. In this model it is assumed that the p.d.f. of the separation of a pair of particles which have separation Δy at time s , i.e. $p_{\Delta X}(t) | \Delta X(s) (\Delta x | \Delta y)$, satisfies the equation

$$\frac{\partial p}{\partial t} = \frac{\partial}{\partial \Delta x^i} \left(K \frac{\partial p}{\partial \Delta x^i} \right)$$

where K , the diffusivity, is proportional to $\Delta^{4/3}$. This assumption can of course also be formulated in terms of a stochastic differential equation for the evolution of the separation $\Delta X(t)$. It is of interest that the new model presented above reduces to this form if we (i) allow C_0 to tend to infinity, (ii) consider only the particle separation and not the centroid motion, and (iii) restrict attention to inertial subrange separations. The reason that the new model reduces to a model of the same form as Richardson's is that, as $C_0 \rightarrow \infty$, the random increments $b^i d\zeta^j$ become large and cause the particle velocities to vary rapidly. As a result the analysis given in §4.2(vi) applies and shows that the model reduces to a diffusion equation model. The analysis also gives a value for the particle separation diffusivity K of $(3.17/C_0) \epsilon^{1/3} \Delta^{4/3}$, where, as indicated in §5.4, we have taken the Kolmogorov constant C equal to 2.0. In the references to Richardson's model given below it will be assumed that K has this value.

The second model which we will consider is perhaps the simplest two-particle model that can be expressed in the form (5.1). It is defined as follows. For a pair of particles originating at position $(\underline{y}_1, \underline{y}_2)$ in $\underline{\hat{x}}$ -space at time s , choose the initial velocities to be correlated, with $\langle U_1^i(s) U_2^j(s) \rangle = \sigma^2 R^{ij} ((\underline{y}_1 - \underline{y}_2) / \sqrt{2})$. To be consistent with the assumptions about \hat{g}_p made in §5.4, we choose $\underline{U}_1(s)$ and $\underline{U}_2(s)$ to be jointly Gaussian. Subsequently each particle moves independently according to (5.11). We will call this the NGLS model since it owes much to the ideas of Novikov (1963), Gifford (1982) and Lee and Stone (1983) (see also Lin and Reid (1963)), although it is not identical to the models proposed by these authors. For example, Novikov (1963) only makes assumptions about the second moments of quantities while Gifford (1982) and Lee and Stone (1983) only consider the component of the motion in one direction, restrict consideration to stationary conditions and do not make any specific assumption about the form of the initial velocity distribution. In addition the models of Gifford (1982) and Lee and Stone (1983) were intended to be used for following clusters of particles rather than just two particles, but can of course be applied to the problem of the dispersion of particle-pairs. We will adopt the NGLS model as a representative example of the class of models which yield a Gaussian p.d.f. for the separation of a pair of particles which are initially coincident (i.e. the models of Lamb (1981), Sawford (1982), Gifford (1982) and Lee and Stone (1983)).

The NGLS model has the advantage of satisfying (5.2); indeed, together with a number of variants, it is the only model of the form (5.1) proposed to date which satisfies (5.2). However it does not satisfy the well-mixed condition, at least not with any physically reasonable form for \hat{g}_p ; if the two particles approach closely at some time after release, the model will not ensure that they have similar velocities. Of course the NGLS equations for the evolution of the particle-pair trajectories are consistent with the form $\hat{g}_p \propto$

$\sigma^{-6} \exp(-\hat{u}^i \hat{u}^i / 2\sigma^2)$, but this form is unrealistic in that it implies zero correlation between velocities at neighbouring points. Also the initial velocity distribution of the particle-pairs is not consistent with this form.

The third model which we will consider is based on the one-dimensional model proposed by Durbin (1980), a model which has been discussed and applied more widely in recent years than any other (Durbin 1982; Sawford 1983, 1985; Egbert and Baker 1984; Sawford and Hunt 1986; Thomson 1986b). Here we will consider the extension of this model to non-stationary conditions (suggested by Durbin and reported in Stapountzis et al (1986)). This extension takes the form

$$\begin{aligned}
 d\Delta X &= \Delta\tilde{U} \sigma (1-f)^{1/2} dt \\
 d\Sigma X &= \Sigma\tilde{U} \sigma (1+f)^{1/2} dt \\
 d\Delta\tilde{U} &= - (\Delta\tilde{U}/\tau) dt + (2/\tau)^{1/2} d\zeta \\
 d\Sigma\tilde{U} &= - (\Sigma\tilde{U}/\tau) dt + (2/\tau)^{1/2} d\zeta'
 \end{aligned}
 \tag{5.15}$$

where $\Delta\tilde{U} = \Delta U / (\sigma(1-f)^{1/2})$, $\Sigma\tilde{U} = \Sigma U / (\sigma(1+f)^{1/2})$, ζ and ζ' are independent Wiener processes and the correlation function f has the form (5.6). In the same way as (5.11) was expressed in the form (5.12), it is straightforward to express Durbin's model in the form (5.1), although the equations then appear more complex. The initial values of $\Delta\tilde{U}$ and $\Sigma\tilde{U}$ are chosen to be independent and Gaussian with variance 1. Because this model is one-dimensional, it is appropriate to comment on the physical interpretation of ΔX and ΣX . In most of the applications of the model that have been made to date (Durbin 1980; Sawford 1983, 1985; Sawford and Hunt 1986), the values of ΔX and ΣX are interpreted as the values of one component (say the x-component) of $\Delta\underline{X}$ and $\Sigma\underline{X}$, and attention is restricted to source distributions which are homogeneous in the y- and z-directions (for more general source distributions, the second moments of the concentration cannot be calculated without knowledge of the distributions of the other

components of $\Delta \underline{x}$ and $\Sigma \underline{x}$).

Like the NGLS model, Durbin's model does not satisfy the well-mixed condition, at least not with a form of \hat{g}_ρ which is consistent with ρ being constant; indeed if the contaminant is initially uniform in space (in every realisation), then the model (5.15) predicts that the mean square concentration will be infinite at all times after release (Sawford 1983; Egbert and Baker 1984). Durbin gets round this problem by using the above model to calculate backwards trajectories (with t in (5.15) interpreted as running in the opposite direction to real time) and by using the equation

$$\begin{aligned} \langle c(\underline{x}_1, t_1) c(\underline{x}_2, t_2) \rangle &= \int_{s_1 \leq t_1, s_2 \leq t_2} p_{\underline{x}_1(s_1), \underline{x}_2(s_2) | \underline{x}_1(t_1), \underline{x}_2(t_2)}(\underline{y}_1, \underline{y}_2 | \underline{x}_1, \underline{x}_2) \times \\ &\quad \times \langle S(\underline{y}_1, s_1) S(\underline{y}_2, s_2) \rangle d\underline{y}_1 d\underline{y}_2 ds_1 ds_2 \end{aligned} \quad (5.16)$$

to obtain concentration statistics from the trajectory statistics. This automatically ensures that fluctuations will not appear if the initial conditions are well-mixed. As in the NGLS model, there is a form of \hat{g}_ρ which is consistent with Durbin's model, namely

$$\hat{g}_\rho \propto \frac{1}{\sigma^2(1-f)(1+f)^{1/2}} \exp \left(- \frac{(\Delta u)^2}{2\sigma^2(1-f)} - \frac{(\Sigma u)^2}{2\sigma^2(1+f)} \right),$$

but this form implies infinite $\langle \rho^2 \rangle$ ($\langle \rho(\underline{x}_1) \rho(\underline{x}_2) \rangle$ is proportional to $\int \hat{g}_\rho d\underline{u}$). In a compressible flow the reverse formulation in the form (5.16) is not valid and (3.11) should be used instead. By using (5.16), Durbin is effectively assuming that the behaviour of

$$\frac{\langle c(\underline{x}_1, t_1) c(\underline{x}_2, t_2) \rangle}{\langle \rho(\underline{x}_1, t_1) \rho(\underline{x}_2, t_2) \rangle}$$

in a variable density flow is similar to that of $\langle c(\underline{x}_1, t_1) c(\underline{x}_2, t_2) \rangle$ in a constant density flow. Although it seems reasonable that a model which is not completely consistent with ρ being constant can be corrected by this means, it is far from clear that this is adequate for a model with infinite $\langle \rho^2 \rangle$. Thomson (1986b) showed that, in this

model, particle-pairs released at (y_1, y_2) have an initial mean relative acceleration unless $|y_1 - y_2| \gg l$. Hence this model, like the new model presented in §5.4 above, fails to satisfy (5.2).

In the results obtained with the above models presented below, τ , σ , l and ε are assumed to be related as in the new model described in §5.4.

5.6 Properties of the Two-Particle Transition P.D.F. in the Models.

(i) Introduction.

We can learn something about the models described in §§5.4 and 5.5 above by looking at some of the properties of the two-particle transition p.d.f. $P_{\underline{x}_1, \underline{x}_2}(t_1, t_2) | \underline{x}_1(s_1), \underline{x}_2(s_2)$ as predicted by the models. One of the most important quantities that can be calculated from $P_{\underline{x}_1, \underline{x}_2}(t_1, t_2) | \underline{x}_1(s_1), \underline{x}_2(s_2)$ is the distribution of the particle separation $\Delta \underline{x}$. $p_\Delta(\Delta \underline{x}, t | s)$ will be used to denote the p.d.f. of $\Delta \underline{x}$ at time t for particle-pairs with zero separation at time s , i.e.

$$p_\Delta(\Delta \underline{x}, t | s) = P_{\Delta \underline{x}}(t) | \Delta \underline{x}(s) (\Delta \underline{x} | 0).$$

In terms of $P_{\underline{x}_1, \underline{x}_2}(t_1, t_2) | \underline{x}_1(s_1), \underline{x}_2(s_2)$, p_Δ can be expressed as

$$p_\Delta(\Delta \underline{x}, t | s) = \int P_{\underline{x}_1, \underline{x}_2}(t, t) | \underline{x}_1(s), \underline{x}_2(s) ((\underline{x}_1 + \Delta \underline{x})/\sqrt{2}, (\underline{x}_2 - \Delta \underline{x})/\sqrt{2} | 0, 0) d\underline{x}_1.$$

Because we are considering isotropic turbulence, this p.d.f. is a function of $\Delta = |\Delta \underline{x}|$ only and so is sometimes written as $p_\Delta(\Delta, t | s)$ or, if it is clear what values t and s take, as $p_\Delta(\Delta)$. However this is not the p.d.f. of Δ which is equal to $4\pi\Delta^2 p_\Delta(\Delta)$ (here, and also in similar situations below, it is convenient to use Δ to denote both $|\Delta \underline{x}|$ and $|\Delta \underline{X}|$; it should be clear from the context which is meant). The reason why p_Δ is an important quantity is that it has a strong effect on the mean square concentration, with more strongly peaked shapes leading to larger values of the mean square concentration (see Sawford (1983) and

also the discussion of mean square concentration given in chapter 6 below - in particular equations (6.1) and (6.10)). In the same way $p_{\Sigma}(\Sigma_{\underline{x}}, t|s)$ will denote the p.d.f. of $\Sigma_{\underline{x}}$ at time t for particle-pairs with both particles coincident at the origin at time s . This is a function of $\Sigma = |\Sigma_{\underline{x}}|$ only and so will sometimes be written as $p_{\Sigma}(\Sigma, t|s)$. In addition, for particle-pairs with both particles at the origin at time s , the distributions of $X_{\underline{x}1}$, $\Delta X_{\underline{x}}$ and $\Sigma X_{\underline{x}}$ are spherically symmetric. For this case $\sigma_1(t|s)$, $\sigma_{\Delta}(t|s)$ and $\sigma_{\Sigma}(t|s)$ will be used to denote the root mean square value of one component of $X_{\underline{x}1}$, $\Delta X_{\underline{x}}$ and $\Sigma X_{\underline{x}}$ respectively at time t . For one-dimensional models, such as Durbin's (1980), the above definitions do not apply directly. We note here that, in such models, p_{Δ} , p_{Σ} , σ_{Δ} and σ_{Σ} will be used to denote the p.d.f.s and mean square values of ΔX and ΣX for particle-pairs which are coincident at the origin at time s .

In the following we will investigate the properties of the two-particle transition p.d.f. from the new model for both stationary and decaying turbulence. These properties will be compared with the properties of the other models described in §5.5.

(ii) Stationary turbulence.

Let us first consider the idealised case where the turbulence is stationary. Only forward trajectory statistics will be described here; because the flow is stationary, the discussion in §5.4 on the way to calculate backwards trajectories implies that these statistics can also be interpreted as the statistics of backwards trajectories. Figure 5.1(a) shows the p.d.f. of the distribution of $\Delta X_{\underline{x}}$ in the new model at time t for zero separation at time s . Unfortunately, p_{Δ} cannot be calculated analytically and so numerical results are shown. The details of the numerical calculations are given in Appendix C. In fact, in the numerical simulations it is impossible to start with particles which are truly coincident, and so a small initial separation

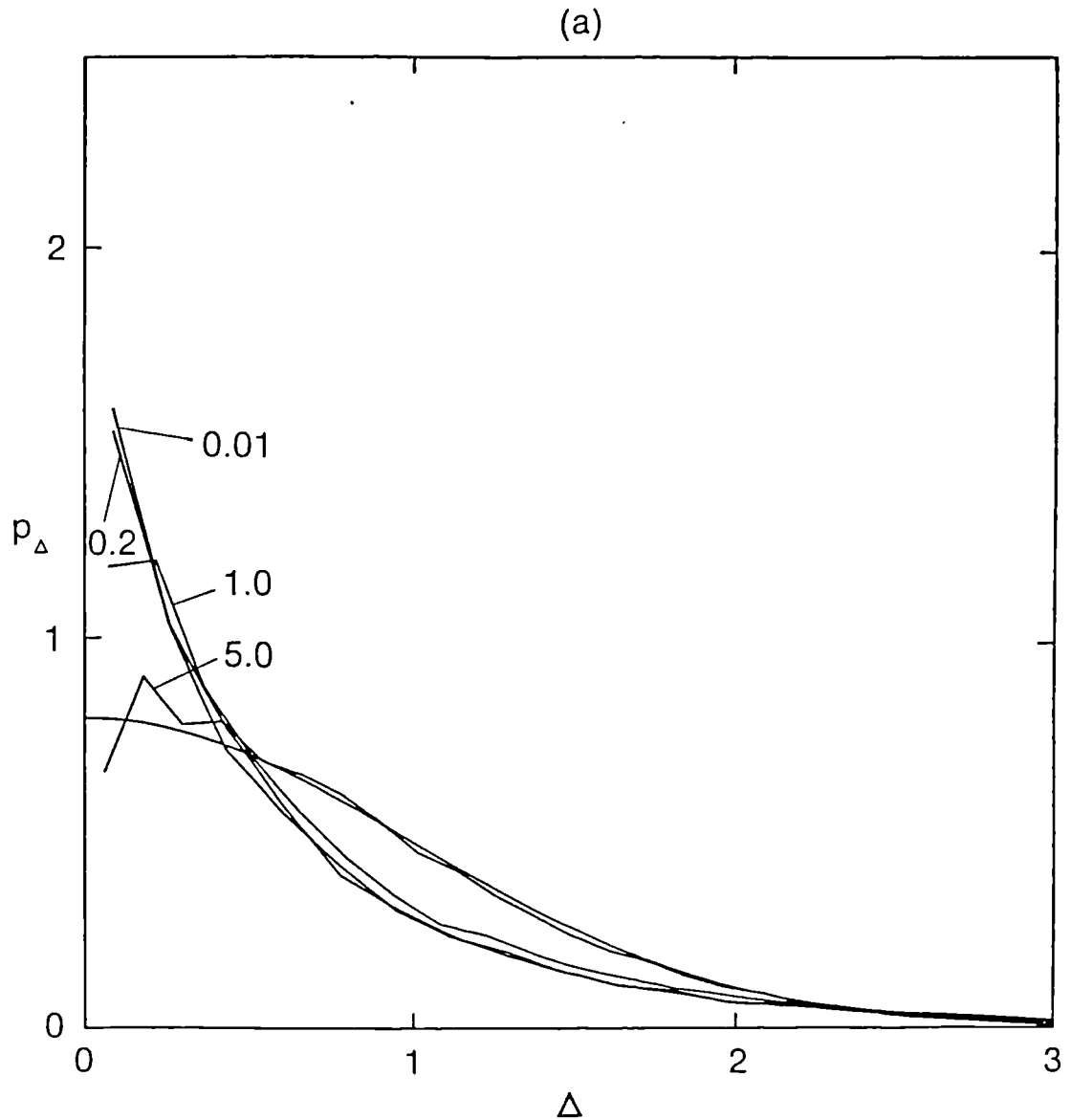


Figure 5.1: The shape of $p_{\Delta}(\Delta, t|s)$ in stationary turbulence. The curves are normalised with zeroth and second moments equal to unity as if they were one-dimensional p.d.f.s. (a), (b), (c), (d) and (e) show the results for the new model: (a) shows the results obtained without "particle splitting", (b) shows results obtained using the particle splitting technique, (c) shows results obtained using the particle splitting technique plotted against $\Delta^{2/3}$ to show the $\alpha-\beta\Delta^{2/3}$ behaviour near $\Delta = 0$, (d) shows $\bar{p}_{\Delta}(\Delta, t|s)$ and (e) shows $\bar{\bar{p}}_{\Delta}(\Delta, t|s)$. (f) shows p_{Δ} from Richardson's (1926) model and (g) shows p_{Δ} from Durbin's (1980) model. In all cases except (f), the numbers attached to the curves indicate values of $t-s$ normalised by σ^2/ϵ , and the unlabelled line is a Gaussian distribution. The shape of p_{Δ} in Richardson's model (figure 5.1(f)) is independent of $t-s$.

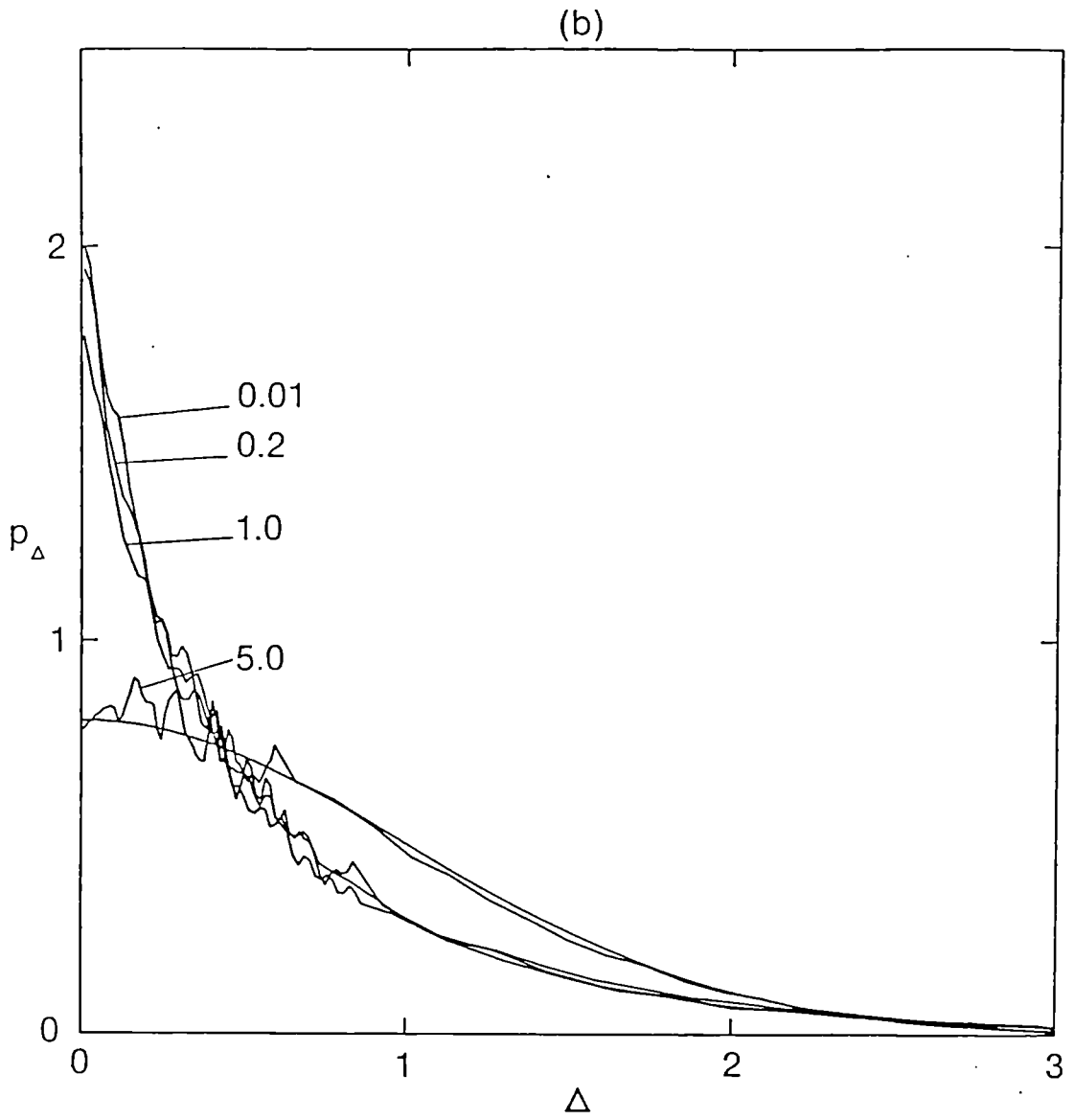


Figure 5.1 continued.

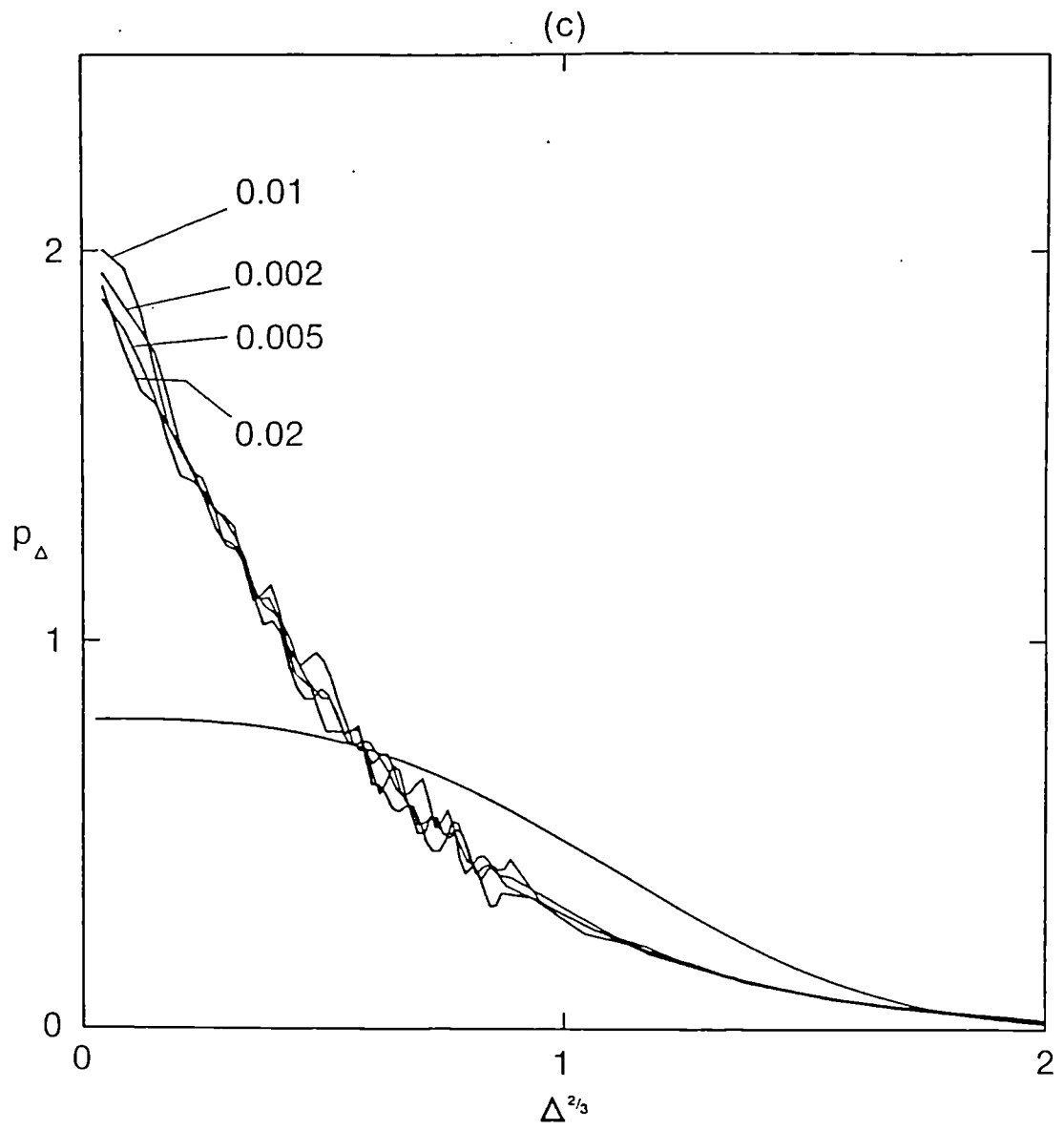


Figure 5.1 continued.

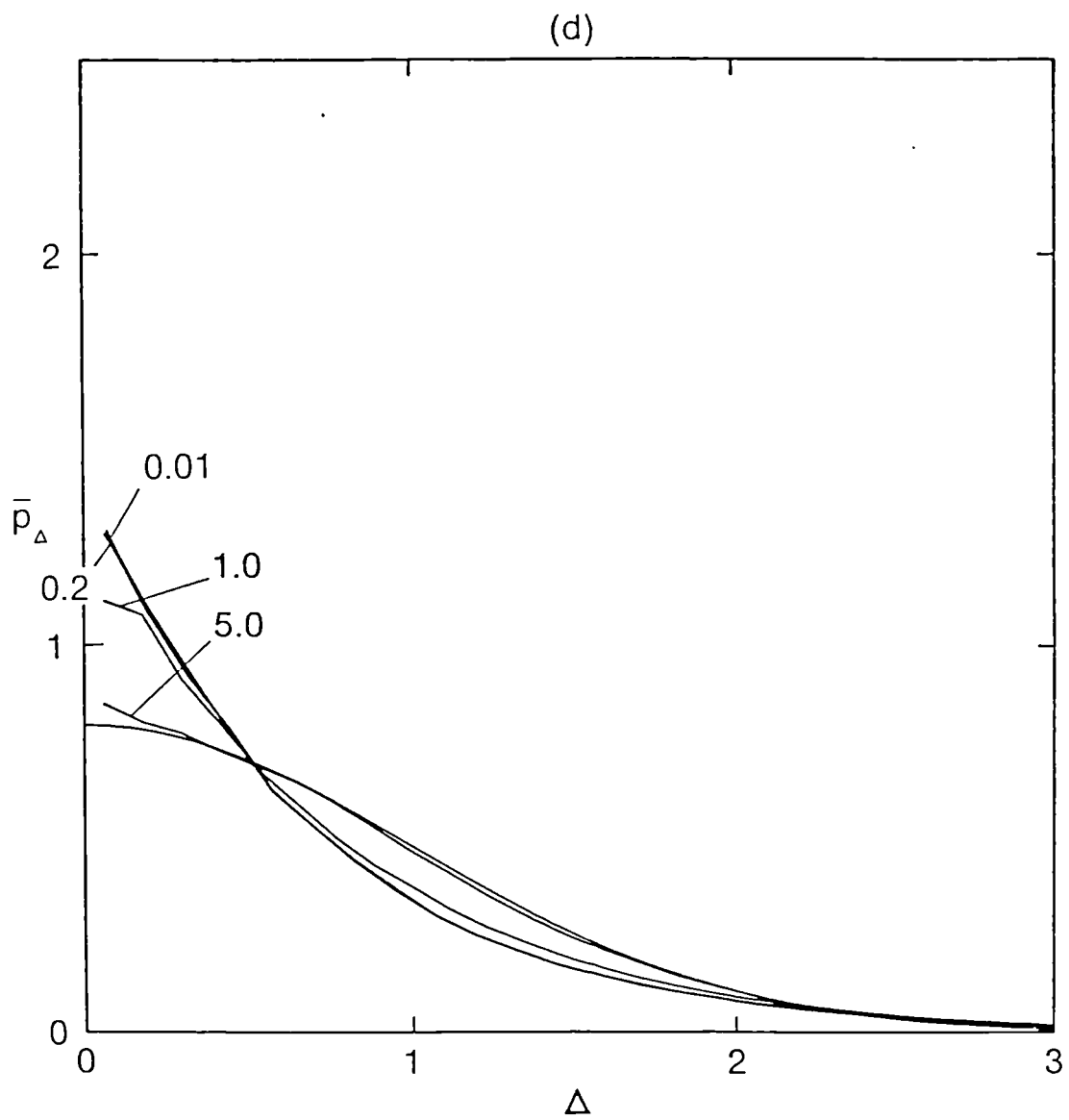


Figure 5.1 continued.

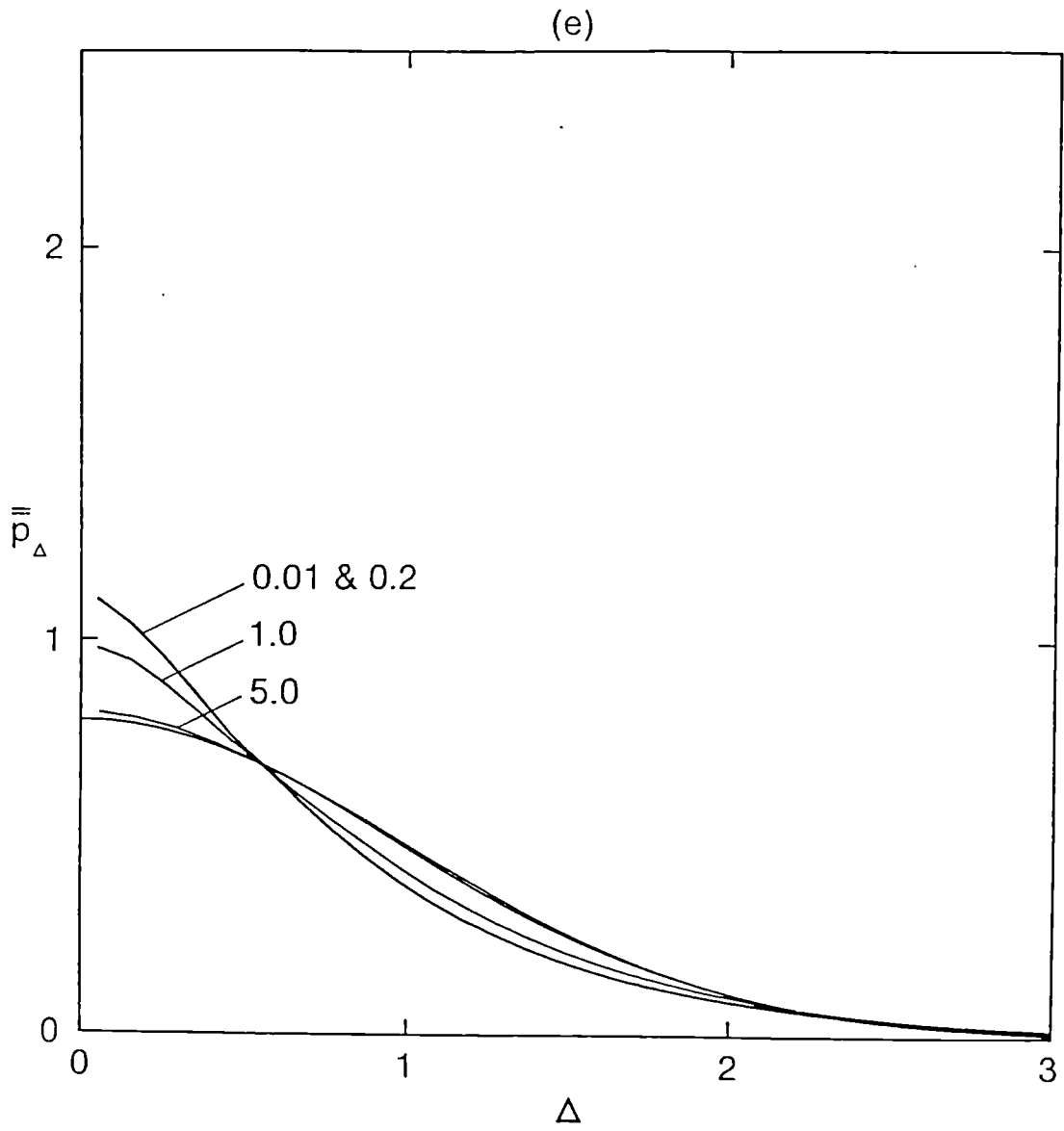


Figure 5.1 continued.

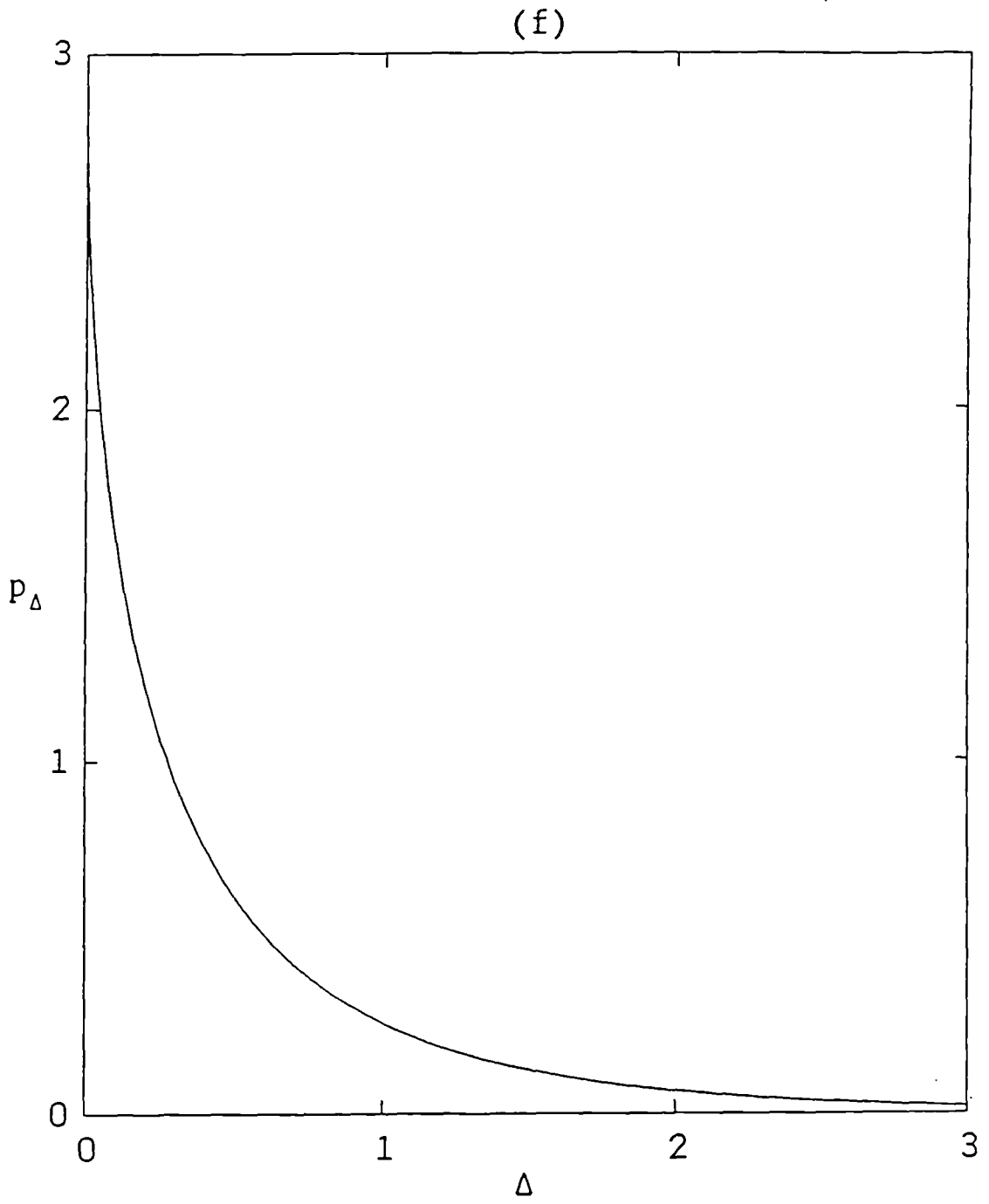


Figure 5.1 continued.

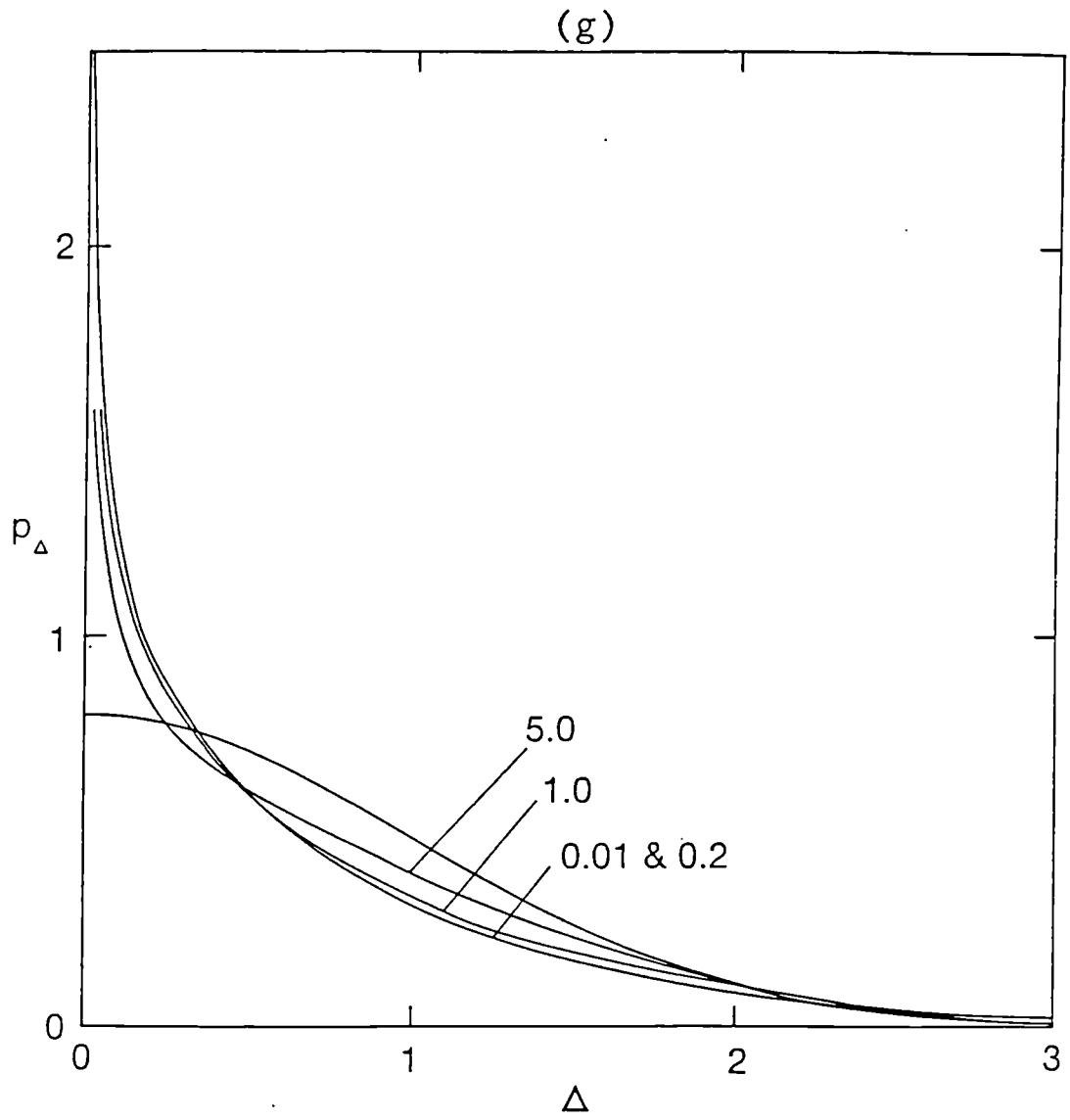


Figure 5.1 continued.

equal to $2 \times 10^{-6} l$ was used. The results are insensitive to changes in this quantity of an order of magnitude. This is discussed further in Appendix C. The curves shown consist of straight lines between a number of data points, each data point representing the average value of p_Δ over a small interval of Δ values. It can be seen that the distribution changes from a strongly peaked distribution to a Gaussian distribution as t increases. This was also observed by Thomson (1986b) using what is essentially a one-dimensional version of the model. At small times, $t-s \ll \tau$, the shape is independent of $t-s$. This is to be expected on dimensional grounds because, from inertial subrange theory, p_Δ should depend only on Δ , $t-s$ and ϵ .

One of the problems of having to calculate p_Δ numerically is that it is very difficult to obtain an accurate value for $p_\Delta(0)$. This is because very few particle-pairs pass sufficiently close to $\Delta = 0$ and so the results show a great deal of statistical scatter. In order to obtain a better estimate of p_Δ near the origin, the following "particle splitting" technique was applied. Each particle-pair is assigned a weight which indicates the importance to be attached to the particle in calculating the statistics. Whenever, for any integer n in the range 0 to 18, the separation of the particles becomes less than $\Delta_n = \sigma_\Delta 2^{n/3} \times 10^{-2}$, having been greater than Δ_n in the previous time-step, the particle-pair is divided into two copies which then move independently, each pair being given a weight equal to half the weight assigned to the parent particle-pair. Similarly whenever the separation of the particles becomes greater than Δ_n (having been less than Δ_n in the previous step) the pair has a probability of 1/2 of being annihilated. If the particle-pair survives, the weighting assigned to it is doubled. This method ensures that there are a lot of particle-pairs with small separations, each having a very small weight. A sketch of a proof showing that this does not introduce a bias into the results but merely alters the accuracy is given in Appendix C. The value of σ_Δ which was

used in defining Δ_n was obtained from the calculations made without the particle splitting technique. The result is shown in figure 5.1(b). Because of the increased accuracy at small separations, it is possible to place the data points from which the curves are constructed closer together. In order to resolve the behaviour near $\Delta=0$, the data points have been placed as close together as is possible without the scatter becoming unacceptable. More accurate results could be obtained by following a greater number of particles; however, as with all Monte Carlo methods, the convergence is slow, the error decreasing as $N^{-1/2}$ where N is the number of particle-pairs.

It is clear from (3.6) that $p_\Delta(\Delta x, t|s)$ is equal to the value of $\langle c(\underline{x}, t)c(\underline{x} + \Delta \underline{x}/2, t) \rangle$ which results from an initially isotropic concentration field with $\langle c(\underline{x}, s)c(\underline{x} + \Delta \underline{x}/2, s) \rangle = \delta(\Delta \underline{x})$. Now, for Δ lying in the inertial subrange, classical theory (e.g. Monin and Yaglom (1975, p384)) predicts that the concentration covariance function $\langle c(\underline{x}, t)c(\underline{x} + \Delta \underline{x}/2, t) \rangle$ has the form $\alpha - \beta \Delta^2/3$. Hence p_Δ should also have this form for small Δ . The model results for small $t-s$ do indeed agree with this as is shown by the straight-line behaviour near the origin in figure 5.1(c). At larger $t-s$ (not shown in figure 5.1(c)) the inertial subrange behaviour ceases to be apparent in the graph of p_Δ ; this is to be expected because the region in which the inertial subrange form should occur ($\Delta \ll 1$) becomes small relative to the length-scale σ_Δ on which p_Δ varies.

Figures 5.1(d) and 5.1(e) show the p.d.f.s of $(\Delta X^2, \Delta X^3)$ and of ΔX^3 . These are functions of $((\Delta x^2)^2 + (\Delta x^3)^2)^{1/2}$ and $|\Delta x^3|$ respectively, and will be written as $\bar{p}_\Delta(\Delta)$ and $\bar{\bar{p}}_\Delta(\Delta)$ where Δ is to be interpreted, with a slight abuse of notation, as $((\Delta x^2)^2 + (\Delta x^3)^2)^{1/2}$ or $|\Delta x^3|$. They are closer to a Gaussian distribution than p_Δ , the peak in p_Δ at small separations being smoothed by the process of integrating p_Δ over Δx^1 or over Δx^1 and Δx^2 . (The use of superscripts for

cartesian components becomes a bit clumsy here, but appears unavoidable - subscripts are already used for distinguishing between particles 1 and 2 and the use of y and z for x^2 and x^3 is liable to be confused with the use of \underline{x} and \underline{y} to denote two points in space.)

Figure 5.1(f) shows the shape of p_Δ in Richardson's (1926) model. For Richardson's model, p_Δ can be found analytically and is equal to $\alpha' \exp(-\beta' \Delta^{2/3})$ where α' and β' are functions of $t-s$ (Monin and Yaglom 1975, p574). As indicated in §5.1, the shape of p_Δ is in agreement with the inertial subrange prediction $\alpha - \beta \Delta^{2/3}$ for small Δ . It is also independent of $t-s$ as is expected on dimensional grounds. The shape is quite similar to that of the new model at small times (fig 5.1(b)) suggesting that, at least as far as the shape of p_Δ is concerned, the new model is behaving in a way that is not very different from its asymptotic form for large C_0 (as noted in §5.5 the new model reduces to Richardson's model as $C_0 \rightarrow \infty$).

In Durbin's (1980) model, p_Δ can also be calculated analytically (Durbin 1980) and the result is shown in figure 5.1(g). In Durbin's model, the distribution is always strongly peaked and infinite at $\Delta = 0$. The singularity in Durbin's p.d.f. would result in infinite mean square concentration if the forward formulation (3.6) were used. This is of course associated with the unphysical form of \hat{g}_p with which Durbin's model is consistent. In the NGLS model p_Δ is exactly Gaussian at all times.

The similarity in the shape of p_Δ at times $t-s \ll \tau$ in the new model and the model of Durbin is striking. However the difference in behaviour near the origin has some important consequences. Firstly the new model can treat the problem of a point source and does not require the explicit treatment of molecular diffusion which is needed to smooth the singularity in Durbin's model (Sawford and Hunt 1986). Also, because of the shapes of p_Δ and p_x (see below for discussion of p_x) and

the fact that σ_Δ and σ_x tend to infinity as $t-s \rightarrow \infty$, it follows that, for any given length-scale, the values of p_Δ and p_x from the new model will show little variation on this scale when $t-s$ is sufficiently large. It seems reasonable to suppose the same is also true of the quantity $P_{\underline{x}_1(t), \underline{x}_2(t) | \underline{x}_1(s), \underline{x}_2(s)}(\underline{x}_1, \underline{x}_2 | \underline{y}, \underline{y})$, and hence (using the above noted fact that the model statistics for forward and backward trajectories are equal in stationary conditions) of the quantity $P_{\underline{x}_1(s), \underline{x}_2(s) | \underline{x}_1(t), \underline{x}_2(t)}(\underline{y}_1, \underline{y}_2 | \underline{x}, \underline{x})$. Now, for an instantaneous spatially-bounded deterministic source, (3.11) can be written (assuming ρ is constant) as

$$\langle c(\underline{x}, t)^2 \rangle = \int P_{\underline{x}_1(s), \underline{x}_2(s) | \underline{x}_1(t), \underline{x}_2(t)}(\underline{y}_1, \underline{y}_2 | \underline{x}, \underline{x}) S(\underline{y}_1) S(\underline{y}_2) d\underline{y}_1 d\underline{y}_2$$

where s is the time at which the contaminant is released (S here has a slightly different meaning to the S introduced in §3.1, being the amount of tracer released per unit volume, not per unit space-time volume). It follows from the above property of the quantity $P_{\underline{x}_1(s), \underline{x}_2(s) | \underline{x}_1(t), \underline{x}_2(t)}(\underline{y}_1, \underline{y}_2 | \underline{x}, \underline{x})$ that this can be approximated when $t-s$ is large by

$$\langle c(\underline{x}, t)^2 \rangle = P_{\underline{x}_1(s), \underline{x}_2(s) | \underline{x}_1(t), \underline{x}_2(t)}(\underline{y}, \underline{y} | \underline{x}, \underline{x}) \int S(\underline{y}_1) S(\underline{y}_2) d\underline{y}_1 d\underline{y}_2,$$

where \underline{y} is some point in the source region. Hence, provided the total amount of material released remains fixed, $\langle c^2 \rangle$ becomes independent of source size in the new model. Similar arguments, using \bar{p}_Δ or \bar{p}_Δ instead of p_Δ , show that $\langle c^2 \rangle$ becomes independent of source "size" (i.e. source thickness) for instantaneous area and line sources also. In contrast, the value of $P_{\underline{x}_1(s), \underline{x}_2(s) | \underline{x}_1(t), \underline{x}_2(t)}(\underline{y}_1, \underline{y}_2 | \underline{x}, \underline{x})$ in Durbin's model shows variations on a length-scale 1 or less at all times due to the singularity in p_Δ . Hence, as discussed by Durbin (1980) and Sawford (1983), $\langle c^2 \rangle$ never becomes independent of the source size for sources of size less than 1. Although it is not clear how to

prove from first principles that this behaviour is wrong, it seems intuitively very unlikely.

A partial justification of the idea that $\langle c^2 \rangle$ should become independent of source size is possible by considering the equality noted above between $p_\Delta(\Delta x, t|s)$ and the spatial covariance function of a hypothetical isotropic concentration field. We have already noted that this implies $p_\Delta \approx \alpha - \beta \Delta^{2/3}$ for Δ lying in the inertial subrange. Now at large times σ_Δ^2 grows like t and so α cannot decrease faster than $t^{-3/2}$. Now α is the variance of our hypothetical concentration field and β is proportional to its rate of dissipation (see e.g. Monin and Yaglom (1975, p384)). Hence β/α must become small, since otherwise α would decrease exponentially. It follows that p_Δ is likely to show little variation on small scales for large t -s. In addition, it seems likely that p_x will also show little variation on small scales at large t -s (see discussion of p_x below). Hence, for the same reasons as given above in discussing the behaviour of $\langle c^2 \rangle$ in the model, it seems likely that the value of $\langle c^2 \rangle$ for instantaneous plane, line and compact sources will become independent of source size at large times.

It should be pointed out that, in most of the applications of Durbin's model made to date (Durbin 1980; Sawford 1983, 1985; Sawford and Hunt 1986), p_Δ is, as noted in §5.5, interpreted as the p.d.f. of one component of $\Delta \underline{x}$ (this is the logical interpretation since the model is one-dimensional). Hence it should be compared with the value of \bar{p}_Δ from the new model (figure 5.1(e)). If this is done the agreement in shape is much worse. It is not proposed here to investigate in detail how much of this difference is due to the one-dimensionality of Durbin's model and how much is a result of the failure to satisfy the "well-mixed condition". However, for $t-s \ll \tau$, the model of Thomson (1986b) (which is essentially a one-dimensional version of the model of §5.4 and which satisfies the well-mixed condition) also shows a much

stronger peak at $\Delta = 0$ than does \overline{p}_Δ from the new model, suggesting that the one-dimensionality of Durbin's model may be an important factor.

Figure 5.2 shows the p.d.f. of the distribution of $\Sigma \underline{X}$. In the new model it is close to Gaussian at all times. As in figure 5.1, the scatter at small ε is statistical noise. The value of p_x in the NGLS model is of course exactly Gaussian at all times. In Durbin's model (not shown) p_x is also close to Gaussian (Sawford 1983). A Gaussian shape for p_x is to be expected at small times (as a consequence of the assumed Gaussianity of the fixed point velocity distribution) and at large times (on the basis of a central limit theorem type argument similar to that in §1.1) and so the observed Gaussianity is not surprising.

Figure 5.3 shows the growth of σ_1 , σ_Δ and σ_x in the new model and in the NGLS model. The behaviour of σ_Δ in Richardson's (1926) model is also shown (in Richardson's model there is of course no prediction for σ_1 or σ_x). At small times σ_1 and σ_x are proportional to $t-s$ as is to be expected since the particle trajectories can be approximated by straight lines over short times. In contrast σ_Δ grows like $(t-s)^{3/2}$ at small times. This is to be expected on dimensional grounds since, for small $t-s$, σ_Δ should depend only on ε and $t-s$ (Monin and Yaglom 1975, p545). The "straight-line approximation" argument does not apply to σ_Δ . This is because this approximation yields $\sigma_\Delta = 0$ and so the departure from straight-line motion dominates the behaviour of σ_Δ . At large $t-s$, σ_1 , σ_Δ and σ_x grow like $(t-s)^{1/2}$. The $(t-s)^{1/2}$ growth of σ_1 is expected on the basis of Taylor's (1921) result (see §1.1). Also σ_Δ and σ_x are expected to grow in the same way as σ_1 at large $t-s$ since, at large $t-s$, the particle-pairs will have spent most of their time at large separations where they travel independently. The values of σ_1 , σ_Δ and σ_x from the NGLS model can be obtained analytically and are as follows:

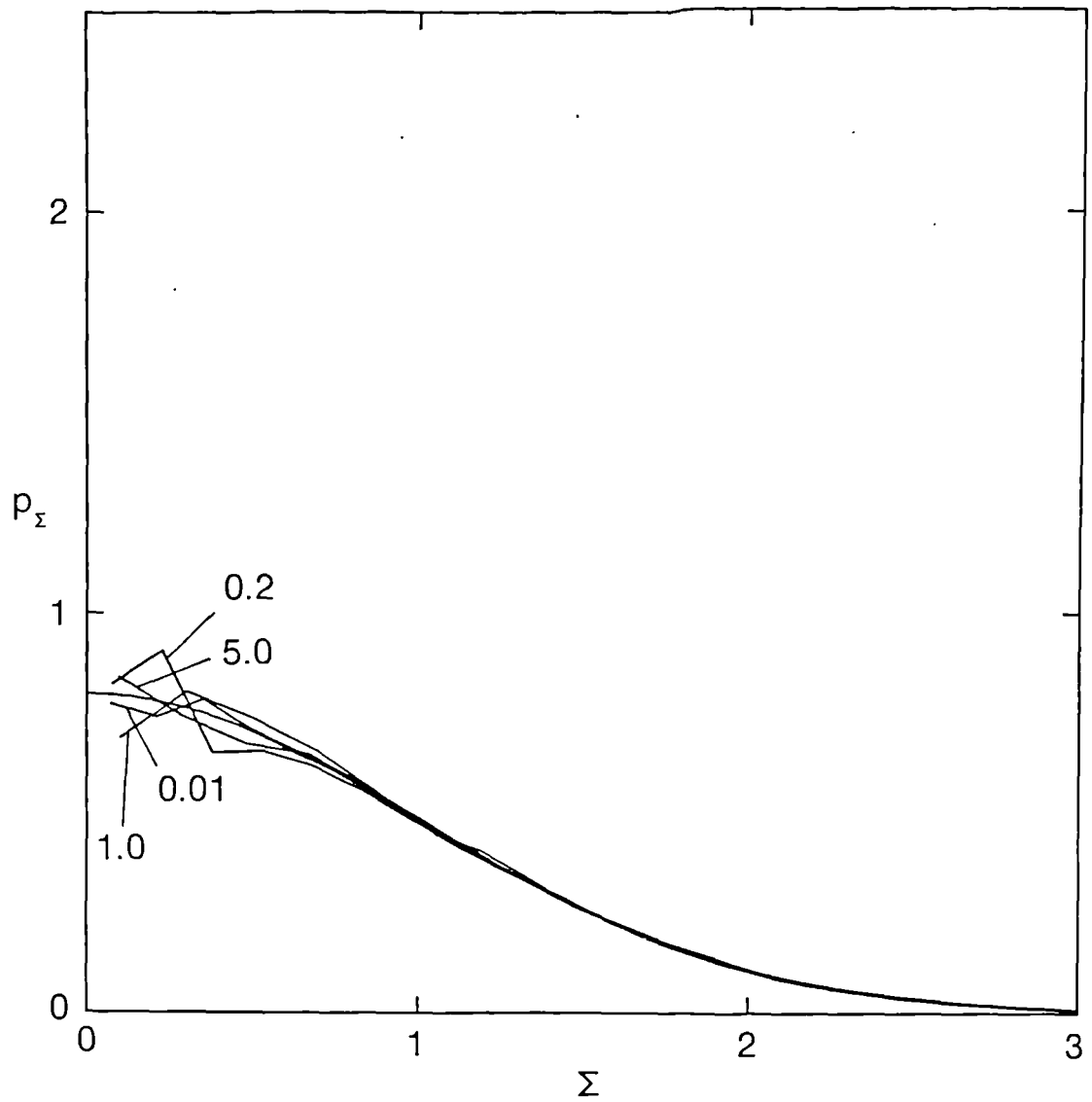


Figure 5.2: The shape of $p_{\Sigma}(\Sigma, t|s)$ from the new model in stationary turbulence. The curves are normalised with zeroth and second moments equal to unity as if they were one-dimensional p.d.f.s. The numbers attached to the curves indicate values of $t-s$ normalised by σ^2/ε , and the unlabelled line is a Gaussian distribution.

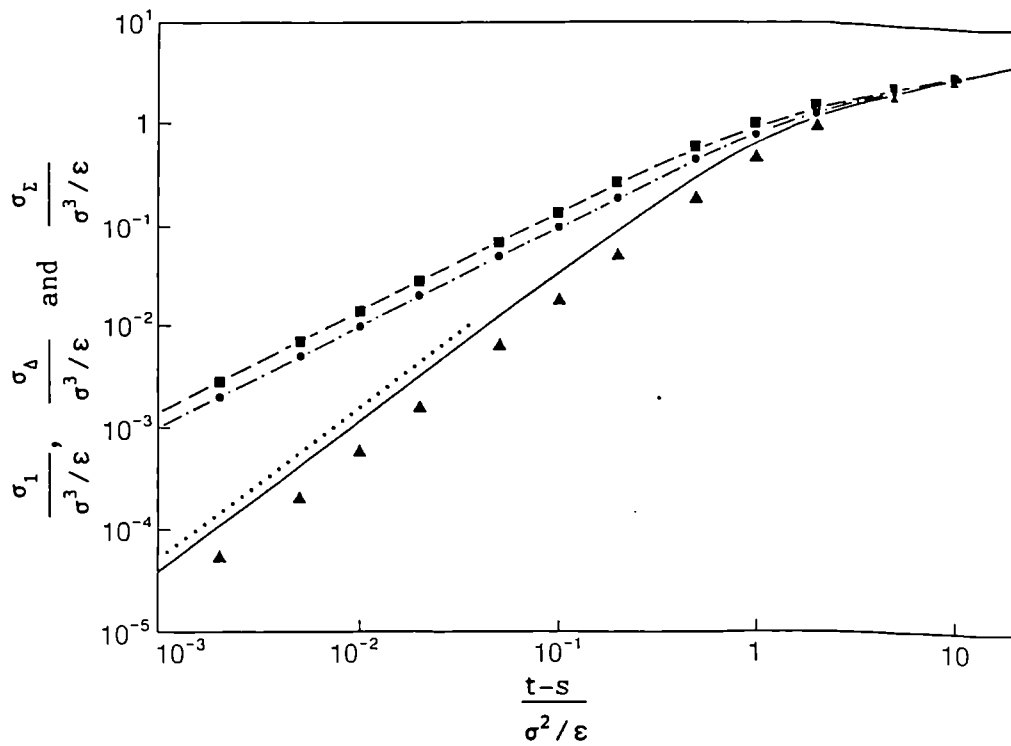


Figure 5.3: $\sigma_1(t|s)$, $\sigma_\Delta(t|s)$ and $\sigma_z(t|s)$ in stationary turbulence. The values of σ_1 , σ_Δ and σ_z obtained from the new model are denoted by \bullet , \blacktriangle and \blacksquare , and the values obtained from the NGLS model are indicated by ---, — and ----. The value of σ_Δ from Richardson's (1926) model is denoted by

$$\sigma_1^2(t|s) = 2\sigma^2\tau^2(\exp(-(t-s)/\tau) - 1 + (t-s)/\tau)$$

$$\sigma_\Delta^2(t|s) = \sigma_1^2 - \sigma^2\tau^2(1 - \exp(-(t-s)/\tau))^2$$

$$\sigma_\varepsilon^2(t|s) = \sigma_1^2 + \sigma^2\tau^2(1 - \exp(-(t-s)/\tau))^2$$

(see Appendix B). In the new model, the value of σ_1 is indistinguishable from that in the NGLS model. This is as it should be if (5.2) is not to be seriously violated. This is because, for large initial separation (with $\underline{x}_1(s) = 0$), $\langle(X_1^1)^2\rangle = \langle(X_1^2)^2\rangle = \langle(X_1^3)^2\rangle = 2\sigma^2\tau^2(\exp(-(t-s)/\tau) - 1 + (t-s)/\tau)$ in the new model (this follows from a calculation similar to the calculations in Appendix B and the fact that, for large initial separations, the motion of single particles obeys (5.11)) and these quantities should be independent of initial separation since they depend on the motion of one particle only. The value of σ_Δ in the new model is smaller than the value from the NGLS model. This is to be expected because, if the particles in the new model approach closely at some time after release, their velocities become highly correlated again, reducing the rate of growth of σ_Δ . The value of σ_Δ in Richardson's model can also be obtained analytically and, taking $K = (3.17/C_0)\varepsilon^{1/3}\Delta^{4/3}$ (see the discussion in §5.5), is equal to $(12.3/C_0^{3/2})\varepsilon^{1/2}(t-s)^{3/2}$ (Monin and Yaglom 1975, p574). This is plotted in figure 5.3 for $C_0 = 4.0$, the value adopted in the new model. Only the values for small $t-s$ are plotted since Richardson's model is of course only applicable to inertial subrange behaviour. In the limit $C_0 \rightarrow \infty$, the new model should give the same results as Richardson's model. The results in figure 5.3 show that σ_Δ is considerably larger in Richardson's model than in the new model, implying that $C_0 = 4.0$ is not sufficiently large for this limiting behaviour to be found. Some further simulations with the new model showed that a value of C_0 as large as 16.0 is needed for the two models to give values of σ_Δ which agree to within 15 per cent, and a value of 32.0 is needed for agreement to within 5 per cent. The Richardson

model will not be considered further here, mainly because it does not give predictions for the motion of the centroid of a pair of particles and so is incapable, in most situations, of leading to predictions for $\langle c^2 \rangle$.

The results of the simulations enable us to see how seriously the new model violates (5.2). Figure 5.4 shows the behaviour of certain statistics of X_1 for various initial values of the separation, which was taken to be in the x^3 -direction. For initial separations much larger than 1, the model reduces to (5.11) and the statistics of X_1 can be calculated analytically. The statistics of X_1 should be independent of $\Delta(s)$ if (5.2) is to be satisfied. The results show little dependence on the initial separation. This is encouraging and suggests that the violation of (5.2) may not be too serious. Further evidence to this effect is given in figure 5.5. The value of $\langle \hat{U}^i \hat{U}^i \rangle$ does not show any strong dependence on the initial separation, indicating either that the higher order terms in (5.14) have a corrective effect or that the power series expansion ceases to be applicable after a short time. The general increase in $\langle \hat{U}^i \hat{U}^i \rangle$ which does occur is due to the size of the time-step used and is, for small initial separation, much less than that predicted by the first two terms in (5.14); if the NGLS model (which satisfies (5.2) exactly) were solved numerically with the same time-step a similar behaviour would be observed. We also note that the distribution of X_1 in the model is Gaussian for large initial separations (this follows from (5.11) using the methods given in Appendix B) and hence that it should be close to Gaussian for all initial separations if (5.2) is to be approximately true. The simulations indicate that this is in fact the case, with the p.d.f.s of X_1 for various initial separations and travel times (not shown) having a degree of scatter about a Gaussian distribution similar to that seen in figure 5.2.

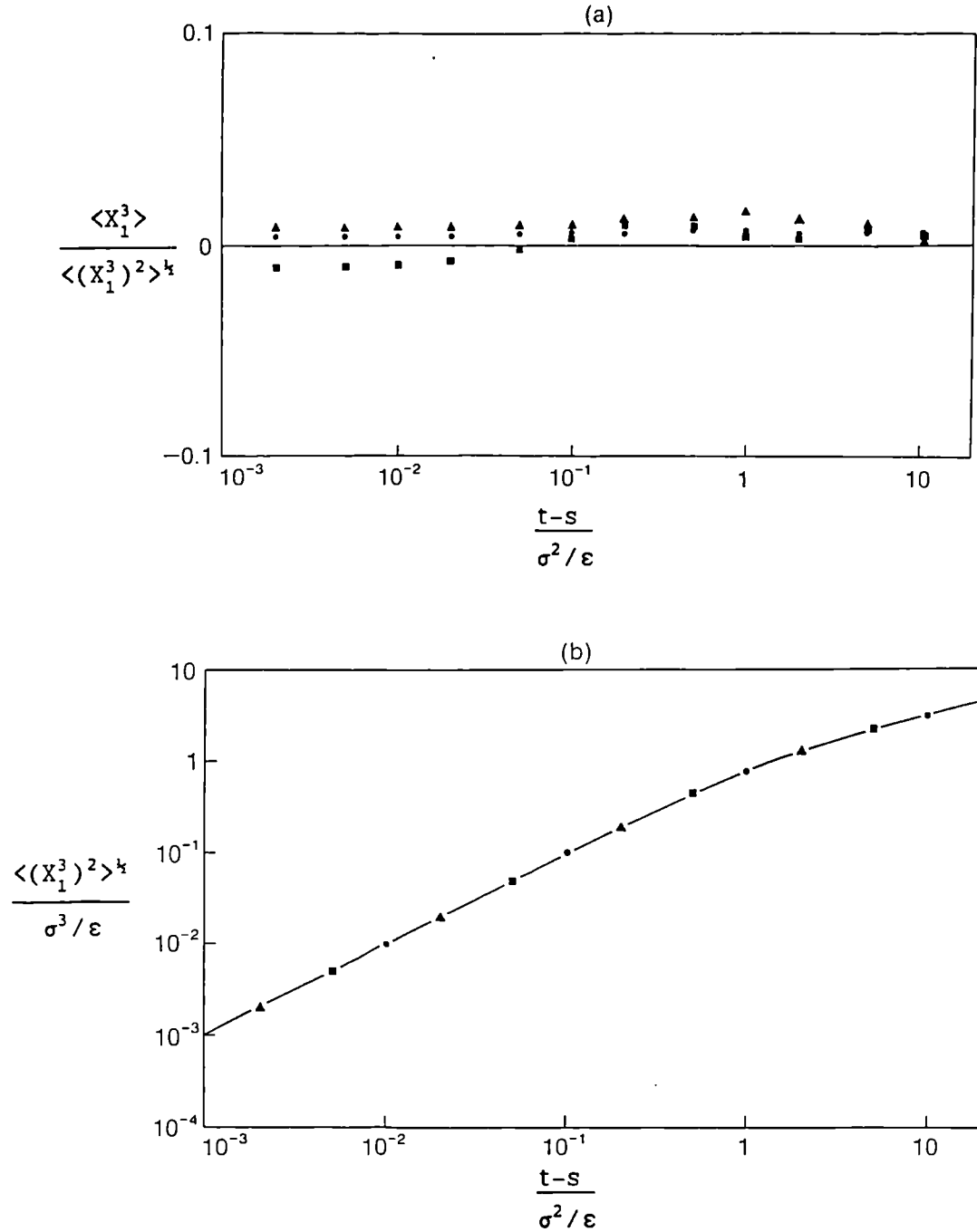


Figure 5.4: (a) and (b) show values of $\langle X_1^3 \rangle$ and $\langle (X_1^3)^2 \rangle$ from the new model for particle-pairs released at time s with various initial separations in stationary turbulence. $X_1(s)$ is zero. \bullet , \blacksquare and \blacktriangle indicate initial separations of 0, 0.021 and 21 respectively, the initial separation being in the x^3 -direction with $X_1^3(s) > X_2^3(s)$. In both figures the solid line indicates the analytic result for large initial separation. The values of $\langle (X_1^1)^2 \rangle$ and $\langle (X_1^2)^2 \rangle$ (not shown) are indistinguishable from $\langle (X_1^3)^2 \rangle$.

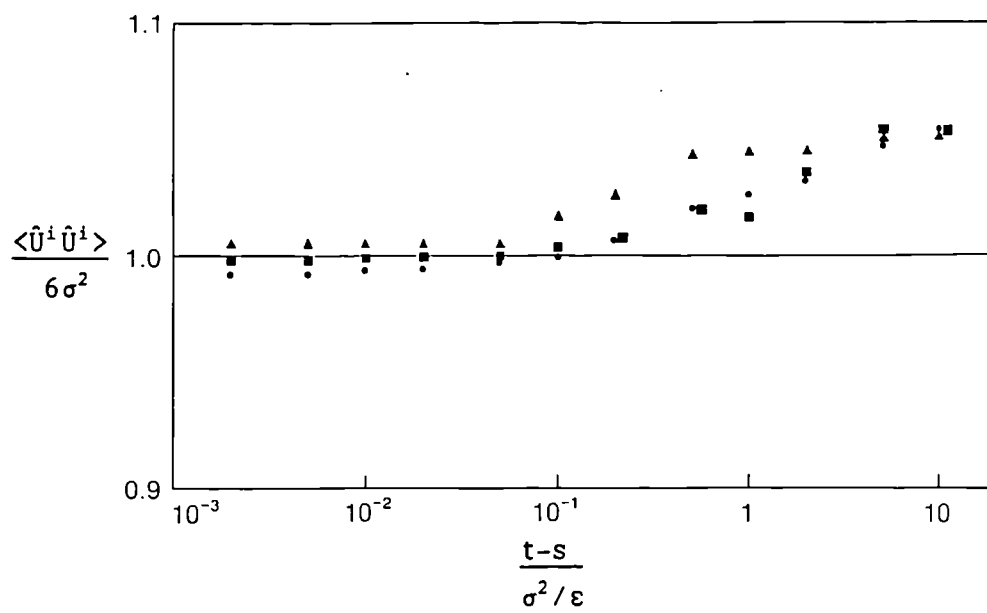


Figure 5.5: $\langle \hat{U}^i \hat{U}^i \rangle$ from the new model for particle-pairs released at time s with various initial separations in stationary turbulence. ●, ■ and ▲ indicate initial separations of 0, 0.021 and 21 respectively. The solid line is the analytic result for large initial separation.

There is however one aspect of the new model which violates (5.2) significantly. Consider the quantity $\delta\tilde{X}_1(t) = \tilde{X}_1(t) - \tilde{X}_1(s) - \underline{U}_1(s)(t-s)$. This represents the departure in the position of a particle from the position it would have had had it moved in a straight line (see figure 5.6). For $t-s \ll \tau$, $\langle |\delta\tilde{X}_1|^2 \rangle$ should grow like $C_0 \varepsilon(t-s)^3$, the value which $\langle |\delta\tilde{X}_1|^2 \rangle$ takes when $\Delta(s) \gg 1$ (this follows from (5.11) by a similar calculation to the calculations given in Appendix B). As in (5.13), the average here is an average over particle-pairs with a given position in \tilde{x} -space at time s . For $\Delta(s) = 0$, the value of $\langle |\delta\tilde{X}_1|^2 \rangle$ from the model is significantly smaller than $C_0 \varepsilon(t-s)^3$ (see figure 5.7). Some insight into why this is so can be obtained by considering $\delta\Delta\tilde{X}$ and $\delta\Sigma\tilde{X}$, defined in a way analogous to $\delta\tilde{X}_1$ (see figure 5.6). It is easy to show that $\langle |\delta\tilde{X}_1|^2 \rangle + \langle |\delta\tilde{X}_2|^2 \rangle = \langle |\delta\Delta\tilde{X}|^2 \rangle + \langle |\delta\Sigma\tilde{X}|^2 \rangle$ and so, by symmetry, $\langle |\delta\tilde{X}_1|^2 \rangle = \frac{1}{2}(\langle |\delta\Delta\tilde{X}|^2 \rangle + \langle |\delta\Sigma\tilde{X}|^2 \rangle)$. Hence, for $t-s \ll \tau$,

$$\frac{1}{2}(\langle |\delta\Delta\tilde{X}|^2 \rangle + \langle |\delta\Sigma\tilde{X}|^2 \rangle) = C_0 \varepsilon(t-s)^3 \quad (5.17)$$

should hold. In the model the leading order term in the Taylor series for $\langle |\delta\Delta\tilde{X}|^2 \rangle$ and $\langle |\delta\Sigma\tilde{X}|^2 \rangle$ is $C_0 \varepsilon(t-s)^3$ (by, for example, applying Itô's formula) and so (5.17) is satisfied at small times. If $\Delta(s) \ll 1$, then, while $\Delta \ll 1$ (i.e. for $t-s \ll \tau$), the stochastic differential equations for $\delta\Sigma\tilde{X}$ and $\delta\Sigma\tilde{U}(t) = \Sigma\tilde{U}(t) - \Sigma\tilde{U}(s)$ can be approximated by

$$d\delta\Sigma\tilde{X} = \delta\Sigma\tilde{U} dt, \quad d\delta\Sigma\tilde{U} = (C_0 \varepsilon)^{1/2} d\zeta$$

with $\delta\Sigma\tilde{U}(s) = 0$ (the terms which have been omitted in this approximation have an effect which is only significant over time-scales of order τ). Hence, again by a calculation similar to the calculations given in Appendix B, $\langle |\delta\Sigma\tilde{X}|^2 \rangle = C_0 \varepsilon(t-s)^3$ for $t-s \ll \tau$. However the equations for $\delta\Delta\tilde{X}$ and $\delta\Delta\tilde{U} = \Delta\tilde{U}(t) - \Delta\tilde{U}(s)$ are much more complex and, in addition to a $(C_0 \varepsilon)^{1/2} d\zeta$ term, the expression for $d\delta\Delta\tilde{U}$ contains terms which, for particle separations lying in the inertial subrange, are of order $(\varepsilon^2/\Delta)^{1/3} dt$. Over a time of order $(\Delta^2/\varepsilon)^{1/3}$ these terms have an

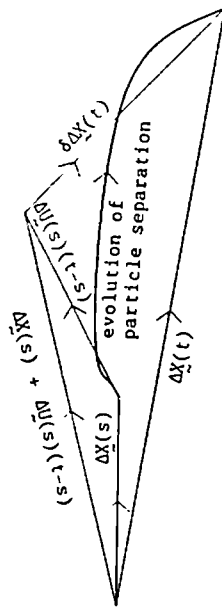
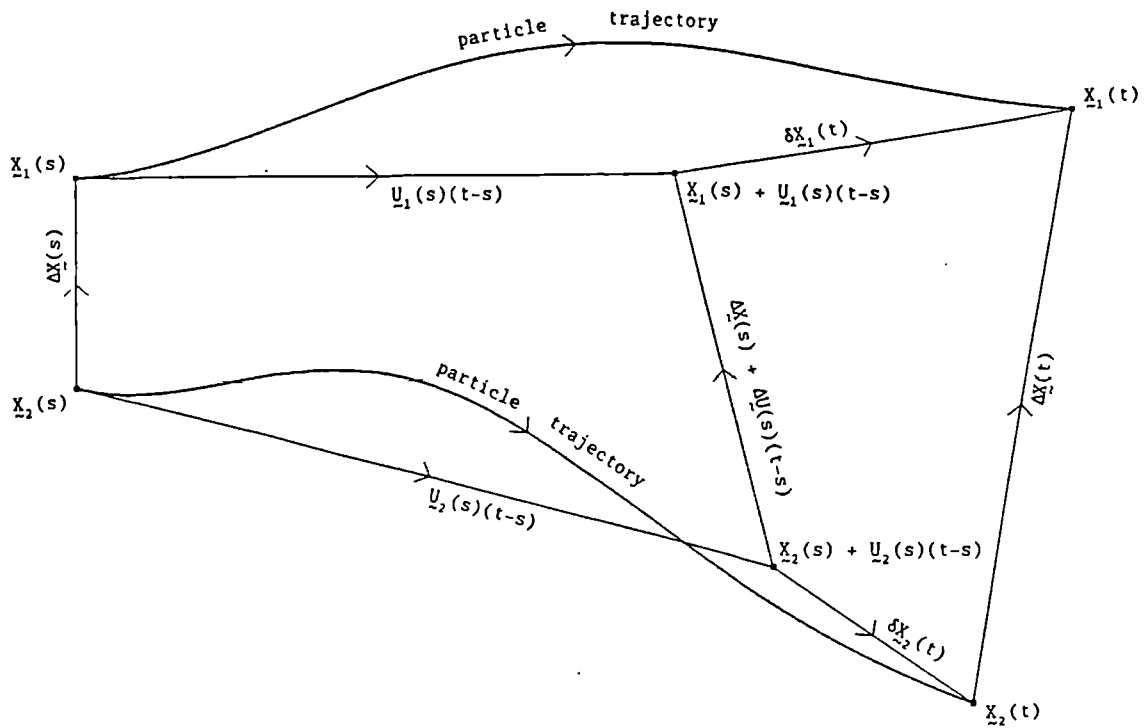


Figure 5.6: Schematic illustration of the quantities $\delta X_1(t)$, $\delta \Delta \underline{X}(t)$ and $\delta \Sigma \underline{X}(t)$ for a pair of particles with given positions at time s . For clarity, factors of $\sqrt{2}$ have been ignored, i.e. we have taken $\Delta \underline{X} = \underline{X}_1 - \underline{X}_2$ and $\Sigma \underline{X} = (\underline{X}_1 + \underline{X}_2)/2$ instead of $\Delta \underline{X} = (\underline{X}_1 - \underline{X}_2)/\sqrt{2}$ and $\Sigma \underline{X} = (\underline{X}_1 + \underline{X}_2)/\sqrt{2}$.

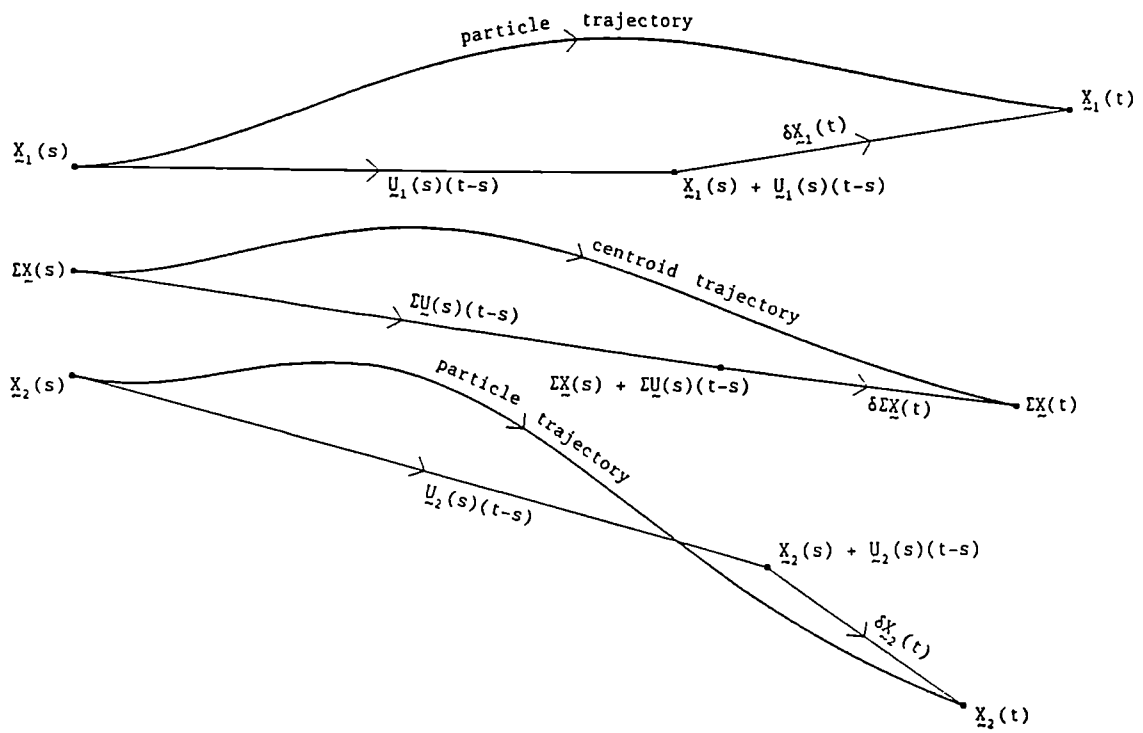


Figure 5.6 continued.

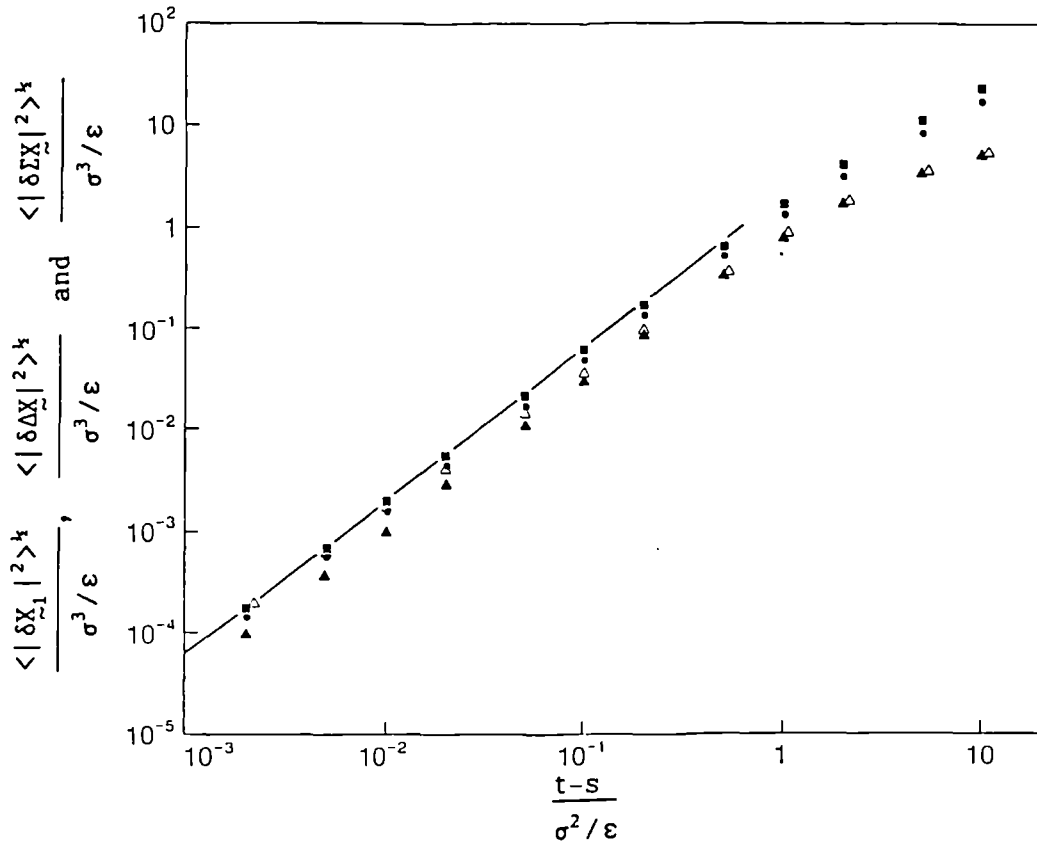


Figure 5.7: $\langle |\delta \underline{X}_1|^2 \rangle$, $\langle |\delta \Delta \underline{X}|^2 \rangle$ and $\langle |\delta \Sigma \underline{X}|^2 \rangle$ from the new model for particle-pairs released at time s in stationary turbulence. \bullet , \blacktriangle and \blacksquare denote $\langle |\delta \underline{X}_1|^2 \rangle$, $\langle |\delta \Delta \underline{X}|^2 \rangle$ and $\langle |\delta \Sigma \underline{X}|^2 \rangle$ respectively for zero initial separation. \blacktriangle denotes $\langle |\delta \Delta \underline{X}|^2 \rangle$ for an initial separation of $2 \times 10^{-3} l$. The solid line is $C_0 \epsilon t^3$.

effect comparable to the effect of the $(C_0 \varepsilon)^{1/2} d\zeta$ term. Hence $\langle |\delta\Delta\tilde{X}|^2 \rangle \approx C_0 \varepsilon (t-s)^3$ only holds for $t-s \ll (\Delta(s)^2/\varepsilon)^{1/3}$. For $(\Delta(s)^2/\varepsilon)^{1/3} \ll t-s \ll \tau$, $\langle |\delta\Delta\tilde{X}|^2 \rangle$ grows like $(t-s)^3$ but with a different coefficient. This difference in the coefficient of $(t-s)^3$ for $t-s \ll (\Delta(s)^2/\varepsilon)^{1/3}$ and for $(\Delta(s)^2/\varepsilon)^{1/3} \ll t-s \ll \tau$ is clearly seen in the results obtained with an initial separation of $2 \times 10^{-3} l$ (figure 5.7). For this value of the initial separation, the "cross-over" time $(\Delta(s)^2/\varepsilon)^{1/3}$ equals $10^{-2} \sigma^2/\varepsilon$.

Consider a pair of particles whose initial separation lies well within the inertial subrange and consider their motion over times for which the evolution of $\delta\tilde{X}_1$ and $\delta\Delta\tilde{X}$ is dominated by inertial subrange eddies. In the model, for which the inertial subrange extends to arbitrarily high wave numbers and frequencies, this means restricting consideration to initial separations with $\Delta(s) \ll l$ and travel times satisfying $t-s \ll \tau$. By assuming that the covariance between the accelerations of two particles whose separation lies in the inertial subrange is negligible, Monin and Yaglom (1975, pp546-547) and Sawford (1984) deduce that $\langle |\delta\tilde{X}_1|^2 \rangle = \langle |\delta\Delta\tilde{X}|^2 \rangle$ for such initial separations and travel times. (Monin and Yaglom (1975) and Sawford (1984) were principally concerned with the case where the initial separation is zero or where the initial separation is non-zero and the travel time is sufficiently large for the particles to forget their initial separation. In this case $\langle |\delta\Delta\tilde{X}|^2 \rangle$ equals the mean square separation $\langle |\Delta\tilde{X}|^2 \rangle$. However their analysis applies more generally.) If this is true it follows that the value of $\langle |\delta\Delta\tilde{X}|^2 \rangle$ in the model is incorrect for times in the range $(\Delta(s)^2/\varepsilon)^{1/3} \ll t-s \ll \tau$. However the argument in Appendix D shows that the inertial subrange acceleration covariances may be important in reality (they certainly are in the model since, as we have noted, the model value of $\langle |\delta\tilde{X}_1|^2 \rangle$ is greater than $\langle |\delta\Delta\tilde{X}|^2 \rangle$ for $(\Delta(s)^2/\varepsilon)^{1/3} \ll t-s \ll \tau$), and that it is more likely that $\langle |\delta\tilde{X}_1|^2 \rangle$ is, in reality, greater than $\langle |\delta\Delta\tilde{X}|^2 \rangle$ for times in the range $(\Delta(s)^2/\varepsilon)^{1/3} \ll t-s \ll \tau$. Hence the model value of $\langle |\delta\Delta\tilde{X}|^2 \rangle$ is not unreasonable and the

cause of the problem could be the model's value for $\langle |\delta \Sigma \underline{x}|^2 \rangle$.

It is not clear if the above problem is a serious flaw in the model. However it should be pointed out that this flaw is not one which is apparent in the single-time statistics of particle-pairs whose trajectories commence at a given position in \underline{x} -space. The single-time statistics, at least as judged by the evidence presented earlier in this section, show little evidence of violation of (5.2). For many purposes, in particular for predicting concentration fluctuations in the situations which will be considered in chapter 6, it is only the single-time statistics which are important. This suggests that the violation of (5.2) may not matter in practice.

(iii) Decaying turbulence.

A number of simulations were also carried out in decaying isotropic turbulence. The velocity field was assumed to decay self-similarly with σ^2 varying as $\sigma_s^2 (t/s)^{-n}$ where σ_s is the value of σ at time s . n was taken to be 1.35, a value within the scatter of values observed in grid turbulence (Warhaft 1984; Warhaft and Lumley 1978). Of course the decay exponent measured in grid turbulence is the exponent for the decay of σ^2 with downwind distance in a steady inhomogeneous flow. However it can be interpreted as the exponent for the decay in time of isotropic turbulence in the usual way (Monin and Yaglom 1975, pp115-116). With this form for σ^2 , ε is equal to $1.5n(\sigma_s^2/s)(t/s)^{-(n+1)}$, which, assuming the relation between σ^2 , ε and l given in §5.4, implies $l = (\sqrt{2/3n})\sigma_s s(t/s)^{1-n/2}$.

Trajectories of particle-pairs were simulated both forward and backwards in time, the particles being coincident at the time of release. The same release time was used in all the simulations. Because the turbulence decays self-similarly, the results can be rescaled (Durbin 1982) to give results for other release times; for

example, for any $\gamma > 0$,

$$P_{\underline{x}_1(t), \underline{x}_2(t) | \underline{x}_1(s), \underline{x}_2(s)}(\underline{x}_1, \underline{x}_2 | 0, 0) = \gamma^{6-3n} P_{\underline{x}_1(\gamma t), \underline{x}_2(\gamma t) | \underline{x}_1(\gamma s), \underline{x}_2(\gamma s)}(\underline{x}_1 \gamma^{1-n/2}, \underline{x}_2 \gamma^{1-n/2} | 0, 0). \quad (5.18)$$

The shape of p_Δ is shown in figure 5.8. Because of the scaling relation (5.18), the shape of p_Δ depends only on t/s . The shape becomes quite close to Gaussian as $t/s \rightarrow 0$; however there is some indication that the shape remains more peaked than a Gaussian distribution as $t/s \rightarrow \infty$. Figure 5.9 shows the values of σ_1 , σ_Δ and σ_z from the new model and from the NGLS model. As is to be expected, the behaviour of σ_1 , σ_Δ and σ_z for small $|t-s|$ is the same as in the stationary case. For the forward trajectories, σ_1 , σ_Δ and σ_z become, at large times, proportional to $(t-s)^{1-n/2}$, which is in turn proportional to $l(t)$. This form of large time behaviour is expected on dimensional grounds - at large times the particles forget the release time s and so the spread can depend only on t (or $t-s$, which differs negligibly from t at large $t-s$) and on $\sigma_s^2 s^n$, which is the only dimensional constant in the problem (and is in fact independent of the chosen value of s). An alternative way of understanding the $(t-s)^{1-n/2}$ growth of σ_1 at large times is to consider Taylor's (1921) result applied to the scaled velocity $u_1(t)/\sigma(t)$, which, because the turbulence is assumed to decay self-similarly, is expected to be a stationary process when expressed as a function of the stretched time t' defined by $dt' = dt/t$ (Batchelor and Townsend 1956; Monin and Yaglom 1971, §9.4). The values from the NGLS model can be obtained analytically and are

$$\sigma_1^2(t|s) = 2\sigma_s^2 s^2 \left(\frac{(t/s)^{r-q} - 1}{r(r-q)} + \frac{(t/s)^{-q} - 1}{rq} \right)$$

$$\sigma_\Delta^2(t|s) = \sigma_1^2 - \sigma_s^2 s^2 \left(\frac{(t/s)^{-q} - 1}{q} \right)^2$$

$$\sigma_z^2(t|s) = \sigma_1^2 + \sigma_s^2 s^2 \left(\frac{(t/s)^{-q} - 1}{q} \right)^2$$

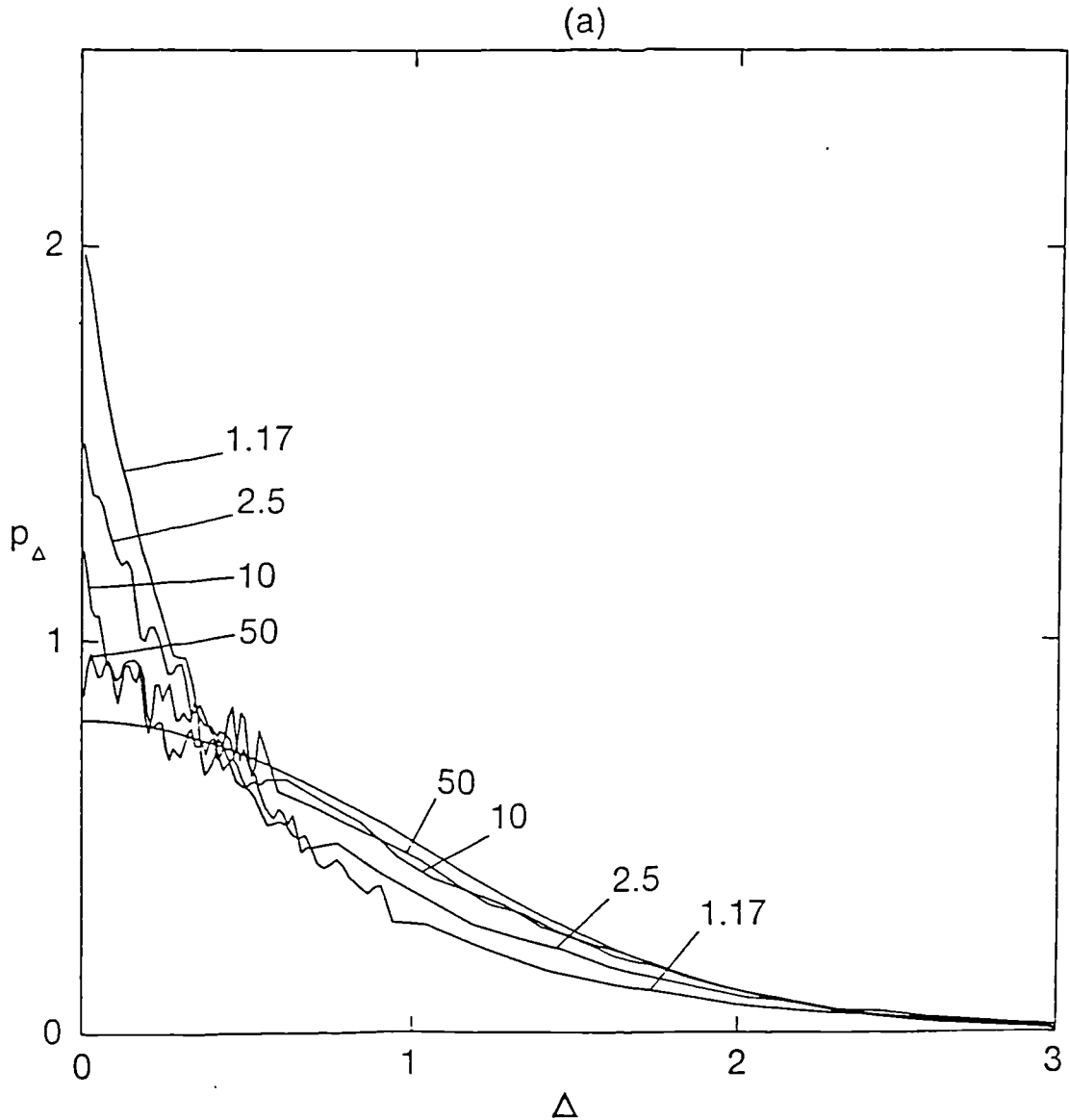


Figure 5.8: The shape of $p_{\Delta}(\Delta, t|s)$ from the new model in decaying turbulence. The curves were obtained using the particle splitting technique and are normalised with zeroth and second moments equal to unity as if they were one-dimensional p.d.f.s. (a) shows results for $t > s$ (forward trajectories) and (b) shows results for $t < s$ (backwards trajectories). The numbers attached to the curves indicate values of t/s for the forward trajectories and s/t for the backwards trajectories. In both figures the unlabelled line is a Gaussian distribution.

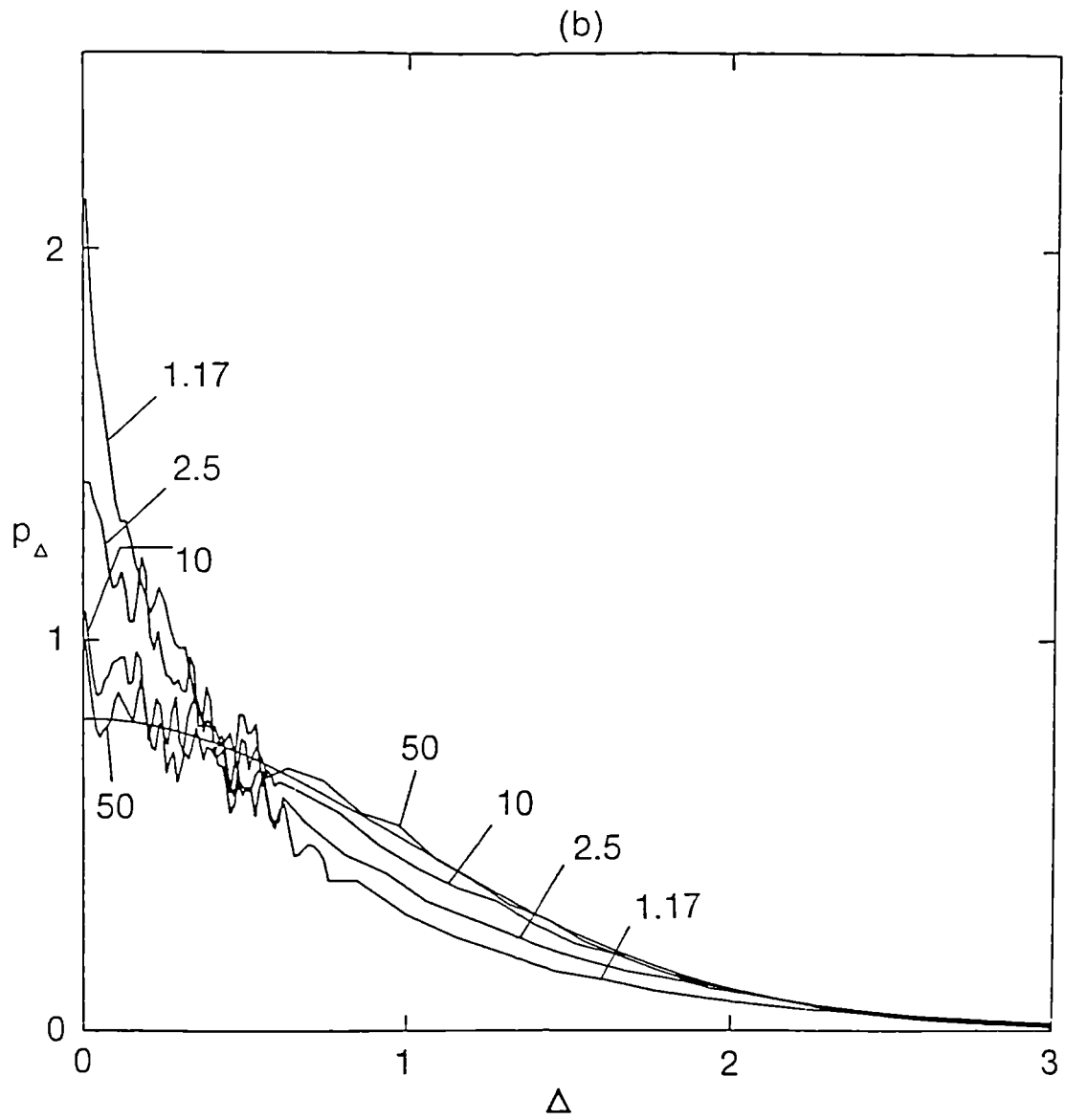


Figure 5.8 continued.

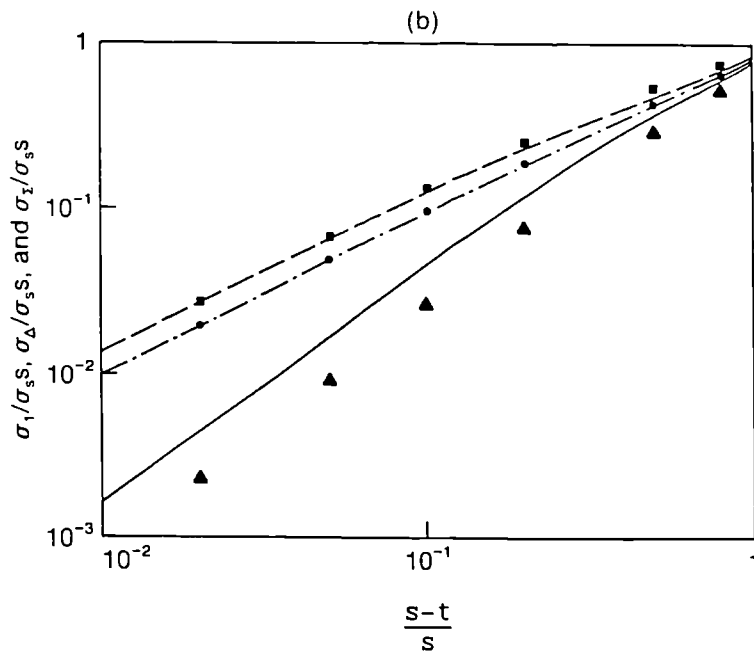
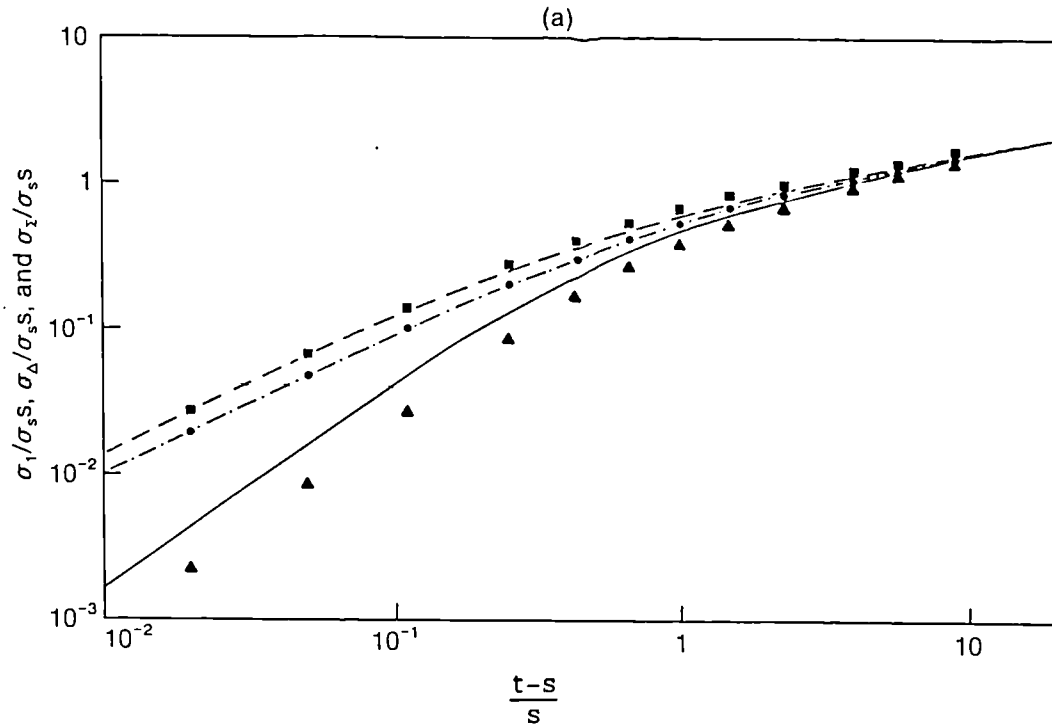


Figure 5.9: $\sigma_1(t|s)$, $\sigma_\Delta(t|s)$ and $\sigma_z(t|s)$ in decaying turbulence. The values of σ_1 , σ_Δ and σ_z obtained from the new model are denoted by \bullet , \blacktriangle and \blacksquare , and the values obtained from the NGLS model are indicated by $---$, $—$ and $- \cdot -$. (a) shows results for $t > s$ (forward trajectories) and (b) shows results for $t < s$ (backwards trajectories).

where $r = \alpha - n/2 + 1$, $q = \alpha + n/2 - 1$ for the forward trajectories ($t > s$) and $r = -\alpha - n/2 + 1$, $q = -\alpha + n/2 - 1$ for the reverse trajectories ($t < s$), with $\alpha = 3nC_0/4$ (see Appendix B). For the forward trajectories these expressions were derived by Anand and Pope (1985), although in a rather different context (Anand and Pope were considering not a random walk model but a so-called p.d.f. model; however with the aid of some approximations, Anand and Pope found that some aspects of their model were related to the NGLS model considered here). As in the stationary case the value of σ_Δ in the new model is considerably smaller than the value from the NGLS model, while the values of σ_1 in the two models are indistinguishable. The close agreement between the values of σ_1 lends support, as in the stationary case, to the idea that (5.2) is not seriously violated. The homogeneity of the flow and equation (3.8) imply that, in reality, $\sigma_1(t|s) = \sigma_1(s|t)$. This is satisfied exactly in the NGLS model and to high accuracy in the new model. It is of interest that the values of $\sigma_1(t|s)/\sigma_\Delta(t|s)$ and $\sigma_1(t|s)/\sigma_2(t|s)$ for the backward trajectories do not tend to unity as $t/s \rightarrow 0$ while the values for the forward trajectories do tend to unity as $t/s \rightarrow \infty$. A consequence of this is that $\sigma_\Delta(t|s) > \sigma_\Delta(s|t)$ in the limit $t/s \rightarrow \infty$, while, as a result of (3.10), $p_\Delta(0, s|t) = p_\Delta(0, t|s)$. It follows that the shape of $p_\Delta(\Delta, t|s)$ must be more peaked in the limit $t/s \rightarrow \infty$ than in the limit $t/s \rightarrow 0$, as is observed in figure 5.8 (note this argument does not apply to the NGLS model which does not satisfy (3.10) because of the inconsistency noted in §5.5 between the initial conditions on the particle velocities and the form of \hat{g}_p with which the model is consistent). It will be seen below that this has implications for the intensity of concentration fluctuations at large times.

5.7 Summary.

The problem of how to formulate two-particle stochastic models has been examined and it has been shown how the one-particle theory discussed in chapter 4 can be applied to the two-particle case. A new model has been designed for calculating dispersion in isotropic constant density flows. The new model yields a well-mixed distribution of particle-pairs in $(\underline{\hat{x}}, \underline{\hat{u}})$ -space which is consistent with the constant density constraint and with a physically reasonable form for the two-point velocity correlation function. Previous models of the form (5.1) (e.g. Durbin (1980), Lee and Stone (1983)) are consistent only with well-mixed distributions which imply $\langle \rho^2 \rangle$ is infinite or which fail to account for the correlation of velocities in space. The new model shows a more physically plausible behaviour for the particle separation p.d.f. which, in contrast to previous models, agrees with inertial subrange theory for small separations. The model is not satisfactory in every respect as it violates the physical constraint (5.2). However the degree of violation appears to be minor. Of course the ultimate test of a model is not whether it satisfies certain physical constraints, but how well it performs in comparison to experimental data. In the next chapter the model is compared against experimental data in some simple flows.

6. PREDICTIONS OF CONCENTRATION VARIANCE FROM THE NEW MODEL.

In this chapter values of concentration variance $\sigma_c^2 = \langle c^2 \rangle - \langle c \rangle^2$ from the new model described in §5.4 are presented and some comparisons with experimental data are made. Two types of situation are considered, namely those involving isotropic concentration fields, and those involving the inhomogeneous concentration fields which result from deterministic source distributions in which all the material is released at a single time. Throughout this chapter it is assumed that the fluid density ρ is constant.

6.1 Isotropic Concentration Fields.

The model described in §5.4 was used to calculate the decay of isotropic scalar fluctuations in decaying isotropic turbulence. This is one of the simplest flows involving scalar fluctuations, with the results depending only on the separation of particle-pairs and not on the motion of the particle-pair centroids. The results will be compared below with the experimental data of Warhaft and Lumley (1978) and Sreenivasan et al (1980). This data refers to the decay of scalar fluctuations with downwind distance in grid turbulence, but we interpret it here in the usual way as pertaining to the decay of scalar fluctuations with time in isotropic turbulence (Monin and Yaglom 1975, pp115-116). One of the interesting features of this flow is the way in which the rate of decay of concentration fluctuations depends on the ratio of the integral scales of the scalar and velocity fields (Warhaft and Lumley 1978; Sreenivasan et al 1980; Antonopoulos-Domis 1981; Newman et al 1981). In the experiments of Warhaft and Lumley (1978) and Sreenivasan et al (1980) the scalar fluctuations were introduced by a heated screen, or "mandoline", situated some distance downwind of the turbulence producing grid. This arrangement enabled a range of values of the length-scale ratio to be obtained. A complicating factor in comparing the experimental data with the model is the low Reynolds

number of the experiments and the consequent lack of any inertial subrange. The model presented above has been designed for high Reynolds number flows and so is not strictly applicable to the experimental situation. However it seems unlikely that the low Reynolds number of the experiments will have a strong qualitative effect on the scalar variance decay rate, although there may well be some quantitative effects.

The time at which the isotropic scalar field is introduced into the flow will be denoted by s . The scalar field will be assumed to have mean zero and $Q(\Delta \underline{x}, t)$ will denote its covariance function $\langle c(\underline{x} + \sqrt{2}\Delta \underline{x}, t) c(\underline{x}, t) \rangle$. As pointed out by Durbin (1982), for this situation (3.11) takes the form

$$Q(\Delta \underline{x}, t) = \int P_{\Delta \underline{X}(s) | \Delta \underline{X}(t)}(\Delta \underline{y} | \Delta \underline{x}) Q(\Delta \underline{y}, s) d\Delta \underline{y} \quad (6.1)$$

where $Q(\Delta \underline{x}, s)$ is the covariance function at the time when the scalar is introduced and $P_{\Delta \underline{X}(s) | \Delta \underline{X}(t)}(\Delta \underline{y} | \Delta \underline{x})$ is the p.d.f. of the particle separation vector at time s given that the particle separation vector equals $\Delta \underline{x}$ at time t . The concentration variance can then be obtained as $\sigma_c^2 = Q(0, t)$. We note in passing that (6.1) leads immediately to the (well known) fact that the Corrsin integral $\int Q(\Delta \underline{x}, t) d\Delta \underline{x}$ is constant in time (Monin and Yaglom 1975, §15.2) and shows that this constancy is a consequence of the conservation of particle-pairs. Two forms of $Q(\Delta \underline{x}, s)$ were adopted, namely

$$\sigma_c^2(s) (1 - (\Delta^4 / (\Delta^4 + l_c^4))^{1/6}) \quad (6.2)$$

and

$$\sigma_c^2(s) (1 - (\Delta^2 / (\Delta^2 + l_c^2))^{1/3}), \quad (6.3)$$

in order to see how sensitive the results are to the shape of $Q(\Delta \underline{x}, s)$. These forms have the correct inertial subrange form at small Δ . The first form is closer to the experimental data on the shape of the correlation function obtained by Yeh and van Atta (1973) downwind of a heated turbulence producing grid, although of course there is no reason

why the data of Yeh and van Atta should be especially relevant to the shape of the scalar correlation function very close to the heated screen (in fact the scalar field will not even be isotropic close to the screen; however we will ignore such complications here). Both forms, and the data of Yeh and van Atta, are shown in figure 6.1. The integral length-scale L_c of the scalar field is equal to $0.662l_c$ for the form (6.2) and $1.06l_c$ for the form (6.3). As in §5.4, L will denote the integral length-scale of the velocity field.

Figure 6.2(a) and (b) show the evolution of σ_c^2 with time as given by the new model. At small times the rate of decay of σ_c^2 depends strongly on the initial value of L/L_c and, except for large values of L/L_c in the simulations with $Q(\Delta x, s)$ given by (6.3), the initial variation of σ_c^2 is close to a power law, $\sigma_c^2 \propto t^{-m}$. This strong dependence on L/L_c was also obtained by Durbin (1982) and is observed in the experimental data. The power law exponent m at small times is plotted in figure 6.3 together with the heated screen (or "mandoline") data of Warhaft and Lumley (1978) and Sreenivasan et al (1980). The model shows the correct qualitative behaviour although the decay exponents are generally slightly too large. Better quantitative agreement could almost certainly be obtained by adjusting the model parameters (in particular the value of C_0); however this has not been attempted here.

The variation of decay rate with the initial length-scale of the concentration field can be understood quite simply in terms of equation (6.1). If $Q(\Delta x, s)$ varies little over distances comparable to the separation at time s of particle-pairs whose separation is zero at time t , then (6.1) implies

$$\begin{aligned}\sigma_c^2(t) &= Q(0, t) \approx Q(0, s) \int P_{\Delta \underline{x}(s) | \Delta \underline{x}(t)}(\Delta \underline{y} | 0) d\Delta \underline{y} \\ &= Q(0, s) = \sigma_c^2(s),\end{aligned}$$

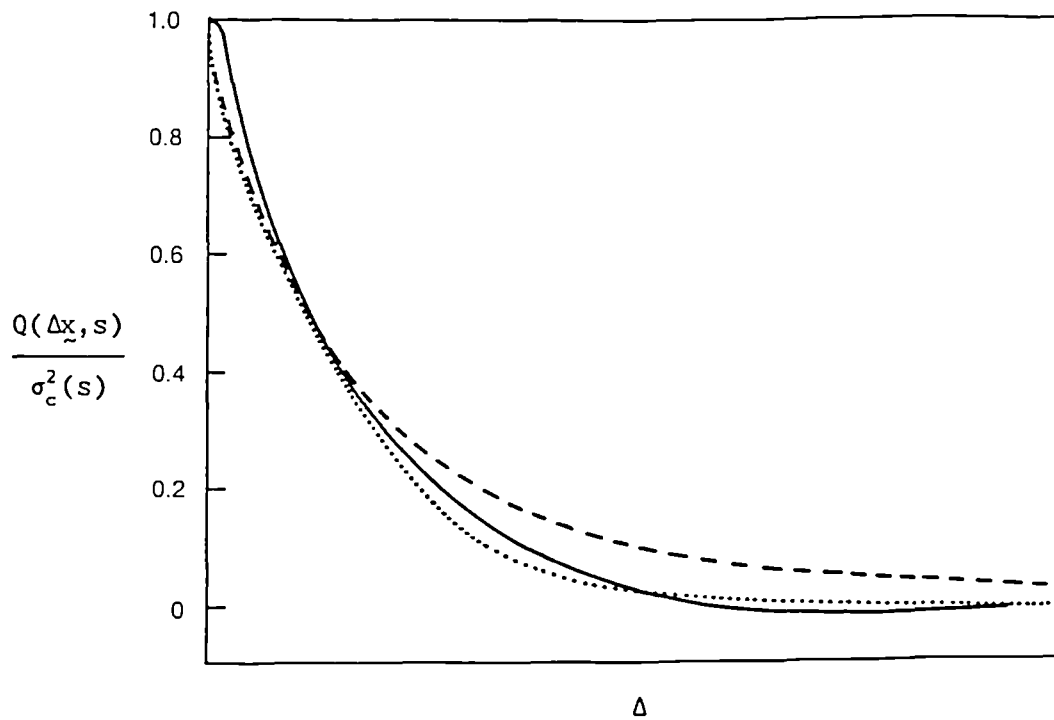


Figure 6.1: The initial correlation function of the concentration field. and ---- indicate equations (6.2) and (6.3) respectively while — is the experimental data of Yeh and van Atta (1973). The curves are normalised so that the separation at which the correlation drops to 0.5 is the same for each curve.

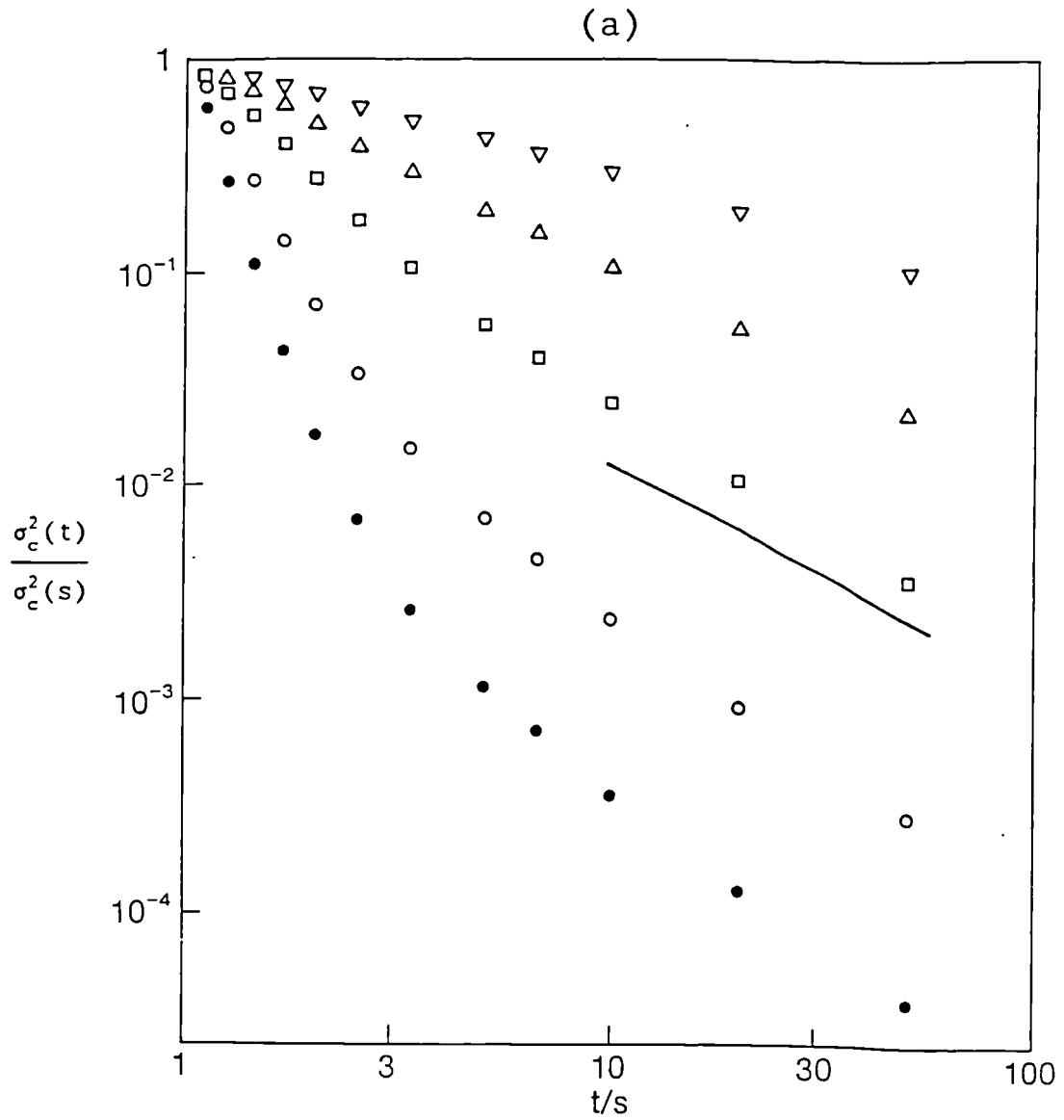


Figure 6.2: The decay of concentration variance σ_c^2 with the time t since the origin of the turbulence. s is the time at which the scalar field is introduced. ∇ , Δ , \square , \circ and \bullet indicate initial values of L/L_c of 0.185, 0.37, 0.74, 1.85 and 3.7 respectively. (a) shows results obtained with Q given by (6.2) and (b) with Q given by (6.3). The solid lines in (a) and (b) represent the theoretical decay rates at large t/s , which are proportional to $t^{-0.975}$ and $t^{-0.65}$ respectively.

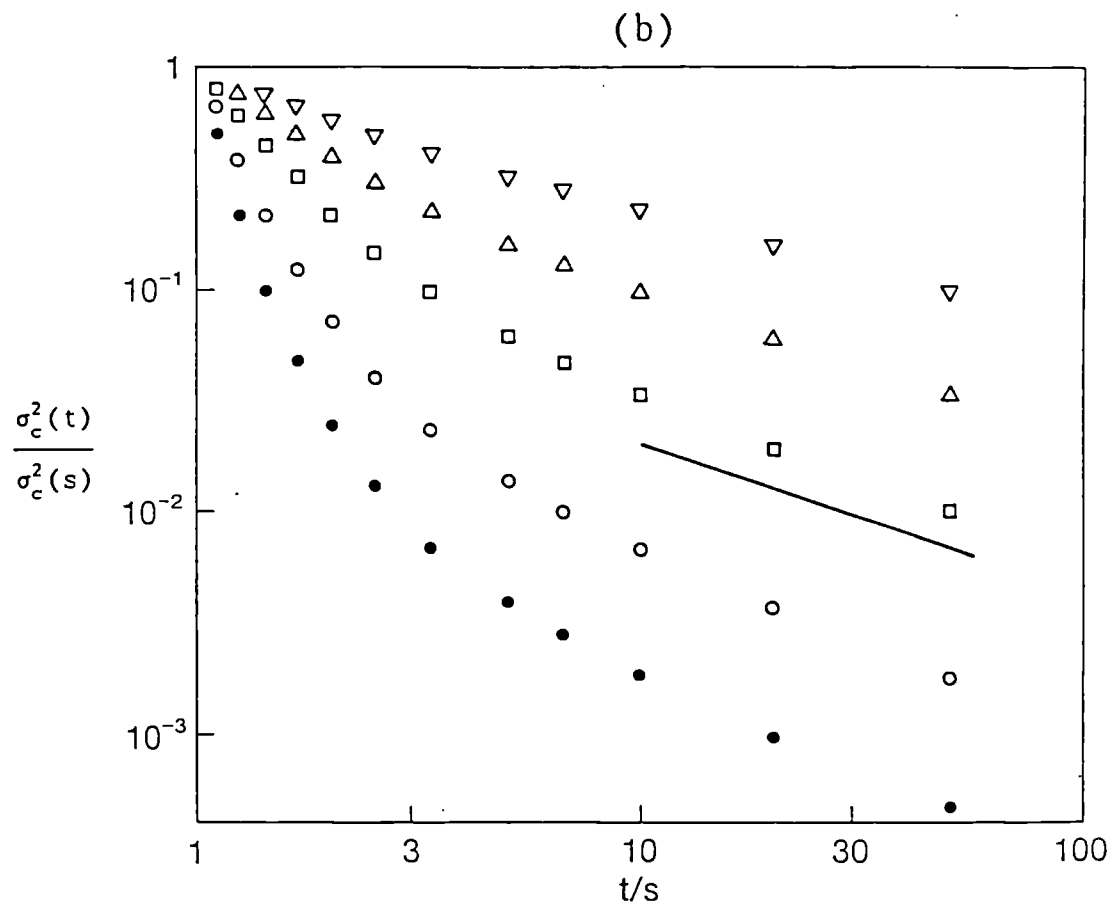


Figure 6.2 continued.

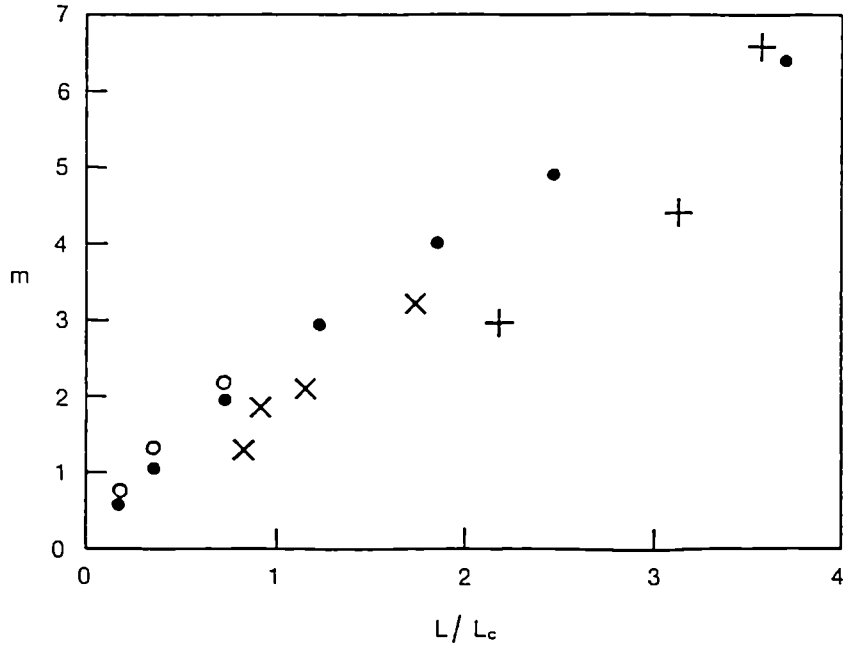


Figure 6.3: Comparison of the decay exponent m from the model with experimental data. ●, model values with $Q(\Delta x, s)$ given by (6.2); ○, model values with $Q(\Delta x, s)$ given by (6.3); ×, values from Warhaft and Lumley (1978); +, values from Sreenivasan et al (1980). The length-scale ratios for Warhaft and Lumley's experiments were estimated from the spectral peak data given in their figure 16. The values of m given for Sreenivasan et al's experiments were obtained by replotting their analytic fit to the data (their equation (5)) against distance from the turbulence grid instead of distance from the heating screen. When plotted in this way, the decay exponent varies with downstream distance. The three values which have been plotted are values obtained at three selected downstream distances. Sreenivasan et al's values of L/L_c also vary with downstream distance, and the values plotted (corresponding to the three selected downstream distances) were obtained from Sreenivasan et al's figure 7.

showing that $\sigma_c^2(t)$ is approximately equal to the initial value $\sigma_c^2(s)$. The larger the length-scale on which $Q(\Delta x, s)$ varies, the more accurately the above approximation holds and the slower is the rate of decay of σ_c^2 . At the other extreme, if $Q(\Delta y, s)$ has a very short length-scale and is negligibly small at values of Δy for which $P_{\Delta X(s)|\Delta X(t)}(\Delta y|\Delta x)$ is significantly different from $P_{\Delta X(s)|\Delta X(t)}(0|\Delta x)$, then (6.1) can be approximated by

$$Q(\Delta x, t) = P_{\Delta X(s)|\Delta X(t)}(0|\Delta x) \int Q(\Delta y, s) d\Delta y. \quad (6.4)$$

Because σ_Δ^2 grows like $(t-s)^3$ at small $t-s$, $P_{\Delta X(s)|\Delta X(t)}(0|0)$, and hence also $\sigma_c^2(t)$, decay like $(t-s)^{-9/2}$. This shows that, in the limit of small scalar length-scale, σ_c^2 decays faster than any power of t at small times after release.

For large times the model decay rates approach a value which is independent of the initial value of L/L_c . The following argument gives a simple explanation of the asymptotic value of the decay exponent. As $t \rightarrow \infty$ the length-scale on which $P_{\Delta X(s)|\Delta X(t)}(\Delta y|\Delta x)$ varies increases indefinitely. It follows that, provided the Corrsin integral $\int Q(\Delta x, s) d\Delta x$ is finite and non-zero, (6.1) can be approximated by (6.4) (this approximation is similar to the approximations considered in §5.6 when discussing whether source size remains important at large times). Because $\sigma_\Delta(s|t)$ varies like $L(t)$ at large times (see §5.6(iii)), it follows that σ_c^2 varies like $1/L^3$, i.e. $t^{-0.975}$, as is observed in the simulations which were carried out with $Q(\Delta x, s)$ given by (6.2) (figure 6.2(a)). For (6.3) however, the Corrsin integral is infinite with $Q(\Delta x, s)$ proportional to $1/\Delta^2$ for large Δ . In this case the dominant contribution to the integral in (6.1) comes, at large times, from large values of $|\Delta y|$. It follows, by a similar argument to that given above, that σ_c^2 decays like $1/L^2$ at large times, as is observed in the simulations (figure 6.2(b)). This difference in behaviour, which is also found in two-point spectral closures such as the eddy-damped

quasi-normal Markovian approximation (Larchevêque et al 1980), shows that the asymptotic value of the decay exponent may be quite sensitive to the form of Q .

The experimental data show little sign of an approach to a universal decay exponent. However, as discussed by Larchevêque et al (1980) and Nelkin and Kerr (1981), this may well be due to the fact that the experimental data do not extend to large enough values of t/s . There seems little merit in a more detailed comparison of the model decay curves with the experimental data since the initial shape of $Q(\Delta y, s)$ is unknown and it was seen above that the large time behaviour is quite sensitive to this shape. However we note that for large initial values of L/L_c , the experimental data (Sreenivasan et al 1980) shows m decreasing as t/s increases in qualitative agreement with the model results shown in figure 6.2 (note Sreenivasan et al plot σ_c^2 against distance from the heated screen instead of distance from the turbulence grid; when plotted in this way the data are quite close to a power law throughout the region in which the measurements were made).

6.2 Instantaneous Deterministic Sources.

(i) Introduction.

In this section deterministic instantaneous sources are considered and the release time will be denoted by s . For $t > s$, (3.9) and (3.11) can then be written as

$$\langle c(\underline{x}, t) \rangle = \int p_{\underline{X}(s) | \underline{X}(t)}(\underline{y} | \underline{x}) S(\underline{y}) d\underline{y} \quad (6.5)$$

and

$$\begin{aligned} \langle c(\underline{x}, t)^2 \rangle = & \int p_{\underline{X}_1(s), \underline{X}_2(s) | \underline{X}_1(t), \underline{X}_2(t)}(\underline{y}_1, \underline{y}_2 | \underline{x}, \underline{x}) \times \\ & \times S(\underline{y}_1) S(\underline{y}_2) d\underline{y}_1 d\underline{y}_2 \quad (6.6) \end{aligned}$$

where $S(\underline{x})$ is the source strength (as in §5.6, S here has a slightly different meaning to the S introduced in chapter 3, being the amount of

tracer released per unit volume, not per unit space-time volume). It is useful to apply an approximation introduced by Sawford (1983) and replace $p_{\underline{X}(s)|\underline{X}(t)}(\underline{y}|\underline{x})$ in (6.5) by

$$G_3(\underline{y}-\underline{x}, \sigma_1^2(s|t)) \quad (6.7)$$

and $p_{\underline{X}_1(s), \underline{X}_2(s)|\underline{X}_1(t), \underline{X}_2(t)}(\underline{y}_1, \underline{y}_2|\underline{x}, \underline{x})$ in (6.6) by

$$p_\Delta(\Delta\underline{y}, s|t) G_3(\Sigma\underline{y}-\underline{x}/2, \sigma_\Sigma^2(s|t)) \quad (6.8)$$

where $\Delta\underline{y} = (\underline{y}_1 - \underline{y}_2)/\sqrt{2}$, $\Sigma\underline{y} = (\underline{y}_1 + \underline{y}_2)/\sqrt{2}$ and $G_\lambda(\underline{x}, \sigma^2)$ denotes a λ -dimensional Gaussian distribution with variance σ^2 , i.e.

$$G_3(\underline{x}, \sigma^2) = \frac{1}{(2\pi)^{3/2} \sigma^3} \exp(-|\underline{x}|^2/2\sigma^2)$$

$$G_2(\underline{x}, \sigma^2) = \frac{1}{2\pi\sigma^2} \exp(-((x^2)^2 + (x^3)^2)/2\sigma^2)$$

$$G_1(\underline{x}, \sigma^2) = \frac{1}{(2\pi)^{1/2} \sigma} \exp(-(x^3)^2/2\sigma^2).$$

The assumptions involved here are that the distribution of \underline{X} and $\Sigma\underline{X}$ are approximately Gaussian (which is true) and that, for particles with separation zero at time s , $\Delta\underline{X}$ and $\Sigma\underline{X}$ are approximately independent. The latter assumption is hard to verify directly but appears reasonable because of the weak dependence of $d\Sigma\underline{X}$ on $\Delta\underline{X}$, the absence of any dependence of $d\Delta\underline{X}$ on $\Sigma\underline{X}$, and the fact that the covariance of $\Delta\underline{X}$ and $\Sigma\underline{X}$ is zero. A comparison presented below between values of σ_c obtained with and without this approximation gives some indirect support for the assumption. The advantages of using the approximations (6.7) and (6.8) are that it reduces statistical noise and makes it easier to see how the different aspects of the one- and two-particle transition p.d.f.s (e.g. σ_1 , σ_Δ , σ_Σ , shape of p_Δ) influence σ_c .

Calculations of $\langle c^2 \rangle$ and $\langle c \rangle$ were carried out for area, line and compact sources centred on the origin. The source size will be denoted by σ_0 . The source is taken to be Gaussian, i.e. $S(\underline{x}) = G_\lambda(\underline{x}, \sigma_0^2)$ where

λ is 1 for an area source, 2 for a line source and 3 for a compact source. As discussed by Sawford (1983), $\langle c \rangle$ and $\langle c^2 \rangle$ are, with the approximations (6.7) and (6.8), given by

$$\langle c(\underline{x}, t) \rangle = G_\lambda(\underline{x}, \sigma_1^2(s|t) + \sigma_0^2) \quad (6.9)$$

and

$$\langle c(\underline{x}, t)^2 \rangle = \int p_\Delta(\Delta \underline{y}, s|t) G_\lambda(\Delta \underline{y}, \sigma_0^2) d\Delta \underline{y} G_\lambda(\underline{x}/2, \sigma_2^2(s|t) + \sigma_0^2). \quad (6.10)$$

Some calculations will also be presented for two parallel Gaussian area sources. For this situation expressions analogous to (6.9) and (6.10) can be easily derived.

(ii) Stationary turbulence.

Figures 6.4(a), (b) and (c) show values of $\sigma_c/\langle c \rangle$ at $\underline{x} = 0$ for area, line and compact sources of various sizes. Some statistical noise is evident at small values of $\sigma_c/\langle c \rangle$, especially at large times. This is because, when $\sigma_c/\langle c \rangle$ is small, small errors in $\langle c^2 \rangle$ and $\langle c \rangle$ can result in a large error in σ_c . The results show clearly the strong effect which source size has near the source and suggest that $\sigma_c/\langle c \rangle$ becomes independent of source size and tends to zero at large time. Because of statistical noise, it is impossible, in the absence of an analytic solution to the model, to state with certainty that the model value of $\sigma_c/\langle c \rangle$ tends to zero. However, if $p_\Delta(\Delta \underline{x}, s|t)$ is exactly Gaussian at large t , then (6.9) and (6.10) imply

$$\frac{\sigma_c}{\langle c \rangle} = \left(\frac{(\sigma_1^2(s|t) + \sigma_0^2)^\lambda}{((\sigma_\Delta^2(s|t) + \sigma_0^2)(\sigma_2^2(s|t) + \sigma_0^2))^{\lambda/2}} - 1 \right)^{1/2} \quad (6.11)$$

at large times. Now $\sigma_1(s|t)/\sigma_\Delta(s|t)$ and $\sigma_1(s|t)/\sigma_2(s|t)$ tend to unity as $t \rightarrow \infty$ and so, if (6.11) is true, $\sigma_c/\langle c \rangle \rightarrow 0$ at large times. This behaviour agrees with that shown by the NGLS model but is in marked contrast to Durbin's (1980) model where $\sigma_c/\langle c \rangle$ tends to a non-zero constant depending on source size. An argument which suggests that $\sigma_c/\langle c \rangle$ tends to zero in reality at large times can be constructed as

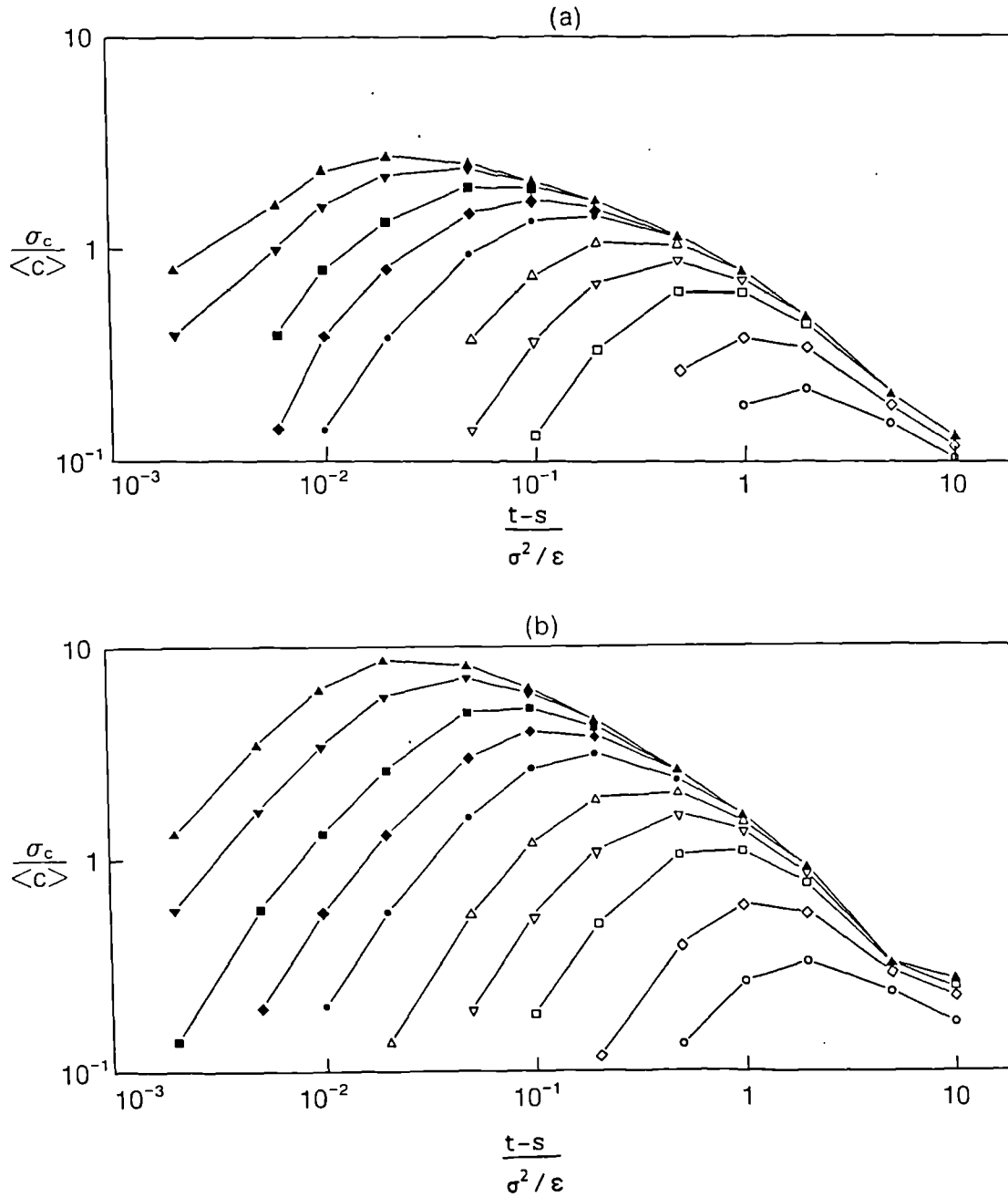


Figure 6.4: Values of $\sigma_c / \langle c \rangle$ at $\tilde{x} = 0$ from the model in stationary conditions. (a) shows results for an area source, (b) for a line source and (c) for a compact source. (d) shows results for an area source calculated without using the approximation (6.8). The different symbols refer to different source sizes: \blacktriangle , $\sigma_0 = 0.001\sigma^3/\epsilon$; \blacktriangledown , $\sigma_0 = 0.002\sigma^3/\epsilon$; \blacksquare , $\sigma_0 = 0.005\sigma^3/\epsilon$; \blacklozenge , $\sigma_0 = 0.01\sigma^3/\epsilon$; \bullet , $\sigma_0 = 0.02\sigma^3/\epsilon$; \triangle , $\sigma_0 = 0.05\sigma^3/\epsilon$; \triangledown , $\sigma_0 = 0.1\sigma^3/\epsilon$; \square , $\sigma_0 = 0.2\sigma^3/\epsilon$; \diamond , $\sigma_0 = 0.5\sigma^3/\epsilon$; \circ , $\sigma_0 = \sigma^3/\epsilon$.

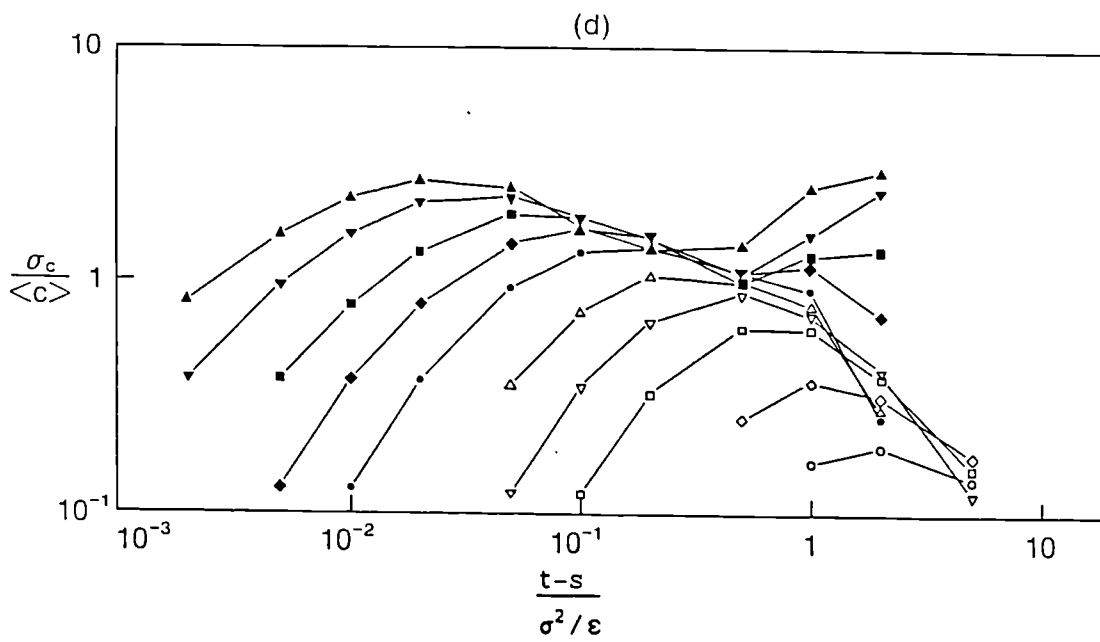
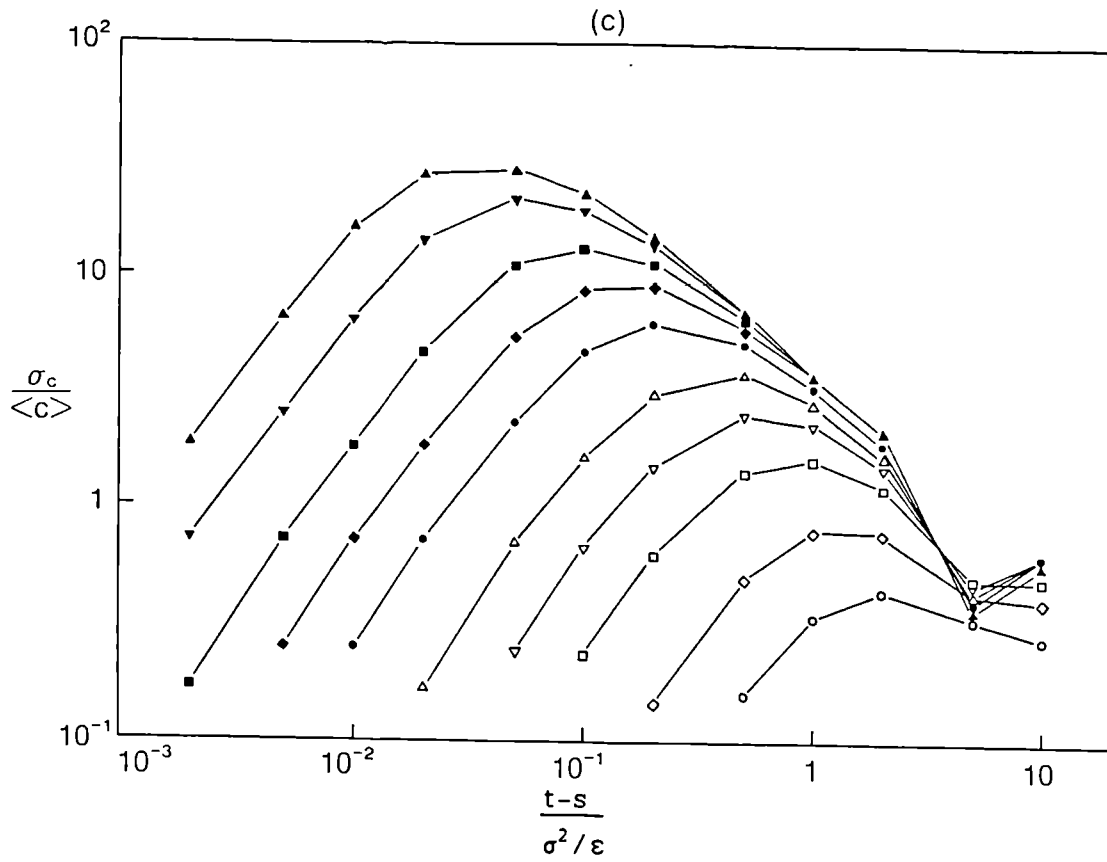


Figure 6.4 continued.

follows. At large times the two particles in a pair will have spent most of their time at large separations where they move independently. Hence it seems likely that $\underline{X}_1(t)$ and $\underline{X}_2(t)$ become asymptotically independent as $t \rightarrow \infty$. As a result, using the fact that the model's forward and reverse statistics are identical in stationary conditions,

$$P_{\underline{X}_1(s), \underline{X}_2(s) | \underline{X}_1(t), \underline{X}_2(t)}(y_1, y_2 | \underline{x}, \underline{x}) = \\ P_{\underline{X}(s) | \underline{X}(t)}(y_1 | \underline{x}) P_{\underline{X}(s) | \underline{X}(t)}(y_2 | \underline{x})$$

at large times and it follows from (6.5) and (6.6) that $\sigma_c / \langle c \rangle \approx 0$.

Values of $\sigma_c / \langle c \rangle$ for an area source, obtained without using the approximation (6.8) (but still using (6.7)) are shown in figure 6.4(d). In evaluating (6.6), the two-particle transition p.d.f. was represented as a sum of a number of delta functions located at the positions of the particle-pairs in the simulation. At small times the results show good agreement with the results obtained using (6.8) (figure 6.4(a)), lending support to the assumption that $\Delta \underline{X}$ and $\Sigma \underline{X}$ are approximately independent. At larger times however the scatter becomes very great due to the small number of particle-pairs passing through the source. For example, for small sources at large times the expected number of particle-pairs passing through the source can be less than one. In this situation either no particle-pairs pass through and the calculated value of $\langle c^2 \rangle$ is zero, or one or more particle-pairs pass through and $\sigma_c / \langle c \rangle$ is large. It may be possible to improve matters by smoothing the two-particle transition p.d.f. and by the use of a suitable form of particle splitting to ensure that there are always a lot of particle-pairs near the source; however this has not been attempted here. For line and compact sources (not shown) the scatter is even greater.

Figure 6.5 shows a comparison between the model results and the experimental wind tunnel data of Fackrell and Robins (1982). In the wind tunnel experiments material was released into a turbulent boundary

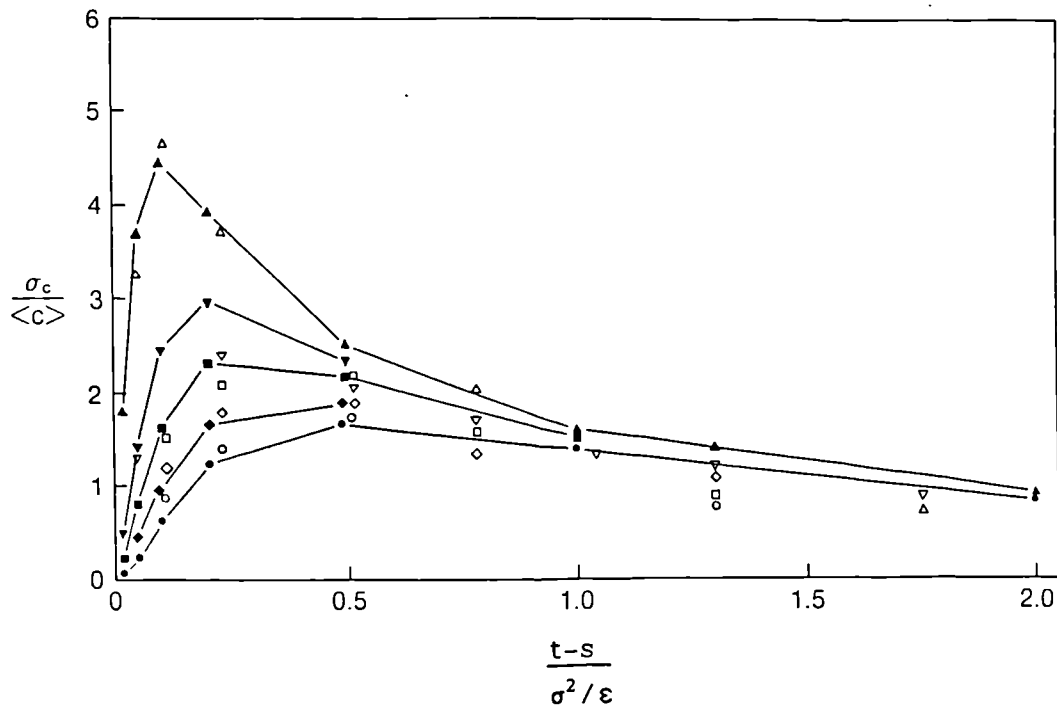


Figure 6.5: Comparison of $\sigma_c / \langle c \rangle$ at $x = 0$ from the model with the experimental data of Fackrell and Robins (1982). Model results are indicated by solid symbols and experimental results by open symbols. The different symbol shapes refer to different source sizes: ▲, $\sigma_0 = 7.41 \times 10^{-3} \sigma^3 / \epsilon$; ▼, $\sigma_0 = 2.22 \times 10^{-2} \sigma^3 / \epsilon$; ■, $\sigma_0 = 3.7 \times 10^{-2} \sigma^3 / \epsilon$; ◆, $\sigma_0 = 6.17 \times 10^{-2} \sigma^3 / \epsilon$; ●, $\sigma_0 = 8.64 \times 10^{-2} \sigma^3 / \epsilon$.

layer from a continuous compact elevated source. For comparison with the model, the experimental data obtained at a distance x downwind of the source is regarded as data obtained at time x/U_0 after the release of an instantaneous line source in stationary isotropic turbulence (here U_0 denotes the mean velocity at the source in the experiments). Provided the anisotropy of the flow can be neglected, this should be a good approximation; this is because the intensity of turbulence in the experiments was small (see e.g. Townsend (1954), Anand and Pope (1985) or Sawford and Hunt (1986) for a discussion of a similar approximation - the approximation of a continuous line source by an instantaneous area source). The wind tunnel results are of course affected by the shear and the inhomogeneity in the flow and the anisotropy of the (one-point) velocity covariance tensor $\langle u_0^i u_0^j \rangle$; however the effect of the shear and inhomogeneity should be unimportant for travel times less than about $0.5\sigma^2/\epsilon$, the time at which the tracer first reaches the ground in significant quantities. In contrast the anisotropy of the velocity covariance tensor is likely to have some effect on the results, but, because the anisotropy is not large, the effect is unlikely to be of major importance. In plotting the experimental results in figure 6.5, σ^2 was taken to be the average of the velocity variances in three orthogonal directions. The agreement between the model and experimental results is good although, because of the uncertainty in the universal constant C_0 and the arbitrary way in which f was chosen (equation (5.6)), this may be partly fortuitous. It is somewhat surprising that the agreement remains good for $t-s > 0.5\sigma^2/\epsilon$ when the effect of shear and inhomogeneity might be expected to be significant. The observed and modelled behaviour is different to the type of behaviour seen in Durbin's model where $\sigma_c/\langle c \rangle$ increases monotonically to an asymptotic value.

Figure 6.6 shows examples of profiles of σ_c for a line source with σ_0 equal to $2.22 \times 10^{-2} \sigma^3 / \epsilon$, the source size used in most of Fackrell and Robins experiments. As time increases the profile evolves through three stages. At first the σ_c profile has its peak away from the origin at the point where the gradient of $\langle c \rangle$ is greatest. As time advances the peak moves towards the origin and, in what will be referred to as the second stage, the peak is at $\underline{x}=0$. This stage lasts from $t-s = 0.05\sigma^2/\epsilon$ to $t-s = 2\sigma^2/\epsilon$. In the third and final stage, the off centre peak reappears. At all times the σ_c profile is somewhat wider than the profile of the mean concentration. Similar behaviour is observed for other small source sizes, although the time of transition between the first and second stages increases with source size. For large sources, with σ_0 comparable to σ^3/ϵ , the behaviour is somewhat different, the first stage lasting so long that it merges into the third stage with the second stage being squeezed out of existence. For area sources the second stage begins later and ends earlier while the reverse is true for compact sources. In the case of compact sources the evidence for the reappearance of the off-centre peak is not so clear cut, the peak appearing and disappearing repeatedly at large times due to the statistical scatter discussed above. The first stage in the evolution of σ_c is to be expected because, at small times after release, the fluctuations arise directly from the local gradients of mean concentration. Some understanding of the second stage can be obtained by considering (6.9) and (6.10). These equations imply that the peak will occur off the centre line when

$$\frac{\langle c(0,t)^2 \rangle}{\langle c(0,t) \rangle^2} \frac{\sigma_1^2(s|t) + \sigma_0^2}{\sigma_2^2(s|t) + \sigma_0^2} < 1; \quad (6.12)$$

in particular, since $\sigma_2^2 \leq 2\sigma_1^2$, the peak must be on the centre line when $\sigma_c / \langle c \rangle \geq 1$. At large times p_Δ becomes close to Gaussian. If p_Δ is exactly Gaussian, then (6.9), (6.10) and the fact that $\sigma_1(s|t)/\sigma_\Delta(s|t)$ and $\sigma_1(s|t)/\sigma_2(s|t)$ tend to unity at large t imply that the left hand

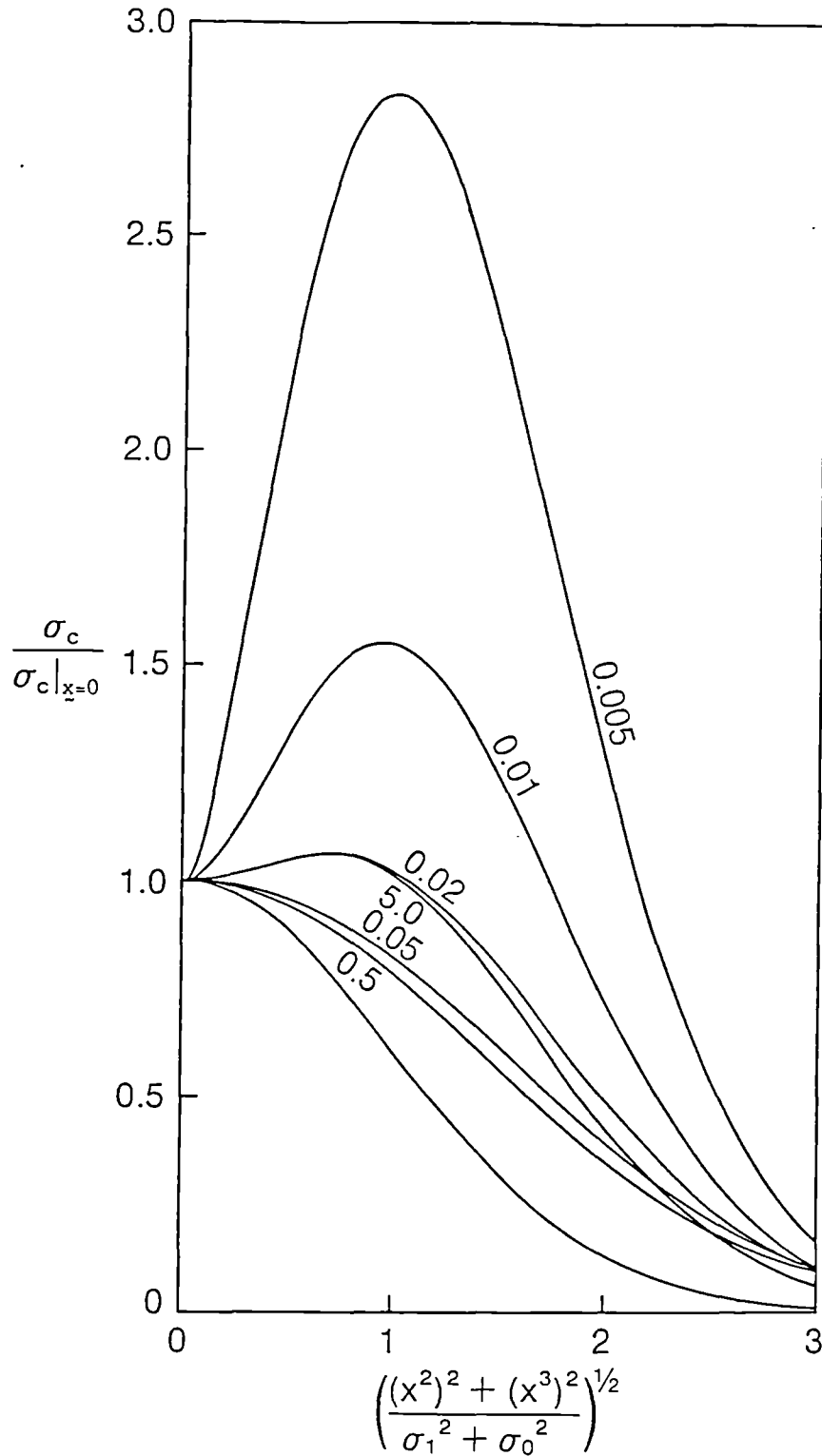


Figure 6.6: Profiles of σ_c from the model for a line source in stationary conditions. $\sigma_0 = 2.22 \times 10^{-2} \sigma^3 / \varepsilon$. The numbers attached to the curves indicate values of $t-s$ normalised by σ^2 / ε . The unlabelled curve is a Gaussian distribution with the same standard deviation as the profile of $\langle c \rangle$.

side of (6.12) is less than 1 at large t (and approaches 1 as $t \rightarrow \infty$) and so explains the reappearance of the off-centre peak in the third stage. The reappearance of the off-centre peak suggests that at large times σ_c is again partly determined by local processes, with σ_c peaking in the vicinity of the point where the production of concentration variance from the local mean concentration gradient is a maximum. The data collected by Fackrell and Robins (1982) were obtained at travel times in the range $0.26\sigma^2/\varepsilon$ to $1.74\sigma^2/\varepsilon$, times which the model predicts will lie within the second stage of evolution. The measured σ_c profiles are consistent with this, showing a centre line peak and a similar form to the model profiles. The width of the model's σ_c profile is in good agreement with the experimental data; for the times at which the experimental data was obtained, both the model and the experimental σ_c profile half widths lie between 1.4 and 1.6 times the half width of the $\langle c \rangle$ profile.

(iii) Decaying turbulence.

Figure 6.7 shows model values of $\sigma_c/\langle c \rangle$ at $\underline{x} = 0$ for dispersion from an area source in decaying turbulence. As in the stationary case the values are strongly affected by the source size at small times, but become independent of source size at large times. However, in contrast to the results obtained in stationary conditions, $\sigma_c/\langle c \rangle$ approaches a small non-zero constant at large time. If $p_\Delta(\Delta\underline{x}, s|t)$ is exactly Gaussian for $t \gg s$ then (6.11) holds and this constant can be expressed as

$$\lim_{t/s \rightarrow \infty} \left(\frac{(\sigma_1(s|t))^2}{\sigma_\Delta(s|t)\sigma_z(s|t)} - 1 \right)^{1/2}.$$

As noted at the end of §5.6, $\sigma_1(s|t)/\sigma_\Delta(s|t)$ and $\sigma_1(s|t)/\sigma_z(s|t)$ do not tend to unity as $t \rightarrow \infty$. Hence, because $\sigma_1^2 = (\sigma_\Delta^2 + \sigma_z^2)/2$ and because arithmetic means are greater than geometric ones, this limit is strictly positive. The simulations indicate that the value of this

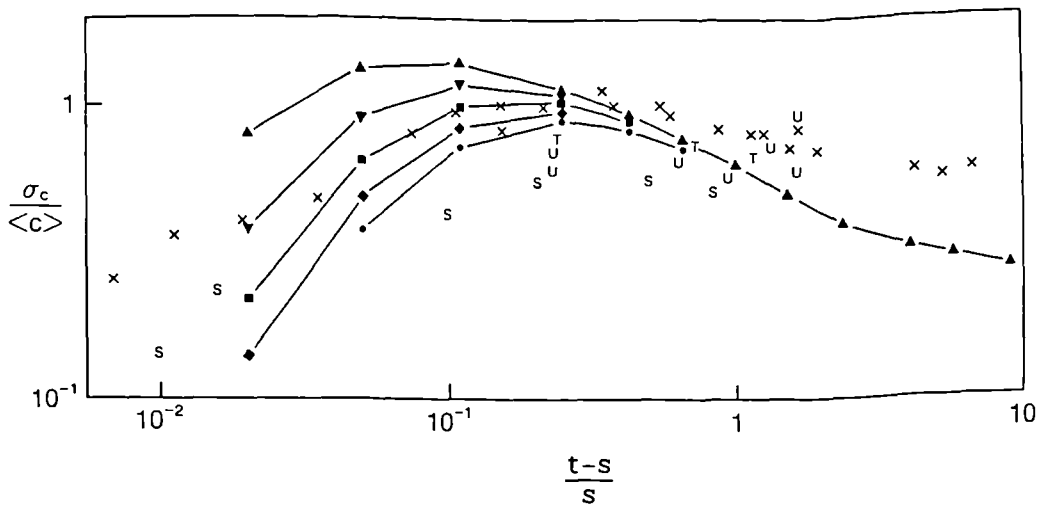


Figure 6.7: Comparison of $\sigma_c / \langle c \rangle$ at $\underline{x} = 0$ from the model with the experimental data of Warhaft (1984). The model results for various source sizes are indicated by the following symbols: \blacktriangle , $\sigma_0 = 0.01\sigma_s s$; \blacktriangledown , $\sigma_0 = 0.02\sigma_s s$; \blacksquare , $\sigma_0 = 0.03\sigma_s s$; \blacklozenge , $\sigma_0 = 0.04\sigma_s s$; \bullet , $\sigma_0 = 0.05\sigma_s s$. The experimental results of Warhaft (1984) are denoted by crosses. Also shown are the experimental results of Uberoi and Corrsin (1952) (U), Townsend (1954) (T) and Stapountzis et al (1986) (S).

limit is about 0.16.

The results of Warhaft's (1984) experiments on dispersion downstream of a cross-stream line source in decaying grid turbulence are also plotted in figure 6.7. In the same way as Fackrell and Robins' (1982) continuous compact source was interpreted as an instantaneous line source, the continuous line source of Warhaft's experiment is regarded here as an instantaneous area source. It is not so easy to interpret these experiments as those of Fackrell and Robins (1982) because the Reynolds number is relatively low and the model being considered here cannot account for molecular diffusivity and viscosity explicitly. Molecular diffusion almost certainly results in an effective source size that is much larger than the width of the wire used in the experiments. It seems reasonable to assume that the effective source size will be of the same order as the Kolmogorov micro-scale, η . The value of η at the source varies between the experiments, lying between $0.01\sigma_s s$ and $0.016\sigma_s s$. The agreement with the model results is best for a slightly larger source size of about $0.03\sigma_s s$. At large times the value of $\sigma_c/\langle c \rangle$ in the model falls off rather too quickly. This is probably because the asymptotic value at large time is too small. Although the agreement could almost certainly be improved by adjusting C_0 and f , it is not proposed to do this here. The agreement is also poor for $(t-s)/s \leq 0.02$. This is however to be expected since molecular diffusion must be significant for $(t-s)/s$ of order τ_η/s , a quantity which is about 0.04 in the experiments. To model this region accurately it would be necessary to take account of molecular diffusivity and viscosity explicitly as in Sawford and Hunt (1986) and to use a source size more closely related to the wire diameter. Also shown in figure 6.7 are the experimental results obtained downwind of a line source in grid turbulence by Uberoi and Corrsin (1952), Townsend (1954) and Stapountzis et al (1986). These data show broadly similar behaviour to Warhaft's data and to the model

results.

Figure 6.8 shows the model profiles of σ_c for $\sigma_0 = 0.03\sigma_g s$. Qualitatively the behaviour is similar to that obtained in stationary conditions (figure 6.6) and to that observed by Warhaft (1984). At small $(t-s)/s$ the profiles have an off-centre peak, although the model peak is rather more pronounced than that in Warhaft's experiments. It seems likely that this discrepancy is due to molecular diffusion which, in the experiments, must play a significant role in the early stages of the plume's development. To represent these early stages accurately, it is probably necessary, as above, to use a source size related to the wire diameter and to use a model which includes molecular diffusion and viscous effects explicitly. For $0.11 \leq (t-s)/s \leq 0.43$ in the model and for $0.073 \leq (t-s)/s \leq 1.92$ in Warhaft's experiments, the peak is at the centre of the ensemble average plume, with the off-centre peak reappearing at large times. Although the off-centre peak reappears sooner in the model than in the experiments, the model peak value is only a few per cent larger than the centre line value until $(t-s)/s \approx 2$. At large $(t-s)/s$ the model off-centre peak is again rather more pronounced than that measured in the experiments. As noted above, the off-centre peak cannot occur if $\sigma_c/\langle c \rangle$ is as large as unity, and so it seems possible that the more pronounced peak in the model is associated with the fact that the value of $\sigma_c/\langle c \rangle$ in the model is too low at large times. The width of the model σ_c profile is in good agreement with the experimental data, the half width in both the model and the experiments lying between about 1.5 and 2.0 times the half width of the $\langle c \rangle$ profile.

Figures 6.9 and 6.10 show model values of the correlation between the concentrations resulting from two parallel instantaneous Gaussian area sources. The sources are taken parallel to the (x^1, x^2) -plane and are separated by a distance d , with the origin (i.e. $x_j = 0$) lying

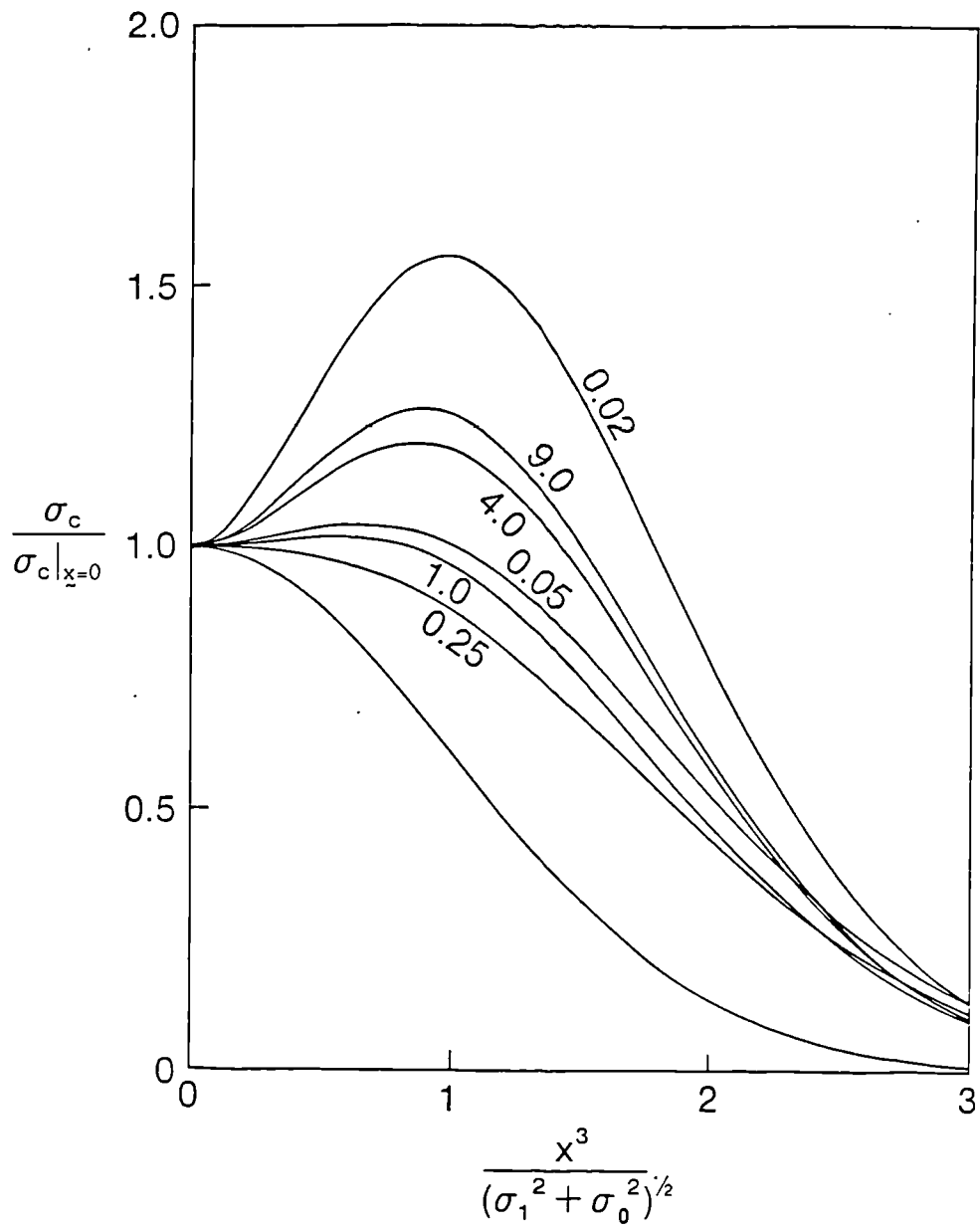


Figure 6.8: Profiles of σ_c from the model for an area source in decaying turbulence. $\sigma_0 = 0.03\sigma_s$. The numbers attached to the curves indicate values of $(t-s)/s$. The unlabelled curve is a Gaussian distribution with the same standard deviation as the profile of $\langle c \rangle$.

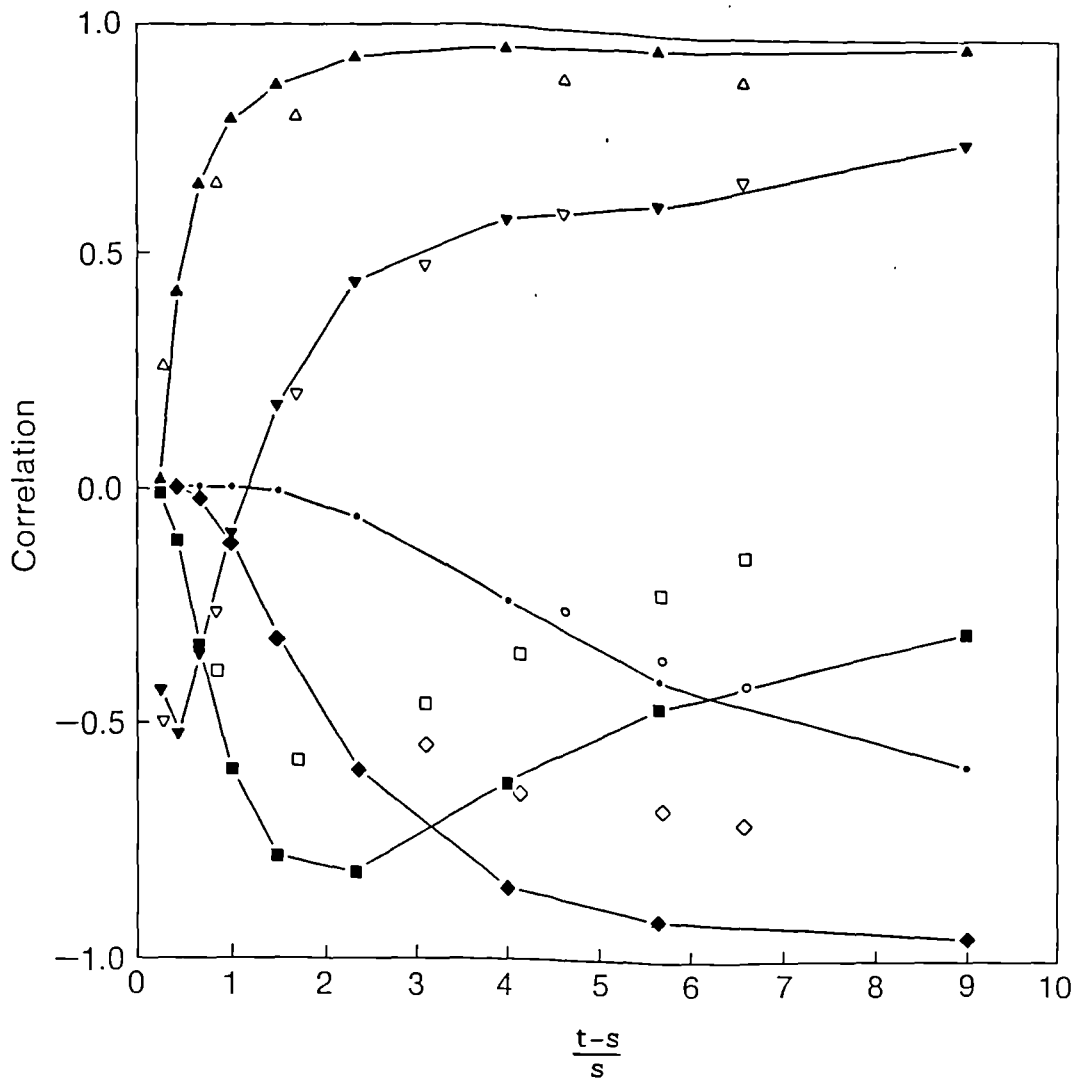


Figure 6.9: Correlation between the concentration resulting from two parallel sources separated by a distance d in decaying turbulence. The correlation is evaluated half way between the two sources. Model results for a source size of $0.03\sigma_s$ are indicated by solid symbols and experimental results from Warhaft (1984) by open symbols. The different symbol shapes refer to different values of d : ▲, $d = 0.122\sigma_s$; ▼, $d = 0.4\sigma_s$; ■, $d = 1.26\sigma_s$; ◆, $d = 2.52\sigma_s$; ●, $d = 5.2\sigma_s$.

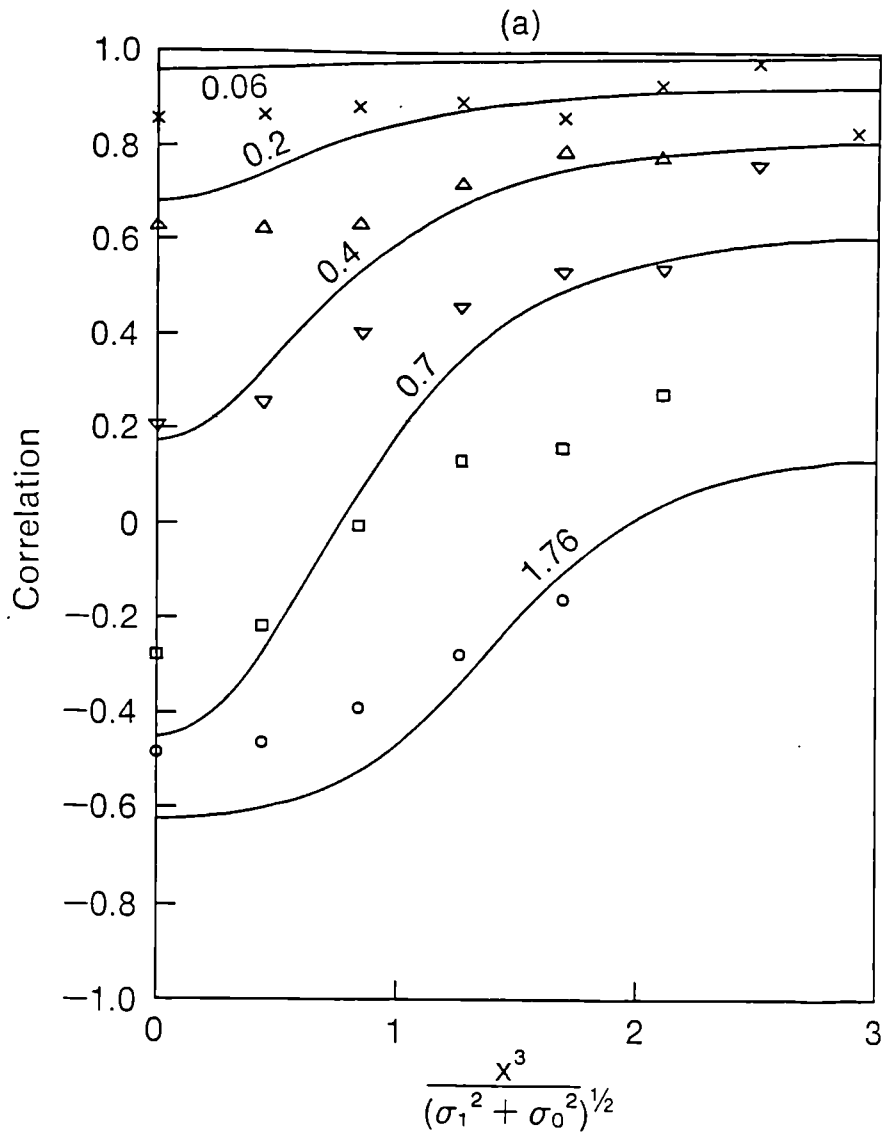


Figure 6.10: Correlation between the concentration resulting from two parallel sources separated by a distance d in decaying turbulence. The correlation is shown as a function of x^3 , the origin of x^3 being taken half way between the two sources. (a) shows model results for $(t-s)/s = 1.5$ and experimental results (Warhaft 1984) for $(t-s)/s = 1.65$, while (b) shows model results for $(t-s)/s = 4.0$ and experimental results for $(t-s)/s = 4.65$. The model results are shown by solid lines and labelled with the value of d/σ_s , while the experimental results for different values of d are indicated as follows: \times , $d = 0.06\sigma_s$; $+$, $d = 0.122\sigma_s$; Δ , $d = 0.2\sigma_s$; ∇ , $d = 0.4\sigma_s$; \square , $d = 0.7\sigma_s$; \diamond , $d = 1.26\sigma_s$; \circ , $d = 1.76\sigma_s$. The experimental results are taken from Warhaft's (1984) figure 13 and the values obtained for positive and negative x^3 have been averaged.

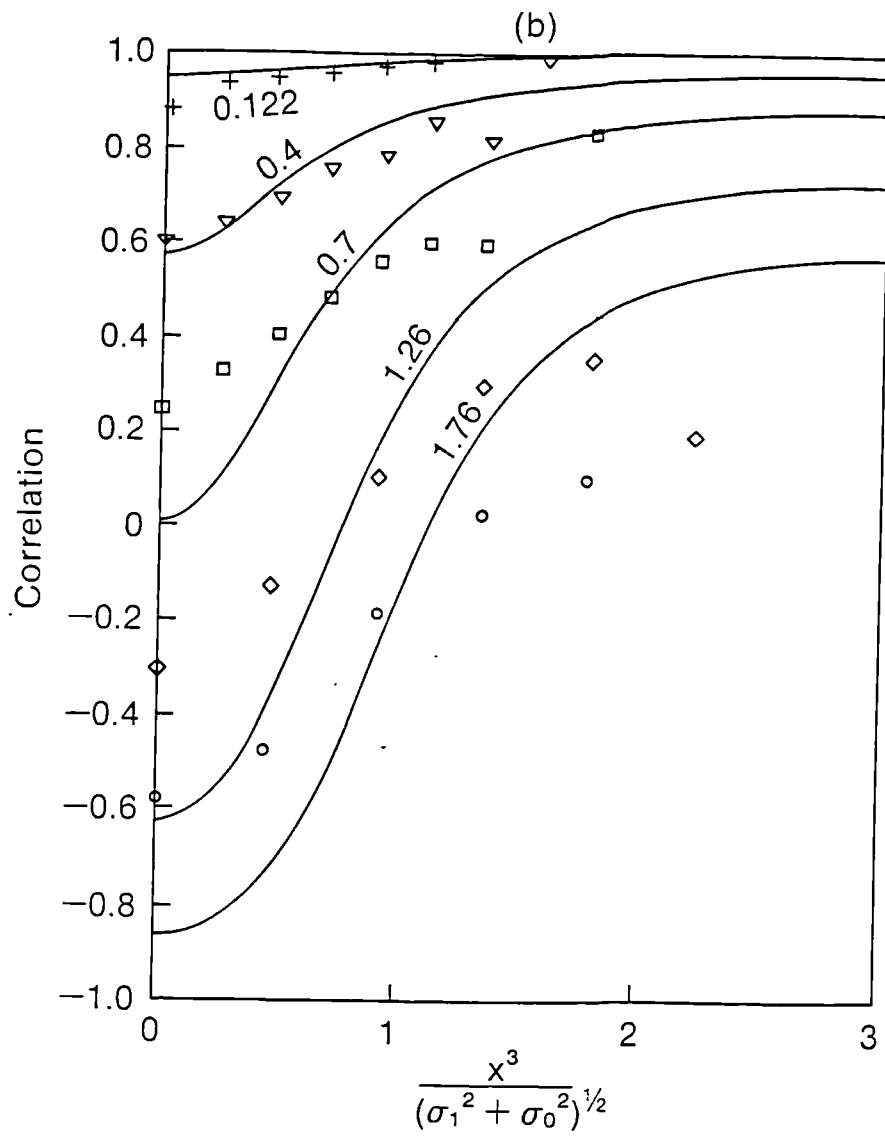


Figure 6.10 continued.

midway between the sources. Also shown are experimental values for two parallel continuous cross-stream line sources in decaying grid turbulence (Warhaft 1984). As for the single sources considered above, the data is interpreted as relating to two instantaneous area sources. In the model the size of each source was taken to be $0.03\sigma_g s$, the value which gives best agreement with the single source data. The values of the correlation at the origin are shown in figure 6.9. The model values show very similar behaviour to that observed although there are some quantitative differences when the correlation is negative. The agreement is much better than that obtained with Durbin's model by Sawford (1985). For example, Sawford's calculations show the correlation approaching a value of 0.15 at large times for $d/l = 0.2$ (see Sawford's figure 7). In contrast, Warhaft's (1984) experimental values of the correlation reach values as large as 0.9 for $d/\sigma_g s$ equal to 0.06 and 0.122 (which correspond, with our assumptions about the turbulence, to values of d/l of 0.17 and 0.35). In Sawford's calculations no account is taken of the decay of the turbulence in the experiments; however this is likely to result in better mixing in the model and hence larger values of the correlation than would otherwise occur.

The behaviour of the correlation can be understood quite simply in terms of the following physical picture. It is easier to visualise this picture in terms of the experimental set-up of two continuous line sources than in terms of two instantaneous area sources, and so we will adopt this view point. At small distances downwind from the sources, the material from the two sources meanders "in phase" due to the correlation between the velocities at the two source locations. As a result the correlation is negative. Also, at very small distances, material only rarely reaches the measurement point and on such occasions only material from one source is present in significant quantities; hence the correlation is small and negative. At large

times the plumes from the two sources mix and the correlation becomes positive. Because the length-scale on which $p_{\Delta}(\Delta x, s|t)$ varies increases without limit as $t \rightarrow \infty$, it can be shown from (6.5), (6.6) and the approximations (6.7) and (6.8) that the correlation (in the model at least) tends to unity at large times. An alternative way to deduce that the correlation tends to unity at large times is as follows. We have seen that the value of σ_c^2 becomes independent of source size at large times and it seems reasonable to expect σ_c^2 to become independent of the source shape also. Hence the value of σ_c^2 due to the two sources should become equal to the value resulting from a single source of twice the strength. This can only happen if the correlation tends to unity. The times at which these different stages in the evolution of the correlation occur vary greatly with the source separation d , as can be seen from figure 6.9.

Figure 6.10 shows some examples of the correlation at points away from the origin. The agreement between the model and the experiments is again encouraging, although the experimental correlation shows less variation with x^3 than does the correlation from the model.

(iv) Summary.

Simulations with the new model show that $\sigma_c/\langle c \rangle$ is strongly dependent on source size at small times, but becomes independent of source size at large times. The simulations also suggest that $\sigma_c/\langle c \rangle$ tends to zero in stationary conditions but approaches a small non-zero value in decaying turbulence. However, because of statistical noise, we cannot be certain of the zero limit in the stationary case. The large time behaviour of $\sigma_c/\langle c \rangle$ in stationary conditions is in marked contrast to that seen in Durbin's (1980) model for which $\sigma_c/\langle c \rangle$ approaches a non-zero constant depending on source size. In some ways the large time limit of $\sigma_c/\langle c \rangle$ in the stationary case is a rather academic question - in reality inhomogeneity or non-stationarity is

nearly always important at large times. However it does serve to highlight the differences in behaviour between the various models considered here.

The agreement between the new model and Fackrell and Robins' (1982) experimental data is encouraging. In particular the effect of varying the source size in the model has the same effect as in the experiments. The agreement with Warhaft's (1984) line source data is not so good, but this may be partly due to the low Reynolds number of the experiments. This data, which was obtained in decaying turbulence, shows clearly a non-zero limit for $\sigma_c / \langle c \rangle$, although the value of this limit is rather larger than the model value. The model also shows encouraging agreement with the data of Warhaft (1984) on the correlation between the concentration from two sources separated in space.

7. THE RANDOM WALK MODELLING TECHNIQUE - AN APPRAISAL.

It seems appropriate to conclude this study of random walk models by discussing the strengths and weaknesses of such models, both in absolute terms and in comparison with other modelling techniques.

Random walk models avoid many of the problems inherent in other approaches to modelling. For example, they do not require the extensive empirical tuning associated with Gaussian plume models. Also they do not need to make crude eddy-diffusivity assumptions, either for the flux of contaminant as in eddy-diffusivity models, or for the flux of some higher order concentration-weighted velocity moment as in high-order closure models. As a result, random walk models can represent the initial stages in the evolution of $\langle c \rangle$ easily and naturally and can also model the dispersion from complex source distributions. In effect, random walk models make a diffusive assumption in phase space instead of in ordinary space. Although such an assumption is of course not exact, it seems to cause few problems in practice and is, as Obukhov (1959) has pointed out, consistent with inertial subrange scaling. In two-particle models, the description of the flow at any time includes a specification of the spatial distribution of pairs of contaminant particles, and hence of the (second-order) spatial structure of the concentration field. As a result, such models can represent effects which depend on the length-scale of the concentration fluctuations. In contrast high-order closure models and p.d.f. models, which represent the concentration field solely in terms of one-point statistics, have difficulty in describing such effects. As noted in §1.3, two-point closure models (such as the eddy-damped quasi-normal approximation) can represent such effects, but have difficulty in modelling the inhomogeneous concentration fields resulting from inhomogeneous source distributions. Random walk models of course have no such difficulty.

One-particle random walk models are particularly suited to situations where the flow is inhomogeneous and have proved able to provide good descriptions of the dispersion in many such situations. For two-particle models, complex flows are likely to prove more difficult; indeed very few attempts at modelling the motion of pairs of particles in flows significantly more complex than the isotropic turbulence considered in chapters 5 and 6 have yet been made. The difficulty is that, although random walk models are conceptually simple, they can be very complex to implement in complex flows. Simple modifications of the model described in §5.4 (e.g. to include, following Durbin (1980), the effect of a uniform shear) are straightforward, but it is not clear how to adapt the model to more complex flows such as surface layers (see Sawford (1985) for an attempt to extend Durbin's (1980) model to a surface layer). For example, it is quite hard even to devise a simple expression for the two-point velocity correlation function which is consistent with incompressibility and surface layer scaling. Such an expression would be a necessary prerequisite to designing a model using the approach developed in this thesis. As a result it seems likely that, for complex flows, it will only be possible to apply the ideas developed in this thesis in a simplified form. For continuous sources or instantaneous area or line sources (as considered in §6.2), the concentration variance is not very sensitive to the shape of the particle separation p.d.f. p_Δ . This is because, for such sources, σ_c^2 depends only on the averaged p.d.f.s \bar{p}_Δ or $\bar{\bar{p}}_\Delta$, and these quantities do not vary as much as p_Δ . This suggests that, with the possible exception of instantaneous compact sources, it may be possible in complex flows to use models based on the simpler NGLS model, at least if we allow ourselves to "tune" the values of C_0 . For surface sources in a neutral surface layer, it seems possible that models based on Richardson's (1926) model might be useful. We saw in §5.6 that the

shape of p_{Δ} in Richardson's model is quite close to that in the new model. The value of σ_{Δ} is rather different, but this could be corrected by adjusting C_0 . Of course, if an approach based on Richardson's model is adopted, it would be necessary to postulate a model for the motion of the particle-pair centroids. For surface sources in a surface layer, it is known that, because the eddy size becomes small as we approach the ground, an eddy-diffusivity approach describes motion of single particles quite well (see §1.3). For the same reason, it seems likely that such a model could describe the motion of the particle-pair centroids. If such a model is adopted in conjunction with Richardson's (1926) model for the particle separations (suitably modified for surface layer scaling), we would then have quite a simple model (of a similar type to that proposed by Thiebaut (1975)) for the motion of particle-pairs from a surface source, in which both the particle separation and the centroid position evolve according to an eddy-diffusivity formulation. Such a model seems worthy of investigation.

A difficulty with the random walk approach is the absence, in most cases of interest, of analytic solutions and the problem of statistical noise in numerical simulations. An example of this difficulty was apparent in §6.2, where, because of statistical noise, it was impossible to conclude with certainty that the model value of $\sigma_c / \langle c \rangle$ tends to zero at large times in stationary conditions. However the difficulty in this case was caused by the need to evaluate a very small difference between two almost equal quantities. For most quantities not involving small differences it seems likely that, by using the "particle splitting" technique appropriately, the statistical noise can be kept under control. It should be pointed out however that this type of problem is likely to be worse in more complex situations where there are fewer symmetries which can be averaged over to reduce the noise.

In many problems, more knowledge than that given by the first two one-point moments of the concentration is required. For example, one may be interested in the variance of the average concentration over a certain region. Such information can be obtained from two-particle random walk models, although no such quantities have been calculated in this thesis. Also it is often necessary to know the p.d.f. of the concentration at a point or averaged over some volume. This is especially true in the case of an atmospheric release of a toxic, inflammable or explosive substance. Unfortunately such quantities cannot be obtained from one- and two-particle random walk models. However there is a growing body of evidence (Lewellen and Sykes 1986; Sawford 1987; Mylne 1988) to suggest that, for passive contaminants in the atmosphere, the p.d.f. of the concentration can be parametrized with reasonable accuracy in terms of the first two moments. In principle the concentration p.d.f. could be obtained from many-particle random walk models (Kaplan and Dinar 1988). However only the first steps in the development of such models have been taken, and it is not yet clear if such models will prove useful.

There are a number of theoretical problems with random walk models, some of which suggest that the goal of a universal model, applicable to all (high Reynolds number) flows may not be achievable. Firstly, except in one-dimensional one-particle models, the theory presented in chapters 4 and 5 does not determine ϕ (or $\hat{\phi}$) uniquely. As pointed out in §4.4, Sawford and Guest (1988) have shown that the choice of ϕ does make some difference to the results and it is not at all clear how arguments can be formulated to determine ϕ . The second problem concerns the value of C_0 . In successful simulations of dispersion in a convective boundary layer, Sawford and Guest (1987) and Weil (1988) used values of C_0 of order 2.0 instead of the value 4.0 adopted in §5.4. This suggests that the value of C_0 may need to be tuned to some extent for different problems - such tuning is of course

inconsistent with the idea that C_0 is the inertial subrange constant which occurs in the Lagrangian velocity structure function (see also Sawford and Guest (1988)). Finally there is the problem discussed in §§5.4 and 5.6, namely the fact that it is not clear how to design a two-particle model to satisfy both the well-mixed condition and (5.2). However this problem does not appear to be too serious in practice.

If random walk models based on (4.1) or (5.1) do prove to have serious limitations, there are a number of possible ways of generalising such models. The most obvious way is to add an equation for the evolution of the acceleration of the particles. This might enable such models to give a better description of the trajectories over time intervals of order τ_η , but it is not clear if there are any other advantages. An alternative approach suggested by Yeung and Pope (1988) is to add an equation for the value of the turbulent energy dissipation rate at the location of the particle. Such a modification might enable the model to take account of the intermittent structure of the turbulence associated with fluctuations in dissipation rate. There are of course many more ways of formulating such models than there are in the case of models of the form (4.1) and (5.1), and the problem of discovering how such a model should be designed has only just begun to be investigated.

To sum up, random walk models constitute a promising approach to the problem of the dispersion of a passive contaminant in a turbulent flow. Though simple in concept, random walk models avoid many of the problems inherent in other techniques. Although they involve a number of assumptions that cannot be justified in any fundamental way, they show good agreement with experimental data in a wide range of flows. It seems likely that such models will be increasingly exploited in the future.

Appendix A. Derivation of the Statistical Relations given in §3.3.

The purpose of this appendix is to give a derivation of the statistical relations (3.4), (3.5), (3.6) and (3.7).

Consider a single realisation $\omega \in \Omega$ of the flow. Let us assume that the total mass M of fluid is finite, as would be the case, for example, if the region occupied by the fluid were bounded. The reason for making this assumption is that it enables us to consider the hypothetical operation of choosing a fluid particle at random from all fluid particles in the flow, with the probability of the fluid particle belonging to any given subset of the set of fluid particles being proportional to the mass of fluid particles in that subset. The assumption is not as restrictive as it might appear since in reality the region of interest is always finite and in any case the results apply in greater generality as can be seen from the obvious limiting argument.

As explained in §3.3, if $\kappa > 0$, the term "fluid particle" means simply a fluid molecule. For simplicity we shall adopt the stochastic differential equation model for the motion of fluid molecules discussed in §2.3, i.e. we shall assume that the molecule trajectories $\underline{X}^\omega(t)$ evolve according to the stochastic differential equation

$$d\underline{X}^\omega = \underline{u}_0(\underline{X}^\omega, t)dt + (\nabla(\kappa\rho)/\rho)dt + (2\kappa)^{1/2}d\underline{\zeta} \quad (\text{A.1})$$

and have an initial distribution given by

$$P_{\underline{X}^\omega(0)}(\underline{x}) = \rho(\underline{x}, 0)/M$$

(the superscript ω in \underline{X}^ω is intended to emphasise that we are considering the realisation ω only). Equation (A.1) is simply (2.3) with \underline{a} and \underline{b} chosen so that the equation for the evolution of $P_{\underline{X}^\omega(t)|\underline{X}^\omega(s)}$, i.e. equation (2.6), takes the same form as (3.3) with $S = 0$. Of course $P_{\underline{X}^\omega(t)}(\underline{x}) = \rho(\underline{x}, t)/M$ is satisfied at times $t > 0$ as well as at time $t=0$.

There are a number of advantages of using this model. Firstly the model molecules have a continuous distribution in space and so there is no need to invoke the continuum hypothesis to relate the distribution of molecules to $c(\underline{x}, t)$. This is a consequence of the idealised picture of the physics embodied in the model (A.1). The spatial distribution of the model molecules can be regarded as being a model for the true distribution of molecules smoothed over a length-scale δ , where δ is much smaller than the length-scale on which continuum quantities vary, but large enough so that a sphere of radius δ contains many molecules. Alternatively, the model distribution of molecules can be regarded as representing an ensemble average over an ensemble of flows which have the same values for the macroscopic quantities \underline{u}_e , ρ and c , but in which the details of the molecular motions are different. Secondly, because of the way we have chosen \underline{a} and \underline{b} , the transition density $P_{\underline{x}^\omega}(t) | \underline{x}^\omega(s)$ satisfies the advection-diffusion equation (3.3) exactly (with $S = 0$). This means that the model is consistent with the description of dispersion embodied in equation (3.3). Of course, as noted in §2.2, the model (A.1) cannot be an exact model of molecular motions. However the equations of §3.1 are generally believed to give an accurate description of turbulent flows and so this should not matter. Finally, when $\kappa=0$, the model molecules become "fluid elements", i.e. points which are advected by the velocity \underline{u}_e . This enables us to treat both the cases $\kappa > 0$ and $\kappa = 0$ together. It follows immediately from (2.6) and (3.3) that $c(\underline{x}, t)$ can be expressed in terms of $P_{\underline{x}^\omega}(t) | \underline{x}^\omega(s)$ as

$$c(\underline{x}, t) = \int_{s \leq t} P_{\underline{x}^\omega}(t) | \underline{x}^\omega(s) (\underline{x} | \underline{y}) S(\underline{y}, s) d\underline{y} ds. \quad (\text{A.2})$$

Let us now consider the entire ensemble of flows and consider choosing a fluid particle at random from all fluid particles in the ensemble. By this we mean first taking a random sample of size one from the set Ω of realisations and then taking a random sample of size

one from the set of fluid particles in the selected realisation. If $\underline{X}(t)$ is the trajectory of the particle so chosen, it is clear that the joint density of $\underline{X}(t_1), \dots, \underline{X}(t_n)$ for various times t_1, \dots, t_n is given by

$$P_{\underline{X}(t_1), \dots, \underline{X}(t_n)}(\underline{x}_1, \dots, \underline{x}_n) = \langle P_{\underline{X}^\omega(t_1), \dots, \underline{X}^\omega(t_n)}(\underline{x}_1, \dots, \underline{x}_n) \rangle.$$

If we now assume that S/ρ is independent of \underline{u}_e and ρ , equation (3.4) can be obtained by taking the ensemble average of (A.2):

$$\begin{aligned} \langle c(\underline{x}, t) \rangle &= \int_{s \leq t} \langle P_{\underline{X}^\omega(t) | \underline{X}^\omega(s)}(\underline{x} | \underline{y}) S(\underline{y}, s) \rangle d\underline{y} ds \\ &= M \int_{s \leq t} \langle P_{\underline{X}^\omega(t), \underline{X}^\omega(s)}(\underline{x}, \underline{y}) S(\underline{y}, s) / \rho(\underline{y}, s) \rangle d\underline{y} ds \\ &= M \int_{s \leq t} P_{\underline{X}(t), \underline{X}(s)}(\underline{x}, \underline{y}) \langle S(\underline{y}, s) / \rho(\underline{y}, s) \rangle d\underline{y} ds \\ &= \int_{s \leq t} P_{\underline{X}(t) | \underline{X}(s)}(\underline{x} | \underline{y}) \langle S(\underline{y}, s) \rangle d\underline{y} ds. \end{aligned}$$

Let us now return to considering a single realisation ω and consider the distribution of $\underline{u}_e(\underline{X}^\omega(t), t)$ which will be denoted by $\underline{U}^\omega(t)$. $\underline{U}^\omega(t)$ is the velocity at the position $\underline{X}^\omega(t)$ of the randomly chosen fluid particle. The conditional p.d.f. $P_{\underline{U}^\omega(t) | \underline{X}^\omega(t)}(\underline{u} | \underline{x})$ of $\underline{U}^\omega(t)$ given that $\underline{X}^\omega(t) = \underline{x}$ is equal to $\delta(\underline{u} - \underline{u}_e(\underline{x}, t))$, as is the conditional p.d.f. $P_{\underline{U}^\omega(t) | \underline{X}^\omega(t), \underline{X}^\omega(s)}(\underline{u} | \underline{x}, \underline{y})$. Hence

$$\begin{aligned} \rho(\underline{x}, t) \delta(\underline{u} - \underline{u}_e(\underline{x}, t)) &= M P_{\underline{X}^\omega(t)}(\underline{x}) P_{\underline{U}^\omega(t) | \underline{X}^\omega(t)}(\underline{u} | \underline{x}) \\ &= M P_{\underline{X}^\omega(t), \underline{U}^\omega(t)}(\underline{x}, \underline{u}) \end{aligned}$$

and

$$\begin{aligned} c(\underline{x}, t) \delta(\underline{u} - \underline{u}_e(\underline{x}, t)) &= \\ &= \int_{s \leq t} P_{\underline{X}^\omega(t) | \underline{X}^\omega(s)}(\underline{x} | \underline{y}) S(\underline{y}, s) d\underline{y} ds P_{\underline{U}^\omega(t) | \underline{X}^\omega(t), \underline{X}^\omega(s)}(\underline{u} | \underline{x}, \underline{y}) \\ &= M \int_{s \leq t} P_{\underline{X}^\omega(t), \underline{U}^\omega(t), \underline{X}^\omega(s)}(\underline{x}, \underline{u}, \underline{y}) S(\underline{y}, s) / \rho(\underline{y}, s) d\underline{y} ds \\ &= M \int_{s \leq t} P_{\underline{X}^\omega(t), \underline{U}^\omega(t), \underline{X}^\omega(s), \underline{U}^\omega(s)}(\underline{x}, \underline{u}, \underline{y}, \underline{v}) S(\underline{y}, s) / \rho(\underline{y}, s) d\underline{y} d\underline{v} ds. \end{aligned}$$

Taking the ensemble average of these equations yields

$$g_p = M p_{\underline{X}(t), \underline{U}(t)}(\underline{x}, \underline{u}) \quad (\text{A.3})$$

and

$$g_c = M \int_{s \leq t} p_{\underline{X}(t), \underline{U}(t), \underline{X}(s), \underline{U}(s)}(\underline{x}, \underline{u}, \underline{y}, \underline{v}) \langle S(\underline{y}, s) / \rho(\underline{y}, s) \rangle d\underline{v} d\underline{y} ds.$$

By using (A.3) and standard relations between conditional p.d.f.s, g_c can be expressed in the form

$$g_c = \int_{s \leq t} p_{\underline{X}(t), \underline{U}(t) | \underline{X}(s), \underline{U}(s)}(\underline{x}, \underline{u} | \underline{y}, \underline{v}) \times \\ \times g_p(\underline{y}, \underline{v}, s) \langle S(\underline{y}, s) / \rho(\underline{y}, s) \rangle d\underline{v} d\underline{y} ds.$$

The results (3.6) and (3.7) for particle-pairs can be derived similarly. Again consider initially a single realisation ω and let $\underline{X}_1^\omega(t)$ and $\underline{X}_2^\omega(t)$ be the trajectories of two randomly and independently chosen fluid particles. Then, from (A.2),

$$c(\underline{x}_1, t_1) c(\underline{x}_2, t_2) = \int_{s_1 \leq t_1, s_2 \leq t_2} p_{\underline{X}_1^\omega(t_1), \underline{X}_2^\omega(t_2) | \underline{X}_1^\omega(s_1), \underline{X}_2^\omega(s_2)}(\underline{x}_1, \underline{x}_2 | \underline{y}_1, \underline{y}_2) \times \\ \times S(\underline{y}_1, s_1) S(\underline{y}_2, s_2) d\underline{y}_1 d\underline{y}_2 ds_1 ds_2.$$

As in deriving (A.3), taking the ensemble average yields

$$\langle c(\underline{x}_1, t_1) c(\underline{x}_2, t_2) \rangle = \int_{s_1 \leq t_1, s_2 \leq t_2} p_{\underline{X}_1(t_1), \underline{X}_2(t_2) | \underline{X}_1(s_1), \underline{X}_2(s_2)}(\underline{x}_1, \underline{x}_2 | \underline{y}_1, \underline{y}_2) \times \\ \times \langle S(\underline{y}_1, s_1) S(\underline{y}_2, s_2) \rangle d\underline{y}_1 d\underline{y}_2 ds_1 ds_2.$$

The phase space result (3.7) for particle-pairs follows similarly.

Appendix B. Some Properties of Various Random Walk Models.

In this appendix some of the analytic results which can be obtained for simple random walk models and which have been quoted above are derived.

First consider the Langevin equation (4.2), which we write here in the form

$$dU = -\frac{U}{\tau} dt + \left(\frac{2\sigma^2}{\tau}\right)^{1/2} d\zeta. \quad (\text{B.1})$$

In addition we assume that the distribution of the initial value of U , $U(0)$, is Gaussian with mean zero and variance σ^2 , and that $U(0)$ is independent of $\zeta(t)$. The Langevin equation can be transformed easily into the form $d(Ue^{t/\tau}) = (2\sigma^2/\tau)^{1/2} e^{t/\tau} d\zeta$ which integrates to give

$$U(t) = U(0)e^{-t/\tau} + \left(\frac{2\sigma^2}{\tau}\right)^{1/2} e^{-t/\tau} \int_0^t e^{t'/\tau} d\zeta(t'). \quad (\text{B.2})$$

Because $U(0)$ and $\zeta(t)$ are (jointly) Gaussian, $U(t)$ is a Gaussian process. Using the independence of $U(0)$ and $\zeta(t)$, the two-time covariance of U can be expressed as

$$\begin{aligned} \langle U(t)U(s) \rangle = & \\ & e^{-(t+s)/\tau} \left(\langle U(0)^2 \rangle + \frac{2\sigma^2}{\tau} \int_0^t \int_0^s e^{(t'+s')/\tau} \langle d\zeta(t')d\zeta(s') \rangle \right). \end{aligned}$$

Now $\langle d\zeta(s')d\zeta(t') \rangle = ds'$ if $s' = t'$ and is zero otherwise. Hence, assuming without loss of generality that s is less than or equal to t , we have

$$\begin{aligned} \langle U(t)U(s) \rangle &= e^{-(t+s)/\tau} \left(\langle U(0)^2 \rangle + \frac{2\sigma^2}{\tau} \int_0^s e^{2s'/\tau} ds' \right) \\ &= e^{-(t+s)/\tau} \left(\langle U(0)^2 \rangle + \sigma^2 (e^{2s/\tau} - 1) \right). \end{aligned} \quad (\text{B.3})$$

Using $\langle U(0)^2 \rangle = \sigma^2$, we obtain $\langle U(t)U(s) \rangle = \sigma^2 e^{-(t-s)/\tau}$ for $s \leq t$, showing that $U(t)$ is a stationary process (because it is Gaussian and $\langle U(t)U(s) \rangle$ depends on $|t-s|$ only), has variance σ^2 , and has an exponential correlation function with integral time-scale τ . (B.2) can

be integrated to yield

$$X(t) = X(0) + U(0)\tau(1 - e^{-t/\tau}) + (2\sigma^2\tau)^{1/2} \int_0^t (1 - e^{(t'-t)/\tau}) d\zeta(t').$$

It follows from the (joint) Gaussianity of $U(0)$ and $\zeta(t)$ that the displacements $X(t)-X(0)$ are Gaussian.

Let us now consider the situation discussed briefly in §4.3(iii), in which $\underline{U}(t)$ satisfies

$$dU^i = -L^{ij}U^j dt + b^{ij}d\zeta^j$$

with \underline{L} symmetric. Note we have set $\underline{U}_e = 0$ as we clearly may do by using a Galilean transformation. It follows immediately that $\langle U^i(t)U^j(s) \rangle$ satisfies

$$\frac{d}{dt} \langle U^i(t)U^k(s) \rangle = -L^{ij} \langle U^j(t)U^k(s) \rangle.$$

By choosing a coordinate system in which \underline{L} is diagonal, it can be seen that the correlation function decays exponentially.

Finally we will describe how to derive the expressions given in §5.6 for the values of σ_1 , σ_Δ and σ_Σ in the NGLS model. In stationary conditions, each component of \underline{U}_1 , $\Delta\underline{U}$ and $\Sigma\underline{U}$ in the NGLS model satisfies (B.1) and, for particle-pairs with both particles coincident at the origin at time zero, $\langle U_1^i(0)U_1^i(0) \rangle = 3\sigma^2$, $\langle \Delta U^i(0)\Delta U^i(0) \rangle = 0$, and $\langle \Sigma U^i(0)\Sigma U^i(0) \rangle = 6\sigma^2$ (for convenience we consider particle-pairs released at time zero instead of time s as considered in §5.6). It follows from (B.3) that

$$\begin{aligned} \langle U_1^i(t)U_1^i(s) \rangle &= 3\sigma^2 e^{-(t-s)/\tau} \\ \langle \Delta U^i(t)\Delta U^i(s) \rangle &= 3\sigma^2 (e^{-(t-s)/\tau} - e^{-(t+s)/\tau}) \\ \langle \Sigma U^i(t)\Sigma U^i(s) \rangle &= 3\sigma^2 (e^{-(t-s)/\tau} + e^{-(t+s)/\tau}) \end{aligned}$$

for $s \leq t$. σ_1 , σ_Δ and σ_Σ can then be found from the relation

$$\frac{d}{dt} \langle X_1^i(t)X_1^i(t) \rangle = 2\langle U_1^i(t)X_1^i(t) \rangle = 2 \int_0^t \langle U_1^i(t)U_1^i(s) \rangle ds$$

and the analogous relations for $\langle \Delta X^i(t)\Delta X^i(t) \rangle$ and $\langle \Sigma X^i(t)\Sigma X^i(t) \rangle$. In

decaying turbulence, σ_1 , σ_Δ and σ_z can be found in the same way, although the algebra is considerably more complex.

Appendix C. Details of the Numerical Simulations.

C.1 Details of Simulations Presented in Chapter 4.

The simulations presented in chapter 4 were carried out by replacing the infinitesimal quantities $d\underline{x}$, $d\underline{u}$, dt and $d\underline{\zeta}$ in (4.1) by finite differences $\Delta\underline{x}$, $\Delta\underline{u}$, Δt and $\Delta\underline{\zeta}$. 20,000 particles were followed for the simulations shown in figure 4.1. For the simulations with \underline{B} constant and $\underline{\phi} = 0$, \underline{a} is a linear function $-L^i j u^j$ of \underline{u} with \underline{L} symmetric; hence the resulting velocity correlation function can be calculated analytically (see Appendix B). A time-step of 0.05τ was found to be sufficiently small to achieve good agreement with the analytic result. The same time-step was used for the other case with constant \underline{B} . For the remaining two simulations in figure 4.1, $\Delta t = 0.05\tau$ proved unsatisfactory, but a time-step of

$$\Delta t = \min(0.05\sigma^2/B^{11}, 0.1\sigma/|\underline{a}|), \quad (\text{C.1})$$

with Δt varying along the trajectory, gave results which appeared realistic and were insensitive to further reductions in Δt . (C.1) ensures that a particle cannot change its velocity by a large amount (relative to the velocity-scale σ) in any time-step.

For the simulation shown in figure 4.2, 10,000 particles were followed. The same time-step as specified in (C.1) above was adopted and proved adequate to achieve good agreement between the analytic and numerical velocity p.d.f.s, as can be seen in figure 4.2.

C.2 Details of Simulations Presented in Chapters 5 and 6.

The model described in §5.4 is quite complex to implement because the expression for \underline{a} contains a large number of terms. In the calculations with this model presented in chapters 5 and 6, the model was simplified by the method used in the one-particle model of Thomson (1986a). This involves using a different set of finite difference equations at alternate time-steps.

When the particle separation is large, the time-scale on which particle velocities change is τ and so we require $\Delta t \ll \tau$ for accurate results. When the particles are close together however, the time-scale of the relative motion of particles is much smaller than τ and so a much smaller time-step is required. In order to allow for this and also avoid unnecessary waste of computing resources, the time-step was made a function of the particle separation and was allowed to vary along the particle-pair trajectory. The time-step Δt used in most of the calculations was chosen to be $0.1\tau(1 - f(\Delta))$. This ensures that $\Delta t \ll \tau$ at all times and also that $\Delta t \ll (\Delta^2/\varepsilon)^{1/3}$ when the particle separation lies in the inertial subrange ($(\Delta^2/\varepsilon)^{1/3}$ is the time-scale of the eddies which make the dominant contribution to the relative motion of the particles). A few experiments were conducted with a time-step of $0.05\tau(1 - f(\Delta))$. This resulted in only small differences (a few per cent) in most statistics. An exception is the statistic $\langle |\delta\Delta\tilde{x}|^2 \rangle$ shown in figure 5.7. In the case where the initial particle separation was $2 \times 10^{-3}l$, a time-step of $0.01\tau(1 - f(\Delta))$ was found necessary to ensure that the results were independent of Δt . This is to be expected since, with $\Delta t = 0.1\tau(1 - f(\Delta))$, the initial time-step is about one third of the time interval between the release of the particles and the time corresponding to the first data point in figure 5.7. Clearly the quantity $\langle |\delta\Delta\tilde{x}|^2 \rangle$, which depends on the departure of the trajectories from straight lines (and so depends on the difference between two nearly equal quantities), is unlikely to be well represented at the time of the first data point when the time-step is so large.

On the occasions when coincident particles needed to be released an initial separation of $2 \times 10^{-6}l$ was used. The results appear insensitive to changes in this quantity of an order of magnitude. It is of course impossible to have truly coincident particles since this would necessitate a time-step of length zero.

30,000 particle-pairs were followed in all the simulations from which p.d.f.s or concentration statistics were calculated, with the exception of the simulations involving the "particle splitting" technique (described in §5.6) for which 10,000 pairs were released. The remaining simulations were used only to calculate quantities such as σ_Δ , $\langle X_1^3 \rangle$ or $\langle |\delta\Delta X|^2 \rangle$. For such quantities, statistical noise is not as great a problem as it is with p.d.f.s and concentration variances, and so only 10,000 pairs were followed in these simulations.

In calculating $\langle c^2 \rangle$ in §§6.1 and 6.2 (with the exception of the calculations made in §6.2 without the aid of the approximation (6.8)), p_Δ was calculated from simulations which utilised the particle splitting technique, and was represented as a series of straight line segments between data points, each data point representing the average value of p_Δ over a small interval of Δ values. The distance between data points was similar to that used in the graphs shown in figures 5.1(b) and 5.8. The use of a much larger distance would tend to smooth the peak in p_Δ observed at small travel times, while a much smaller distance would greatly increase the scatter and would produce inaccurate results when the source size σ_0 or initial length-scale $L_c(s)$ is much less than σ_Δ . (The integrals in (6.10) and - putting $\Delta x=0$ - in (6.1) are in effect averages of p_Δ over regions of size σ_0 and $L_c(s)$. Hence they are most sensitive to statistical noise in p_Δ when σ_0 and $L_c(s)$ are small.) For the area and line sources considered in §6.2, a consequence of (6.9) and (6.10) is that σ_c depends on p_Δ only through \bar{p}_Δ and \bar{p}_Δ respectively. These quantities do not show such a marked peak as p_Δ and so the accuracy of the results might be increased by calculating \bar{p}_Δ and \bar{p}_Δ with a larger distance between data points as in figures 5.1(d) and 5.1(e); however for simplicity this has not been done here.

C.3 Justification of the "Particle Splitting" Technique.

Here a sketch of a proof that the particle splitting technique does not bias the (single-time) statistics from the model is given. Suppose we are computing an ensemble of realisations of the trajectory in \underline{x} -space of a particle-pair, with the initial positions and velocities of the two particles in the pair having a given probability distribution. Consider the probability $P(\Gamma_A)$ of the event Γ_A that the phase space position of the pair at time t , $(\hat{\underline{X}}(t), \hat{\underline{U}}(t))$, lies in a region A of phase space. Knowledge of $P(\Gamma_A)$ for all "hyper-cubes" A in phase space determines the distribution of $(\hat{\underline{X}}(t), \hat{\underline{U}}(t))$ and hence enables any statistic derived from $(\hat{\underline{X}}(t), \hat{\underline{U}}(t))$ to be calculated. Hence we need only show that the estimate of $P(\Gamma_A)$ obtained from the model is not biased by the particle splitting technique. Let us also suppose that we decide to split particle-pairs when they enter a certain region B of phase space and let Λ denote the event that the pair enter B before time t . Λ' will denote the event that Λ does not occur. In the simulations we consider a series of nested regions of phase space in which splitting occurs as described in §5.6. Here however we will consider only one region for simplicity. Also, again for simplicity, we will consider the situation in which splitting and chance annihilation occur on the first time of entering and leaving B only.

Without particle splitting, the numerical estimate e of $P(\Gamma_A)$ would be equal to the fraction of particle-pairs in the simulation which lie in A at time t , i.e.

$$e = \frac{1}{n} \sum_{i=1}^n \chi_i$$

where n is the number of pair trajectories computed, and χ_i equals unity if the i th particle-pair trajectory lies in A and is zero otherwise. For each i , the expectation of χ_i is equal to $P(\Gamma_A)$ and so the expectation of e also equals $P(\Gamma_A)$.

Suppose now that when particle-pairs enter the region B of phase space for the first time they are "split" into two pairs, each having a weight of 1/2. If the i th particle-pair is split prior to time t , the two daughter pairs will be labelled i_1 and i_2 and X_{i_1} and X_{i_2} will be defined as for X_i above. $P(\Gamma_A)$ would then be estimated as

$$e' = \frac{1}{n} \sum_{i=1}^n X'_i.$$

where $X'_i = \frac{1}{2}(X_{i_1} + X_{i_2})$ if the i th pair is split and $X'_i = X_i$ if it isn't. Now the expectation of X_{i_1} and X_{i_2} , conditional on splitting occurring, equals the conditional probability $P(\Gamma_A|\Lambda)$ while the expectation of X_i , conditional on splitting not occurring, equals $P(\Gamma_A|\Lambda')$. Hence, because the probability of splitting equals $P(\Lambda)$, the expectation of X'_i equals $P(\Gamma_A)$ and so the expectation of e' also equals $P(\Gamma_A)$. This shows that splitting of particle-pairs does not introduce any bias.

Now suppose that, as well as particle splitting occurring on entering B for the first time, each particle-pair has equal chances of being annihilated or of having its weight doubled on the first occasion of leaving B. It can be shown in the same way as above that this does not bias the results either (instead of considering two possibilities for each particle-pair we need to consider five possibilities corresponding to whether the particle-pair is split prior to time t and, if it is split, whether the first daughter pair, the second daughter pair, both pairs or neither pair leave region B before time t).

Appendix D. The relation between $\langle |\delta \underline{x}_1|^2 \rangle$ and $\langle |\delta \Delta \underline{x}|^2 \rangle$.

In this appendix, the relation between $\langle |\delta \underline{x}_1|^2 \rangle$ and $\langle |\delta \Delta \underline{x}|^2 \rangle$ is discussed.

In reality, the variance of $\delta \underline{x}_1$ and $\delta \Delta \underline{x}$ at time t can be expressed as

$$\begin{aligned} \langle |\delta \underline{x}_1|^2 \rangle &= \int_S^t \int_S^t \langle \delta \underline{U}_1(t_1) \cdot \delta \underline{U}_1(t_2) \rangle dt_1 dt_2 \\ \langle |\delta \Delta \underline{x}|^2 \rangle &= \int_S^t \int_S^t \langle \delta \Delta \underline{U}(t_1) \cdot \delta \Delta \underline{U}(t_2) \rangle dt_1 dt_2 \end{aligned}$$

with

$$\begin{aligned} \langle \delta \underline{U}_1(t_1) \cdot \delta \underline{U}_1(t_2) \rangle &= \int_S^{t_1} \int_S^{t_2} \langle \underline{A}_1(s_1) \cdot \underline{A}_1(s_2) \rangle ds_1 ds_2 \\ \langle \delta \Delta \underline{U}(t_1) \cdot \delta \Delta \underline{U}(t_2) \rangle &= \int_S^{t_1} \int_S^{t_2} \langle \Delta \underline{A}(s_1) \cdot \Delta \underline{A}(s_2) \rangle ds_1 ds_2 \end{aligned}$$

where $\underline{A}_i(t)$ is the acceleration of particle i and $\Delta \underline{A} = (\underline{A}_1 - \underline{A}_2)/\sqrt{2}$. As in §5.6, the average is over particle-pairs with a given position in \underline{x} -space at time s . Also $\langle \Delta \underline{A}(s_1) \cdot \Delta \underline{A}(s_2) \rangle$ can be written in the form

$$\langle \underline{A}_1(s_1) \cdot \underline{A}_1(s_2) \rangle - \langle \underline{A}_1(s_1) \cdot \underline{A}_2(s_2) \rangle. \quad (D.1)$$

For simplicity we will only consider the case where the initial separation lies well within the inertial subrange and restrict consideration to travel times over which the evolution of $\delta \underline{x}_1$ and $\delta \Delta \underline{x}$ are dominated by inertial subrange eddies (in the model this means, as noted in §5.6, imposing the restrictions $\Delta(s) \ll l$ and $t-s \ll \tau$). We first recall that the acceleration field is only well-correlated over very short length-scales of the order of the Kolmogorov micro-scale η (Monin and Yaglom 1975, §21.5). From this Monin and Yaglom (1975, pp546-547) and Sawford (1984) argue that the second term in (D.1) makes a negligible contribution to $\langle |\delta \Delta \underline{x}|^2 \rangle$ for times $t-s \ll \tau$. If this is so, it follows that $\langle |\delta \underline{x}_1|^2 \rangle = \langle |\delta \Delta \underline{x}|^2 \rangle$ for $t-s \ll \tau$. Although it is true that $\langle \underline{A}_1(s_1) \cdot \underline{A}_2(s_2) \rangle$ is small, the following argument suggests

that it may not be negligible over such times (note it is clearly not negligible at very large times when $\langle |\delta X_1|^2 \rangle \sim \langle |U_1(s)|^2 \rangle (t-s)^2$ and $\langle |\delta \Delta X|^2 \rangle \sim \langle |\Delta U(s)|^2 \rangle (t-s)^2$; these cannot be equal unless the initial separation is so large that the initial velocities of the two particles are uncorrelated). In the inertial subrange, the Eulerian acceleration covariance $\langle \underline{a}_e(\underline{x}, t) \cdot \underline{a}_e(\underline{x} + \underline{r}, t) \rangle$ (where \underline{a}_e is the Eulerian acceleration field Du_e/Dt) between the acceleration at two points separated by a distance $r = |\underline{r}|$ is proportional to $\epsilon^{4/3} r^{-2/3}$ (Monin and Yaglom 1975, p371). On dimensional grounds this covariance is expected to persist over a time of order $\epsilon^{-1/3} r^{2/3}$, i.e. we expect $\langle \underline{a}_e(\underline{x}, s_1) \cdot \underline{a}_e(\underline{x} + \underline{r}, s_2) \rangle$ to be of order $\epsilon^{4/3} r^{-2/3}$ for $|s_1 - s_2| < \epsilon^{-1/3} r^{2/3}$. Provided that the Eulerian and Lagrangian acceleration covariances are of the same order of magnitude and that s_1 lies well inside the interval $[s, t_2]$, this implies that, for two particles with separation r at time s_1 ,

$$\int_s^{t_2} \langle \underline{A}_1(s_1) \cdot \underline{A}_2(s_2) \rangle ds_2$$

is of order $(\epsilon^{4/3} r^{-2/3})(\epsilon^{-1/3} r^{2/3}) = \epsilon$. It follows that, provided $t-s \gg (\Delta(s)^2/\epsilon)^{1/3}$ (so that the acceleration covariance $\langle \underline{A}_1(s_1) \cdot \underline{A}_2(s_2) \rangle$ has time to act), the contribution to $\langle |\delta \Delta X|^2 \rangle$ from the second term in (D.1) is of order ϵt^3 , which is (on dimensional grounds) comparable to $\langle |\delta \Delta X|^2 \rangle$ itself. This suggests that the second term in (D.1) is not negligible and that $\langle |\delta \Delta X|^2 \rangle$ is not equal to $\langle |\delta X_1|^2 \rangle$ for times in the range $(\Delta(s)^2/\epsilon)^{1/3} \ll t-s \ll \tau$.

In fact, for initially coincident particles, $\langle |\delta \Delta X|^2 \rangle$ cannot be greater than $\langle |\delta X_1|^2 \rangle$ and so, if we accept the above argument, must be less than $\langle |\delta X_1|^2 \rangle$. To see this consider a single realisation and consider all particles in the realisation which are at \underline{y} at time s . The phase space trajectories of such particles will be denoted by $(\underline{X}^\omega(t), \underline{U}^\omega(t))$ as in Appendix A. q_1 will denote the average of $|\underline{X}^\omega(t) - \underline{y} - \underline{U}^\omega(s)(t-s)|^2$ for such particles and q_2 will denote the average

of $\frac{1}{2}|X_1^\omega(t) - X_2^\omega(t)|^2$ for pairs of such particles. q_2 is equal to the mean square of the displacement $|X^\omega(t) - X_{CM}^\omega(t)|$ of such particles relative to their centre of mass $X_{CM}^\omega(t)$ (Batchelor 1952) and so $q_1 = q_2 + |X_{CM}^\omega(t) - y - U^\omega(s)(t-s)|^2$ and, in particular, $q_1 \geq q_2$. Now, for initially coincident particles, $\delta\Delta X = \Delta X$ and so $\langle |\delta X_1|^2 \rangle$ and $\langle |\delta\Delta X|^2 \rangle$ are equal to the ensemble average of q_1 and q_2 respectively. Hence $\langle |\delta X_1|^2 \rangle \geq \langle |\delta\Delta X|^2 \rangle$. Equality is only possible if $X_{CM}^\omega(t) = y + U^\omega(s)(t-s)$ with probability one. This seems unlikely to be true, lending further support to the idea that $\langle |\delta\Delta X|^2 \rangle$ is less than $\langle |\delta X_1|^2 \rangle$.

For pairs of particles which are not initially coincident, it seems likely that the particles will eventually forget their initial separation and behave in the same way as initially coincident particles (Batchelor 1950, 1952). On dimensional grounds we expect this to happen after a time of order $(\Delta(s)^2/\epsilon)^{1/3}$ (assuming the initial particle separation is well within the inertial subrange). Hence, in the case of particles which are not initially coincident, the arguments in the previous paragraph support the idea that $\langle |\delta\Delta X|^2 \rangle$ is less than $\langle |\delta X_1|^2 \rangle$ for travel times $t-s$ much greater than $(\Delta(s)^2/\epsilon)^{1/3}$.

References.

- Anand M.S. and Pope S.B. 1985 "Diffusion behind a line source in grid turbulence". Turbulent shear flows 4, Springer-Verlag.
- Antonopoulos-Domis M. 1981 "Large-eddy simulation of a passive scalar in isotropic turbulence". J. Fluid Mech., 104, 55-79.
- Batchelor G.K. 1949 "Diffusion in a field of homogeneous turbulence. I. Eulerian Analysis". Aust. J. Sci. Res., 2, 437-450.
- Batchelor G.K. 1950 "The application of the similarity theory of turbulence to atmospheric diffusion". Q. J. R. Meteorol. Soc., 76, 133-146.
- Batchelor G.K. 1952 "Diffusion in a field of homogeneous turbulence. II. The relative motion of particles". Proc. Camb. Phil. Soc., 48, 345-362.
- Batchelor G.K. 1953 "The theory of homogeneous turbulence". Cambridge University Press.
- Batchelor G.K. 1959 "Small-scale variation of convected quantities like temperature in turbulent fluid. Part 1. General discussion and the case of small conductivity". J. Fluid Mech., 5, 113-133.
- Batchelor G.K. 1964 "Diffusion from sources in a turbulent boundary layer". Archiwum Mechaniki Stosowanej, 16, 661-670.
- Batchelor G.K. 1967 "An introduction to fluid dynamics". Cambridge

University Press.

Batchelor G.K., Howells I.D. and Townsend A.A. 1959 "Small-scale variation of convected quantities like temperature in turbulent fluid. Part 2. The case of large conductivity". J. Fluid Mech., 5, 134-139.

Batchelor G.K. and Townsend A.A. 1956 "Turbulent diffusion". Surveys in mechanics, Cambridge University Press.

Brière S. 1987 "Diffusion de polluant: comparaison d'un modèle Lagrangien et d'un modèle Eulerien fermé à l'ordre trois". Note de travail de l'Établissement d'Études et de Recherches Météorologiques No. 173.

Chatwin P.C. 1971 "On the interpretation of some longitudinal dispersion experiments". J. Fluid Mech., 48, 689-702.

Chatwin P.C. and Sullivan P.J. 1979 "The relative diffusion of a cloud of passive contaminant in incompressible turbulent flow". J. Fluid Mech., 91, 337-355.

Corrsin S. 1952 "Heat transfer in isotropic turbulence". J. Appl. Phys., 23, 113-118.

De Baas A.F., van Dop H. and Nieuwstadt F.T.M. 1986 "An application of the Langevin equation for inhomogeneous conditions to dispersion in a convective boundary layer". Q. J. R. Meteorol. Soc., 112, 165-180.

Deardorff J.W. 1978 "Closure of the second- and third-moment rate

equations for diffusion in homogeneous turbulence". Phys. Fluids, 21, 525-530.

Draxler R.R. 1976 "Determination of atmospheric diffusion parameters". Atmos. Environ., 10, 99-105.

Durbin P.A. 1980 "A stochastic model of two-particle dispersion and concentration fluctuations in homogeneous turbulence". J. Fluid Mech., 100, 279-302.

Durbin P.A. 1982 "Analysis of the decay of temperature fluctuations in isotropic turbulence". Phys. Fluids, 25, 1328-1332.

Durbin P.A. 1983 "Stochastic differential equations and turbulent dispersion". NASA reference publication 1103.

Durbin P.A. 1984 "Comment on papers by Wilson et al (1981) and Legg and Raupach (1982)". Boundary-Layer Meteorol., 29, 409-411.

Egbert G.D. and Baker M.B. 1984 "Comments on paper 'The effect of Gaussian particle-pair distribution functions in the statistical theory of concentration fluctuations in homogeneous turbulence' by B.L. Sawford (Q.J. April 1983, 109, 339-353)". Q. J. R. Meteorol. Soc., 110, 1195-1199.

Einstein A. 1956 "Investigations on the theory of the brownian movement". Dover Publications.

Fackrell J.E. and Robins A.G. 1982 "Concentration fluctuations and fluxes in plumes from point sources in a turbulent boundary layer". J. Fluid Mech. 117, 1-26.

- Feller W. 1971 "An introduction to probability theory and its applications". Vol 2, J Wiley and Sons.
- Gifford F.A. 1982 "Horizontal diffusion in the atmosphere: A Lagrangian dynamical theory". Atmos. Environ., 16, 505-512.
- Gihman I.I. and Skorohod A.V. 1979 "The theory of stochastic processes III". Springer-Verlag.
- Gihman I.I. and Skorohod A.V. 1980 "The theory of stochastic processes I". Springer-Verlag.
- Hall C.D. 1975 "The simulation of particle motion in the atmosphere by a numerical random walk model". Q. J. R. Meteorol. Soc., 101, 235-244.
- Hanna S.R. 1979 "Some statistics of Lagrangian and Eulerian wind fluctuations". J. Appl. Met., 18, 518-525.
- Hanna S.R. 1981 "Lagrangian and Eulerian time-scale relations in the daytime boundary layer". J. Appl. Met., 20, 242-249.
- Haworth D.C. and Pope S.B. 1986 "A generalised Langevin model for turbulent flows". Phys. Fluids, 29, 387-405.
- Hunt J.C.R. 1985 "Turbulent diffusion from sources in complex flows". Ann. Rev. Fluid Mech., 17, 447-485.
- Janicke L. 1983 "Particle simulation of inhomogeneous turbulent diffusion". Air pollution modelling and its application II,

Plenum Press.

Jonas P.R. and Bartlett J.T. 1972 "The numerical simulation of particle motion in a homogeneous field of turbulence". J. Comp. Phys., 9, 290-302.

Kaplan H. and Dinar N. 1988 "A stochastic model for dispersion and concentration distribution in homogeneous turbulence". J. Fluid. Mech., 190, 121-140.

Lamb R.G. 1981 "A scheme for simulating particle pair motions in turbulent fluid". J. Comp. Phys., 39, 329-346.

Lamb R.G. 1982 "Diffusion in the convective boundary layer". Atmospheric turbulence and air pollution modelling, D. Reidel Publishing Company.

Langevin P. 1908 "Sur la théorie du mouvement brownien". Comptes Rendus Hebdomadaires des Séances, 146, 530-533.

Larchevêque M., Chollet J.P., Herring J.R., Lesieur M., Newman G.R. and Schertzer D. 1980 "Two-point closure applied to a passive scalar in decaying isotropic turbulence". Turbulent shear flows 2, Springer-Verlag.

Lee J.T. and Stone G.L. 1983 "The use of Eulerian initial conditions in a Lagrangian model of turbulent diffusion". Atmos. Environ., 17, 2477-2481.

Legg B.J. 1983 "Turbulent dispersion from an elevated line source: Markov chain simulations of concentration and flux profiles".

Q. J. R. Meteorol. Soc., 109, 645-660.

Legg B.J. and Raupach M.R. 1982 "Markov-chain simulation of particle dispersion in inhomogeneous flows: The mean drift velocity induced by a gradient in Eulerian variance". *Boundary-Layer Meteorol.*, 24, 3-13.

Lesieur M. 1987 "Turbulence in fluids". Martinus Nijhoff Publishers.

Leslie D.C. 1973 "Developments in the theory of turbulence". Clarendon Press.

Lewellen W.S. and Sykes R.I. 1986 "Analysis of concentration fluctuations from lidar observations of atmospheric plumes". *J. Clim. Appl. Met.*, 25, 1145-1154.

Ley A.J. 1982 "A random walk simulation of two-dimensional diffusion in the neutral surface layer". *Atmos. Environ.*, 16, 2799-2808.

Ley A.J. and Thomson D.J. 1983 "A random walk model of dispersion in the diabatic surface layer". *Q. J. R. Meteorol. Soc.*, 109, 867-880.

Libby P.A. and Williams F.A. 1980 "Fundamental aspects". *Turbulent reacting flows*, Springer-Verlag.

Lin C.C. and Reid W.H. 1963 "Turbulent flow. Theoretical aspects". *Handbuch der Physik*, vol VIII/2, Springer-Verlag.

Lumley J.L. 1970 "Stochastic tools in turbulence". Academic Press.

- Lumley J.L. and Van Cruyningen I. 1985 "Limitations of second order modeling of passive scalar diffusion". *Frontiers in fluid mechanics*, Springer-Verlag.
- Lundgren T.S. 1981 "Turbulent pair dispersion and scalar diffusion". *J. Fluid Mech.*, 111, 27-57.
- Monin A.S. and Yaglom A.M. 1971 "Statistical fluid mechanics". Vol 1, M.I.T. Press.
- Monin A.S. and Yaglom A.M. 1975 "Statistical fluid mechanics". Vol 2, M.I.T. Press.
- Mylne K.R. 1988 "Experimental measurements of concentration fluctuations". *Proc. 17th NATO/CCMS International Technical Meeting on Air pollution modelling and its applications*, Cambridge.
- Nelkin M. and Kerr R.M. 1981 "Decay of scalar variance in terms of a modified Richardson law for pair dispersion". *Phys. Fluids*, 24, 1754-1756.
- Newman G.R., Launder B.E. and Lumley J.L. 1981 "Modelling the behaviour of homogeneous scalar turbulence". *J. Fluid Mech.*, 111, 217-232.
- Novikov E.A. 1963 "Random force method in turbulence theory". *Soviet Physics JETP*, 17, 1449-1454.
- Obukhov A.M. 1959 "Description of turbulence in terms of Lagrangian variables". *Adv. Geophys.*, 6, 113-116.

- Pasquill F. 1974 "Atmospheric diffusion". Ellis Horwood.
- Pasquill F. and Smith F.B. 1983 "Atmospheric diffusion". Ellis Horwood.
- Pope S.B. 1983 "Consistent modeling of scalars in turbulent flows".
Phys. Fluids, 26, 404-408.
- Pope S.B. 1985 "Pdf methods for turbulent reactive flows". Prog. Energy
Combust. Sci., 11, 119-192.
- Pope S.B. 1987 "Consistency conditions for random walk models of
turbulent dispersion". Phys. Fluids, 30, 2374-2379.
- Reid J.D. 1979 "Markov chain simulations of vertical dispersion in the
neutral surface layer for surface and elevated releases".
Boundary-Layer Meteorol., 16, 3-22.
- Richardson L.F. 1926 "Atmospheric diffusion shown on a
distance-neighbour graph". Proc. Roy. Soc., A , 110, 709-737.
- Runca E., Bonino G. and Posch M. 1983 "Lagrangian modeling of air
pollutants dispersion from a point source". Air pollution
modelling and its application II, Plenum Press.
- Saffman P.G. 1960 "On the effect of the molecular diffusivity in
turbulent diffusion". J. Fluid Mech, 8, 273-283.
- Sawford B.L. 1982 "Lagrangian Monte Carlo simulation of the turbulent
motion of a pair of particles". Q. J. R. Meteorol. Soc., 108,
207-213.

- Sawford B.L. 1983 "The effect of Gaussian particle-pair distribution functions in the statistical theory of concentration fluctuations in homogeneous turbulence". Q. J. R. Meteorol. Soc., 109, 339-353.
- Sawford B.L. 1984 "The basis for, and some limitations of, the Langevin equation in atmospheric relative dispersion modelling". Atmos. Environ., 18, 2405-2411.
- Sawford B.L. 1985 "Lagrangian statistical simulation of concentration mean and fluctuation fields". J. Clim. Appl. Met., 24, 1152-1166.
- Sawford B.L. 1986 "Generalized random forcing in random-walk turbulent dispersion models". Phys. Fluids, 29, 3582-3585.
- Sawford B.L. 1987 "Conditional concentration statistics for surface plumes in the atmospheric boundary layer". Boundary-layer Meteorol., 38, 209-223.
- Sawford B.L. and Guest F.M. 1987 "Lagrangian stochastic analysis of flux-gradient relationships in the convective boundary layer". J. Atmos. Sci., 44, 1152-1165.
- Sawford B.L. and Guest F.M. 1988 "Uniqueness and universality of Lagrangian stochastic models of turbulent diffusion". 8th symposium on turbulence and diffusion, San Diego.
- Sawford B.L. and Hunt J.C.R. 1986 "Effects of turbulence structure, molecular diffusion and source size on scalar fluctuations in

homogeneous turbulence". J. Fluid Mech., 165, 373-400.

Schumann U. and Friedrich R. 1986 "Direct and large eddy simulation of turbulence". Vieweg.

Schuss Z. 1980 "Theory and applications of stochastic differential equations". J Wiley and Sons.

Smith F.B. 1968 "Conditioned particle motion in a homogeneous turbulent field". Atmos. Environ., 2, 491-508.

Smith F.B. 1984 "The integral equation of diffusion". Air pollution modelling and its application III, Plenum Press.

Smith F.B. and Thomson D.J. 1984 "Solutions of the integral equation of diffusion and the random walk model for continuous plumes and instantaneous puffs in the atmospheric boundary layer". Boundary-Layer Meteorol., 30, 143-157.

Spalding D.B. 1971 "Concentration fluctuations in a round turbulent free jet". Chem. Eng. Sci., 26, 95-107.

Sreenivasan K.R., Tavoularis S., Henry R. and Corrsin S. 1980 "Temperature fluctuations and scales in grid generated turbulence". J. Fluid Mech., 100, 597-621.

Stapountzis H., Sawford B.L., Hunt J.C.R. and Britter R.E. 1986 "Structure of the temperature field downwind of a line source in grid turbulence". J. Fluid Mech., 165, 401-424.

Sullivan P.J. 1971 "Some data on the distance-neighbour function for

relative diffusion". J. Fluid Mech., 47, 601-607.

Sykes R.I., Levellen W.S. and Parker S.F. 1984 "A turbulent-transport model for concentration fluctuations and fluxes". J. Fluid. Mech., 139, 193-218.

Taylor G.I. 1921 "Diffusion by continuous movements". Proc. Lond. Math. Soc., Ser. 2, 20, 196-211.

Tennekes H. 1979 "The exponential Lagrangian correlation function and turbulent diffusion in the inertial subrange". Atmos. Environ., 13, 1565-1567.

Thiebaut M.L. 1975 "The linear mean gradient model for two-particle turbulent diffusion". J. Atmos. Sci., 32, 91-101.

Thomson D.J. 1984 "Random walk modelling of diffusion in inhomogeneous turbulence". Q. J. R. Meteorol. Soc., 110, 1107-1120.

Thomson D.J. 1986a "A random walk model of dispersion in turbulent flows and its application to dispersion in a valley". Q. J. R. Meteorol. Soc., 112, 511-530.

Thomson D.J. 1986b "On the relative dispersion of two particles in homogeneous stationary turbulence and the implications for the size of concentration fluctuations at large times". Q. J. R. Meteorol. Soc., 112, 890-894.

Thomson D.J. 1987 "Criteria for the selection of stochastic models of particle trajectories in turbulent flows". J. Fluid Mech., 180, 529-556.

- Townsend A.A. 1954 "The diffusion behind a line source in homogeneous turbulence". Proc. Roy. Soc., A, 224, 487-512.
- Townsend A.A. 1976 "The structure of turbulent shear flow". Cambridge University Press.
- Uberoi M.S. and Corrsin S. 1952 "Diffusion of heat from a line source in isotropic turbulence". National Advisory Committee for Aeronautics, Technical Note 2710.
- Van Dop H., Nieuwstadt F.T.M. and Hunt J.C.R. 1985 "Random walk models for particle displacements in inhomogeneous unsteady turbulent flows". Phys. Fluids, 28, 1639-1653.
- Van Stijn Th.L. and Nieuwstadt F.T.M. 1986 "On the relation between a Lagrangian and a Eulerian model of diffusion in homogeneous, stationary and non-Gaussian turbulence". Atmos. Environ., 20, 1111-1120.
- Warhaft Z. 1984 "The interference of thermal fields from line sources in grid turbulence". J. Fluid Mech., 144, 363-387.
- Warhaft Z. and Lumley J.L. 1978 "An experimental study of the decay of temperature fluctuations in grid-generated turbulence". J. Fluid Mech., 88, 659-684.
- Wax N. 1954 "Selected papers on noise and stochastic processes". Dover Publications.
- Weil J.C. 1988 "Stochastic modeling of dispersion in the convective

boundary layer". Proc. 17th NATO/CCMS International Technical Meeting on Air pollution modelling and its applications, Cambridge.

Willis G.E. and Deardorff J.W. 1976 "A laboratory model of diffusion into the convective planetary boundary layer". Q. J. R. Meteorol. Soc., 102, 427-445.

Willis G.E. and Deardorff J.W. 1978 "A laboratory study of dispersion from an elevated source within a modeled convective planetary boundary layer". Atmos. Environ., 12, 1305-1311.

Willis G.E. and Deardorff J.W. 1981 "A laboratory study of dispersion from a source in the middle of the convectively mixed layer". Atmos. Environ., 15, 109-117.

Wilson J.D., Thurtell G.W. and Kidd G.E. 1981a "Numerical simulation of particle trajectories in inhomogeneous turbulence, I: Systems with constant turbulent velocity scale". Boundary-Layer Meteorol., 21, 295-313.

Wilson J.D., Thurtell G.W. and Kidd G.E. 1981b "Numerical simulation of particle trajectories in inhomogeneous turbulence, II: Systems with variable turbulent velocity scale". Boundary-Layer Meteorol., 21, 423-441.

Wilson J.D., Legg B.J. and Thomson D.J. 1983 "Calculation of particle trajectories in the presence of a gradient in turbulent-velocity variance". Boundary-layer Meteorol., 27, 163-169.

Yeh T.T. and van Atta C.W. 1973 "Spectral transfer of scalar and velocity fields in heated-grid turbulence". J. Fluid Mech., 58, 233-261.

Yeung P.K. and Pope S.B. 1988 "Lagrangian statistics from direct numerical simulations of isotropic turbulence". Technical report FDA-88-16, Sibley School of Mechanical and Aerospace Engineering, Cornell University.